(12)

FAA-EE-80-46, Vol. I

Office of Environment
and Energy
Washington, D.C. 20591

Evaluation of Alternative Procedures for Atmospheric Absorption Adjustments During Noise Certification

Volume I: Analyses and Results

Alan H. Marsh
DyTec Engineering, Inc.
2750 East Spring Street
Long Beach, CA 90806

October 1980

Final Report

U.S. Department of Transportation
Federal Aviation Administration

NOTICE

This document is disseminated under the sponsorship of the Department of Transportation in the interest of information exchange. The United States Government assumes no liability for its contents or use thereof.

The method of American National Standard S1.26-1978 for determining the atmospheric absorption of sound has not been approved by the Federal Aviation Administration for use in aircraft-noise type certification under Part 36 of the Federal Aviation Regulations.

Technical Report Documentation Page

1. Report No.	2. Government Accession No.	3. Recipient's Catalog No.
FAA-EE-80-46, Vol. I		

4. Title and Subtitle
Evaluation of Alternative Procedures for Atmospheric Absorption Adjustments During Noise Certification
Volume I: Analyses and Results

5. Report Date

6. Performing Organization Code

8. Performing Organization Report No.
DyTec Report 7926

7. Author(s)
Alan H. Marsh

9. Performing Organization Name and Address
DyTec Engineering, Inc.
2750 East Spring Street
Long Beach, CA 90806

10. Work Unit No. (TRAIS)

11. Contract or Grant No.
DOT-FA78WA-4121

13. Type of Report and Period Covered
Final Report

12. Sponsoring Agency Name and Address
U. S. Department of Transportation
Federal Aviation Administration
Office of Environment and Energy
Washington, DC 20591

14. Sponsoring Agency Code
AEE-110

15. Supplementary Notes
Richard N. Tedrick, Chief of the Noise Policy and Regulations Branch of the Noise Abatement Division of the Office of Environment and Energy, was the FAA Technical Project Manager.

16. Abstract
The work reported here extends that in FAA-RD-77-167, December 1977 to the problem of adjusting actual aircraft noise 1/3-octave-band spectra measured at 0.5-s intervals. Test-day spectra are used to calculate PNL, PNLT, EPNL, AL, and SEL. The test-day spectrum at the time of PNLTM and at the time of ALM are adjusted to acoustical-reference conditions using the atmospheric-absorption method in American National Standard ANSI S1.26-1978 and applied, using measurements of air temperature and relative humidity at various heights above the ground, by integrating over the frequency range of the passband of ideal filters and by calculating the absorption at the exact band-center frequencies only. SAE ARP866A is also used with the vertical-profile temperature/humidity data and with data at 10 m to determine adjustments from test-to-reference conditions. The adjustment methods are applied to noise data from nine aircraft.

Volume I describes the analyses and results of the study. Volume II presents the computer program that was developed and illustrates its use with a test case. Volume III presents tables of attenuation due to atmospheric absorption over a 300-m path. Attenuations were calculated using ANSI S1.26-1978 for pure tones at band-center frequencies and for three noise spectral slopes by a band-integration method, and using SAE ARP866A. For each of the five methods, the tables cover 34 air temperatures from 2 to 35° C, 10 relative humidities from 10 to 100 percent, and 24 nominal band-center frequencies from 50 to 10,000 Hz.

17. Key Words	18. Distribution Statement
Atmospheric absorption of sound Aircraft noise certification ANSI S1.26-1978 SAE ARP866A FAR Part 36	Availability unlimited. Report is available to the public through the National Technical Information Service, Springfield, VA 22161

19. Security Classif. (of this report)	20. Security Classif. (of this page)	21. No. of Pages	22. Price
Unclassified	Unclassified	215	

Form DOT F 1700.7 (8-72) Reproduction of completed page authorized

Section Page

Description of Test Cases. 97

Test-Time Meteorological Data. 101

Sound Propagation Paths. 112

Data Analysis and Adjustment Procedures. 121

Description of Band-Integration Procedure. 126

Results of Comparative Evaluations of Alternative Atmospheric-Absorption Adjustment Procedures 140

Measured Perceived Noise Levels and A-Weighted Sound Levels. 141

1/3-Octave-Band Sound Pressure Levels at the Time of PNLTM 151

Atmospheric Sound Absorption Coefficients 155

Band-Level Test-to-Reference-Day Adjustment Factors 159

Effect of Different Adjustment Procedures on Reference-Day Sound Pressure Levels 184

Effect of Different Adjustment Procedures on Reference-Day EPNL and SEL. 188

5. CONCLUSIONS. 199

6. REFERENCES 203

CONTENTS

Section		Page
1.	INTRODUCTION.	1
2.	EFFECTS OF ATMOSPHERIC CONDITIONS ON CALCULATIONS OF ABSORPTION-ADJUSTMENT FACTORS FOR BROADBAND SOUND.	9
	Spectra at the Source	11
	Spectra at the Receiver	17
	Exact Test-to-Reference-Day Band-Level Adjustment Factors.	25
	Approximation of Source Band Levels by Band-Integration Method	27
	Approximation of Source Band Levels by Band-Center-Frequency Method.	37
	Approximate Test-to-Reference-Day Band-Level Adjustment Factors	40
3.	EFFECTS OF NON-IDEAL FILTER CHARACTERISTICS ON CALCULATIONS OF ABSORPTION-ADJUSTMENT FACTORS	45
	Filter Transmission Response.	45
	Spectra at the Source	52
	Spectra at the Receiver	54
	Test-to-Reference-Day Band-Level Adjustment Factors.	67
4.	ADJUSTMENT OF AIRCRAFT NOISE DATA FROM TEST TO REFERENCE METEOROLOGICAL CONDITIONS.	75
	Requirements for Atmospheric-Absorption Adjustments During Noise Certification.	75
	Requirements for a Layered-Atmosphere Analysis.	78
	Reference Meteorological Conditions	81
	General Requirements of FAR 36 for Aircraft Noise Measurement and Analysis.	82
	Basic Assumptions Related to Atmospheric Absorption Adjustments.	88
	Assumptions Regarding Calculation of Tone-Correction Factors	90
	Assumptions Regarding Calculation of Duration-Correction Factors	95

ILLUSTRATIONS

Figure		Page
1.	Power spectra, $G_S(f)$, of the sound pressure at the source for several spectral slopes.	15
2.	1/3-octave-band sound pressure levels, LS, at the source for sound pressure spectral densities of Fig. 1 and ideal filters.	16
3.	1/3-octave-band sound pressure levels, LR, at the receiver for sound pressure spectral densities of Fig. 1. Ideal filters: Air temperature of 25° C; relative humidity of 70%; air pressure of 1.0 standard atmosphere. Propagation distances as noted. Attenuation by atmospheric absorption only: no spreading loss. .	22
4.	1/3-octave-band sound pressure levels, LR, at the receiver for the same condition as for Fig. 3, except a relative humidity of 10% instead of 70%	23
5.	Attenuation (difference due to atmospheric absorption between band levels at the source, LS, and band levels at the receiver, LR) as a function of frequency and propagation distance. Two relative humidities and band-level source spectrum slopes. Air temperature is 25° C; air pressure is 1.0 standard atmosphere. Ideal filters. No geometric spreading loss.	24
6.	True or exact band-level adjustment factor as a function of frequency and propagation distance. Difference in band level at the receiver under simulated reference and test atmospheric conditions [(LR at 70% relative humidity) - (LR at 10% relative humidity)]. Air temperature is 25° C; air pressure is 1.0 standard atmosphere. Ideal filters.	26
7.	Hypothetical spectrum of aircraft noise.	29
8.	Comparison of band-slope estimating procedures for certain bands from hypothetical aircraft noise spectrum of Fig. 7.	31
9.	Illustrations of straight-line approximations to sound pressure spectral density $G_R(f)$ with slopes ℓ^L and ℓ^U over passband of ideal filter with band center frequency f_c	33
10.	Example of determination of (1) attenuation, (2) accuracy of approximate band-integration method of calculating atmospheric absorption, and (3) exact band-loss adjustment factor from test (10% relative humidity) to reference (70% relative humidity) meteorological conditions. Air temperature is 25° C; air pressure is 1.0 standard atmosphere; spectral slope at the source is -12 dB/band; ideal filters; sound propagation pathlength is 600 m; no geometric spreading loss	35

Figure Page

11. Illustration of ability to accurately calculate atmospheric absorption over a sound propagation path using band sound pressure levels at the receiver. Calculated band levels at the source are compared with known, exact band levels at the source for three sound propagation pathlengths, two slopes for the pressure spectrum of the sound at the source, and two relative humidities. Air temperature is 25° C; air pressure is 1.0 standard atmosphere. Sound spectrum at the receiver is approximated by band-level slopes over the lower and upper halves of the passband of ideal 1/3-octave-band filters. Absorption over the propagation path is calculated by integration over filter passband. 36

12. Similar comparisons of ability to accurately calculate atmospheric absorption over a sound propagation path as in Fig. 11, except that absorption factor for band sound pressure level is determined only at the center frequency of the ideal filters instead of by integration over the frequency range of the passband. Air temperature is 25° C; air pressure is 1.0 standard atmosphere 39

13. Example of determination of exact and approximate band-loss adjustment factors for differences in atmospheric absorption under test (10% relative humidity) and reference (70% relative humidity) conditions. Air temperature is 25° C; air pressure is 1.0 standard atmosphere; spectral slope at the source is -12 dB/band; ideal filters; sound propagation pathlength is 600 m; no geometric spreading loss 42

14. Comparison of approximate and exact band-loss adjustment factors for ideal filters. Difference in source levels ($LS_{10,10} - LS_{70,10}$) calculated from receiver levels, LR_{10}, determined for 10% relative humidity (test-day conditions) assuming first 10 and then 70% relative humidity (reference-day conditions), compared with difference in receiver levels ($LR_{70} - LR_{10}$) for 70 and 10% relative humidity. Air temperature is 25° C; air pressure is 1.0 standard atmosphere. Three sound propagation pathlengths; two true slopes for the sound spectrum at the source; and two approximate methods for calculating atmospheric absorption: integration over filter passband and absorption at band center frequency, f_c, only . . . 43

15. Power transmission response of 1/3-octave-band filters 48

16. Transmission-loss response characteristics of 1/3-octave band filters in real time analyzers compared with response calculated from "practical-filter" transmission-response equation; f_c is band center frequency. 51

Figure Page

17. Power spectra of the sound pressure at the source for calculations of band levels at the receiver with 'practical' rather than ideal filters. 53

18. Effect of filter characteristics on band level at the receiver for various slopes of the sound pressure level spectrum at the source. 300-m sound propagation pathlength; 70% relative humidity; 25° C air temperature; 1.0 standard atmosphere air pressure. 58

19. Same as Fig. 18, except 10% relative humidity. 60

20. Effect of filter transmission response characteristics on band level at the receiver for three sound propagation pathlengths, two relative humidities, and a slope of the sound pressure level spectrum at the source of +1 dB/band. 25° C air temperature; 1.0 standard atmosphere air pressure. . . 64

21. Same as Fig. 20, except slope of sound pressure level spectrum at the source is -12 dB/band. 65

22. Determination of band-loss adjustment factors when band levels at the receiver location are calculated with the filter transmission-response characteristics of the practical filters from Fig. 15; compare with results for ideal filters in Fig. 13. 69

23. Comparison of band-loss adjustment factors, calculated at band center frequency, f_c, only and calculated by integration over passband of ideal filter, for receiver band levels determined with practical-filter transmission-response characteristics. Compare with Fig. 14 for receiver levels determined with ideal filters. See Fig. 22 for definition of terms. 25° C air temperature; 1.0 standard atmosphere air pressure. Three sound propagation pathlengths, two sound pressure spectrum slopes at the source. . 72

24. Measured vertical profiles of air temperature and relative humidity for test cases; also profiles of difference between atmospheric absorption coefficient by SAE ARP866A at 3150 Hz at height and at 10 m height. 104

25. Measured vertical profiles of molar concentration of water vapor for test cases; reference molar concentration of water vapor at 25° C, 70-percent relative humidity, and one standard atmosphere of air pressure is 2.18774 percent. 110

26. Geometrical relationships between aircraft and microphone at different relative times during a flyover. 115

Figure		Page
27.	Definition of quantities used in calculating angles ϕ, η, and ψ; sound propagation distance PD; and aircraft height above the microphone height at the time of sound emission AHS.	117
28.	Illustration of procedure for calculating incremental distances, along sound propagation path of length PD from R to E, which correspond to heights HM(K) where meteorological data were measured	119
29.	Illustration of rules for calculating band-level differences . .	134
30.	Substitute slopes for 1/3-octave-band levels of broadband aircraft noise in the free field	136
31.	Variation of normalized PNLT and AL with time during a DC-9-14 flyover, from run 272	142
32.	Variation of normalized PNLT and AL with time for the Raisbeck-Learjet, run 12	150
33.	Aircraft sound pressure level spectra at the time of occurrence of the maximum test-time tone-corrected perceived noise level, $PNLTM_{test}$	152
34.	Pure-tone atmospheric sound absorption coefficients by ANSI S1.26-1978 and SAE ARP866A	156
35.	Band sound-pressure-level adjustment factors at the time of $PNLTM_{test}$ for DC-9-14 runs at nearly-equal sound propagation distances, PD, and emission angles, ψ, but different meteorological conditions along the sound path	160
36.	Illustration, for DC-9-14 runs 272 and 358, of difference between reference-day sound pressure levels calculated by adjustment procedures (2) and (3). Propagation distances and sound emission angles are for the time of $PNLTM_{test}$	168
37.	Band sound pressure level adjustment factors at the time of $PNLTM_{test}$ and of ALM_{test} for DC-9-14 run 374, PD = 369.4 m, $\psi = 113.1^{\circ}$	170
38.	Sound pressure level spectra for test and reference meteorological conditions from DC-9-14 runs 358 and 374 at nearly equal sound-emission angles but different propagation distances	173
39.	For nominally equal sound-emission angles (110.5° and 113.1°), illustration of effect of choice of atmospheric-absorption model on ability to extrapolate reference-day SPLs	177

Figure Page

40. Band sound-pressure-level adjustment factors at the time of $PNLTM_{test}$ and of ALM_{test} for Raisbeck-Learjet, run 12, PD = 1925.7 m, ψ = 135.2°. 181

41. Sound-pressure-level spectra for test and reference meteorological conditions for Raisbeck-Learjet at time of $PNLTM_{test}$ or ALM_{test}, run 12, PD = 1925.7 m, ψ = 135.2°. 185

42. Test-to-reference-day adjustment factors by the four adjustment procedures for PNLT and AL for DC-9 test cases (runs 272 to 378) and Learjet (run 12) 196

TABLES

Number		Page
1.	Description of aircraft used for test cases.	98
2.	Test and airplane parameters	100
3.	Meteorological conditions for test cases	103
4.	Engine/airplane parameters for DC-9 runs	145
5.	Measured and approximate duration factors for EPNL and SEL . . .	148
6.	Comparison of results from present study with those from Ref. 25 for five DC-9 runs.	189
7.	Comparison of test-time quantities calculated by BBN and by present study (P. S.) for data obtained from BBN	192
8.	Summary of frequency-weighted and time-integrated noise levels for DC-9 and Learjet test cases where meteorological data aloft were measured	194
9.	Summary of frequency-weighted and time-integrated noise levels for 727, HS-748, and Beech Debonair test cases where only surface meteorological data were measured	195

METRIC CONVERSION FACTORS

Approximate Conversions to Metric Measures

Symbol	When You Know	Multiply by	To Find	Symbol
		LENGTH		
in	inches	*2.5	centimeters	cm
ft	feet	30	centimeters	cm
yd	yards	0.9	meters	m
mi	miles	1.6	kilometers	km
		AREA		
in^2	square inches	6.5	square centimeters	cm^2
ft^2	square feet	0.09	square meters	m^2
yd^2	square yards	0.8	square meters	m^2
mi^2	square miles	2.6	square kilometers	km^2
	acres	0.4	hectares	ha
		MASS (weight)		
oz	ounces	28	grams	g
lb	pounds	0.45	kilograms	kg
	short tons (2000 lb)	0.9	tonnes	t
		VOLUME		
tsp	teaspoons	5	milliliters	ml
Tbsp	tablespoons	15	milliliters	ml
fl oz	fluid ounces	30	milliliters	ml
c	cups	0.24	liters	l
pt	pints	0.47	liters	l
qt	quarts	0.95	liters	l
gal	gallons	3.8	liters	l
ft^3	cubic feet	0.03	cubic meters	m^3
yd^3	cubic yards	0.76	cubic meters	m^3
		TEMPERATURE (exact)		
°F	Fahrenheit temperature	5/9 (after subtracting 32)	Celsius temperature	°C

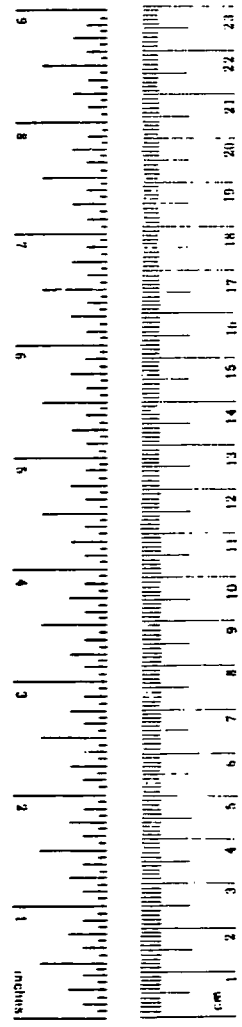

Approximate Conversions from Metric Measures

Symbol	When You Know	Multiply by	To Find	Symbol
		LENGTH		
mm	millimeters	0.04	inches	in
cm	centimeters	0.4	inches	in
m	meters	3.3	feet	ft
m	meters	1.1	yards	yd
km	kilometers	0.6	miles	mi
		AREA		
cm^2	square centimeters	0.16	square inches	in^2
m^2	square meters	1.2	square yards	yd^2
km^2	square kilometers	0.4	square miles	mi^2
ha	hectares (10,000 m^2)	2.5	acres	
		MASS (weight)		
g	grams	0.035	ounces	oz
kg	kilograms	2.2	pounds	lb
t	tonnes (1000 kg)	1.1	short tons	
		VOLUME		
ml	milliliters	0.03	fluid ounces	fl oz
l	liters	2.1	pints	pt
l	liters	1.06	quarts	qt
l	liters	0.26	gallons	gal
m^3	cubic meters	35	cubic feet	ft^3
m^3	cubic meters	1.3	cubic yards	yd^3
		TEMPERATURE (exact)		
°C	Celsius temperature	9/5 (then add 32)	Fahrenheit temperature	°F

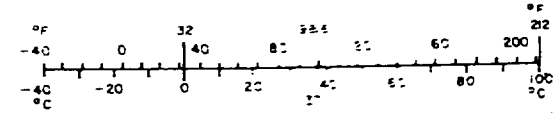

ACKNOWLEDGMENT

It is a pleasure to acknowledge the many helpful suggestions and constructive comments provided by the author's colleague Dr. Robert L. Chapkis.

EVALUATION OF ALTERNATIVE PROCEDURES FOR ATMOSPHERIC ABSORPTION ADJUSTMENTS DURING NOISE CERTIFICATION

VOLUME I: ANALYSES AND RESULTS

1. INTRODUCTION

To certify the noise of an aircraft, the only approved procedure for adjusting measured sound pressure levels for differences between atmospheric absorption under test and acoustical-reference conditions uses the method in the Society of Automotive Engineers (SAE) Aerospace Recommended Practice ARP866A for calculating atmospheric sound absorption coefficients. That atmospheric-absorption model was developed by the SAE A-21 Committee in 1962 and 1963 and published in 1964. It was re-issued in 1975 as ARP866A[1] and is used to adjust from test-to-reference conditions in Part 36 of the Federal Aviation Regulations (FAR36) and in Annex 16 to the International Standards and Recommended Practices of the International Civil Aviation Organization. ARP866A is also incorporated in International Standard IS 3891 as part of the procedure recommended by the International Standards Organization for describing noise around an airport.

The American National Standard Method for the Calculation of the Absorption of Sound by the Atmosphere, ANSI S1.26-1978,[2] was published in 1978. It contains a series of equations that permit calculation of the atmospheric sound absorption coefficient for a pure-tone sound with a frequency between 40 and 1,000,000 Hz (at an air pressure of one standard atmosphere). The equations are stated to be applicable for air temperatures between 0° and 40° C, relative humidities between 10 and 100 percent, and air pressures less than 2 atmospheres. The analytical expressions that form the basis for the calculation method were validated by laboratory tests[3] over a wide range of atmospheric conditions and frequencies, specifically frequencies from 4000 to 100,000 Hz at 1/12-octave intervals, temperatures from -17.8° C to +37.8° C at 5.6° C intervals, and relative humidities from 0 to 100 percent at 10-percentage-point intervals.

The analytical model in ARP866A for atmospheric absorption is based on aircraft flyover noise data and an earlier and less-complete theoretical understand-

ing of the various physical mechanisms than the analytical model in ANSI S1.26. In ARP866A the analytical model is applied to broadband sound spectra analyzed by 1/3-or 1/1-octave-band filters without regard for spectral shape or propagation distance. Attenuation over a pathlength is calculated by determining an absorption coefficient (at a particular frequency) and multiplying by the distance. The nominal band center frequency is used for calculations at center frequencies to 4000 Hz. To allow for the rapid high-frequency spectral rolloff rate often encountered in measurements of aircraft noise, absorption coefficients for 1/3-octave bands with center frequencies from 5000 to 10,000 Hz are calculated using the nominal lower bandedge frequency for those bands.

Section 5 of ANSI S1.26-1978 provides general guidance on how to apply the pure-tone calculation method of the Standard to the problem of calculating the absorption loss experienced by a sound with energy distributed over a wide frequency range and analyzed by fractional-octave-band filters. It recommends evaluation of a pair of integrals over a range of frequency for each band. The pressure spectral density of the sound must be known. Additional guidance is given in Appendix E of the Standard regarding a method for numerically evaluating the integrals of Section 5 when it is necessary to consider the power transmission response of practical 1/3-octave-band filters and when the pressure spectral density of the sound at the beginning of the propagation path can be approximated by a function proportional to frequency to some power.

A study[4] was conducted for the FAA in 1977 to develop a digital computer program, in the extended FORTRAN IV programming language, that was capable of calculating adjustment factors to be applied to 1/3-octave-band sound pressure levels to account for differences in atmospheric absorption losses experienced under test and reference meteorological conditions over an assumed sound propagation path. The program computed pure-tone atmospheric absorption losses by the method in the then-proposed, but essentially final, version of ANSI S1.26-1978. The integrals were numerically evaluated by the approximation scheme outlined in Appendix E of the Standard and, in more detail, in Ref. 3. The pressure spectral density of the sound at the microphone was estimated by a simple power function over the theoretical bandwidth of 1/3-octave-band filters. The slope ℓ of the line

(or the exponent of the normalized frequency, normalized by the exact band geometric mean frequency, f_c) was obtained from the difference between the level in the band below and the level in the band above the band of interest. Thus, at a general frequency f_j, the pressure spectral density was proportional to $(f_j/f_c)^{\ell}$.

The numerical integration procedure developed for the computer program in the 1977 study[4] used the procedure described in Refs. 2 and 3 for approximating the frequency dependence of atmospheric absorption by a power function $(f_{j+1}/f_j)^K$ over small ranges of logarithmically spaced frequency from f_j to f_{j+1}. With those approximations for the absorption function and the sound pressure spectral density, the general integral expression could be replaced by a summation of integrals each of which could be integrated exactly in closed form.

The power transmission response of the 1/3-octave-band filters was assumed in Ref. 4 to be that of ideal filters because the objective of the analysis and the computer program was to start with 1/3-octave-band sound pressure levels measured at some receiver location and to calculate an adjustment factor to be added to the measured band levels in order to determine what the band levels would have been had the sound propagated through an atmosphere with acoustical-reference meteorological conditions rather than the actual meteorological conditions existing on the day when the band levels were measured. The assumption that the filter response was that of an ideal filter was considered to be most appropriate for that problem.

The assumption of ideal filter-transmission characteristics was justified on the grounds that (1) the pressure spectral density has to be estimated from measured band levels, (2) there is no unique, one-to-one relationship between a set of measured band levels and the true pressure spectral density of the sound that impinges on the microphone, and (3) there is no way of knowing how much, if any, the indicated band-level value is influenced by energy transmitted in the stopband frequency ranges due to inadequate filter-rejection capability.

The assumption of ideal filters was also considered to be consistent with the other assumptions regarding the approximation of the absorption function, the adequacy of the number of horizontal layers into which the atmosphere had been subdivided and over which test-day meteorological conditions could be assumed to be constant, and the length of the sound propagation path. The sound propagation path was assumed to be a single straight line from an equivalent source location to the microphone, neglecting any bending (refraction) of the direction of propagation as a result of temperature gradients or winds. The aircraft was assumed to be always far enough away that the various complex noise sources could be replaced by a single equivalent acoustic source located at an aircraft reference point. The true pressure spectral density of the aircraft noise signal was assumed to be continuous with no pure-tone components.

Given those assumptions, the atmospheric absorption model of ANSI S1.26-1978 was applied, using the specific numerical integration method described above, to calculate band adjustment factors for differences between atmospheric absorption losses under test-day and acoustical-reference-day meteorological conditions. The method was applied to 1/3-octave-band sound pressure levels from simulated level-flight aircraft flyover noise measurements. Each set of 24 levels was assumed to be complete with no band levels missing because of contamination by high-level background noise. Two test cases with different spectral shapes, propagation pathlengths, and test-day meteorological conditions were examined as a means of checking out the computer program and illustrating the magnitude of the band-adjustment factors.

The scope of the 1977 study in Ref. 4 was limited, as indicated above, essentially to the development of a computer program to use the atmospheric absorption model of ANSI S1.26-1978 and to implement the general recommendations of the standard regarding the calculation of atmospheric absorption loss for a band of noise. To satisfy the limited objective, it was not necessary to include the capability of examining 1/3-octave-band sound pressure levels at 0.5-s intervals throughout a flyover, or to calculate any psychoacoustical measures, or to develop a method of estimating pressure spectral density functions when a complete set of 24 band levels (for center frequencies from 50 to 10,000 Hz) was not available because of contamination by background

noise, or to evaluate differences between the method and alternative methods of calculating absorption-loss adjustment factors. However, the program that was developed did consider the problem of calculating absorption losses over segments of the sound propagation path through horizontal layers of the atmosphere defined by the heights where meteorological data were measured.

Paragraph (d)(2) of Section A36.9 of Appendix A of FAR 36[5] requires use of a "layered-atmosphere" procedure for calculating atmospheric-absorption adjustment factors when the atmospheric-absorption coefficient at 3150 Hz over the sound propagation path from the aircraft to the microphone varies by more than ± 0.23 dB/100 m from the value calculated using the air temperature and relative humidity measured near the microphone at a height of 10 m above the ground surface at the time of the measurement. The layered-atmosphere procedure requires that the atmosphere be divided into horizontal strata no thicker than 30.5 m (100 ft). The average air temperature and relative humidity must be computed for each layer from measurements made as a function of height above the ground surface within 25 minutes of the noise measurement and interpolated to the time of the measurement. The average temperatures and relative humidities must be used to calculate average absorption coefficients for each layer. An average attenuation rate over the total propagation path must be calculated from the ratio of the sum of the attenuations over the segments of the path to the total propagation pathlength. That average attenuation rate (instead of the rate calculated simply from the air temperature and relative humidity measured at the 10 m height) must then be used in making the absorption adjustments in accordance with Paragraph (d) of Section A36.11 of Appendix A. All absorption coefficients are to be calculated using SAE ARP866A-1975.

The purpose of the study described in this report was to employ actual, measured aircraft noise and accompanying meteorological data in a comparative evaluation of different procedures for determining test-day-to-reference-day atmospheric-absorption-loss adjustment factors. The study required further development and extension of the digital computer program reported in Ref. 4. The revised program can perform all the additional tasks noted above as being outside the scope of the Ref. 4 program.

Four alternative procedures for calculating 1/3-octave-band atmospheric-absorption adjustment factors were included in the study. They were

- absorption coefficients and band attenuation by SAE ARP866A-1975 and meteorological data measured only at 10 m
- absorption coefficients and band attenuation by SAE ARP866A-1975 a layered-atmosphere analysis using meteorological data measured at various heights
- absorption coefficients by ANSI S1.26-1978, a band-integration method to calculate attenuation, and a layered-atmosphere analysis using meteorological data aloft
- absorption coefficients by ANSI S1.26-1978, attenuation calculated at the band center frequencies only, and a layered-atmosphere analysis using meteorological data aloft.

The report is organized into three Volumes. Volume I describes the analyses that were performed and presents the results. Volume II contains the listing of the statements for the computer program, the input data for a sample test case, and the corresponding output listings. Volume III supplements the information in Volumes I and II with extensive tables of the attenuation caused by atmospheric absorption over a 300-m path. Attenuation values are computed for five methods for each of 340 combinations of 34 air temperatures and 10 relative humidities. The tables permit a variety of comparative analyses of the differences between the analytical atmospheric-absorption models of ANSI S1.26-1978 and SAE ARP866A-1975 and between the attenuation at the band center frequency for a pure-tone sound and the attenuation for broadband sounds with constant slopes of +1, -6, and -12 dB/band.

The analyses and results presented here in Volume I are contained in Sections 2-4. Sections 2 and 3 describe the results of an analytical study of the effects of different atmospheric conditions and 1/3-octave-band filter-transmission-response characteristics on the calculation of atmospheric-absorption adjustment factors for broadband sound. The magnitude of the errors that can occur in the values of the band levels at a distant receiver, and the values of the band levels when adjusted from test to reference conditions, are calculated for practical filters meeting the minimum transmission-loss

requirements of ANSI S1.11-1966 for Class III filters.[6] The accuracy of determining atmospheric-absorption adjustment factors is demonstrated for band-integration and band-center-frequency methods.

Section 4 describes the basis for the new computer program for calculating atmospheric-absorption band-adjustment factors. The program was used to evaluate the differences among the four procedures described above for calculating band-adjustment factors. Evaluations are presented in terms of perceived noise level, tone-corrected perceived noise level, effective perceived noise level, A-weighted sound level, and sound exposure level for each of the four procedures for nine sets of actual aircraft flyover noise measurements from jet- and propeller-powered aircraft.

Conclusions concerning the alternative procedures for determining atmospheric absorption losses during an aircraft noise-certification test are drawn from the analyses in Sections 2 to 4 and presented in Section 5.

2. EFFECTS OF ATMOSPHERIC CONDITIONS ON CALCULATIONS OF ABSORPTION-ADJUSTMENT FACTORS FOR BROADBAND SOUND

Evaluation of alternative procedures for determining band-adjustment factors for atmospheric-absorption losses was performed in two phases. The first phase consisted of analyses to show the validity, or need for refinement, of the band-adjustment method of Ref. 4. The second phase included development of a new computer program and evaluation of four alternative procedures for adjusting various aircraft noise signals from test to reference atmospheric conditions. This Section discusses the analyses that were conducted for the first part of the first phase for which the filters were assumed to have ideal transmission-response characteristics.

The most-critical issue in developing any method for determining band-adjustment factors to account for atmospheric-absorption losses is how to obtain a good estimate of the true pressure spectral density of the sound that impinged on the microphone. For this reason, the original plan for assessing the validity of the method of Ref. 4 to account for atmospheric-absorption losses was to obtain a narrow-band analysis of samples of aircraft-noise measurements for which 1/3-octave-band sound pressure levels and test-day meteorological data were also available.

Narrow-band analyses were obtained at three different times (before, near, and after the time of maximum overall sound pressure level) during the duration of a recording of the flyover noise signals from four aircraft. The four aircraft represented jet- and propeller-powered airplanes and consisted of a Boeing 727-100 commercial jet transport, a Raisbeck-modified Gates Learjet business/executive jet, a Hawker-Siddely HS-748 twin-turboprop transport, and a Beech Debonair single-engine, propeller-powered, general-aviation airplane.

A digital signal processor was used to obtain the narrow-band analyses. The upper limit of the frequency range was set to 9000 Hz giving a rate for sampling the analog signal from the tape recorder of 18,432 samples/second. The processor was set to per form a single-length Fourier

transform with 1024 data samples needed to complete one block of data. The time required to fill the memory of the input buffer for one block of data was then 1024/18,432 = 55.56 ms.

There were 500 frequency resolution points in the frequency range for the 1024-point block of sampled data. The 500 points, then, meant that there was an 18-Hz nominal spacing between the frequency components in the spectrum analysis from 0 to 9000 Hz. The effective bandwidth around each spectral component at the 18-Hz spacing was approximately 32 Hz because of the use of the rounded, cosine-squared Hanning function for time-limiting (or time-weighting) in the fast-Fourier-transform algorithm.

The statistical confidence of the narrow-band spectra was increased by averaging eight consecutive 55.56-ms blocks of data to give an ensemble average with an effective averaging time of about 444 ms. This ensemble averaging time is close to the averaging time used in 1/3-octave-band real-time analyzers that provide data at nominal 500-ms intervals.

Although considerable effort was devoted to obtaining the narrow-band spectra, the results were disappointing. The 60-to-70-dB dynamic range of the instruments (microphone, tape recorder, and digital signal processor), and the relatively high level of high-frequency background noise (instrument noise plus ambient noise) with typical values between 15 to 20 dB for the equivalent 32-Hz-bandwidth sound pressure levels at frequencies above 3000 Hz, combined to eliminate any useful data above 2500 to 4000 Hz. Furthermore, the narrow-band spectrum was not at all smooth and would have been difficult to interpret even if the background levels had been lower. Attempts to use narrow-band spectra to obtain a better approximation to the true sound pressure spectral density were therefore abandoned.

Because the narrow-band spectral approach had to be abandoned, it was necessary to develop an alternative procedure for assessing the validity of a 1/3-octave-band atmospheric-absorption adjustment method. The alternative procedure started with a specification for the power spectrum of the sound pressure at an equivalent source location. The power spectrum at a distant receiver location was then calculated for an atmosphere with acoustical

reference conditions and for atmospheric conditions yielding a very high rate of atmospheric absorption. One-third-octave-band sound pressure levels at the receiver location were calculated for filters having ideal transmission-response characteristics. The calculated band levels at the receiver were used to find band-adjustment factors. Comparison with what the adjustment factors should have been (values which were known exactly since the true spectrum was known at the source and at the receiver) gave a measure of the accuracy of the calculation methods. The results are presented in a series of spectral plots that assess the effects of atmospheric conditions, propagation distance, and adjustment-factor calculation method.

Spectra at the Source

The analysis began with a set of assumed broadband power spectra for the sound pressure at the location of the source.

For convenience, the spectrum was assumed to be a simple power function of frequency as

$$G_S(f) = |G_S(f_c)| \, (f/f_c)^{\ell^S} \qquad (1)$$

where $G_S(f)$ is the sound pressure spectral density at any frequency f, $G_S(f_c)$ is the pressure spectral density at some particular frequency f_c (which later will be taken to be the exact center frequency of a 1/3-octave band), and ℓ^S is the slope of the straight line that represents the spectrum on logarithmic scales.

The exact 1/3-octave-band sound pressure levels, LS, at the source are found from

$$LS(f_c) = 10 \log \left\{ \left[\int_{f_L}^{f_U} G_S(f) \, df \right] / p_{ref}^2 \right\} \qquad (2)$$

where the numerator term represents the mean-squared pressure at the source in the band at f_c, and f_L and f_U are the exact lower and upper bandedge frequencies that represent the limits of integration over the passband of the filter. The filter, by definition, has ideal transmission-response characteristics around the exact band center frequency f_c. The sound pressure levels have units of decibels and are calculated relative to a reference pressure, p_{ref} = 20 μPa.

With Eq. (1) for the power spectrum, the band levels at the source can be calculated exactly from Eq. (2) as

$$LS(f_c) = 10 \log \left\{ \int_{f_L}^{f_U} [G_S(f_c)] \, (f/f_c)^{\ell^S} \, df \right\}$$

$$- 10 \log p_{ref}^2$$

$$= 10 \log \int_{f_L}^{f_U} (f/f_c)^{\ell^S} \, df$$

$$+ 10 \log G_S(f_c) - 10 \log p_{ref}^2 \qquad (3)$$

where the constant, $G_S(f_c)$, has been taken outside the integral.

The integral term in Eq. (3) can be evaluated as

$$\int_{f_L}^{f_U} (f/f_c)^{\ell^S} \, df = f_c \, [1/(\ell^S + 1)] [(f_U/f_c)^{\ell^S + 1} - (f_L/f_c)^{\ell^S + 1}] \qquad (4)$$

when $\ell^S \neq -1$, and

$$= f_c \ln (f_U/f_L) \qquad (5)$$

when $\ell^S = -1$.

For a constant-slope spectrum, the slope, ℓ^S, of the pressure spectral density (log $G_S(f)$ *vs* log f) can be readily related to the slope of the sound pressure level spectrum (LS (f_c) *vs* band center frequency). The relationship is given by

$$\ell^S = SL - 1 \qquad (6)$$

where SL is the band-level slope in dB/band.

The ratio of bandedge frequencies, f_U/f_L, for ideal filters is a constant which was given the symbol RF in Ref. 4. The band center frequency is the geometric mean of f_U and f_L and thus

$$f_U/f_L = RF \tag{7}$$

$$f_U/f_c = RF^{1/2} \tag{8}$$

and

$$f_L/f_c = RF^{-1/2}. \tag{9}$$

The frequency ratio RF is specified in applicable standards[6] for filters. For 1/3-octave-band filters, the exact ratio is

$$RF = 10^{1/10}. \tag{10}$$

The exact band-center frequency is found from

$$f_c = 10^{ISBN/10} \tag{11}$$

where ISBN represents the set of International Standard Band Numbers[6] for the filters. For 1/3-octave-band filters, the values of ISBN range from 17 to 40 for nominal band center frequencies ranging from 50 to 10,000 Hz.

With Eqs. (6) to (9), the expressions in Eqs. (4) and (5) can be written in a more-convenient form as

$$\int_{f_L}^{f_U} (f/f_c)^{\ell^S} df = (f_c/SL)(RF^{SL/2} - RF^{-SL/2}) \tag{12}$$

when $\ell^S \neq -1$ or $SL \neq 0$, and

$$= f_c \ln (RF) \tag{13}$$

when $\ell^S = -1$ or $SL = 0$.

The spectrum of the sound pressure at the source [Eqs. (1) or (3)] can be calculated once the slope, ℓ^S of SL, is specified and some value is assigned for $G_S(f_c)$ at some frequency f_c. For convenience, the value of 10^6 Pa^2/Hz was chosen at $f_c = 1000$ Hz, i.e.,

$$G_S (1000) = 10^6 \ Pa^2/Hz, \tag{14}$$

in order to provide values for band levels at the source that were consistent with reasonable values for corresponding band levels at a distant receiver location.

Making use of the various terms defined above, the expression for the band level at the source for the 1000-Hz center frequency becomes

$$LS(1000) = 10 \log G_S(1000) + 10 \log 1000 - 10 \log p_{ref}^2$$

$$+ 10 \log [(1/SL)(RF^{SL/2} - RF^{-SL/2})]$$

$$= 190.0 - 10 \log 4 + 10 \log [(1/SL)(RF^{SL/2} - RF^{-SL/2})] \quad (15)$$

when $SL \neq 0$, and

$$LS(1000) = 190.0 - 10 \log 4 + 10 \log (\ln (RF)] \quad (16)$$

when $SL = 0$.

Band levels at higher center frequencies are found by successive addition of the band-level slope SL. Note that, for a white-noise spectrum with SL = +1 dB/band, the third term in Eq. (15) reduces to the relative bandwidth of an ideal filter which, for 1/3-octave-band filters, is given exactly by

$$RF^{1/2} - RF^{-1/2} = 10^{1/20} - 10^{-1/20} = 0.23077$$

giving

$$LS(1000) = 177.6 \text{ dB}$$

in the 1000-Hz band for SL = 1 and $G_S(1000) = 10^6$ Pa^2/Hz.

Figures 1 and 2 show spectral plots for $G_S(f)$ and $LS(f_c)$ calculated from the above equations using band-level slopes of +1, -3, -6, and -12 dB/band. The slope SL = +1 dB/band corresponds to a white-noise spectrum with $\ell^S = 0$. Negative values for the other slopes were chosen for the example because most aircraft noise sources have a spectrum that decreases with increasing frequency at high frequencies. The frequency range covered by the eleven 1/3-octave bands with center frequencies between 1000 and 10,000 Hz was chosen as representing the frequency range of most interest to atmospheric absorption studies for propagation outdoors.

The next step was to calculate the band levels at receiver locations for different atmospheric conditions and then to use the receiver levels to attempt to reproduce the known source levels in Fig. 2.

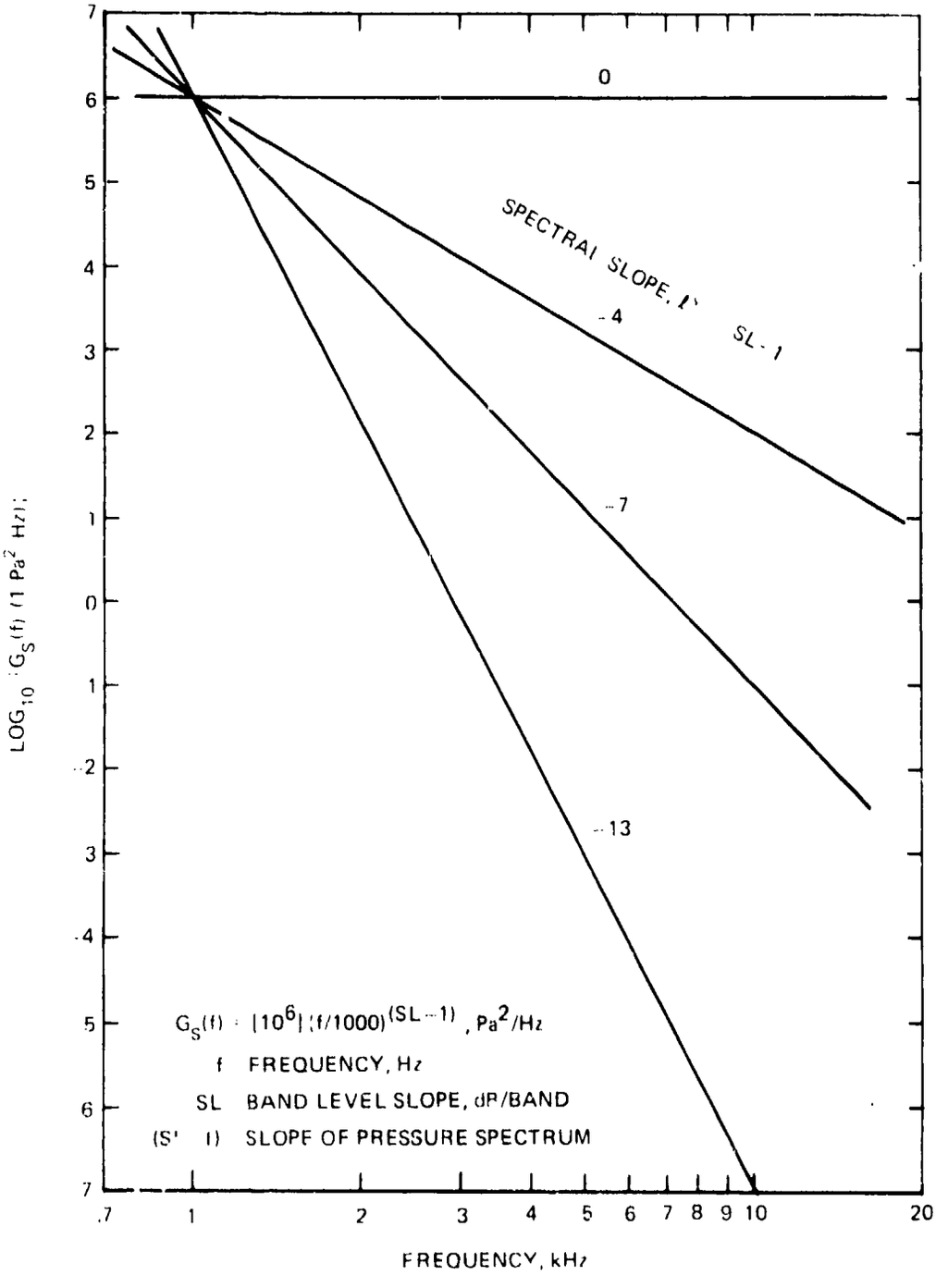

Figure 1.-Power spectra, $G_S(f)$, of the sound pressure at the source for several spectral slopes.

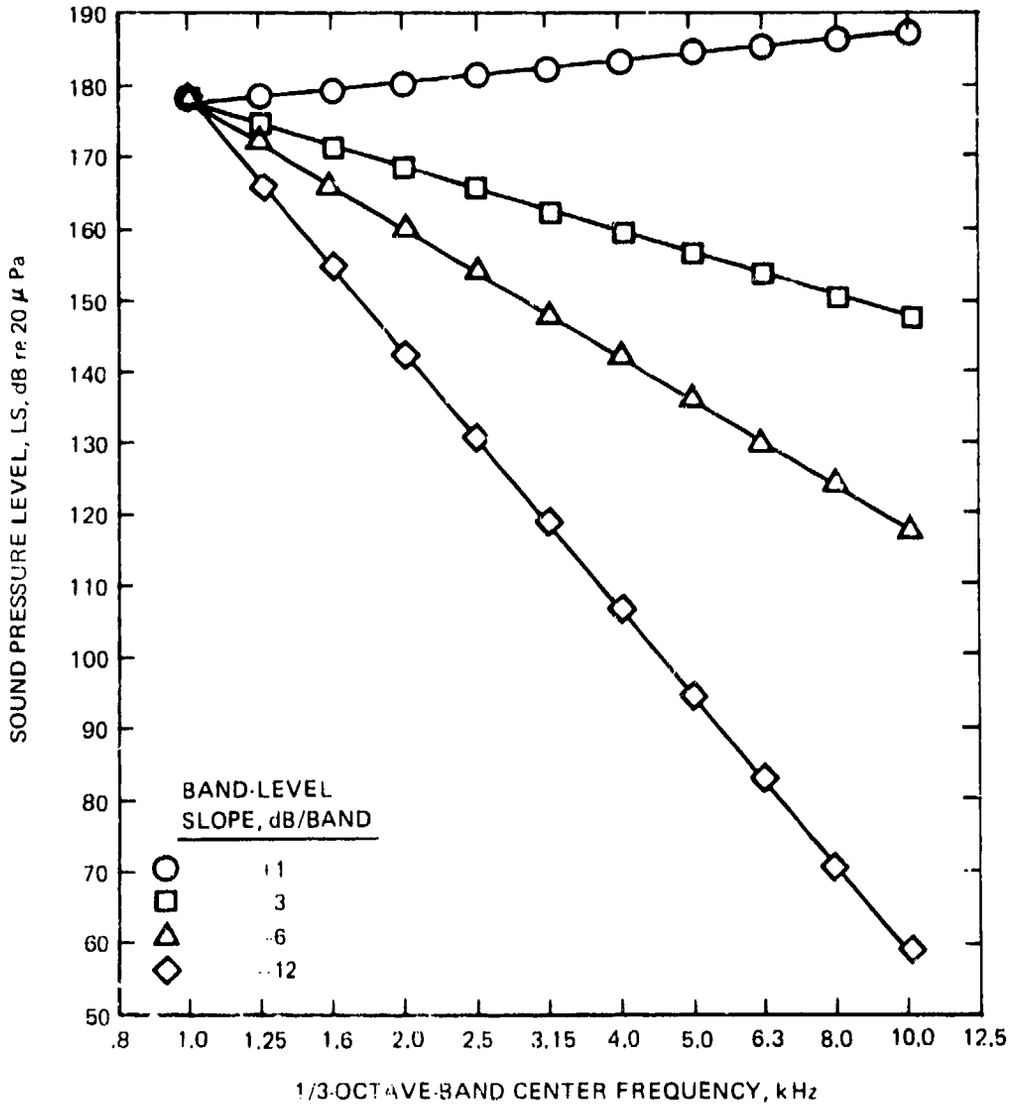

Figure 2.-1/3-octave-band sound pressure levels, LS, at the source for sound pressure spectral densities of Fig. 1 and ideal filters.

Spectra at the Receiver

Neglecting the reduction in the amplitude of the pressure caused by spreading the acoustic power over increasingly larger surfaces as the sound propagates through the atmosphere to the receiver, the general expression for the pressure spectrum at the receiver relative to that at the source is

$$G_R(f) = [G_S(f)][AF^-(f)] \tag{17}$$

where $AF^-(f)$ represents the atmospheric-absorption function applicable to the meteorological conditions over the sound propagation path and the length of the path. The minus sign in the superscript indicates propagation from the source to the receiver. For the analysis here, the model in ANSI S1.26-1978 was used to calculate atmospheric absorption at a specified frequency. The power spectrum of the pressure at the source, $G_S(f)$, was found from Eqs. (1) and (14) for the example considered here, although it could have any other desired functional dependence on frequency.

By analogy to Eq. (2), the exact band levels, LR, at the receiver were found from

$$LR(f_c) = 10 \log \left\{ \left[\int_{f_L}^{f_U} G_R(f)\, df \right] / p_{ref}^2 \right\} \tag{18}$$

where the range of integration has again been restricted to f_L to f_U for ideal filters because the exact values of the band levels at the receiver are those that would be measured with filters having ideal response characteristics. The next section discusses the magnitude of the problems that result from using practical filters having non-ideal transmission-response characteristics.

Using the form of Eq. (17), the expression for the band levels becomes

$$LR(f_c) = 10 \log \left\{ \left[\int_{f_L}^{f_U} [G_S(f)][AF^-(f)]\, df \right] / p_{ref}^2 \right\} \tag{19}$$

If the sound propagation path can be considered to be divided into k segments over which the temperature, humidity, and pressure of the air can be assumed to be constant, then, as shown in Refs. 3 and 4, the absorption

function can be expressed as

$$AF^{-}(f) = 10^{-\sum_k a_k \ell_k / 10} \tag{20}$$

where a_k is the atmospheric sound absorption coefficient over the k-th path segment at frequency f, in, say, decibels per meter, and ℓ_k is the length of one of the segments of the propagation path in meters.

Because $AF^{-}(f)$ has a complicated, though smooth and continuous, dependence on frequency, Eq. (19) must, in general, be evaluated numerically. Note also that the attenuation due to atmospheric absorption is not independent of the length of the propagation path because the pure-tone absorption coefficient and the length of a propagation-path segment are linked as a product in Eq. (20). The pathlength, therefore, cannot be taken outside the integral in Eq. (19). As a consequence, the concept of an absorption coefficient is not strictly applicable to broadband noise analyzed by passband filters except in the sense of a total attenuation rate over the total pathlength, where the pathlength as well as the atmospheric conditions and band center frequency must be stated.

For the purpose of demonstrating the validity of a method for adjusting measured band levels from test to reference conditions, the meteorological conditions of the atmosphere were assumed to be constant over the total propagation path. Thus, the absorption function of Eq. (20) reduced to

$$AF^{-}(f) = 10^{-[a(f)][PD/10]} \tag{21}$$

where a(f) is determined in decibels per meter for any frequency f by the equations in ANSI S1.26-1978 and PD is the propagation distance in meters.

With the specific expression for $G_S(f)$ from the previous Section and with Eq. (21) for $AF^{-}(f)$, the expression for the band levels at the receiver location becomes

$$LR(f_c) = 10 \log \left\{ [G_S(f_c)]/p_{ref}^2 \right\} + 10 \log \left\{ \int_{f_L}^{f_U} (f/f_c)^{\ell S} \; 10^{-[a(f)][PD/10]} df \right\} \tag{22}$$

The problem of numerically evaluating the integral in Eq. (22) was addressed in Refs. 3 and 4. The method used in those references of summing a series of special integrals, where the absorption function was approximated by a power function of frequency over small logarithmically-spaced frequency intervals, was not used here because it was considered unnecessarily cumbersome and because an approximation for $\Delta F^{-}(f)$ was not really needed since the numerical evaluation would have to be done by a digital computer in any case.

The numerical integration method used to calculate band levels at the receiver was one of the standard methods given in the IBM Scientific Subroutine Package in common use at many installations of large digital computers. A number of other standard calculation routines could also have been used. The method that was used, however, utilized Simpson's rule and Newton's 3/8 rule.

To apply the method, the frequency range from f_L to f_U for each band was divided into a number of equally-spaced frequency intervals on a linear frequency scale, the number of intervals being a function of the bandwidth of the particular filter band and increasing as bandwidth increased. The value of the product in the integrand in Eq. (22) was calculated at each frequency step between f_L and f_U and then used by the standard subroutine to evaluate the integral. The subroutine is named by the acronym QSF for quadrature/Simpson's/function; it was also used to calculate band-adjustment factors. Details for the various steps in QSF are given by the subroutine statements in the program listings in Vols. II and III.

Before adopting the QSF subroutine, a study was conducted to select a single set of numbers to be used in all cases for subdividing the passbands of the filters into equally-spaced frequency intervals. Since the intervals were spaced along a linear frequency scale, it was necessary to increase the number of intervals as the bandwidth increased. Judgments as to how many intervals to include were made after considering the sizes of the logarithmically-spaced frequency intervals used for the calculation method of Refs. 3 and 4.

The numerical-integration method from Ref. 4 was also re-programmed for the problem of calculating band levels at the receiver. Parallel computations were made using the numerical-integration method of Ref. 4 and the method of standard subroutine QSF. Identical results were obtained for non-uniform and uniform atmospheric conditions, pathlengths to 900 m, and all four spectral slopes. Computing times for the two methods were also essentially the same for calculations using ideal filters.

The final values selected for the number of frequency intervals to use with subroutine QSF were as shown below along with the bandwidths and stepsizes.

Nominal band center frequency, Hz	Approx. bandwidth, $f_U - f_L$, Hz	Number of intervals N	Approx. frequency, stepsize $\Delta f = (f_U - f_L)/N$, Hz
1000	230.77	10	23.077
1250	290.51	12	24.209
1600	365.75	14	26.125
2000	460.43	16	28.777
2500	579.67	18	32.204
3150	729.75	20	36.488
4000	918.69	22	41.759
5000	1156.58	24	48.191
6300	1456.03	26	56.001
8000	1833.06	28	65.466
10,000	2307.71	30	76.924

Increasing the number of intervals would tend to increase accuracy but would also increase computation time. The intervals defined above required calculations at 231 frequencies over the 11 bands.

After the integral in Eq. (22) had been evaluated for a specified spectral slope at the source, ℓ^S, atmospheric conditions, and propagation distance, the band levels, $LR(f_c)$, were calculated according to Eq. (22) with $G_S(1000) = 10^6$ Pa^2/Hz and $p_{ref} = 20$ μPa.

Calculations of band levels at a receiver location were made for two atmospheric conditions, three propagation distances, and the four spectral slopes at the source of Fig. 1. The two atmospheric conditions were (1) those of a uniform-atmosphere acoustical reference day with air temperature of 298.15 K (25.0° C), relative humidity of 70.0 percent, and air pressure of 1.0 standard sea-level atmosphere (or a pressure of 101.325 kPa), and (2) those which resulted in very high atmospheric absorption coefficients.

By inspection of the data in Table II of ANSI S1.26-1978, it was clear that highly absorptive conditions were those for a warm and dry atmosphere; the conditions of an acoustical reference day yield near-minimum absorption coefficients. The highly-absorptive conditions were therefore chosen to be an air temperature of 298.15 K (25.0° C), a relative humidity of 10.0 percent, and an air pressure of 1.0 standard atmosphere. Thus, the only difference was the change in relative humidity from 70.0 to 10.0 percent.

Propagation distances selected for the analysis were 300, 600, and 900 m. Calculated band levels are shown in Figs. 3 and 4 for relative humidities of 70.0 and 10.0 percent, respectively. Figure 3 shows the band levels for all four source band-level slopes; Fig. 4 omits the intermediate slopes and only presents results for the highest and lowest slopes, +1 and -12 dB/band. Note that different ordinate scales are used for Fig. 3 and Fig. 4.

The band levels at the receiver, as expected, decrease rapidly with increasing frequency and increasing propagation distance. For the highly absorptive conditions, the attenuation is large and the level at the receiver becomes very low in the high-frequency bands, even for a source slope of +1 dB/band. The actual levels at the receiver location would be even lower than those shown in Figs. 3 and 4 because the attenuation due to geometric spreading losses has not been included in the calculations.

However, as shown in Fig. 5, attenuation over the path due to atmospheric absorption (i.e., the difference between the source level, LS, and the receiver level, LR) does not have a strong dependence on the spectral slope at the source. Note that three different ordinate scales were required to conveniently encompass the range of attenuation values for the three propagation pathlengths.

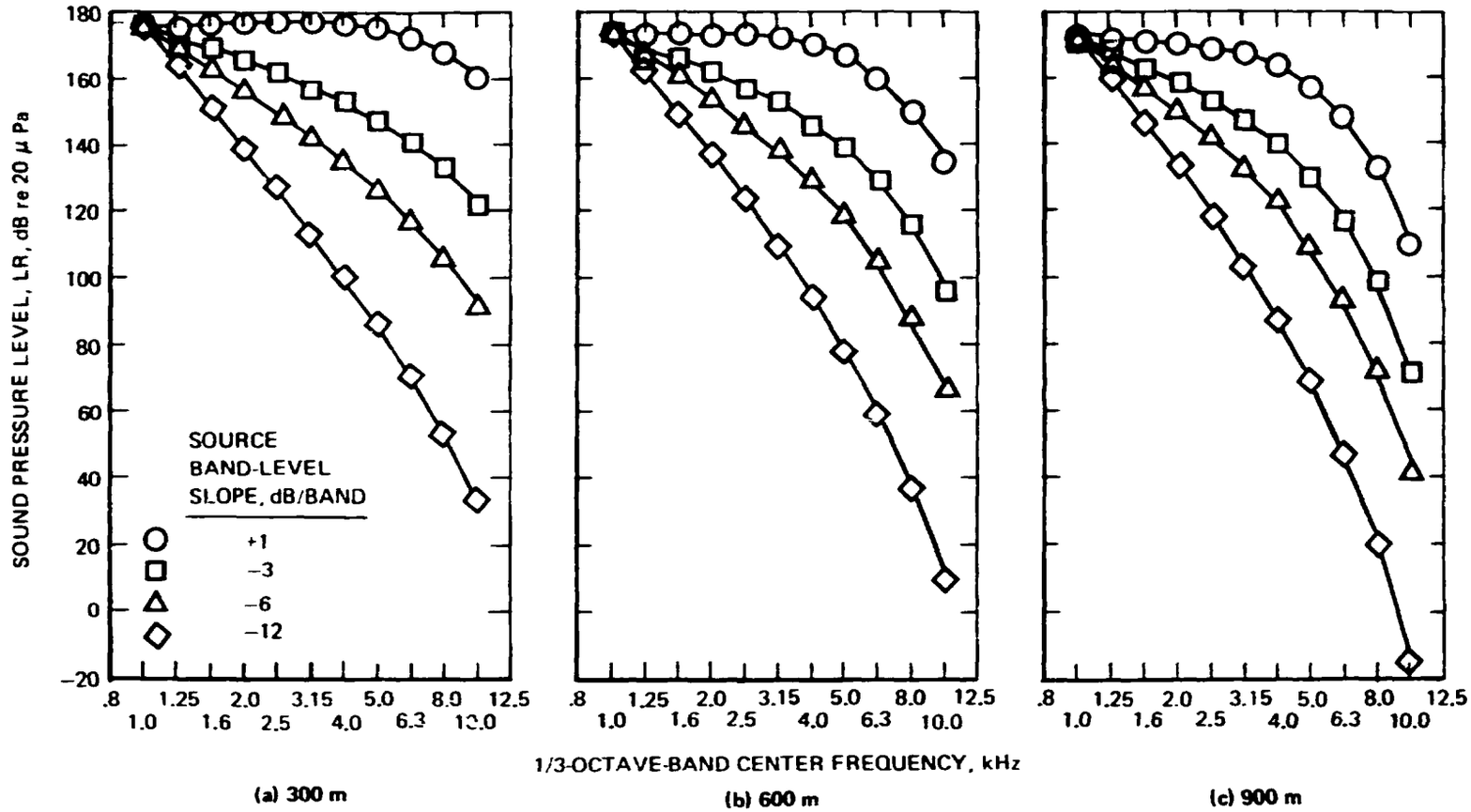

Figure 3.-1/3-octave-band sound pressure levels, LR, at the receiver for sound pressure spectral densities at the source of Fig. 1. Ideal filters; air temperature of 25°C; relative humidity of 70%; air pressure of 1.0 standard atmosphere. Propagation distances as noted. Attenuation by atmospheric absorption only; no spreading loss.

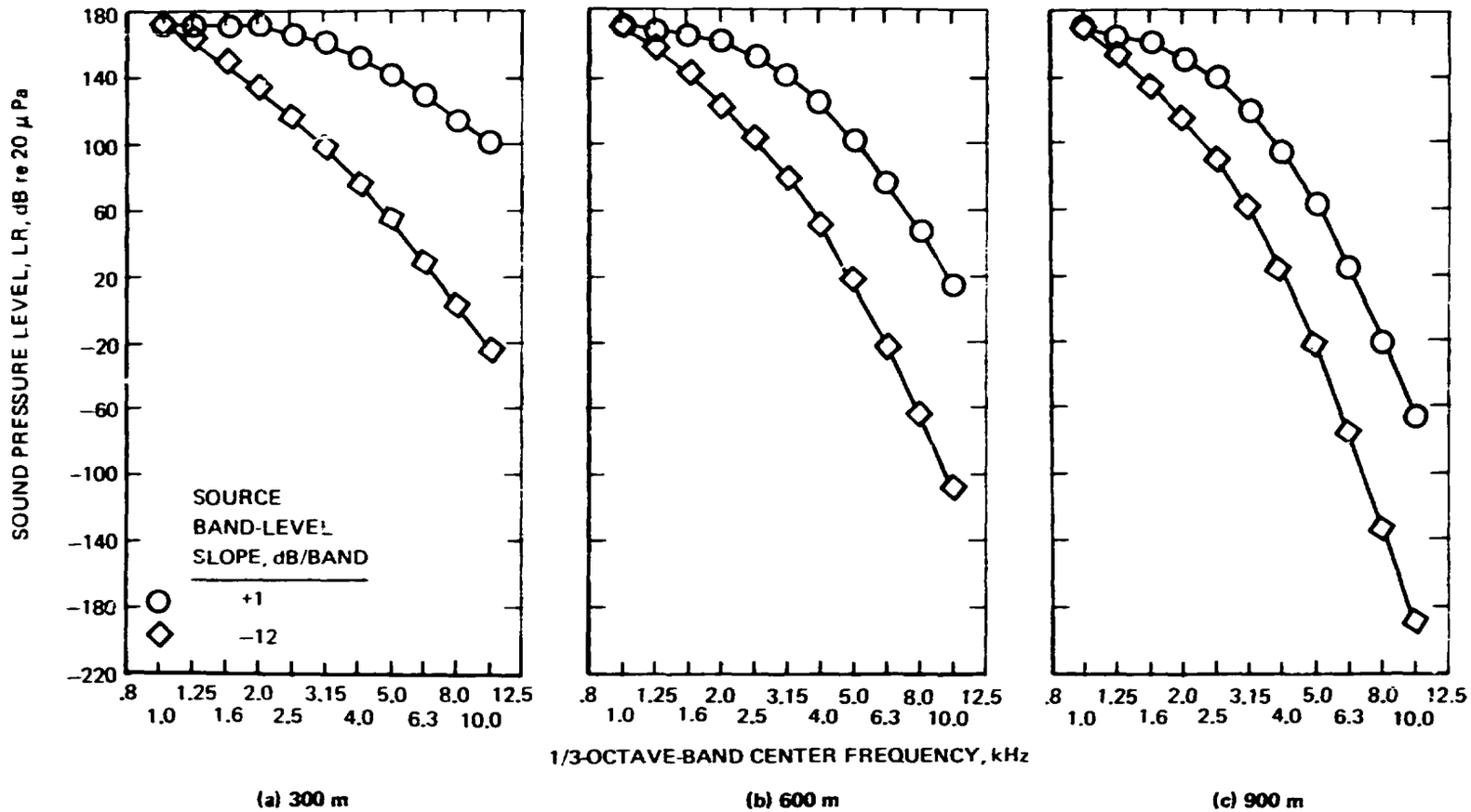

Figure 4.-1/3-ocatve-band sound pressure levels, LR, at the receiver for the same condition as for Fig. 3, except a relative humidity of 10% instead of 70%.

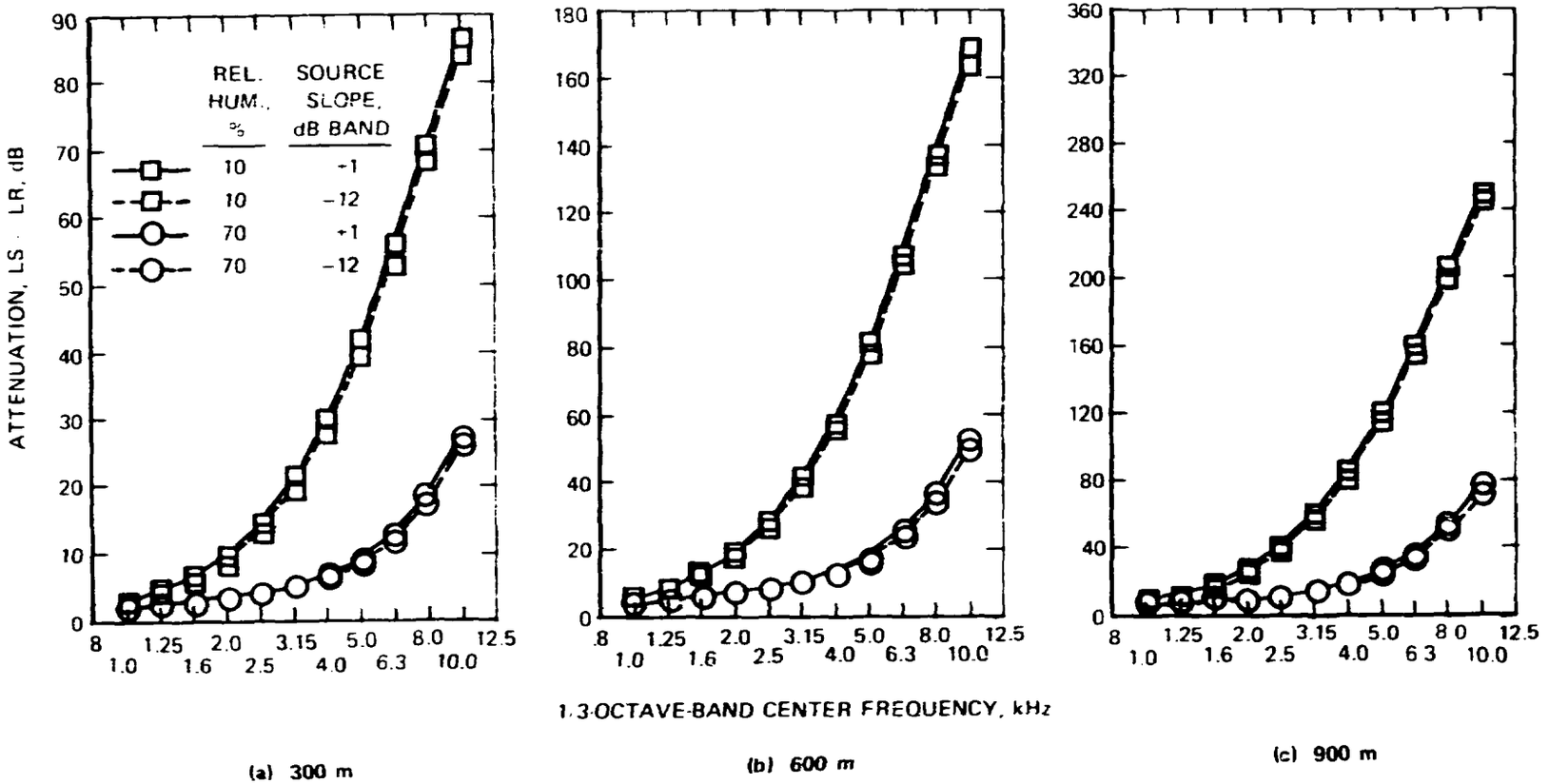

Figure 5.-Attenuation (difference due to atmospheric absorption between band levels at the source, LS, and band levels at the receiver, LR) as a function of frequency and propagation distance. Two relative humidities and band-level source spectrum slopes. Air temperature is 25°C; air pressure is 1.0 standard atmosphere. Ideal filter. No geometric spreading loss.

Exact Test-to-Reference Day Band-Level Adjustment Factors

If the receiver levels calculated for the 10-percent relative humidity condition at 25° C temperature are regarded as representing the exact values for test-day sound pressure levels, then the differences between the attenuation data in Fig. 5 represent exact values for band-level adjustment factors from test-to-reference conditions.

To see why this is true, let LR_{10} be the measured band level for a 10-percent relative-humidity test day and let LR_{70} be the band level that would have been measured at the receiver had the relative humidity been 70 percent. Then

$$LR_{70} = LR_{10} + (LR_{70} - LR_{10}) \tag{23}$$

where the difference $(LR_{70} - LR_{10})$ is the band-level adjustment factor, BA, to be added to the measured test-day level to determine the equivalent reference-day level.

Since the source level, LS, is always the same, the exact value of the test-to-reference band-adjustment factor can be found from

$$BA = (LS - LR_{10}) - (LS - LR_{70}) \tag{24}$$

for any band center frequency. The exact (LS - LR) values in Eq. (24) are just the attenuation values in Fig. 5.

Figure 6 shows the variation of the exact band-level adjustment factor with frequency, propagation distance, and spectral slope at the source. The adjustment factors are exact because all terms in Eq. (24) are known exactly. Note that three different ordinate scales were again needed to cover the range of values. Note also that the magnitude of the adjustments that would, theoretically, be required can become very large - even for the 300-m distance. Moreover, as noted for the attenuation values in Fig. 5, there is only a weak dependence of the exact band-adjustment factor on the slope of the sound spectrum at the source.

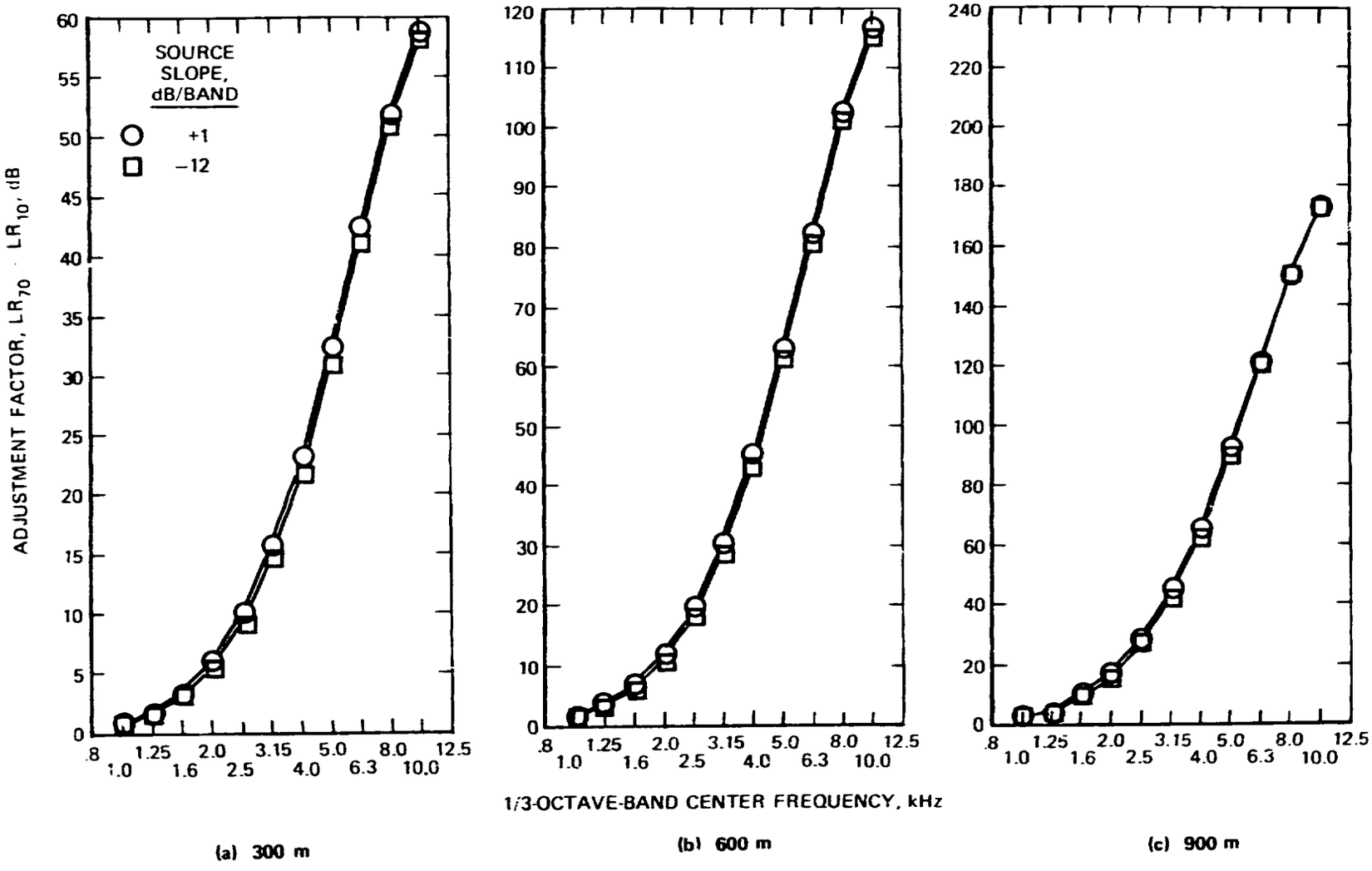

Figure 6.-True or exact band-level adjustment factor as a function of frequency and propagation distance. Difference in band level at the receiver under simulated reference and test atmospheric conditions [(LR at 70% relative humidity) − (LR at 10% relative humidity)]. Air temperature is 25°C; air pressure is 1.0 standard atmosphere. Ideal filters.

Approximation of Source Band Levels by Band Integration Method

If the true source levels are not known, as they usually are not, and only the band levels at the receiver are known, then some approximation method must be used to estimate the sound pressure spectrum at the receiver so that the band level at the source can be calculated. This requirement, of course, is the essence of the band-adjustment calculation problem as was also pointed out in Ref. 4.

The problem of calculating the band level at the source is the inverse of the problem of calculating the band level at the receiver. Hence, referring to Eqs. (17) and (18), the source band levels are found from

$$LS = 10 \log \left\{ \left[\int_{f_L}^{f_U} G_S(f)\, df \right] / p_{ref}^2 \right\} \tag{25}$$

where

$$G_S(f) = [G_R(f)][AF^+(f)] \tag{26}$$

and where an expression for $G_R(f)$ has to be found from the band levels LR. The notation AF^+ is used to signify that the path is from the receiver location to the source location. The notation that the source band level, LS, is for some particular band with center frequency f_c has also been omitted in Eq. (25).

Although it would have been entirely feasible to work directly with Eq. (25) and to have determined source band levels LS and then to have calculated adjustment factors by subtracting the corresponding receiver band levels LR, it was decided to use an alternative approach and calculate the receiver-to-source band-adjustment factors directly. Thus, the problem of calculating source band levels was formulated, in a manner similar to that in Eqs. (23) and (24), as

$$LS = LR + (LS - LR) = LR + BA \tag{27}$$

where BA is the adjustment factor to be added to the measured receiver level to obtain the estimated source level.

Using previous expressions, the receiver-level-to-source-level band-adjustment factor can be written

$$BA = LS - LR = 10 \log \overline{p_S^2}/\overline{p_R^2}$$

$$= 10 \log \left\{ \left[\int_{f_L}^{f_U} [G_R(f)][|AF^+(f)|] \right] / \int_{f_L}^{f_U} G_R(f)df \right\} \quad (28)$$

The form of Eq. (28) has the advantage over that of Eq. (25) in that the constants $G_R(f_c)$ and p^2_{ref} are eliminated because they appear in both the numerator and denominator.

To proceed, we need an expression for $G_R(f)$. The expression for $AF^+(f)$ is obtained from Eq. (20) or Eq. (21) for a layered or a homogeneous atmosphere and with a plus instead of a minus sign.

In Ref. 4, the pressure spectral density function $G_R(f)$, applicable to the frequency range from f_L to f_U for some band center frequency f_c, was estimated from the measured band levels by a single straight line over the passband. The slope of the line was determined by the difference between the level above and the level below the band of interest. Special rules were adopted for the first and last bands where the slope over half of the band was extrapolated over the other half of the band.

For the study described in this report, it was decided to modify the procedure used in Ref. 4. The single-straight-line approximation for $G_R(f)$ over the frequency range of a filter passband is considered to be appropriate when the band-level spectrum is reasonably smooth and not too steep, i.e., slopes less than approximately ±6 dB/band. The spectrum of many noise sources, including significant portions of many aircraft noise signals, is consistent with this assumption. For general applicability, however, the single-straight-line approximation was not considered adequate.

Most aircraft noise signals have a rather complex spectrum because the total noise signal is the result of a variety of noise sources — broadband and discrete frequency. The analysis in this report is applicable to the complex spectra resulting from a number of broadband noise sources. As stated earlier, the problem of calculating atmospheric-absorption adjustments for discrete-frequency components is considered a separate issue.

The procedure for estimating $G_R(f)$ that was adopted for this report uses a 2-slope approximation over the passband instead of a single-slope approximation. To help visualize the effect of the change in the approximation method, consider the hypothetical aircraft noise spectrum represented in Fig. 7 by the set of 1/3-octave-band sound pressure levels as a function of either the logarithm of the band center frequency or, as here, the international standard band numbers as used in Eq. (11).

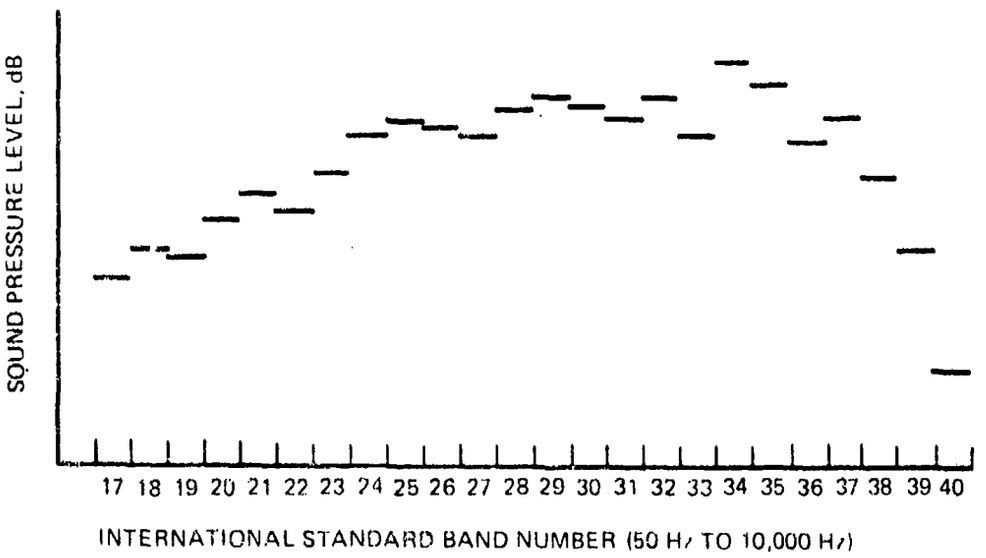

Figure 7.-Hypothetical spectrum of aircraft noise.

In the high-frequency bands, say ISBN = 37 to 40, the band-level slope usually becomes increasingly more negative as frequency increases. The slope, however, rarely, changes sign in the very high-frequency bands. In the lower-frequency bands, there often are several changes in slope. With a single-slope approximation, band-to-band slope changes can cause anomalous results in calculated absorption factors. The 2-slope approximation alleviates the anomalies, though it remains only an approximation to the true pressure spectral density.

Even, as here, with the assumption that the filters have ideal transmission response, there is no way to recover the true sound pressure spectrum at the receiver given only the band levels, except for special cases with constant-slope spectra. Furthermore, if the power-transmission response

of the real filters cannot be assumed to be that of an ideal filter (i.e., if the filter's rejection rate is not high enough in the stopbands), or if the slope of the sound spectrum changes rapidly with frequency, then the filter frequency response must be considered in the calculation of atmospheric-absorption-loss adjustment factors. In such a case, the problem of estimating the true or actual spectrum of the sound pressure at the microphone becomes much more difficult because there is no way to distinguish readily between the effects of the atmosphere and the effects of the filter on the resulting band sound pressure level. Reference 7 proposed an "iterative" method as one possibility. The "iterative" method, however, would have required considerable effort to develop a practical implementation and was not considered for this study. Additional discussion of filter effects is given in the next Section.

Figure 8 illustrates the differences between using the single-straight-line approximation method of Ref. 4 and the 2-slope method of approximating the pressure spectrum. The examples are taken from the hypothetical spectrum of Fig. 7.

Figure 8(a) shows two cases where the band slope changes from negative to positive over a band. Figure 8(b) shows two cases where the band slope changes from negative to more-negative over a band. When there is a large change in noise-level slope over a band, the spectral slope estimate based on the difference in band level between that of the band above and the band below the band of interest (i.e., the short dashed lines in Fig. 8) does not yield a good approximation, especially when the slope changes sign as around bands 33 and 36 in Fig. 8(a). When there is little difference in band slope, as around band 38 in Fig. 8(b), the single-line spectral-slope estimate based on the difference between the level of the band above and the band below may be as reasonable as the 2-slope approximation.

When the pressure spectrum over the passband of a filter is approximated by two straight line segments, the single integrals in the numerator and denominator of Eq. (28) are replaced by the sum of two integrals ranging from f_L to f_c and from f_c to f_U. In each frequency range, the pressure spectrum, $G_R(f)$, is approximated by a power function of frequency. The

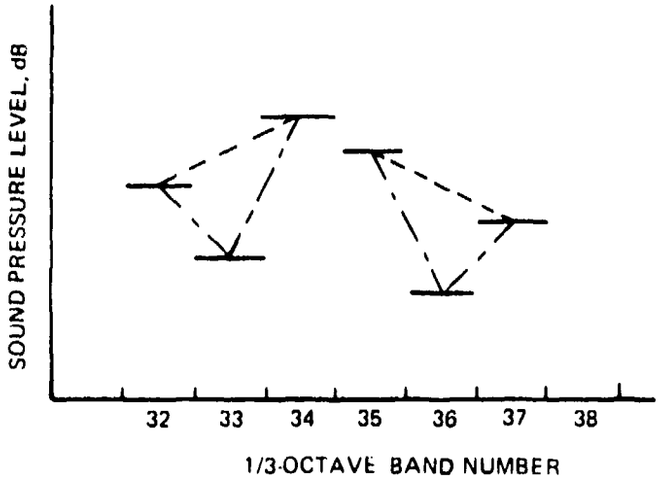

(a) OVER PASSBANDS OF BANDS 33 AND 36.

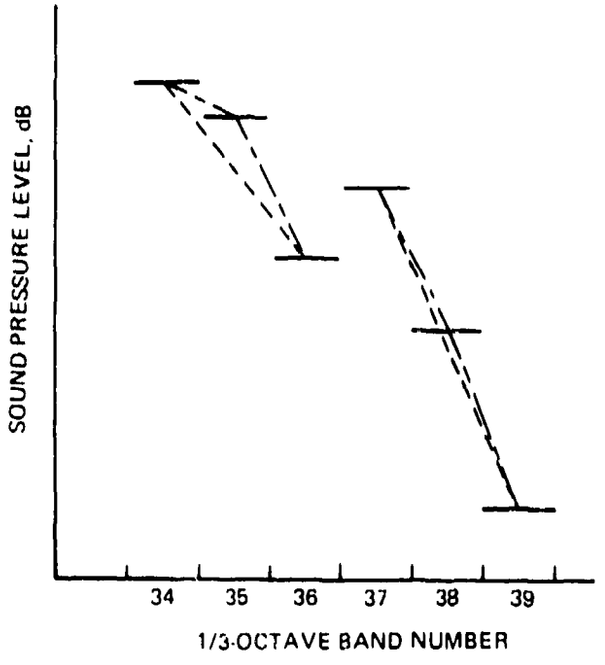

(b) OVER PASSBANDS OF BANDS 35 AND 38.

Figure 8.-Comparison of band-slope estimating procedures for certain bands from hypothetical aircraft noise spectrum of Fig. 7.

- - - - - Band slope procedure of Ref. 4.

——— Band slope procedure based on level differences in adjacent bands.

exponent for the frequency (the slope of the line segment on logarithmic scales) is determined from the difference between the level of adjacent bands. Figure 9 illustrates the process and defines the applicable symbols. Note that at $f = f_c$, $G_{RL}(f_c) = G_{RU}(f_c) = G_R(f_c)$ or a constant which can be factored out and canceled from the ratio in Eq. (28).

Given these considerations the ratio of integrals in Eq. (28) is written as

$$\frac{NUM1 + NUM2}{DEN1 + DEN2} = \frac{\int_{f_L}^{f_c} (f/f_c)^{\ell^L} \Delta F^+ df + \int_{f_c}^{f_U} (f/f_c)^{\ell^U} \Delta F^+ df}{\int_{f_L}^{f_c} (f/f_c)^{\ell^L} df + \int_{f_c}^{f_U} (f/f_c)^{\ell^U} df} \qquad (29)$$

where the pressure spectral density slopes, ℓ^L and ℓ^U, are related to the corresponding normalized, non-dimensional band-level slopes, SLL and SLU, by

$$\ell^L = SLL - 1 \qquad (30a)$$

and

$$\ell^U = SLU - 1 . \qquad (30b)$$

The normalized band-level slopes are found from the differences between the sound pressure levels in adjacent bands using

$$SLL = [LR(f_c) - LR(f_{c-1})]/[10 \log (RF)] \qquad (31a)$$

and

$$SLU = [LR(f_{c+1}) - LR(f_c)]/[10 \log (RF)] \qquad (31b)$$

where $LR(f_c)$ represents the set of sound pressure levels at the receiver and RF is the band frequency ratio f_U/f_L. For 1/3-octave bands, $RF = 10^{0.1}$.

The slope of the line over the lower half of the first band in the set is assumed to be the same as that over the upper half of the first band. Similarly, the slope of the line over the upper half of the last band is assumed to be the same as that over the lower half of the last band.

As for Eq. (22), the integrals in the two numerator terms, NUM1 and NUM2, in Eq. (29) were evaluated using the QSF numerical-integration subroutine

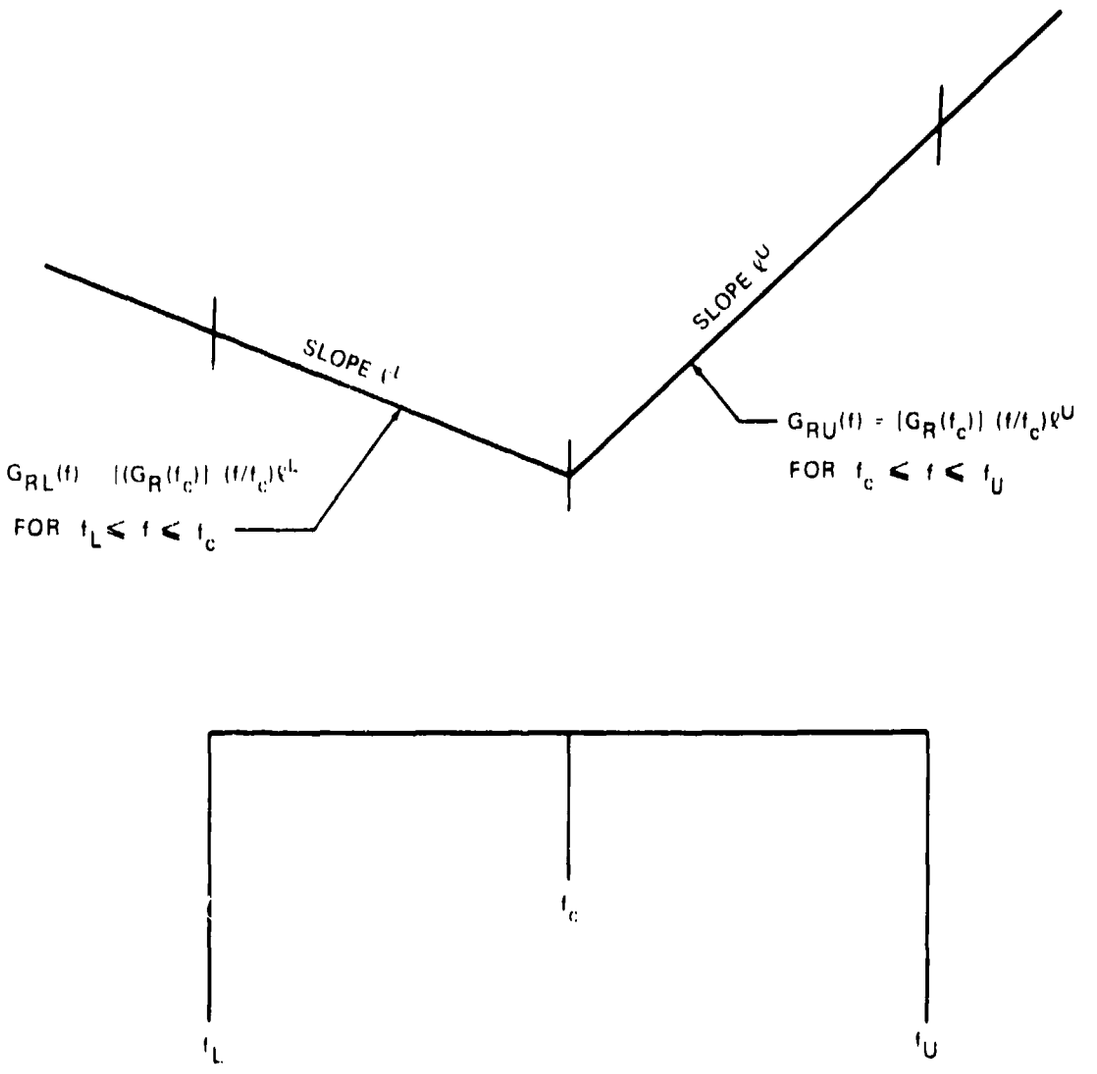

Figure 9.-Illustrations of straight-line approximations to sound pressure spectral density $G_R(f)$ with slopes ℓ^L and ℓ^U over passband of ideal filter with band center frequency f_c.

and the same number of frequency intervals in each passband as determined previously.

The denominator terms, DEN1 and DEN2, in Eq. (29) are evaluated directly. By analogy with the development of Eqs. (12) and (13) for the evaluation of Eq. (3), the denominator terms become

$$DEN1 = (f_c/SLL)(1 - RF^{-SLL/2}) \tag{32a}$$

and

$$DEN2 = (f_c/SLU)(RF^{SLU/2} - 1) \tag{32b}$$

when $\ell^L \neq -1$ (or $SLL \neq 0$) and $\ell^U \neq -1$ (or $SLU \neq 0$), respectively, and

$$DEN1 = DEN2 = (f_c/2) \ln (RF) \tag{33}$$

when $\ell^L = \ell^U = -1$ (or $SLL = SLU = 0$).

With Eqs. (32) and (33), all terms in Eq. (29) can be calculated and used in Eq. (28) to determine the adjustment factors to be added to the band levels at the receiver location to give the estimated band levels at the source. Comparison with the known band levels at the source provides a measure of the accuracy of the process and the appropriateness of the approximation of the true pressure spectral density.

Figure 10 shows the results of applying the method over a propagation distance of 600 m and for a true source-band-level slope of -12 dB/band. Starting with the receiver band levels calculated for either 70 or 10-percent relative humidity, the approximate method is seen to provide a very good estimate of the true source band levels.

Figure 10 also indicates the true attenuation caused by atmospheric absorption over the 600-m distance ($LS - LR_{70}$ or $LS - LR_{10}$ for the 70 and 10-percent relative humidity conditions) as well as the exact test-to-reference-day adjustment factor $LR_{70} - LR_{10}$.

The magnitude of the differences between the exact and the approximate source band levels is shown in Fig. 11 for the three propagation distances and the +1 and -12 dB/band slopes. The largest differences are in the 10-kHz

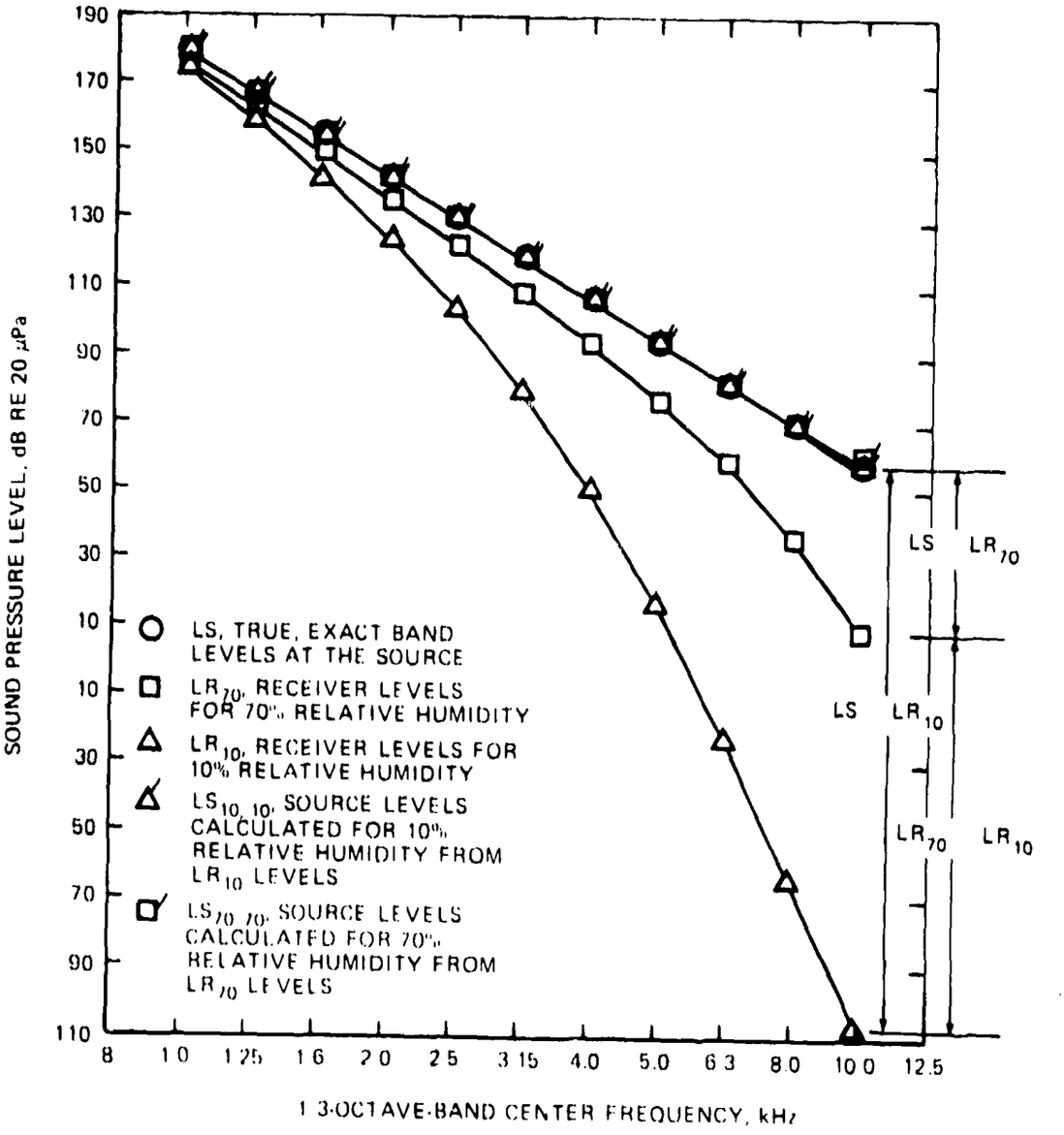

Figure 10.-Example of determination of (1) attenuation, (2) accuracy of approximate band-integration method of calculating atmospheric absorption, and (3) exact band-loss adjustment factor from test (10% relative humidity) to reference (70% relative humidity) meteorological conditions. Air temperature is 25°C; air pressure is 1.0 standard atmosphere; spectral slope at the source is −12 dB/band; ideal filters; sound propagation pathlength is 600 m; no geometric spreading loss.

- Attenuation by atmospheric absorption = $LS - LR_{70}$ or $LS - LR_{10}$.
- Accuracy of approximate method = $LS_{10,10} - LS$ or $LS_{70,70} - LS$.
- Exact band-loss adjustment factor = $LR_{70} - LR_{10}$.

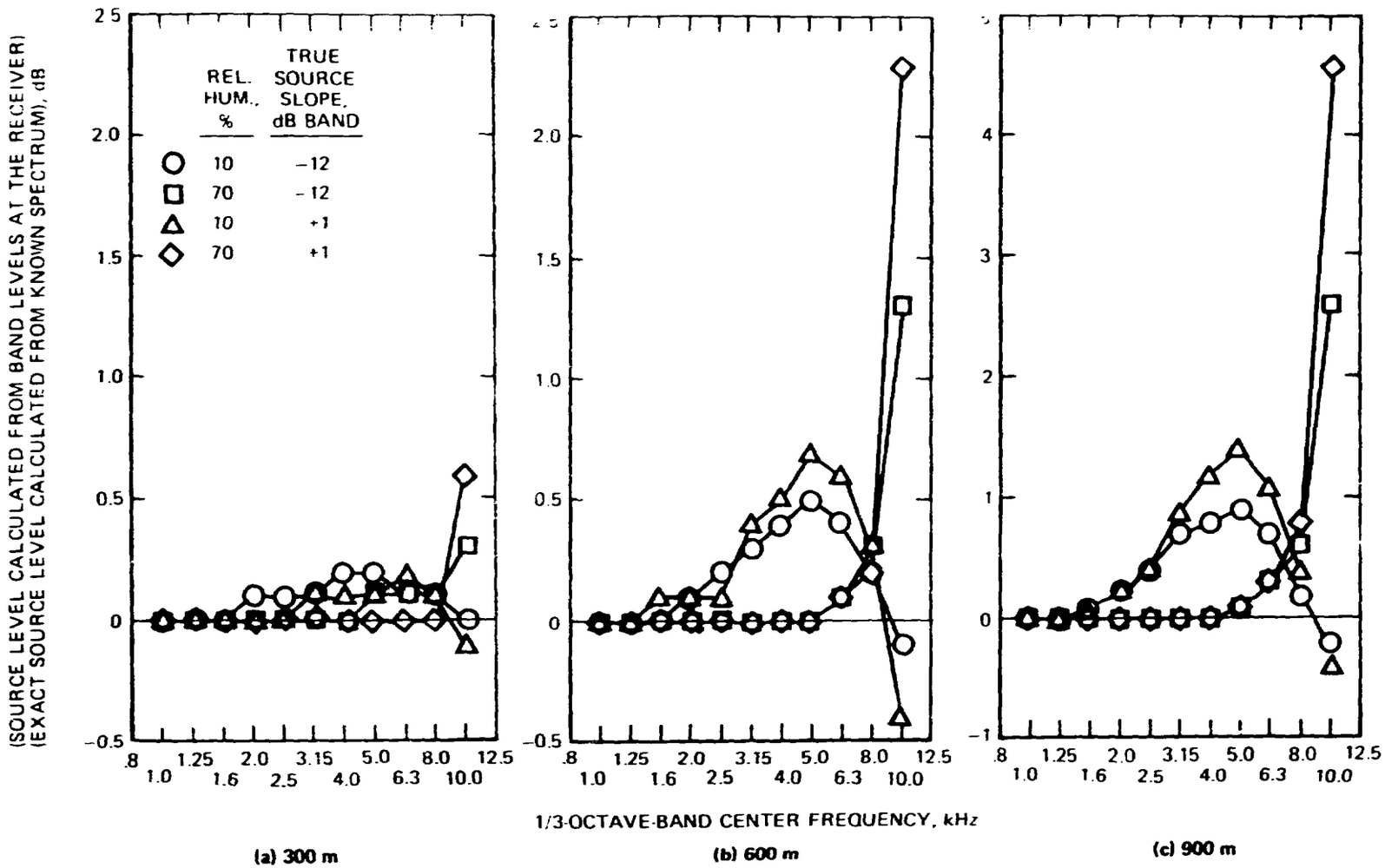

Figure 11.-Illustration of ability to accurately calculate atmospheric absorption over a sound propagation path using band sound pressure levels at the receiver. Calculated band levels at the source are compared with known, exact band levels at the source for three sound propagation path lengths, two slopes for the pressure spectrum of the sound at the source, and two relative humidities, air temperature is 25°C; air pressure is 1.0 standard atmosphere. Sound spectrum at the receiver is approximated by band-level slopes over the lower and upper halves of the passband of ideal 1/3-octave-band filters. Absorption over the propagation path is calculated by integration over filter passband.

band, probably because of the extrapolation of the slope over the lower half of the band to the upper half of the band.

Neglecting the differences in the 10-kHz band, the approximate method is seen to always give an estimate for the source band level that is either equal to or slightly greater than the true source band levels, the larger differences occurring for the much-more-absorptive 10-percent-relative-humidity conditions. For the 70-percent conditions, the difference between the estimated and the exact band level was never more than 0.2 dB and usually was 0.0 dB. For the 10-percent humidity conditions, the largest differences occurred in the 5-kHz band but did not exceed 1.4 dB over the 900-m distance.

As a matter of interest, the calculations of source band level for all the cases shown in Fig. 11 were performed twice, once with the QSF numerical-integration method and once with the closed-form-integral-summation method of Ref. 4 reprogrammed for this application. Identical results were obtained as they were for the calculations of receiver band levels. Thereafter, only the QSF subroutine was used for evaluating the integrals in a calculation of the attenuation over the propagation path.

Approximation of Source Band Levels by Band-Center-Frequency Method

The very good agreement in Fig. 11 between the exact source band levels and source band levels estimated using Eqs. (27) and (28) was anticipated since the receiver band levels had been calculated using ideal filters and the pressure spectral density at the receiver was closely approximated by the two constant-slope lines over the lower and upper halves of each passband.

Since SAE ARP866A uses, essentially, a band-center-frequency method, a natural question was how well would a band-center-frequency method approximate the attenuation over the propagation path.

Thus, instead of evaluating an integral to determine the attenuation over the pathlength, the source band levels were simply calculated from

$$LS(f_c) = LR(f_c) + |a(f_c)||PD| \qquad (34)$$

where $a(f_c)$ is the atmospheric absorption coefficient at the band center frequency. Absorption coefficients were determined by the method of ANSI S1.26-1978 at the exact band center frequencies determined from Eq. (11).

Comparisons of the differences between source band levels calculated from Eq. (34) and the exact source band levels are shown in Fig. 12. The differences are significantly larger than the corresponding differences in Fig. 11 for the band-integration method. Note that two different ordinate scales were required as they were for Fig. 11.

The difference between the exact source band level and the source band level estimated using Eq. (34) increases as the slope of the spectrum at the receiver increases, i.e., as the source spectrum slope increases, as the propagation distance increases, and as the atmospheric conditions become more absorptive. The reason for this result is that the attenuation at the band-center frequency becomes a poorer and poorer estimate of the true attenuation as the slope steepens because the actual attenuation over the frequency range of the filter passband is determined by frequencies near the lower bandedge frequency for steep, negative spectral slopes. The true attenuation is less at the lower bandedge frequency than at the band center frequency. This observation is the basis for the use in SAE ARP866A of the nominal lower bandedge frequency instead of the nominal band center frequency for calculations applicable to the 5-kHz to 10-kHz bands.

The results in Fig. 12 also indicate that if the spectrum is not too steep, or the propagation distance not too long, or the atmospheric conditions not too absorptive (or not too different from reference conditions), then the band-center frequency method is capable of estimating the true attenuation within 1 to 2 dB for band center frequencies as high as 5 to 8 kHz depending on conditions. The levels in the 5 to 10-kHz bands, moreover, are often so low that they are below the level of the background noise and hence cannot be measured with current instruments. Thus, although not as accurate as the band-integration method, the band-center-frequency method may be adequate in many practical situations.

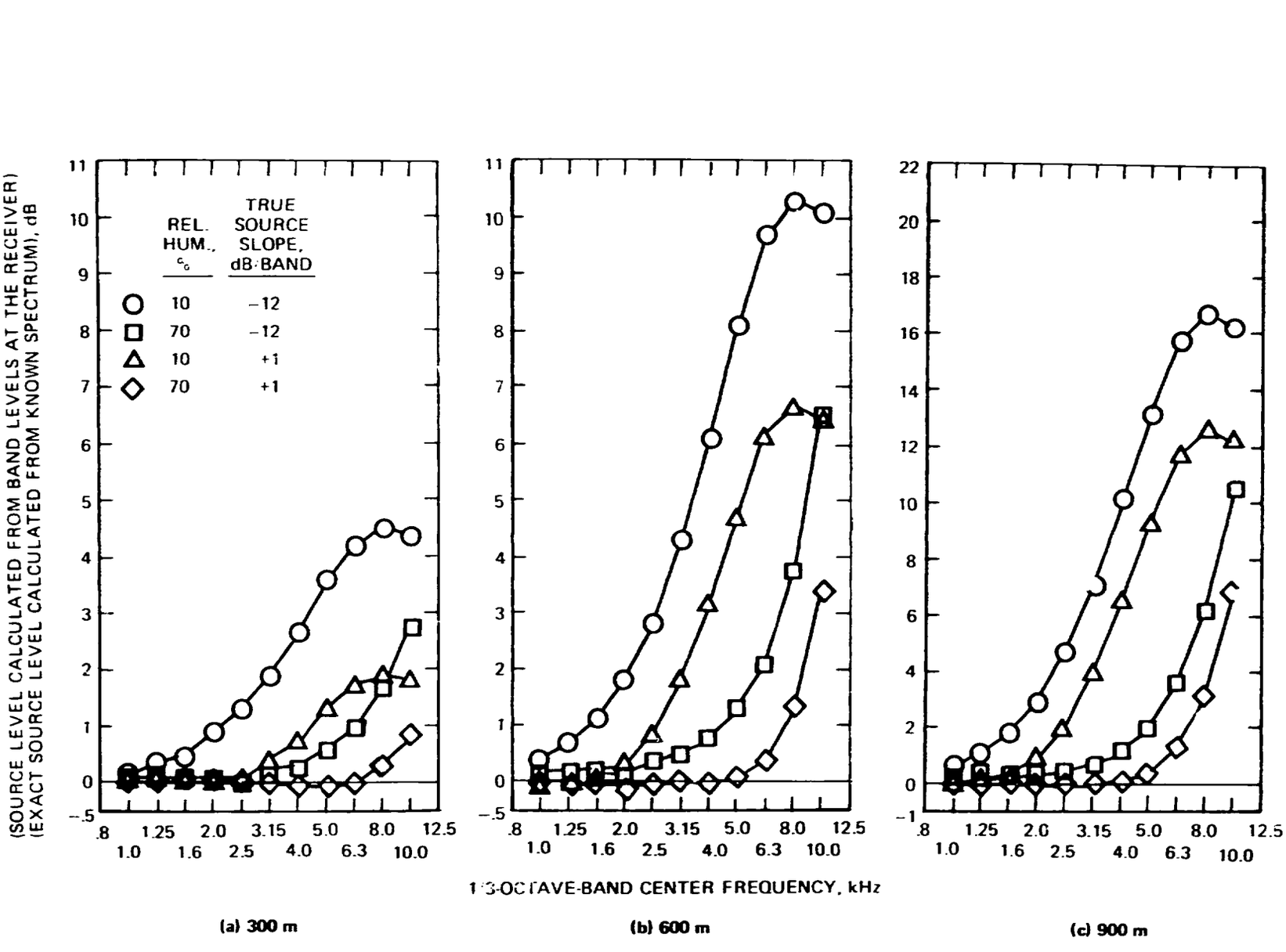

Figure 12.-Similar comparisons of ability to accurately calculate atmospheric absorption over a sound propagation path as in Fig. 11, except that absorption factor for band sound pressure level is determined only at the center frequency of the ideal filters instead of by integration over the frequency range of the passband. Air temperature is 25°C; air pressure is 1.0 standard atmosphere.

Approximate Test-to-Reference-Day Band-Level Adjustment Factors

The exact value for the factor to be added to the receiver band levels for the 10-percent-relative-humidity test-day conditions in order to determine what the receiver band levels would have been on a 70-percent-relative-humidity reference day was found from the difference in the exact values of the attenuation over the propagation path under the two atmospheric conditions.

Thus, from Eq. (24), the exact band-adjustment factor can be written as

$$BA_{exact} = att_{10,exact} - att_{70,exact} \tag{35}$$

$$= (LS_{exact} - LR_{10,exact}) - (LS_{exact} - LR_{70,exact}) \tag{36}$$

$$= LR_{70,exact} - LR_{10,exact} \tag{37}$$

for the known, exact source band levels with the results as shown in Fig. 6.

However, if we start with the exact receiver band levels for the simulated test-day condition, $LR_{10,exact}$, and calculate the approximate attenuation over the path for 10-percent and 70-percent-relative-humidity conditions in order to estimate what the source band levels would have been under the two atmospheric conditions, then the approximate band-adjustment factor from test-to-reference conditions can be determined. By analogy with the calculation for the exact band-adjustment factor, the approximate band-adjustment factor is found from

$$BA_{approx} = att_{10,approx} - att_{70,approx} \tag{38}$$

$$= (LS_{10,10,approx} - LR_{10,exact}) - (LS_{70,10,approx} - LR_{10,exact}) \tag{39}$$

$$= LS_{10,10,approx} - LS_{70,10,approx} \tag{40}$$

where the subscript 10,10 means that the source levels are computed for 10-percent relative humidity starting from receiver levels for a 10-percent-humidity atmosphere while the subscript 70,10 indicates source levels calculated for a 70-percent humidity atmosphere but starting from the same

exact receiver band levels calculated for the 10-percent-humidity condition. Air temperature and pressure are constant for all calculations.

Figure 13 presents an example of the calculation of approximate band-adjustment factors for the same 600-m propagation distance and -12 dB/band exact source slope shown in Fig. 10. Attenuation over the path was determined by the band-integration method. The magnitude of the exact and approximate band-adjustment factors is indicated for the 10-kHz band. The subscripts approx and exact have been omitted in the figure.

A measure of the accuracy of a method of accounting for atmospheric absorption over a propagation path is given by the difference between the approximate and the exact band-adjustment factors, Eqs. (40) and (37). For the example shown in Fig. 13, this difference is shown to be 1.1 dB in the 10-kHz band.

Calculations of approximate band-adjustment factors and comparisons with the corresponding exact band-adjustment factors were made for the three propagation distances and for the +1 and -12 dB/band true source-spectrum slopes. Attenuation over the path was calculated by the band-integration method and by the band-center-frequency method.

Figure 14 summarizes the results of those calculations. The data in Fig. 14 confirm the trends from Figs. 11 and 12 which indicated that the band-integration method provides a more-accurate calculation of attenuation over the path than the band-center-frequency method. Note that three different ordinate scales are used in Fig. 14. Note also that the approximate adjustment factor is almost always greater than the exact adjustment factor; the small negative values shown in the figure are the result of round-off errors.

A summary of the range of the largest differences between the approximate and the exact adjustment factors is shown below for the two methods of calculating attenuation and the three propagation distances.

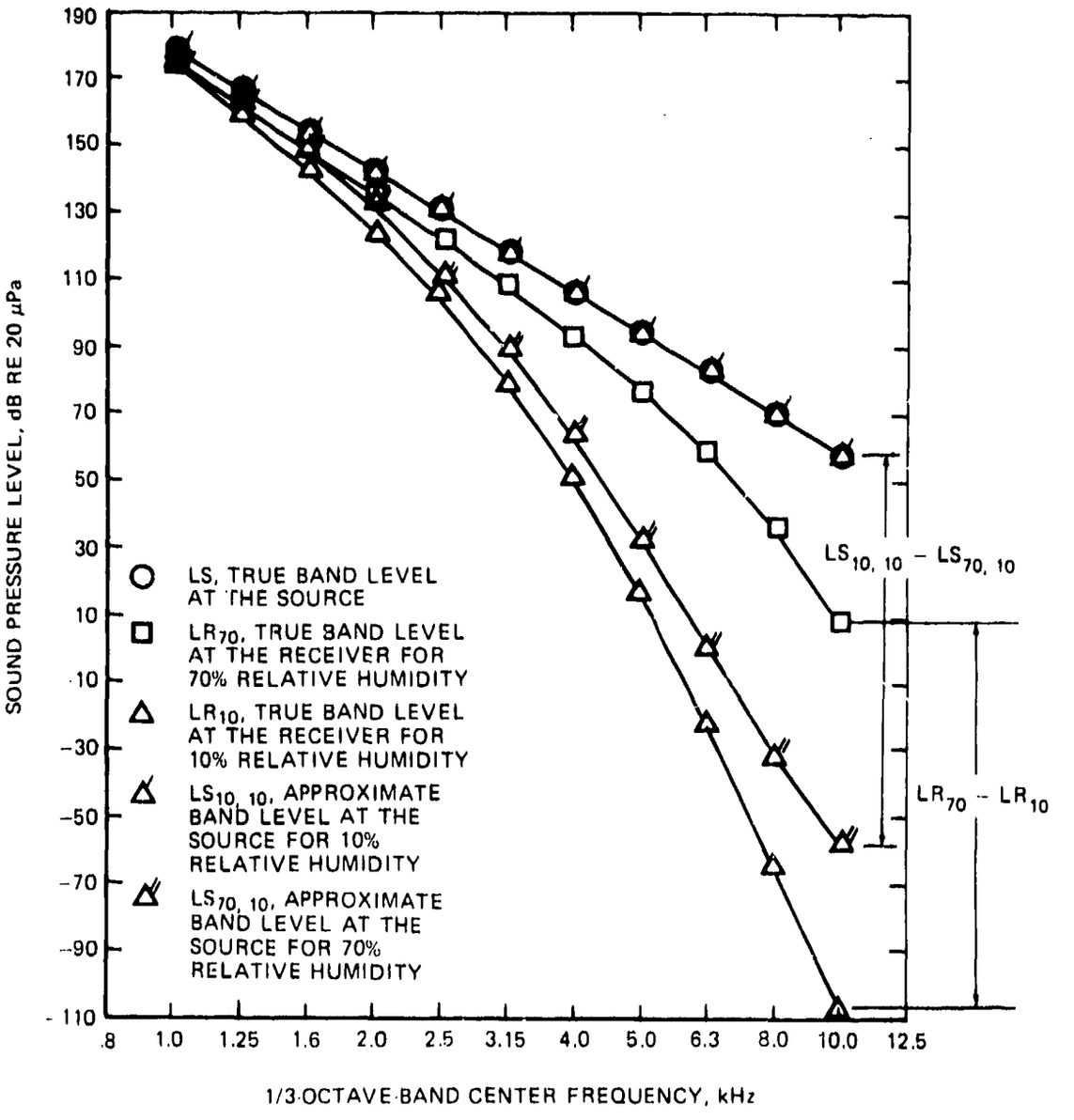

Figure 13.-Example of determination of exact and approximate band-loss adjustment factors for differences in atmospheric absorption under test (10% relative humidity) and reference (70% relative humidity) conditions. Air temperature is 25°C; air pressure is 1.0 standard atmosphere; spectral slope at the source is − 12 dB/band; ideal filters; sound propagation pathlength is 600 m; no geometric spreading loss.

Approximate band-loss adjustment factor for receiver levels under 10% relative humidity is ($LS_{10,10} - LS_{70,10}$). Exact band-loss adjustment factor is ($LR_{70} - LR_{10}$). Comparison of the difference for the 10 kHz band for this example yields ($LS_{10,10} - LS_{70,10}$) − ($LR_{70} - LR_{10}$) = (58.8 − (−58.1)) − (9.0 − (−106.8)) = 116.9 − 115.8 = 1.1 dB.

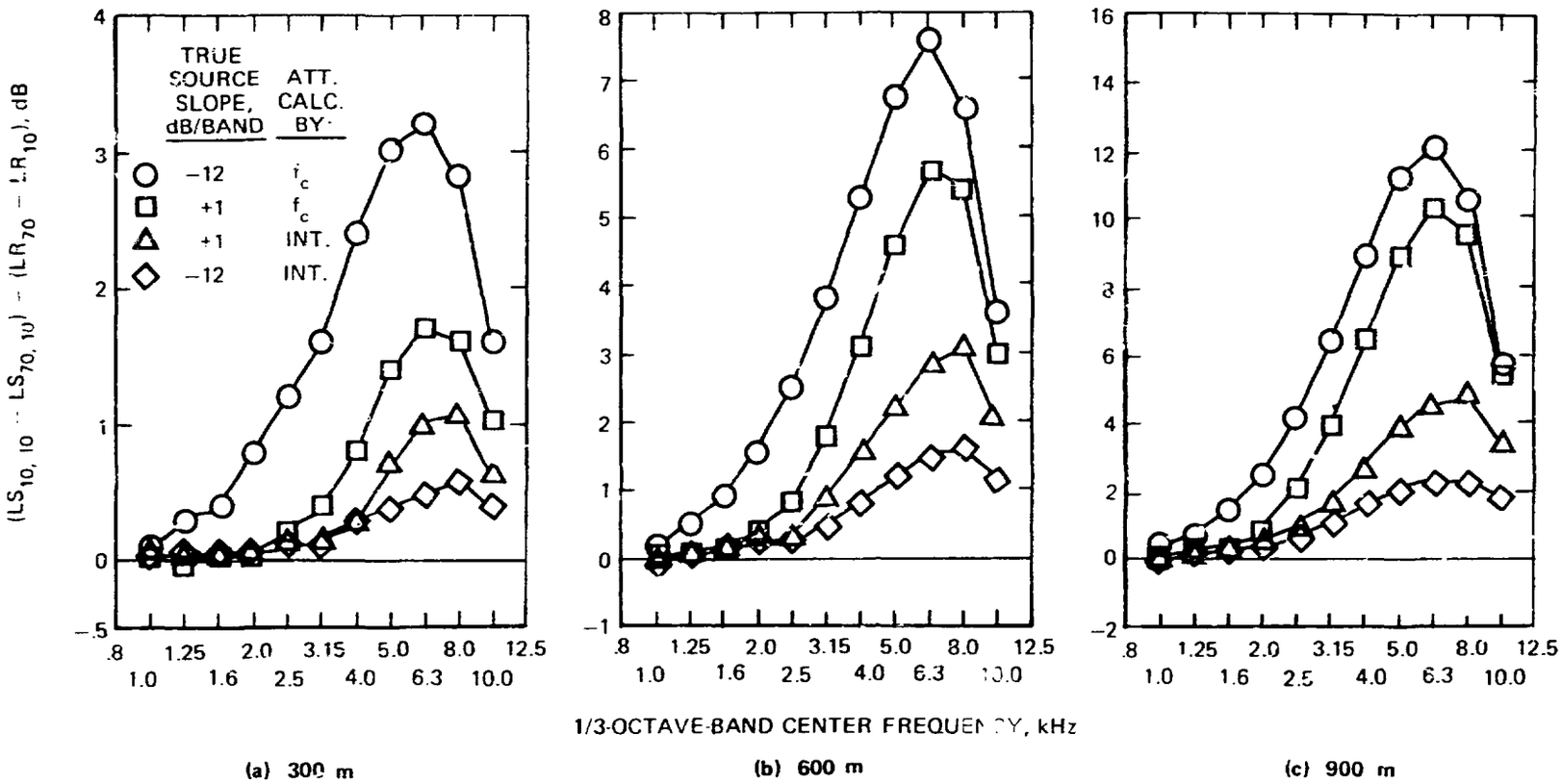

Figure 14.-Comparison of approximate and exact band-loss adjustment factors for ideal filters. Difference in source levels ($LS_{10,10} - LS_{70,10}$), calculated from receiver levels LR_{10}, determined for 10% relative humidity (test-day conditions) assuming first 10 and then 70% relative humidity (reference-day conditions), compared with difference in receiver levels ($LR_{70} - LR_{10}$) for 70 and 10% relative humidity. Air temperature is 25°C; air pressure is 1.0 standard atmosphere. Three sound propagation pathlengths; two true slopes for the sound spectrum at the source; and two approximate methods for calculating atmospheric absorption: integration over filter passband and absorption at band center frequency, f_c, only.

attenuation calculation method	range of largest error, dB		
	pathlength, m		
	300	600	900
integration	0.6 - 1.1	1.6 - 3.1	2.1 - 4.8
center frequency	1.7 - 3.2	5.7 - 7.6	10.3 - 12.2

The error in the calculation of attenuation by the band-integration method is larger for the +1 dB/band source-spectrum slope than for the -12 dB/band slope, a result also shown in Fig. 11 for calculations of source band levels.

For the band-center-frequency method, the error was larger for the steep, -12 dB/band slope than for the +1 dB/band, white-noise source spectrum, a result which is consistent with the trends in Fig. 12.

As a further observation from the results in Fig. 14, we note that, for a specified level of tolerable accuracy, the band-integration method is able to satisfy the criterion to higher frequencies than is the band-center-frequency method for any combination of propagation distance and source spectrum slope.

As a final remark, we reiterate the comment made earlier that although the band-integration method appears, on the basis of the analyses presented here, to be generally more accurate than the band-center-frequency method (significantly so in many cases), the greater accuracy may be of limited practical consequence when differences in atmospheric absorption are judged in terms of psychoacoustic descriptors or time-integrated measures such as perceived noise level or sound exposure level.

3. EFFECTS OF NON-IDEAL FILTER CHARACTERISTICS ON CALCULATIONS OF ABSORPTION-ADJUSTMENT FACTORS

All the analyses in the previous Section were performed under the assumption that the 1/3-octave-band filters in the noise-measurement system at the receiver location had the power-transmission-response characteristics of an ideal filter. A real, or practical, filter has response characteristics that approach those of an ideal filter. The most-important difference, for atmospheric-absorption analyses, is that the practical filter has finite, rather than infinite, rejection at frequencies in the stopbands below the lower-bandedge and above the upper-bandedge frequencies. In this Section, we examine some of the effects of non-ideal filter characteristics at the receiver on atmospheric-absorption calculations.

Filter Transmission Response

An ideal filter has a relative power-transmission ratio or power transfer function (i.e., the ratio of the power transmitted at some frequency to the power transmitted at the band center frequency) of 1.0 in the filter passband and 0.0 in the stopbands on each side of the passband. It was this characteristic that permitted the expressions for determining levels in the previous Section [e.g., Eqs. (2) and (18)] to be integrated only over the passband frequency range from f_L to f_U rather than over the infinite range from 0 to ∞.

Practical 1/3-octave-band filters (analog or digital) are designed to comply with the Class II or Class III requirements of national[6] and international[8] standards. Class III requirements are more stringent than Class II requirements. Very few, if any, Class II 1/3-octave-band filters are used to analyze aircraft noise measurements. Most, if not all, of the 1/3-octave-band filters currently being manufactured are designed to meet the ANSI, or IEC, Class III requirements.

The Class III requirements specify such properties as the exact, or design, band-center frequency, the tolerable ripple in the passband, the rejection rate in the stopbands, and the effective noise bandwidth. The effective noise bandwidth defines the relative filter response at the lower

and upper bandedge frequencies such that the filter will transmit the same power as an ideal filter excited by a broadband electrical noise signal having a white noise spectrum.

The analyses in Refs. 9 and 10 showed that the bandwidth error for filtering of white noise was minimized when the relative response of a practical filter was down 4.5 dB at the bandedge frequencies with a passband relative response of 0.0 dB.

Appendix E of ANSI S1.26-1978 contains a discussion of guidelines for evaluating the atmospheric absorption loss of broadband sound analyzed by practical filters. Table E-1 of Appendix E contains an equation which approximates, but is slightly more conservative than, the minimum transmission-response requirements for a Class III filter. [The maximum transmission response is that of an ideal filter.]

The equation for the relative power transfer function, $\tau(f)$, from Table E-I of ANSI S1.26 is

$$\tau(f) = \left\{a + b\left[(ef/f_c) - (ef/f_c)^{-1}\right]^6\right\}^{-1} \qquad (41)$$

and the corresponding expression for the filter transmission loss, in decibels, is

$$T(f) = 10 \log |\tau(f)|. \qquad (42)$$

The constants a, b, and c in Eq. (41) have specific values applicable to the frequency ranges defined for the stopbands and the passband. Values given in Refs. 6 and 8 for b and c were modified slightly in Table E-I of ANSI S1.26 in order to satisfy the requirement for a transmission loss of -4.5 dB at the exact bandedge frequencies.

The coefficients are defined in Table E-I of ANSI S1.26 for Class III 1/3-octave-band filters as:

Filter frequency region	coefficient a	b	c
lower stopband: $0.1 < f/f_c < f_1/f_c$	8/13	2547	$10^{-1/60}$
passband: $f_1/f_c < f/f_c < f_2/f_c$	1	0	—
upper stopband: $f_2/f_c < f/f_c < 10$	8/13	2547	$10^{1/60}$

where the special frequencies f_1/f_c and f_2/f_c define the width of the 0.0-dB transmission-loss region for the passband. The special relative frequencies have the values

$$f_1/f_c = 10^{-1/30} \approx 0.9261 \tag{43a}$$

and

$$f_2/f_c = 10^{1/30} \approx 1.0798. \tag{43b}$$

Using the values for the coefficients given above, the transmission loss in the stopbands at the relative bandedge frequencies $10^{-1/20}$ and $10^{1/20}$ [Eqs. (8) - (10)] has the value of -4.47 dB (or a power transmission ratio of 0.357).

Figure 15 shows comparisons of the transmission response calculated using Eqs. (41) and (42), the minimum transmission loss permitted for ANSI Class III filters, and the transmission response of an ideal filter. Figure 15(a) presents the comparisons on logarithmic scales to emphasize the differences in the filter responses over the two decades of the stopband frequency regions. Figure 15(b) shows the response on linear scales in order to emphasize the differences at frequencies around the special relative frequencies of Eq. (43) and the relative bandedge frequencies at $f/f_c = 0.8913$ and 1.1220. Equations (41) and (42) are seen to provide a good, somewhat conservative, prediction of the minimum ANSI Class III requirements. Note that the curve in Fig. 15(b) for the equation from Table E-1 of Appendix E of ANSI S1.26 crosses the ideal-filter line at a relative power transmission ratio of 0.357.

The point of this discussion has been to clarify the differences between ANSI Class III 1/3-octave-band filter requirements, ideal-filter response, and the filter response predicted by Eqs. (41) and (42). The next issue is how well does the response of actual filters compare with the ANSI requirements or the predictions of Eqs. (41) and (42).

At the present time, most 1/3-octave-band analyses of aircraft flyover noise measurements are made using one of three models of a real-time analyzer having several contiguous filters in parallel: the Hewlett-Packard Model

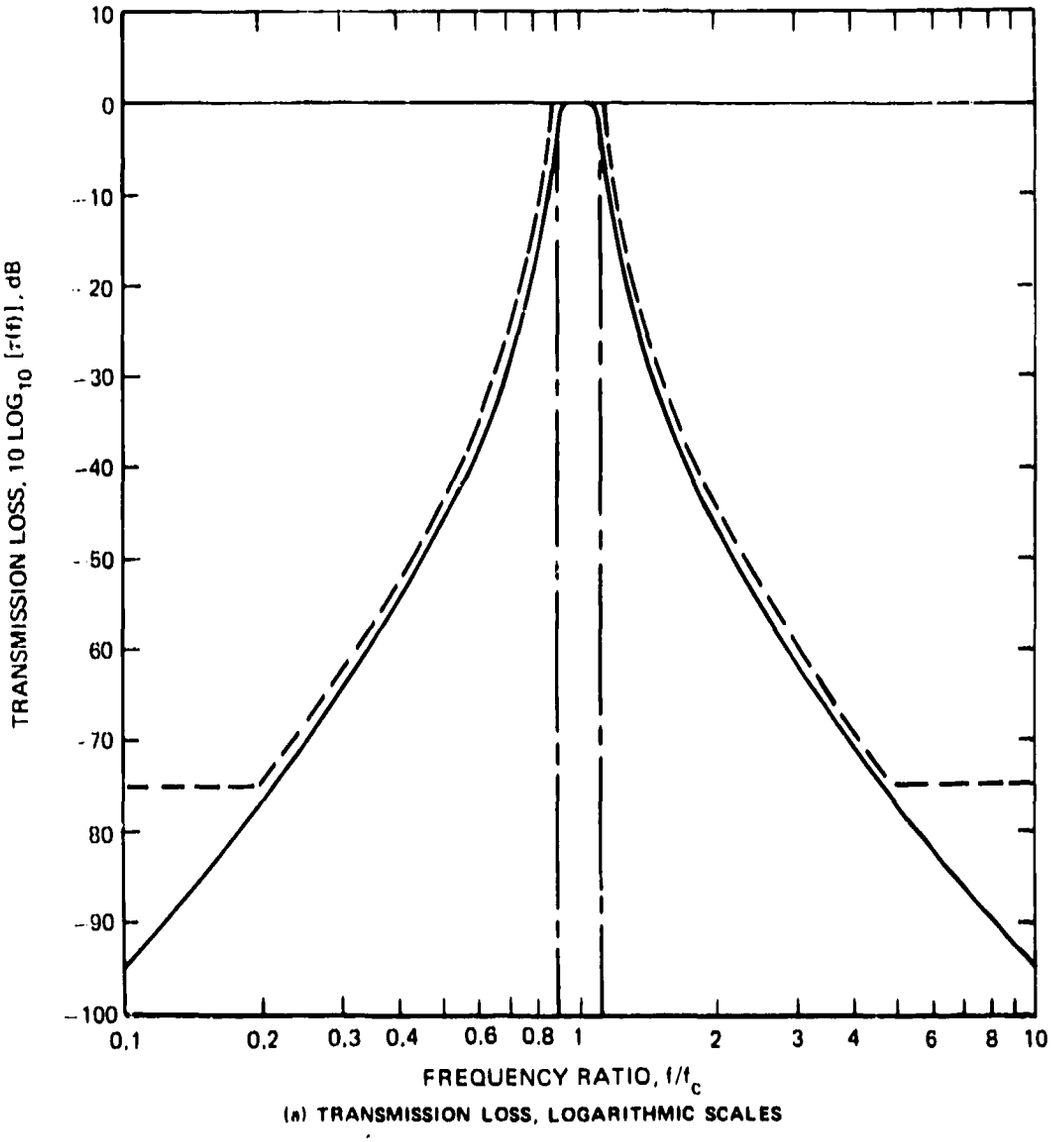

(a) TRANSMISSION LOSS, LOGARITHMIC SCALES

Figure 15.-Power transmission response of 1/3-octave-band filters.

— — — Minimum TL for ANSI Class III; ——— Eqs. (41) & (42) —·— Ideal filter

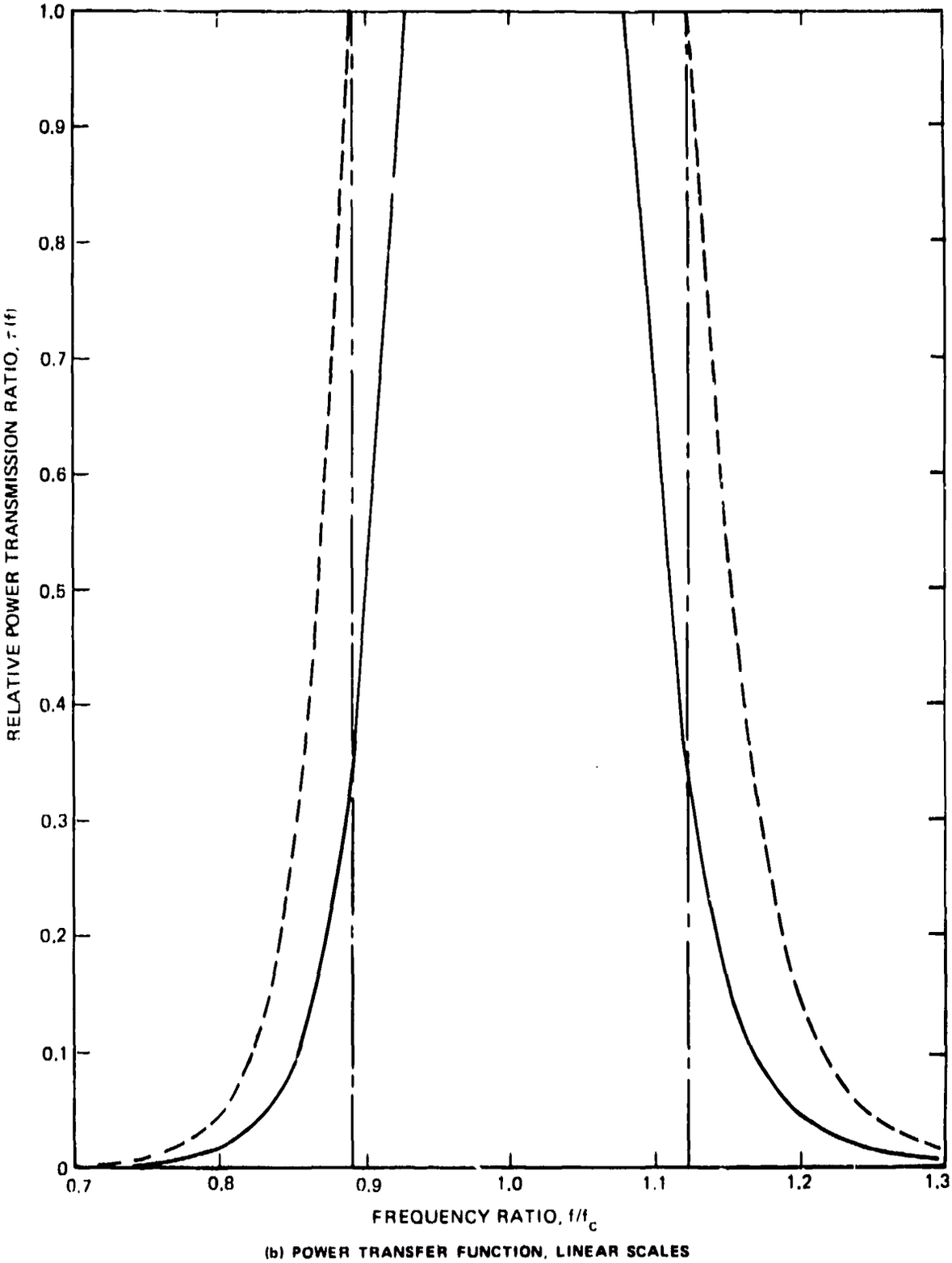

(b) POWER TRANSFER FUNCTION, LINEAR SCALES

Figure 15.-Concluded.

8054A, the Gen Rad Model 1921, and the Brüel and Kjaer Model 2131. Of these three, the GR Model 1921 probably has been the most-widely used.

Response data on a representative sample of each instrument were obtained. Design specification data for the GR 1921 were also obtained and compared with the measured response data.

The HP 8054A and the GR 1921 (which incorporates the GR 1925 multifilter) use analog devices for the filters and, unless carefully adjusted, there can be small differences between the response characteristics of individual filters in a set of contiguous filters as well as between different instruments of the same model. The B&K 2131, however, uses digital filtering and all filters in all instruments should have the same response characteristics.

Figure 16 shows a comparison between typical filter-response data and the response calculated from Eqs. (41) and (42). In the lower-stopband region, the typical response data for all three real-time analyzers are better (by as much as 7 dB) than the response calculated from Eqs. (41) and (42). For the upper-stopband region, the typical response data are either equal to, or slightly better than, the response from Eqs. (41) and (42).

Since the comparisons in Fig. 15 showed that response calculated from Eqs. (41) and (42) was slightly better than the ANSI Class III requirement, and since the typical real-time-analyzer filter-response data were slightly better than the calculations of Eqs. (41) and (42), the actual practical filters must meet the ANSI Class III requirements. Also, the response of an actual 1/3-octave-band filter seems to be very well approximated by Eqs. (41) and (42) using the coefficients listed above. Thus, the typical practical-filter response as predicted from Eqs. (41) and (42) was considered satisfactory for use in calculating sound pressure levels at the receiver location.

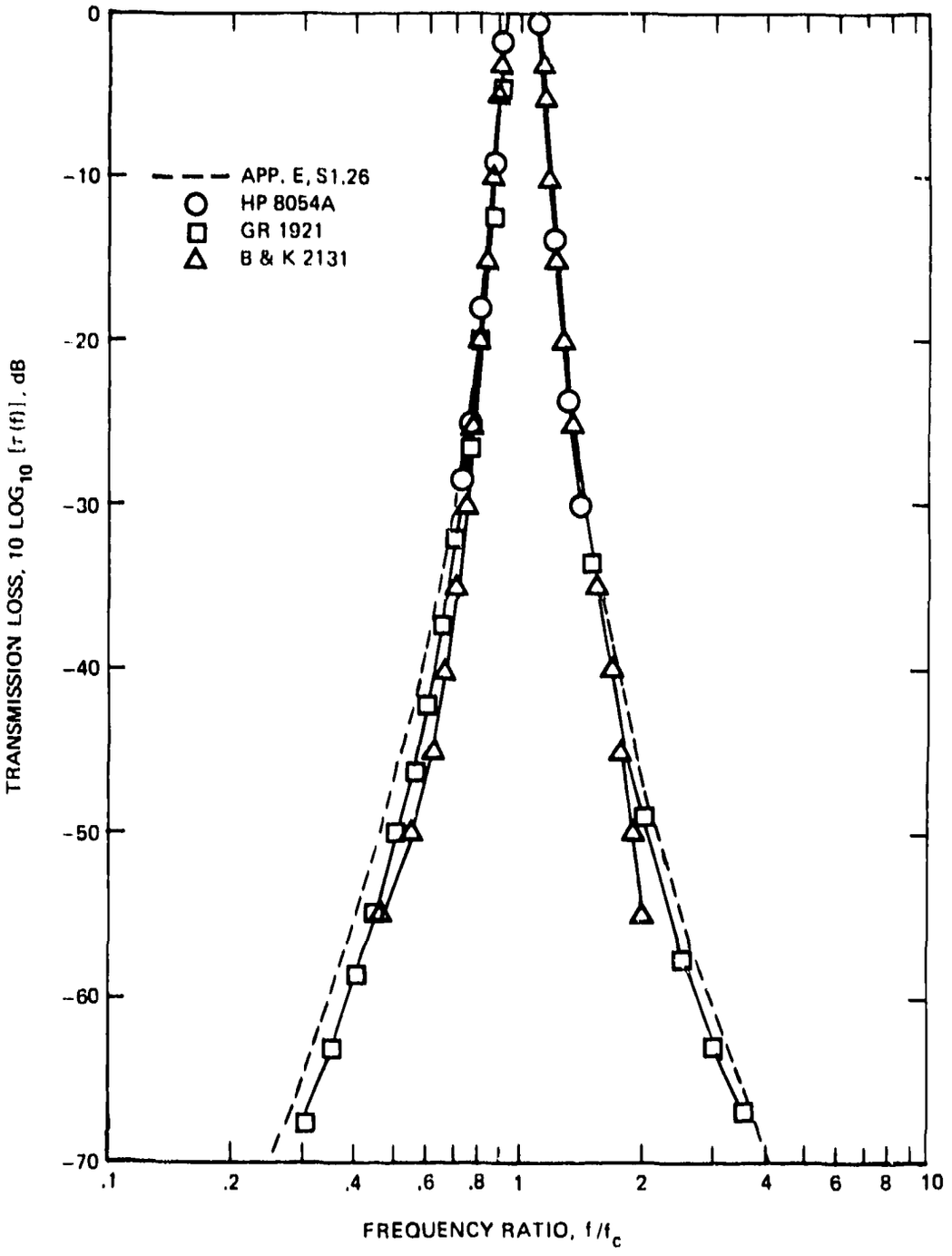

Figure 16.-Transmission-loss response characteristics of 1/3-octave-band filters in real time analyzers compared with response calculated from 'practical-filter' transmission-response equation; f_c is band center frequency.

Spectra at the Source

In order to calculate the 1/3-octave-band sound pressure levels at the receiver it was necessary to modify the sound pressure spectrum at the source from that used in the previous Section.

The power spectrum of the pressure shown in Fig. 1 would, theoretically, apply to any frequency. For ideal filters there was no concern about contributions at frequencies outside the passband because of the infinite rejection in the stopbands. A practical filter, however, can have significant contribution from the stopbands and therefore it was necessary to modify the low-frequency portion of the source spectrum. There was no need to be concerned about the high-frequency portion of the source spectrum since the high-frequency spectral slopes were all negative, or at most, flat. The decreasing high-frequency pressure spectrum in combination with the decreasing high-frequency filter response assured minimal, or negligible, upper-stopband contributions.

Since from Figs. 15 and 16 the low-frequency part of the lower-stopband response has an effective slope of about -7 to -8 dB/band, any sound pressure spectrum that increases in the lower-stopband region of a filter by more than +8 dB/band will ultimately transmit power faster than the filter can reject it. In such a situation, the power from the lower-stopband region can exceed that from the passband. The converse, of course, could be true for the upper-stopband region and indefinitely rising sound pressure spectra.

To preserve a sense of realism in the calculations, the sound pressure spectra of Fig. 1 were extended down to the lower bandedge frequency at one band below the band centered at 1000 Hz, i.e., using Eqs. (7), (9), (1), and (11), down to a frequency given by $10^3 \cdot RF^{-1} \cdot RF^{-0.5} = 10^{2.85} \approx 707.946$ Hz. Below $10^{2.85}$ Hz, the pressure spectra were maintained at a constant value defined by the value of the pressure spectrum at $10^{2.85}$ Hz. A flat, low-frequency pressure spectrum (rather than a decreasing one) was selected because many jet-powered aircraft have rather-flat low- and mid-frequency spectra.

Figure 17 shows the source spectra that were developed on the basis of the preceding analysis. The absolute value of the pressure spectral density

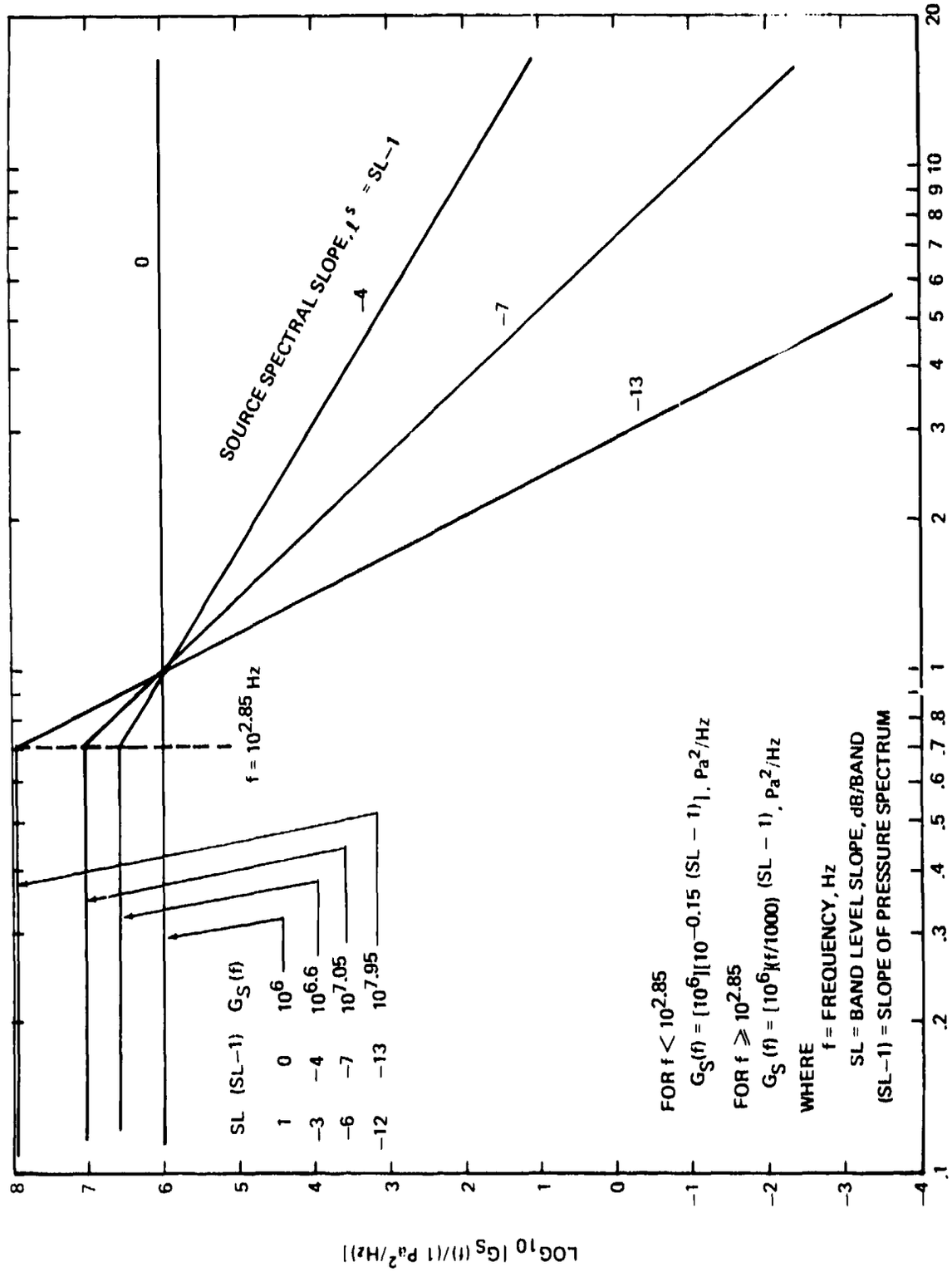

Figure 17.-Power spectra of the sound pressure at the source for calculations of band levels at the receiver with 'practical' rather than ideal filters.

at 1000 Hz has the same value (10^6 Pa^2/Hz) as used in Fig. 1 for the ideal-filter calculations. The values of $G_S(f)$ at frequencies below $10^{2.85}$ Hz are given on the figure.

The 1/3-octave-band sound pressure levels at the source, LS, are the same as shown in Fig. 2 for the 11 bands between 1000 and 10,000 Hz. There is no change in the true source band levels because the actual filters are considered to be located only at the receiver. The true source band levels are always those that would be obtained with ideal filters.

Spectra at the Receiver

Ignoring, as in the previous Section, any change in the amplitude of the sound pressure as a result of spreading the source's acoustic power over increasingly larger surface areas as propagation proceeds from the source to the receiver, the band levels at the receiver location were calculated using the same basic Fourier transform relation as was used in Eq. (18) but including the filter power transfer function $\tau(f)$ from Eq. (41) and integrating over all positive frequencies.

Thus, with the response of a practical filter at the receiver, the band levels are, theoretically, to be found from

$$LR = 10 \log \left\{ \left[\int_0^\infty |G_R(f)|\,|\tau(f)|\, df \right] / p_{ref}^2 \right\} \qquad (44)$$

where $G_R(f)$ is still related to the source spectrum $G_s(f)$ [as defined in Fig. 17] by Eq. (17) and $\Delta F(f)$ is still determined by Eq. (21) for uniform atmospheric conditions.

The transmission response of a practical filter is defined, as noted above, over the frequency range from $f/f_c = 0.1$ to $f/f_c = 10.0$. At the stopband limiting frequencies, the response is down approximately 94 dB (or by a factor of $10^{-9.4}$) from the response at the band center frequency, see Fig. 15(a).

With the limitation on the frequency range of applicability associated with the choice of the definition of $\tau(f)$ from Table E-I of ANSI S1.26-1978

and making use of Eqs. (1), (17) and (21), the working expression for the sound pressure level at the receiver in some 1/3-octave-band can be written as

$$LR = 10 \log \left\{[G_S(f_c)]/p_{ref}^2\right\} + 10 \log \left\{\int_{f_c/10}^{10f_c} \left[(f/f_c)^{\ell^S}\right]\left[10^{-[a(f)][PD/10]}\right]\left[\tau(f)\right] df\right\} \quad (45)$$

which can be compared with Eq. (22) for ideal filters.

The integral in Eq. (45) must be evaluated numerically. The QSF numerical-integration subroutine was again selected to perform the evaluation.

One way of accomplishing the evaluation would be to adopt the approach used in Ref. 3 and break the frequency range into three parts: lower stopband, passband, and upper stopband. Each subrange would be further divided into a number of intervals and the contributions from each subrange calculated separately.

The contribution in the passband from f_1/f_c to f_2/f_c, see Eq. (43), would be calculated first and used to define a reference value. Then the contribution from each stopband would be calculated -- that from the upper stopband proceeding from f_2/f_c to $f/f_c = 10$, and that from the lower stopband proceeding toward lower frequencies from f_1/f_c to $f/f_c = 0.1$. The advantage of this approach is that the passband reference value can be used to define a convergence test which can be used to shorten computation time. At each step over the intervals in the stopbands the calculated value of the integrand can be compared with a specified fraction of the passband reference value (1/1000th of it, for example) and the calculations can be terminated when an integrand value becomes less than the specified fraction of the passband reference value.

Breaking the integration range into three subranges and making use of some type of convergence test would save computation time, especially for the upper stopbands where the absorption function decreases with increasing

frequency for propagation from the source to the receiver and where the sound pressure spectrum function $(f/f_c)^{\ell^s}$ also decreases with increasing frequency for three out of the four values selected for ℓ^s. The convergence test is based on a predetermined judgment of when to stop the integration. The judgment is based on the assumption that the next, and subsequent, contribution in the stopband only provides a negligible amount to the total value of the integral.

The 3-subrange/convergence-test procedure of Ref. 3 was not used to evaluate Eq. (45) because the effort needed to define a meaningful convergence test would have exceeded the savings in computation cost. Also, for many cases examined here, the contribution at successive steps over the lower stopband became successively larger rather than smaller because the product of the pressure-spectrum function and the absorption function increased faster than the filter transmission function decreased. Indeed, for one of the atmospheric conditions examined and for the band centered at 10,000 Hz with a source slope of -12 dB/band, the value of the integrand at the end of the lower stopband at $f = f_c/10 = 1000$ Hz was larger by a factor of approximately 3×10^{11} than it was at the band center frequency.

The procedure that was adopted was the straightforward approach, similar to that used in evaluating Eqs. (22) and (29), in which the entire frequency range, $10f_c - (f_c/10)$, was just divided into a number of intervals and the numerical integration by the QSF subroutine proceeded directly from $f_c/10$ to $10f_c$ for each band.

After some experimentation, the values tabulated below were selected to subdivide the frequency ranges for the eleven bands. The frequency step-sizes over the frequency range for any band are comparable to those used over the passband frequency ranges of the ideal filters in the previous Section. There are, however, 9911 frequencies at which calculations are required here for the 11 bands compared with 231 for ideal filters. The computation time was on the order of 8 times longer for evaluations of Eq. (45) than for Eq. (22).

Nominal band center frequency, Hz	Approx. frequency range $10f_c - (f_c/10)$, Hz	Number of intervals, N	Approx. frequency stepsize Δf = range/N, Hz
1000	9900.00	400	24.75
1250	12,463.36	500	24.93
1600	15,690.44	600	26.15
2000	19,753.10	700	28.22
2500	24,867.68	800	31.08
3150	31,306.55	900	34.79
4000	39,412.61	1000	39.41
5000	49,617.54	1100	45.11
6300	62,464.78	1200	52.05
8000	78,638.50	1300	60.49
10,000	99,000.00	1400	70.71

Some results are presented in Figs. 18 and 19 to show the impact of including the filter transmission response of Eq. (41) in the determination of band levels at the receiver. Figure 18 shows 1/3-octave-band sound pressure levels for the 300-m pathlength and the 70-percent relative-humidity condition; Fig. 19 also shows data for the 300-m pathlength but for 10-percent relative humidity. Data for the four true spectral slopes at the source are included in each figure. For each source slope, comparisons are shown between the exact source band levels, the exact receiver band levels calculated with ideal filters, and the receiver band levels calculated with the response of the practical filter.

In Fig. 18 for 70-percent relative humidity, there is little difference between the exact and the practical-filter receiver band levels for source slopes of +1, -3, and -6 dB/band, except for the 10-kHz band and the -6 dB/band slope.

For the -12 dB/band slope, however, significant differences start to occur in the 2.5-kHz band and become very large in the 10-kHz band. The practical-filter band levels exceed the ideal-filter receiver band levels

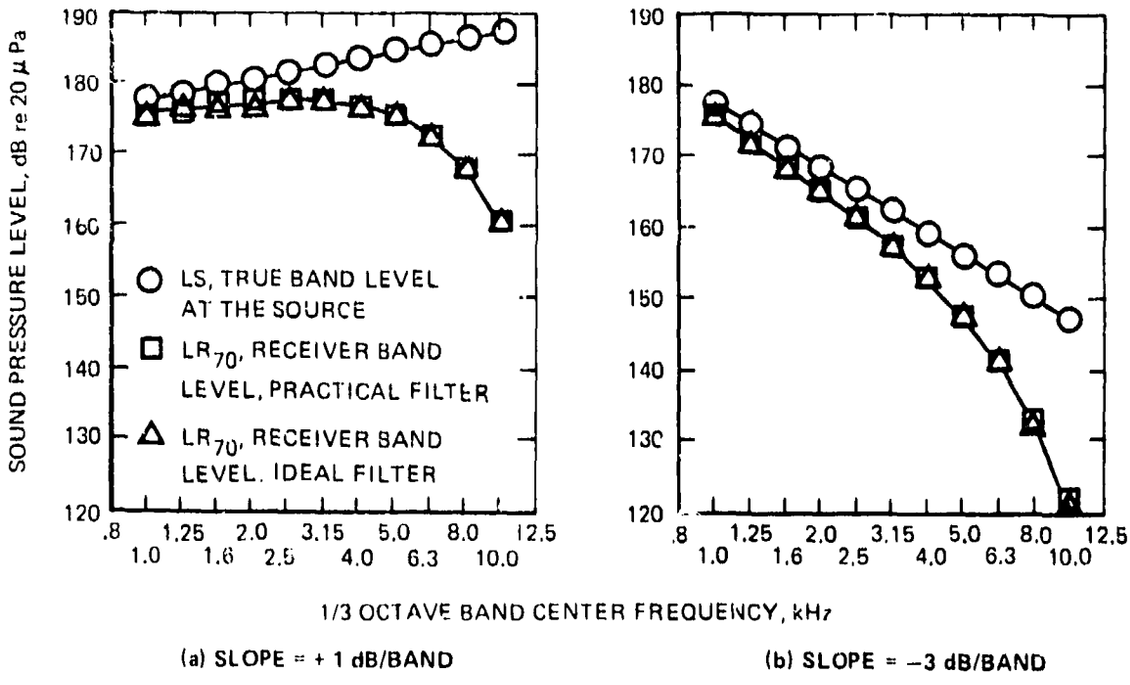

Figure 18.-Effect of filter characteristics on band level at the receiver for various slopes of the sound pressure level spectrum at the source. 300-m sound propagation pathlength; 70 % relative humidity; 25 °C air temperature; 1.0 standard atmospheric air pressure.

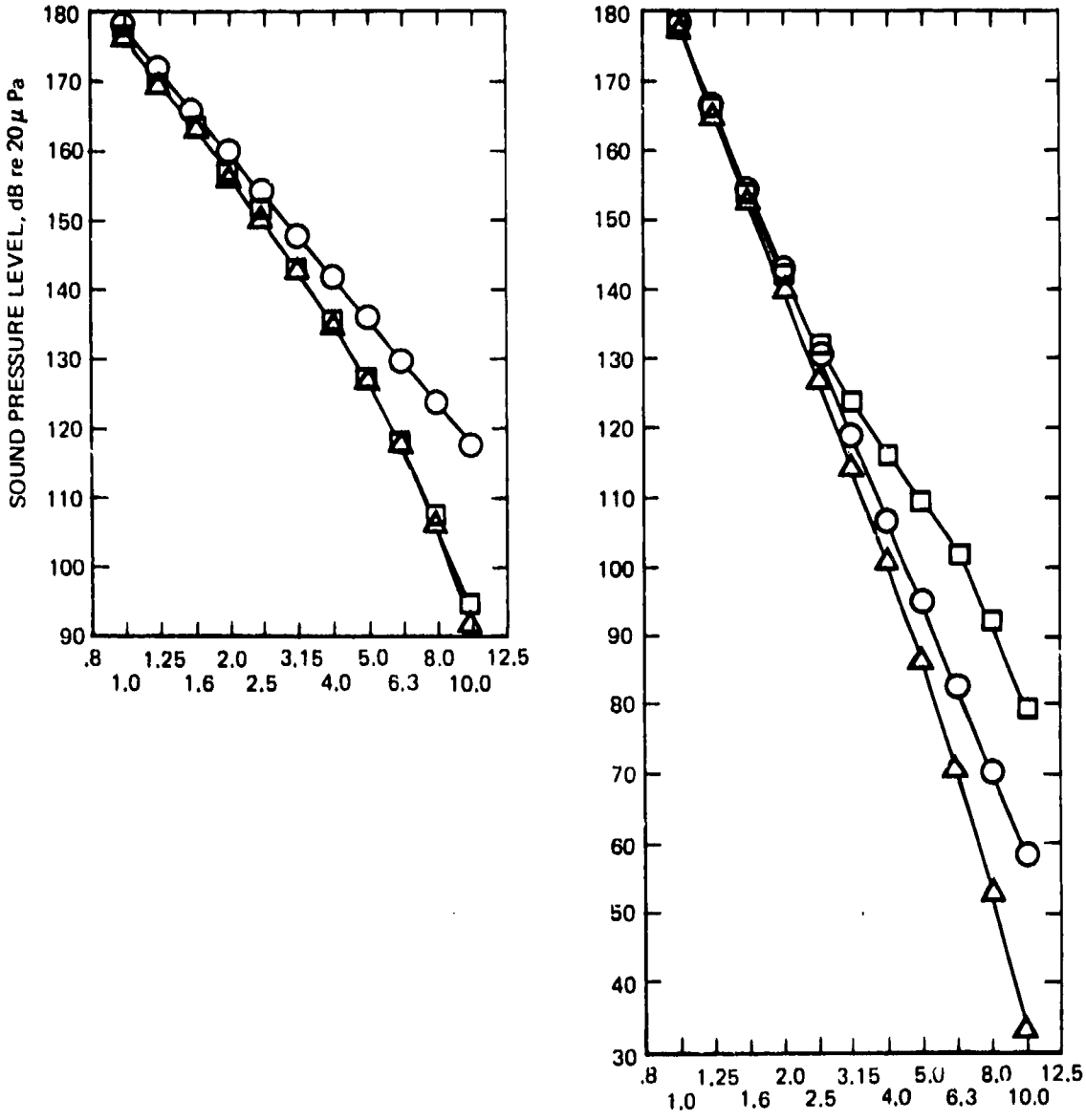

(c) SLOPE = −6 dB/BAND

(d) SLOPE = −12 dB/BAND

Figure 18.-Concluded.

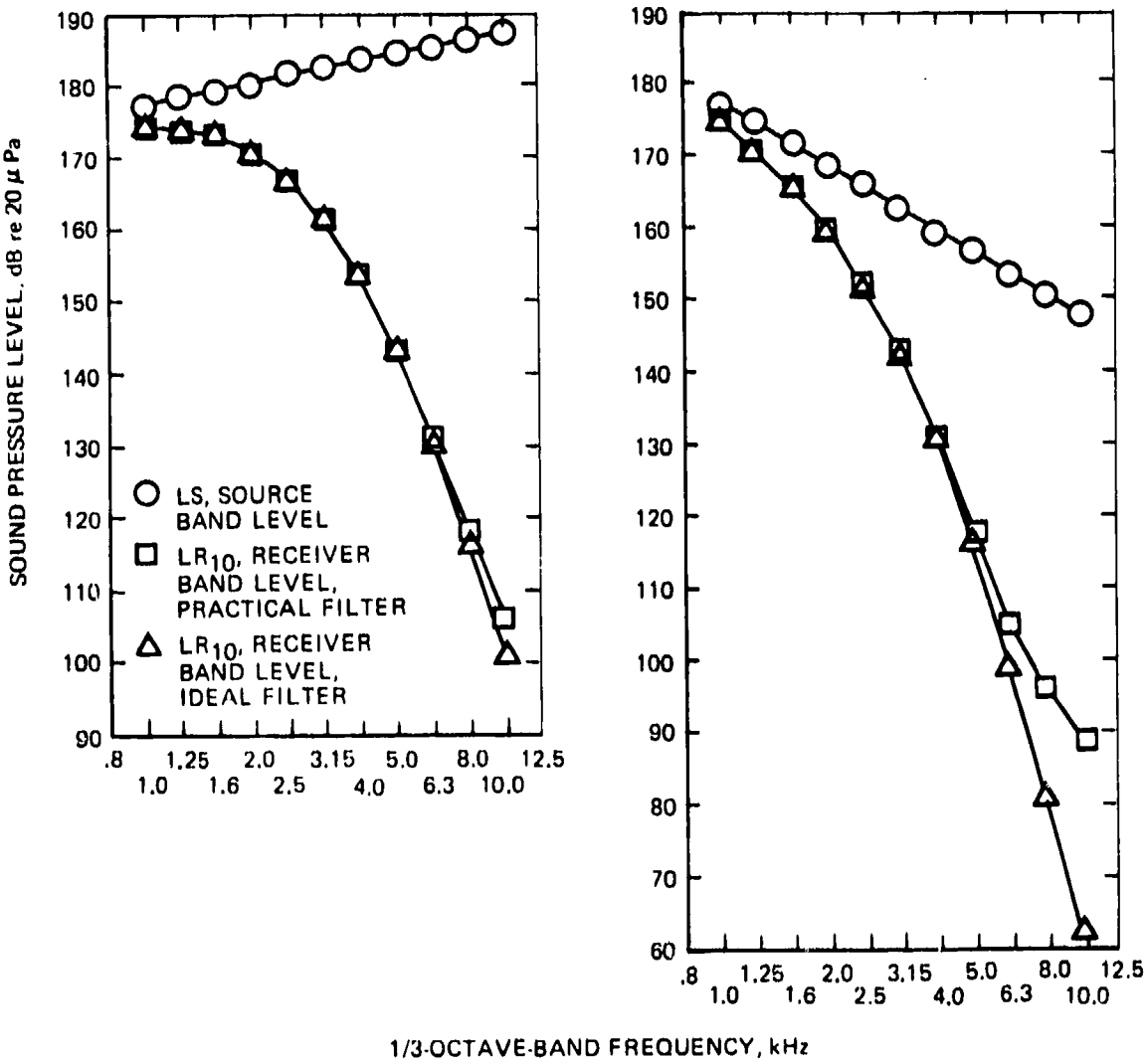

Figure 19.- Same as Fig. 18, except 10% relative humidity.

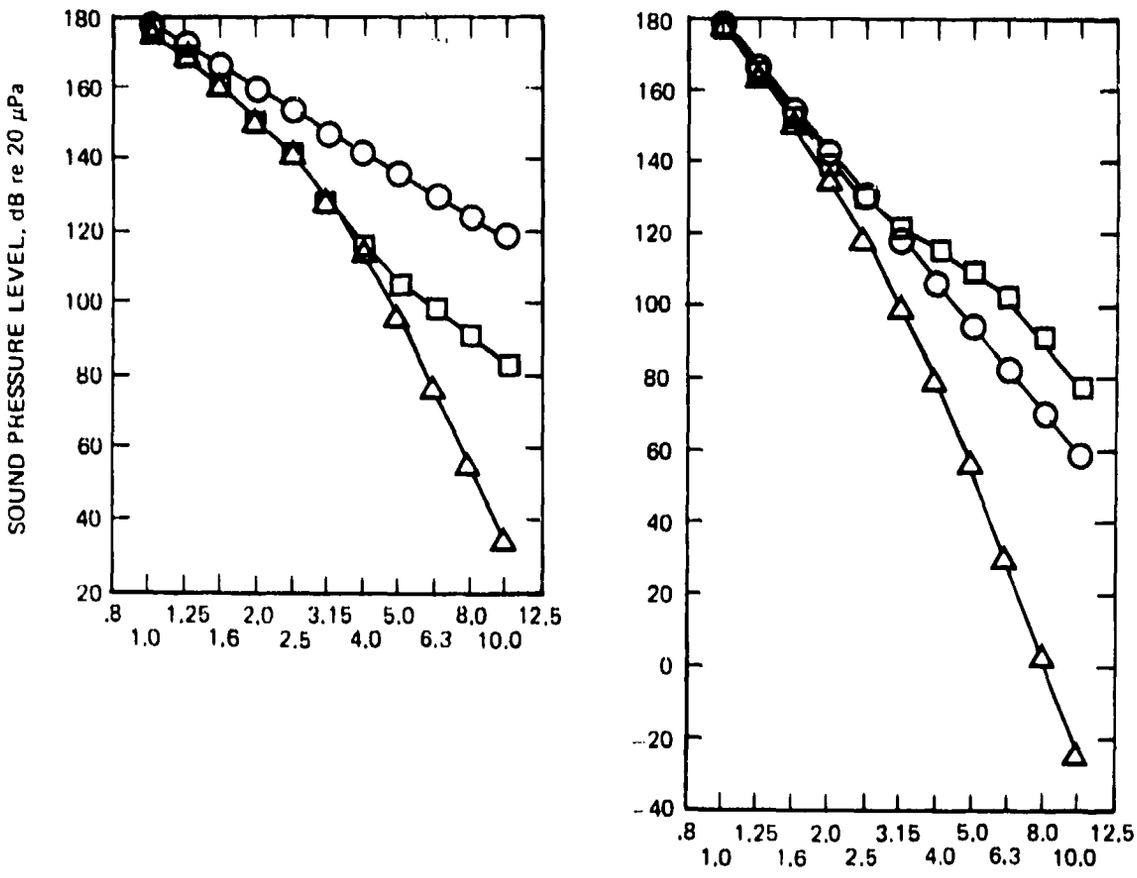

(c) SLOPE = −6 dB/BAND

(d) SLOPE = −12 dB/BAND

Figure 19.-Concluded.

and indeed even exceed the source band levels! In the 10-kHz band, for example, the practical-filter receiver band level exceeds the source band level by about 20 dB and the ideal-filter receiver band level by about 45 dB.

For the highly-absorptive 10-percent relative-humidity conditions of Fig. 19, the situation is substantially more critical than it was for the 70-percent reference-day conditions of Fig. 18. Note that whereas it was feasible to use an ordinate scale with 10-dB per major division for all plots in Fig. 18, it was necessary to use both 10-dB and 20-dB per major division in Fig. 19 because of the much-steeper slopes over the lower stop-band under the more-absorptive conditions.

As the source spectral slope became more and more negative, the deviation between the practical-filter and the ideal-filter receiver band level occurred at a lower and lower frequency: 6.3 to 4.0 to 3.15 to 1.25 kHz as the source slope changed from +1 to -3 to -6 to -12 dB/band.

For comparison with the example quoted above for the 70-percent condition, the -12 dB/band slope data in Fig. 19 show that the practical-filter receiver band level in the 10-kHz band exceeds the source band level by about 19 dB but exceeds the exact receiver band level by 104 dB compared with 45 dB in Fig. 18(d).

The message from these results is that high-frequency 1/3-octave-band sound pressure levels, measured at a receiver location with a filter meeting the most-stringent ANSI requirements, may differ from the expected band levels by significant amounts depending on how steep was the slope of the spectrum of the noise source and how absorptive was the atmosphere.

The results in Figs. 18 and 19 showed the effect on the band levels at the receiver of increasing the spectral slope at the source for a fixed propagation distance of 300 m. If the propagation distance were to be increased, then similar, but more-pronounced, trends would be expected.

Figures 20 and 21 present comparisons in the format of Figs. 18 and 19 for propagation distances of 300, 600, and 900 m. Figure 20 presents results for a source spectral slope of +1 dB/band, Fig. 21 for a slope of -12 dB/band. Each plot in Figs. 20 and 21 includes the band levels at the source and the band levels at the receiver for 70 and 10-percent relative humidities and for ideal and practical 1/3-octave-band filters.

For the +1 dB/band-slope results in Fig. 20, there was no significant difference between the exact receiver band levels and those with the practical filter when the atmospheric absorption had the minimal values associated with 70-percent relative humidity at 25° C air temperature. The largest difference was only about 8 dB in the 10-kHz band for the 900-m pathlength.

For the 10-percent relative-humidity, highly-absorptive atmospheric conditions, however, there were large differences between the exact and the practical-filter receiver band levels. For a given band center frequency (e.g., 10 kHz), the difference increased as the pathlength increased. The frequency, at which the difference between the exact and the practical-filter band level first becomes significant, decreases as the pathlength increases.

For the 10-percent relative-humidity data in Fig. 20, there appeared to be a saturation-like effect that occurred for the high-frequency receiver band levels for the 600 and 900-m pathlengths. Apparently, the power transmitted through the lower stopband becomes more and more the controlling factor in the total power transmitted as the absorption function steepens with increasing pathlength. As an example, consider the 10-kHz band where the practical-filter band level only decreased about 8 dB for the 10-percent relative-humidity conditions between the 600 and 900-m pathlengths. The corresponding difference in exact band levels was about 82 dB. For the 70-percent conditions, the receiver band level decreased by 18 and 24 dB for the practical and ideal filters, respectively. Thus, the level for the 10-percent condition should have decreased by much more than 8 dB.

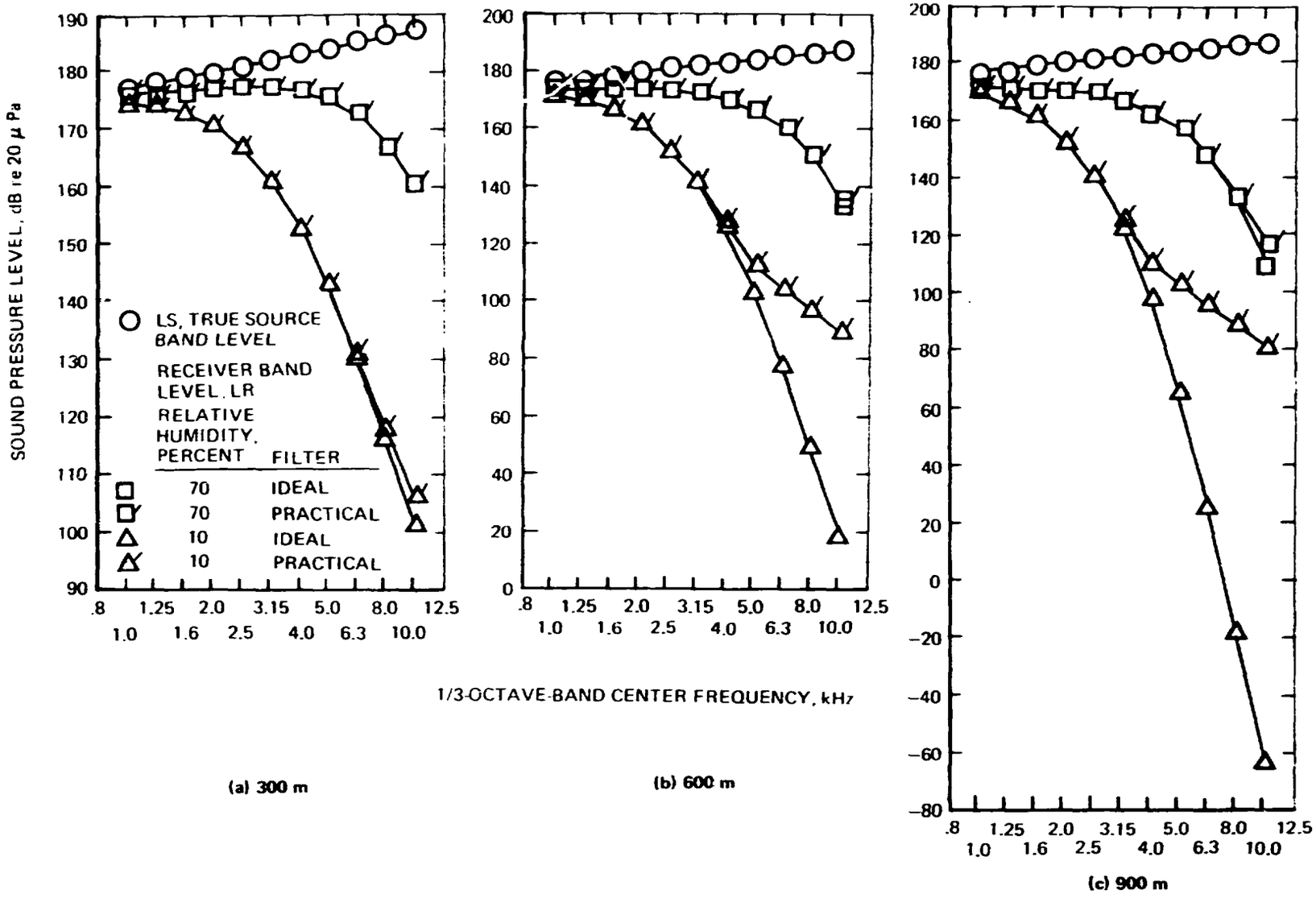

Figure 20.-Effect of filter transmission response characteristics on band level at the receiver for three sound propagation pathlengths, two relative humidities, and a slope of the sound pressure level spectrum at the source of +1 dB/band. 25°C air temperature; 1.0 standard atmosphere air pressure.

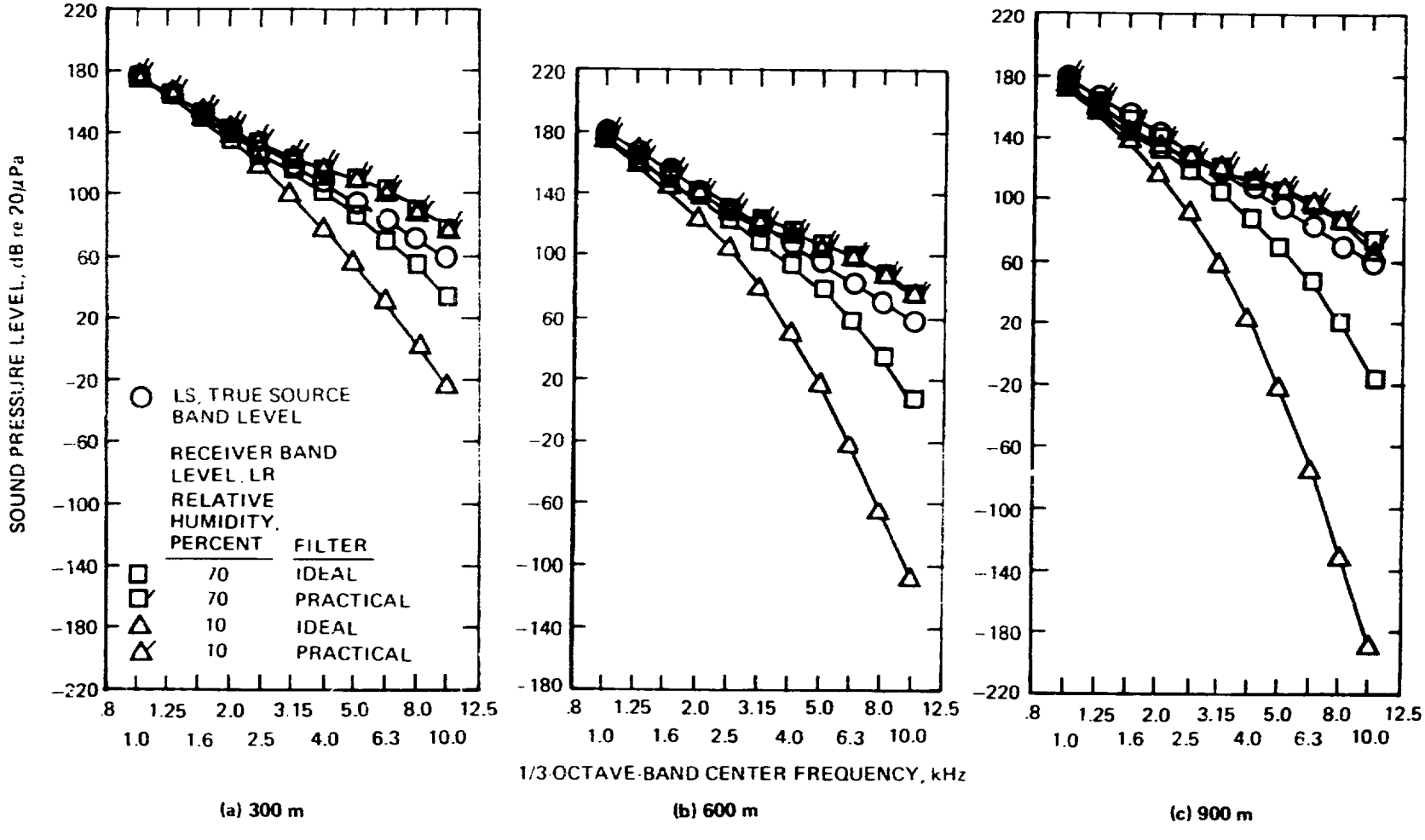

Figure 21.-Same as Fig. 20, except slope of sound pressure level spectrum at the source is −12 dB/band.

It is noted that presumably valid measurements of aircraft flyover noise spectra for relatively absorptive conditions have been reported which have a high-frequency "tail off" similar in appearance to those shown in Figs. 20(b) and 20(c) for the 10-percent relative-humidity condition. The suggestion is that the reported levels, which were said to be well above the corresponding background noise levels, may not be valid because of contamination by power transmitted through the lower stopbands of the practical filters used in analyzing the tape-recorded signals.

The results presented in Fig. 21 show additional evidence of a saturation-like effect when the source slope is -12 dB/band. The receiver band levels, as in Figs. 18(d) and 19(d), are higher, instead of lower, than the source band levels in the high-frequency bands. There was essentially no difference between the practical-filter band levels for the 70 and the 10-percent conditions for any of the three pathlengths. In contrast, the difference between the exact receiver band levels for the 70 and 10-percent conditions was large, as expected, and increased as the pathlength increased. Note that an ordinate scale with 40 dB per division was required for the data in Fig. 21 compared with 10 or 20 dB per division for the data in Fig. 20.

The inference drawn from the data in Fig. 21, and from the comparisons in Figs. 18(c), 18(d), 19(c), and 19(d), is that once either the receiver spectral density function, or the absorption function, or their product, starts to increase faster than the filter lower-stopband response decreases, as the integration proceeds from the passband toward the lowest defined frequency at $f_c/10$, then the band levels at a receiver location which would result from using a practical filter meeting ANSI Class III requirements will be higher than the expected or exact values and by very large amounts for some conditions. Indeed, if, as in Fig. 21, the source slope is as steep as -12 dB/band, then the receiver band levels indicated for the response of a practical filter can become essentially independent of how absorptive the atmosphere is or how long the propagation path is. There were differences between the practical-filter receiver band levels for the 70 and 10-percent conditions and for the three distances, but they were small and are hard to see with a 40-dB-per-division scale.

Two corollaries follow from the above inference. The first is that aircraft-noise data-analysis systems in current use may not be able to provide meaningful measurements of high-frequency 1/3-octave-band sound pressure levels if the noise source spectrum is too steep, or the atmosphere is too absorptive, or the propagation path too long. The second is that attempts to use measured aircraft noise 1/3-octave-band sound pressure levels to derive, or verify, the high-frequency absorption characteristics of the atmosphere may not be feasible and could lead to incorrect conclusions.

The differences between the practical- and ideal-filter receiver band levels could also affect the validity of attempts to adjust measured data from test-to-reference conditions, as well as attempts to use measured aircraft noise data to validate or develop aircraft-noise-prediction methods or to judge the effectiveness of high-frequency noise-suppression devices installed in an engine. Analyses of nonlinear propagation effects and the effects of atmospheric turbulence on sound propagation may also be influenced by the use of practical-filter band levels that are higher than the corresponding ideal-filter band levels.

The potential problems introduced by the response characteristics of practical filters as well as possible solutions, would clearly seem to be areas deserving additional study.

Test-to-Reference-Day Band-Level Adjustment Factors

Although the results were expected to be much different than those obtained using the exact or true band levels at the receiver, it was considered that it would be instructive to use the receiver band levels calculated for the response of a practical filter in determinations of band-level adjustment factors from test to reference atmospheric conditions.

Determinations of adjustment factors would use the analysis described in the previous Section. The "measured" band levels would be assumed to have the values that would have been obtained with ideal filters. Integra-

tion would only cover the frequency range from the exact lower-bandedge to the exact upper-bandedge frequency. The 2-slope procedure would be used to approximate the pressure spectral density function over the frequency range of each ideal-filter passband.

This calculation procedure was felt to simulate the procedure that would likely be used in practice where, in general, there would be no *a priori* knowledge about whether the indicated band levels were or were not contaminated by excessive power transmitted in the stopband frequency ranges. The calculation procedure described above was felt to be especially applicable as a simulation of the procedure that would be used by an automated data-processing system which only provides limited opportunity for operator intervention and inclusion of human judgment concerning the validity of a particular step in the calculation process.

Figure 22 shows the results of applying the procedure described above to the case of a 600-m propagation distance and a -12 dB/band source spectrum slope. Comparable results for ideal filters at the receiver were given in Fig. 13. The practical-filter receiver band levels in Fig. 22 are those from Fig. 21(b). Symbols and their subscripts have meanings as described previously; PF stands for practical filter.

Source band levels, calculated from the practical-filter receiver band levels for 10-percent relative humidity, were determined for test (i.e., 10 percent) and reference (i.e., 70 percent) atmospheric conditions. The calculated source levels have the symbols $LS_{10,10,PF}$ and $LS_{70,10,PF}$ and their difference, as before, is a measure of the band-level adjustment factor to account for differences in attenuation caused by atmospheric absorption under the two conditions. The source band levels were calculated using the band-integration method and the QSF numerical-integration subroutine.

The other measure of the band-level adjustment factor is the difference in the values that were calculated for the receiver band levels starting from the exact source spectrum, or $LR_{70,PF} - LR_{10,PF}$. This difference can be interpreted as representing the "measured" value of the test-to-reference-day adjustment factor; the difference in source levels can be taken as representing the "calculated" value of the adjustment factor.

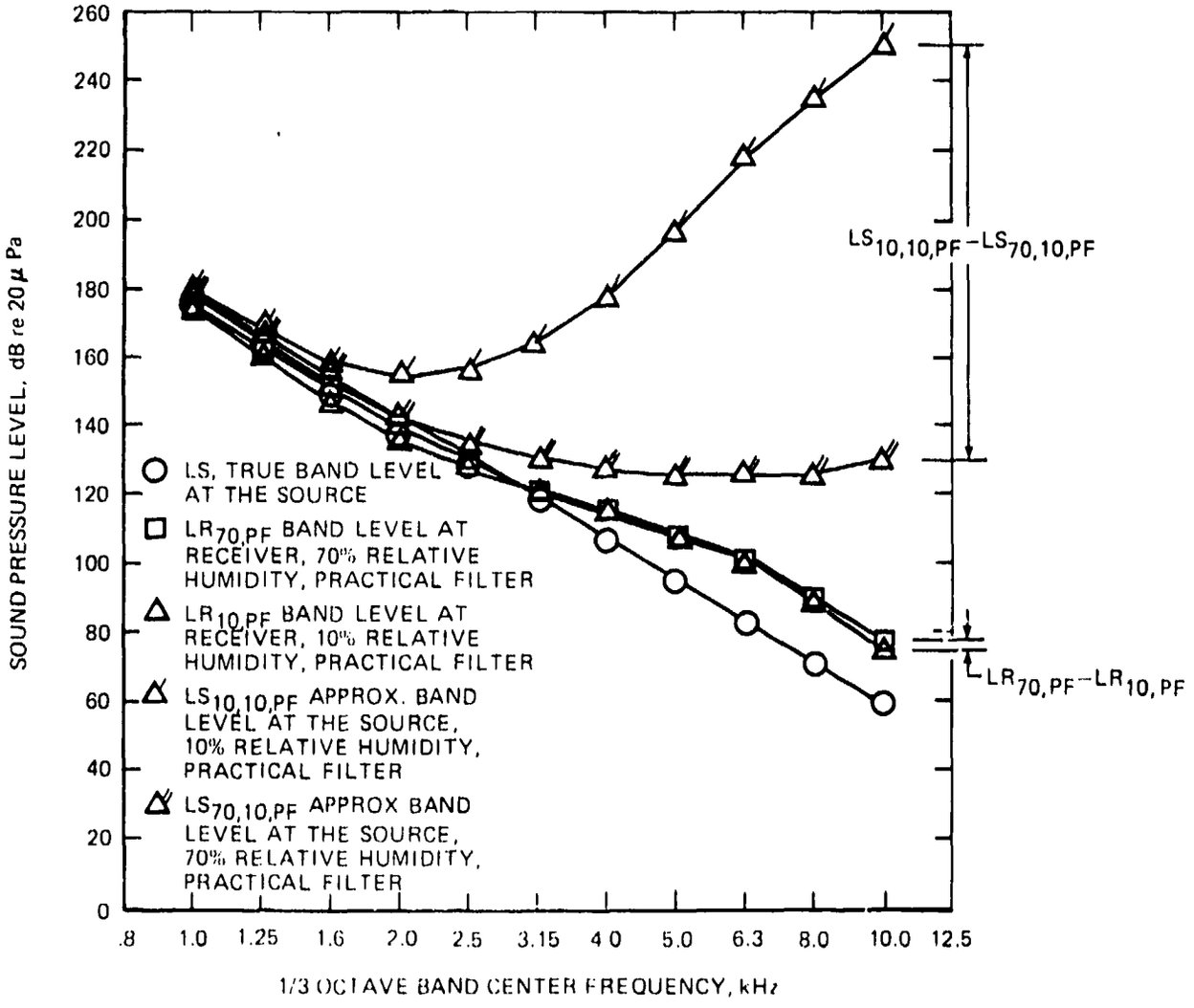

Figure 22.-Determination of band-loss adjustment factors when band levels at the receiver location are calculated with the filter transmission-response characteristics of the practical filters from Fig. 15; compare with results for ideal filters in Fig. 13.
25°C air temperature; 1.0 standard atmosphere air pressure; −12 dB/band spectral slope at the source; 600-m sound propagation pathlength; integration method for absorption loss.
Band-loss adjustment factor from levels at the source(integrating over passband of ideal filters) is $(LS_{10,10,PF}-LS_{70,10,PF})$.

Band-loss adjustment factor from levels at the receiver is $(LR_{70,PF}-LR_{10,PF})$.

Difference here, for 10 kHz band, is (250.2−129.9)−(77.0−74.1) = 120.3−2.9 = 117.4 dB.

Using the 10-kHz band for an example, as before, the results in Fig. 22 indicate that the difference in calculated source levels is a reasonably accurate measure of the true difference in atmospheric absorption under the two conditions. From the data in Fig. 22, the difference is $LS_{10,10,PF}$ - $LS_{70,10,PF}$ = 250.2 - 129.9 = 120.3 dB compared with the exact value of 115.8 dB from Fig. 13.

The adjustment factor determined from the difference in practical-filter receiver band levels is much different than the difference in source levels because of the lower-stopband contamination problem. Thus, using data from Fig. 22, $LR_{70,PF}$ - $LR_{10,PF}$ = 77.0 - 74.1 = 2.9 dB in the 10-kHz band.

Therefore, if the practical-filter "measured" receiver band levels for test and reference conditions were to be used to assess the accuracy of determining band-level adjustment factors, the results in Fig. 22 would indicate a huge error. In the 10-kHz band, the above calculations indicate that the error would be 120.3 - 2.9 = 117.4 dB for the 600-m pathlength and -12 dB/band source spectrum slope.

In addition to the extreme value of the calculated error, use of the contaminated practical-filter receiver band levels to estimate the source levels results in a severe distortion of the true shape of the source spectrum and exceedingly large indicated source band levels as shown in Fig. 22. It is noted that calculations of "source" spectra have appeared in the literature with shapes very similar to those shown by the $LS_{70,10,PF}$ and $LS_{10,10,PF}$ spectra in Fig. 22. The suggestion is that, although the calculated attenuation caused by atmospheric absorption may be approximately correct, the adjustment factor has been applied to contaminated, or incorrect, receiver band levels.

To complete the analysis of test-to-reference-day band-level adjustment factors as applied to sound pressure levels at the receiver which were determined using the response curve of a practical filter, it was decided to examine the differences between the calculated source band levels ($LS_{10,10,PF}$ - $LS_{70,10,PF}$) and the calculated receiver band levels ($LR_{70,PF}$ - $LR_{10,PF}$). Analyses were carried out for the two source spectral

slopes of +1 and -12 dB/band ed for the three propagation distances of 300, 600, and 900 m. As in Section 2 for the analyses using ideal filters, adjustment factors were calculated by the band-integration metho' and the band-center-frequency method for the eleven bands with center freque from 1000 to 10,000 Hz.

Figure 23 shows the results of the analyses. Comparable ideal-filte results were presented i Fig. 14. Note that the ordinate scale in Fig. 23(c) is diff nt from that in Figs. 23(a) and 23(b).

The "error" in the calculation of the band-level adjustment factor is seen to be small to egligible from 1000 Hz to some frequency and then to increase very rapidly. The largest errors in Fig. 23 are bigger by a factor of 15 to 20 than the largest errors in Fig. 14 for receiver levels calculated with filters having ideal response characteristics. The frequency where the error starts to increase corresponds to the frequency where the practical-filter receiver band levels start to deviate from the ideal-filter receiver band levels as seen by comparing the results in Figs. 20 and 21 with the error analyses in Fig. 23.

Aside from the difference in the shape of the curves and the very large difference in the magnitude of the results, the other major difference between the ideal-filter results in Fig. 14 and the practical-filter results in Fig. 23 is that in Fig. 23 the "error" in calculating the band-adjustment factor is somewhat larger by the band-integration method than by the band-center-frequency method. The reasons the band-center-frequency method gave relatively smaller indications of error than it did in Fig. 14 is probably because the spectrum of the sound pressure at the receiver, that was calculated for the practical filters, is significantly less steep than the spectrum calculated using ideal filters, see Figs. 20 and 21.

The differences shown in Fig. 23 between the two methods are not regarded as significant, however, because the basis for the comparisons (the so-called measured adjustment factor or difference between reference-day and test-day receiver band levels) is obviously not correct in many bands as can be seen by inspection of the data in Figs. 20 and 21.

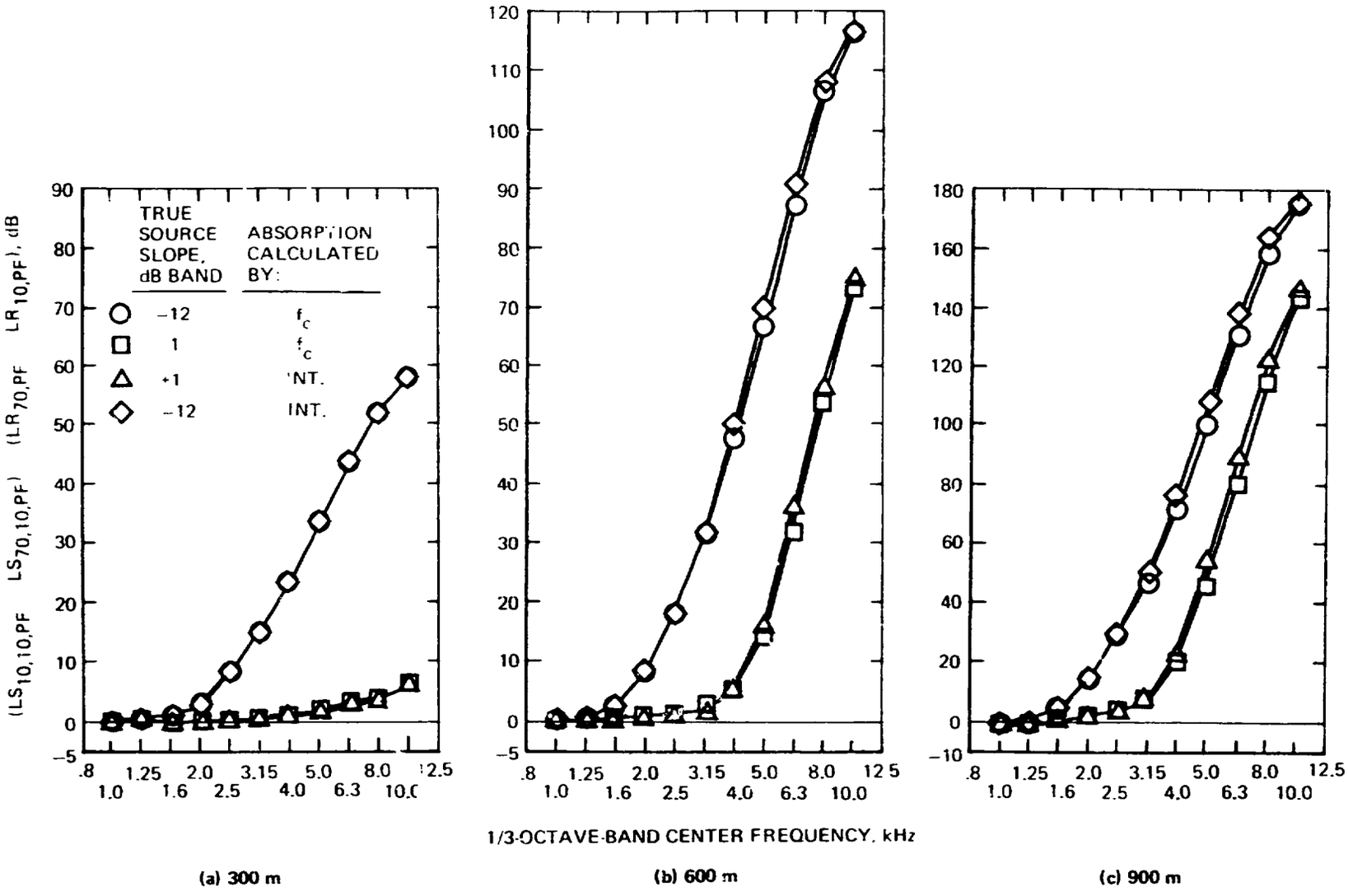

Figure 23.-Comparison of band-loss adjustment factors, calculated at band center frequency, f_c, only and calculated by integration over passband of ideal filter, for receiver band levels determined with practical-filter transmission-response characteristics. Compare with Fig. 14 for receiver levels determined with ideal filters. See Fig. 22 for definition of terms. 25°C air temperature; 1.0 standard atmosphere air pressure. Three sound propagation pathlengths; two sound pressure spectrum slopes at the source.

Thus, it is considered that the conclusion of Section 2 is still valid with regard to the accuracy of the band-integration and the band-center-frequency methods: namely, that when the band levels at the receiver are properly determined, the band-integration method is preferred because it produces smaller errors for steep, negative, high-frequency spectral slopes than the band-center-frequency method. For moderate spectral slopes, however, there is no significant difference in the accuracy of the two methods and either one can be used equally well for determining band-adjustment factors.

The critical issues in the choice of calculation method seem to be: how accurately are the correct receiver band levels known and, for the band-integration method, how accurately does the 2-slope method, or some other method, approximate the pressure spectrum of the sound at the microphone. As a practical matter, there does not appear to be any feasible way to resolve these issues. The next Section provides additional guidance as a result of applying the analytical procedures to actual aircraft flyover noise measurements.

4. ADJUSTMENT OF AIRCRAFT NOISE DATA FROM TEST TO REFERENCE METEOROLOGICAL CONDITIONS

The objective of the second phase of the study was to make a quantitative evaluation of various procedures to adjust measured aircraft flyover noise data for differences between atmospheric absorption under test and reference meteorological conditions. A primary application for such adjustment procedures would be during analysis of data taken to demonstrate compliance with the effective perceived noise level requirements associated with aircraft noise certification. Another application would be to adjust data acquired for specifying A-weighted sound levels and sound exposure levels. Sound exposure levels (SEL) are the basis for calculations of day-night average sound levels, a noise descriptor that is widely used in assessments of the environmental impact of noise. Since the two applications used similar procedures, it is sufficient to describe the application to aircraft noise certification, specifically the requirements of Part 36 of the Federal Aviation Regulations.[5] The next sections describe the requirements of FAR Part 36 relevant to atmospheric absorption adjustments and the interpretations and assumptions made in conducting the evaluations reported here.

Requirements for Atmospheric-Absorption Adjustments During Noise Certification

All transport-category, large airplanes and all turbojet or turbofan-powered airplanes must demonstrate compliance with the applicable noise-level requirements of Appendix C of FAR Part 36 (or FAR 36). Noise levels must be measured and adjusted in accordance with the requirements of Appendix A of FAR 36. The noise evaluation quantity is the effective perceived noise level (EPNL) which must be calculated, in accordance with the requirements of Appendix B of FAR 36, from the psychoacoustic descriptor called perceived noise level (PNL) after addition of appropriate tone-correction factors to determine tone-corrected perceived noise levels (PNLT) and a duration-correction factor (DCF). Requirements for calculation of tone- and duration-correction factors are also given in Appendix B of FAR 36.

If the test-time meteorological conditions do not conform to the

acoustical reference-day conditions specified in §A36.5(c)(1) of Appendix A of FAR 36, then the measured data must be adjusted for differences in atmospheric absorption to determine noise levels equivalent to those that would have been measured under acoustical reference-day conditions.

Currently, the requirements of FAR 36 specify that only the 1/3-octave-band sound pressure level spectrum associated with the maximum test-time tone-corrected perceived noise level ($PNLTM_{test}$) has to be adjusted for differences between reference and test-time atmospheric absorption.

The procedure specified in FAR 36 to account for differences between test and reference atmospheric absorption assumes that there is no difference between the directivity of tone-corrected perceived noise level under the two atmospheric conditions, i.e., that there is no change in the sound-emission angle or propagation pathlength associated with the maximum value of the tone-corrected perceived noise level. The assumption that there is no change in the directivity of tone-corrected perceived noise level is equivalent to assuming that the duration-correction factor is the same under test and reference atmospheric conditions.

However, if each set of 0.5-second-average sound pressure levels was to be adjusted to reference meteorological conditions, and if reference-day tone-corrected perceived noise levels were to be calculated for each 0.5-second interval, and if that set of tone-corrected perceived noise levels were then to be searched to find the maximum reference-day tone-corrected perceived noise, that maximum value might not be the same as the value of the reference-day tone-corrected perceived noise level calculated by the procedure specified in FAR 36. The difference would be caused by changes in the spectrum of the sound at the microphone, as a result of the test-to reference-day atmospheric-absorption adjustments, such that the directivity of the tone-corrected perceived noise level was altered.

To distinguish between the maximum tone-corrected perceived noise levels calculated according to the two methods, we use the abbreviation $PNLTM_{ref}$ to represent the maximum value of the reference-day tone-corrected perceived noise levels for the set of tone-corrected perceived noise levels at 0.5-second intervals

and $PNLT'_{ref}$ to represent the reference-day tone-corrected perceived noise level determined in accordance with the method specified in FAR 36.

By the rules in FAR 36, the reference-day effective perceived noise level, EPNL, is calculated from

$$EPNL_{ref} = EPNL_{test} + (PNLT'_{ref} - PNLTM_{test}) = PNLT'_{ref} + DCF_{test} \qquad (46)$$

where DCF_{test} is the duration-correction factor under test-time atmospheric conditions.

Equation (46) is strictly applicable only when the reference and test flight paths, power settings, and airspeeds are the same. If the flight paths are not the same, then additional adjustments are included to account (1) for the differences in reference-weather atmospheric absorption because of the different propagation pathlengths and (2) for the difference in inverse-square divergence loss over the two propagation pathlengths. Other corrections have to be included for differences in engine power setting and airspeed.

If the test and reference flight paths are not the same, then SA36.11(e) also requires the addition of an adjustment which is proportional to the ratio of the minimum distances to the flight paths. The basis for this geometric factor is an assumption that the airspeeds along the test and reference flight paths are the same. The adjustment thus accounts for the longer, or shorter, duration between the same sound-propagation angles for test-time flight paths that are higher, or lower, than the reference flight path.

The analyses reported here did not consider any effects caused by differences between the test and reference flight paths as a result of differences in height overhead or flight-path angle since such differences are not relevant to comparisons of different procedures for determining atmospheric absorption losses. Nor were differences in engine power setting or airspeed considered. The analyses followed the requirements as given in the 3 April 1978 version of Appendix A of FAR 36. Adjustments for differences in atmospheric absorption losses were applied only to the spectra at the time

of occurrence of the maximum test-time tone-corrected perceived noise level, $PNLTM_{test}$. Similarly, reference-day sound exposure level was determined by calculating absorption-loss adjustments for the pathlengths at the time of occurrence of the maximum test-time A-weighted sound level, ALM_{test}.

No investigation was made of the differences in atmospheric-absorption adjustments that would have resulted from using the procedure required by some European noise-certification authorities for determining reference-day EPNL. That procedure requires that the spectrum at each 0.5-s interval throughout the 10-dB-down duration, instead of just the spectrum at the time of $PNLTM_{test}$, be adjusted for differences in atmospheric absorption under test and reference conditions. For effective perceived noise level, the value of $PNLTM_{ref}$ is determined from the set of $PNLT_{ref}$ values. A duration-correction factor under reference conditions is determined from the $PNLT_{ref}$ values and used to calculate the reference-day effective perceived noise level from $EPNL_{ref} = PNLTM_{ref} + DCF_{ref}$.

Requirements for a Layered-Atmosphere Analysis

The original issue of FAR 36 required the measurement of air temperature and relative humidity at a height of 10 m above the ground surface at a location near the microphones. Test-time meteorological conditions were acceptable only if the 10-m (or "surface") temperature was between 5° and 30° C and the relative humidity was between 30 and 90 percent, and there was no inversion (or positive gradient) of the temperature lapse rate. In determining adjustments for differences in atmospheric absorption under test and reference conditions, only the surface conditions were used to calculate the test-time atmospheric-absorption coefficients.

While vertical profiles of air temperature above the surface had to be measured to assure the certifying authorities that there was no temperature inversion present at the time of the noise recordings, there was no requirement to measure relative humidity aloft or to consider absorption losses over the sound propagation path. Thus, a test could be conducted under conditions where the actual absorption losses were large over a significant fraction of the

propagation path, but the adjustment factors from test-to-reference conditions were relatively small because the surface conditions were not too different from the reference conditions.

The 3 April 1978 version of Appendix A of FAR 36 permits noise-certification compliance testing under a wider range of meteorological conditions than those of the original issue. The change gives an applicant for a noise-type certificate more flexibility in choice of test sites and test schedules. Air temperature and relative humidity, however, must both be measured from the surface (i.e., from 10 m above the ground plane) to a height greater than the greatest height of the airplane during the time when $PNLT_{test}$ is within 10 dB of $PNLTM_{test}$.

Over that portion of the sound propagation path (presumably at the time of $PNLTM_{test}$) between the aircraft (presumably meaning at the location of the equivalent aircraft noise source at the aircraft reference point) and a point 10 m above the ground at the noise measuring station, the requirements in §A36.1(c) for 3 April 1978 are that

- the air temperature must be between 2.2° and 35° C
- the relative humidity must be between 20 and 95 percent
- the atmospheric absorption coefficient, as calculated using SAE ARP866A, must not exceed 12 dB/100 m at a frequency of 7100 Hz for the 1/3-octave band having a nominal band center frequency of 8000 Hz.

Compared with the original issue, the so-called weather window was thus made considerably larger in the 3 April 1978 version of FAR 36. Testing is now permitted in the presence of temperature inversions. Atmospheric conditions aloft can be more absorptive than at the surface as long as the 12 dB/100 m rule is observed for the 1/3-octave band at 8 kHz.

However, because testing is now permitted when temperature inversions are present, a layered-atmosphere procedure was developed by the FAA to help provide consistent and repeatable results. Meteorological data must be measured periodically throughout the day of the test from a height of 10 m

to the height of the airplane and at times that are within 25 minutes of each aircraft noise measurement. At each height where data are measured (at height intervals not exceeding 30 m), the measured meteorological data must be interpolated to the time of the noise measurement.

The average air temperature and relative humidity must be determined over each horizontal layer of the atmosphere using the meteorological data, at 10 m and aloft, interpolated to the time of the noise measurement. Atmospheric absorption coefficients must be calculated by the method of SAE ARP866A (for the 1/3-octave band with nominal band center frequency of 3150 Hz) for the average temperature and relative humidity over each layer.

According to §A36.9(d)(2), if the atmospheric absorption coefficients over all the layers up to the height of the airplane (at the time of $PNLTM_{test}$) do not vary by more than ±0.23 dB/100 m (or ±0.7 dB/1000 ft) from the value calculated from the test-time air temperature and relative humidity at the 10-m height, then only the meteorological data at the 10-m height need be used to determine the test-time atmospheric-absorption coefficients for use in calculating test-to-reference-day adjustment factors. If desired, the full set of meteorological data may also be used, instead of just the 10-m data, to determine adjustment factors when the conditions aloft permit the ±0.23 dB/100 m deviation criterion at 3150 Hz to be met. All temperatures and relative humidities aloft must also satisfy the weather-window criteria cited above from §A36.1(c).

When the meteorological conditions aloft are such that the ±0.23 dB/100 m deviation criterion cannot be satisfied, then an average test-time atmospheric-absorption coefficient must be determined for each of the 24 bands with nominal 1/3-octave center frequencies from 50 to 10,000 Hz. The average coefficient must be computed using the coefficients calculated for the average temperature and relative humidity in each layer. The attenuation applicable to each 1/3-octave band must be calculated for the entire sound propagation path (at the time of $PNLTM_{test}$) from the sum of the attenuations over the lengths of the segments of the path contained within each layer. An average test-time atmospheric-absorption coefficient is then found from the ratio of the total attenuation over the path to the length of the propagation path. The average

test-time absorption coefficients must be used in determining the adjustment factors required in §A36.11(d). The process just described for determining the average attenuation rates is known as the layered-atmosphere analysis method. The alternative procedure, which may be used when the meteorological conditions aloft permit its use, is known as the 10-m, or surface-weather, method.

Reference Meteorological Conditions

Meteorological conditions for the acoustical reference day are defined in §A36.5(c)(1) of FAR 36. They are

(1) sea level pressure of 1.0 standard atmosphere (0.760 m of mercury);
(2) an air temperature of 25° C (298.15 K);
(3) a relative humidity of 70 percent; and
(4) zero wind.

The reference meteorological conditions must be used to establish the reference takeoff flight path; the reference takeoff and landing airspeeds; the reference takeoff, cutback, and landing engine-power settings; as well as the reference pure-tone atmospheric-absorption attenuation rates.

A uniform, reference atmosphere with constant conditions at any height was selected by the FAA for a layered-atmosphere analysis on the grounds that such a definition provided consistent, repeatable, and creditable test results. A uniform, reference atmosphere was also regarded as being consistent with the process of determining average atmospheric-absorption sound attenuation rates when the test-time meteorological conditions aloft were such as to require the use of a layered-atmosphere adjustment method.

During the period of time that the proposed rule, which led to the 3 April 1973 version of Appendix A, was out for public comment, it was suggested to the FAA that the requirement to consider atmospheric absorption losses along the sound propagation paths from the aircraft to the microphone should also mean that reference lapse rates should be included in the definition of reference meteorological conditions. This suggestion was not accepted by the FAA for the 3 April version of Appendix A or for use as an FAA-approved equivalent procedure.

General Requirements of FAR 36 for Aircraft Noise Measurement and Analysis

This report is primarily concerned with evaluation of alternative procedures for adjusting measured aircraft noise data for differences between the atmospheric absorption that occurred at the time of the measurement and that which would have occurred if the atmosphere had had acoustical reference meteorological conditions. The adjustments would be applied as part of the analysis of measurements made to demonstrate compliance with aircraft noise-certification requirements of FAR 36. The major elements of the general requirements of FAR 36 for measurement and analysis of aircraft noise are reviewed here to establish the basis for the structure of the computer program that was prepared to evaluate the alternative procedures. Subsequent discussions present some of the interpretations and assumptions that were made to carry out the evaluations.

Appendix A of FAR 36 contains a host of detailed requirements for measuring, analyzing, and reporting aircraft noise data and associated airplane and meteorological parameters. The measurement requirements fall into two categories: data acquisition and data processing. We are concerned here with data acquisition, data processing and analysis.

There are five principal measurement systems involved in acquiring aircraft noise data. The systems are for measuring (1) acoustical data, (2) airplane tracking data, (3) meteorological data, (4) airplane/engine-parameter data, and (5) time-code data for synchronizing the recording of the acoustical, tracking, and airplane/engine data.

For each noise measurement, data acquisition consists of the following sequence of five general steps:

(1) meteorological data are measured at the surface and aloft;

(2) background noise (ambient noise plus electrical instrument noise) is recorded;

(3) the test airplane is set up to fly over, or to the side of, a microphone at constant conditions (i.e., constant engine power setting, airspeed, airplane configuration, airplane attitude, and flight path angle);

(4) as the airplane flies over the microphone, simultaneous recordings are made of sychronizing time-code signals and (a) the aircraft noise signal, (b) airplane parameters, and (c) the location in space of the airplane reference point; and

(5) after the test airplane has cleared the area, meteorological data are again measured at the surface and aloft.

Data processing is considered to include those steps which lead to generation of the basic data which are subsequently analyzed and reported. Analysis includes all the adjustments from test-to-reference conditions, calculation of effective perceived noise levels under reference conditions, and determination of compliance with the noise certification requirement.

Data processing includes the following four general steps:

(1) determine meteorological data, at the surface and aloft, which are appropriate for the time of the noise measurement by interpolating the surface (i.e., 10 m) data on time of day and interpolating the data aloft, on height and time of day, to produce data at heights that are not more than 30 m apart;

(2) at nominal 0.5-s intervals throughout the duration of the flyover noise recording, determine 1/3-octave-band sound pressure levels at each microphone for the 24 nominal band center frequencies between 50 and 10,000 Hz;

(3) determine the coordinates of the airplane reference point throughout the duration of the aircraft noise recording in time synchronization with the aircraft noise data; and

(4) determine the values of the (nominally constant) airplane and engine parameters throughout the duration of the aircraft noise recording in time synchronization with the aircraft noise data.

The sound pressure levels must be corrected for nonideal frequency-response factors such as the effect of a microphone windscreen on frequency response and sensitivity, microphone diffraction effects on the frequency response of the microphone when the sound impinges on the microphone's sensing element at other than a grazing incidence angle, the effect of using an electrical pre-emphasis network to boost the sensitivity of the recording system at high frequencies in order to capture more of the high-frequency content of the aircraft's noise signal, and the effect that various components of the data-acquisition/data processing system have on the flatness or uniformity of the system's frequency response. The filters must conform to the ANSI or IEC Class III requirements for 1/3-octave-band filters. Corrections for effective noise bandwidth must be included for each filter.

More importantly, the sound pressures must be suitably time averaged as

well as corrected for the contaminating influence of high levels of background noise.

With regard to time averaging, FAR 36 requires that the 1/3-octave band sound pressure levels be generated at time intervals that are spaced at 500 ms ± 5 ms. Further, a time interval of no more than 50 ms can be used to read out the 24 values and no more than 5 ms of data out of every 500 ms sample may be excluded from the average. The real-time analyzers most often used for processing aircraft noise recordings satisfy those requirements. The electrical signal from the tape recorder is supplied to each filter band simultaneously. The output of the filters is sampled at a high rate, squared, and summed over a period close to 500 ms. Summations from the parallel-connected filters are scanned sequentially by an electronic scanner and stored with time-code signal on a recorder. The time average of the electrical analog of the squared pressures is found by dividing by the averaging time. The logarithm of the result is taken to produce, with suitable scaling, sound pressure levels relative to a reference pressure of 20 μPa.

The process described above is sometimes referred to as linear averaging. Some sound level meters and analog types of data-processing instruments use resistor-capacitor networks to perform an effective integration of the input signal; that process is referred to as exponential averaging. With exponential averaging, the time constant, and hence the damping, of the signal can be adjusted. To facilitate the measurement of fluctuating as well as relatively steady signals, sound level meters incorporate both low-damping (or FAST) and high-damping (or SLOW) dynamic-response characteristics.[11]

A linear average over a 500-ms period corresponds, approximately, to the FAST response characteristics of a sound level meter. Appendix A of Part 36, however, requires that the dynamic response of the data-processing system simulate the damping characteristics of the SLOW response of a sound level meter. To meet that requirement, additional smoothing is often introduced by employing a running average, on a mean-square basis, of sequential values of two or three of the 500-ms linear-averaged time-integrated data samples.

The running average is performed by a digital computer after the 1/3-octave band real-time analyzer has produced the series of data samples at 500-ms intervals. The number of data samples to include in each running average is determined empirically for the particular characteristics of the data-processing system relative to the detailed requirements in Appendix A and to the rates at which the noise signals vary with time during the flyover noise recording. References 12 and 13 contain additional discussions of data averaging methods to meet the dynamic response requirements of FAR 36 when analyzing transient aircraft noise signals (which can include rapidly rising and rapidly decaying signals from a flyover at a low altitude).

The discussion of averaging is included here because the averaging process is relevant to atmospheric absorption. The averaging process not only affects the magnitude of the sound pressure levels, it also influences the choice of the time to associate with each data sample and hence the identification of the average angle of sound propagation and the propagation pathlength. Moreover, the running-average method distorts the time variation of the noise levels by foreshortening the time before the time at the closest point of approach and lengthening the time after the time at the closest point of approach, see the discussion in Ref. 14. The running average method can thus affect the value of the duration correction factor.

For the study reported here, all sound pressure levels were obtained using only a 500-ms averaging time. Shorter averaging times, which would have improved angular resolution at the expense of statistical reliability, were not considered. No attempt was made to obtain additional smoothing or to match the SLOW response characteristics of sound level meter because the running average method complicates the correlation between a sample of aircraft noise and the corresponding location of the aircraft on the flight path at the time when it emitted the sound characterized by the particular data sample. Moreover, there was a concern that if the present Part 36 requirement should be changed in the future to make it consistent with the European practice of determining atmospheric-absorption adjustments at 0.5-s intervals, instead of just at the time of $PNLTM_{test}$, then it might be more correct, technically, to compute the running-average values after, instead of before, applying the atmospheric-absorption adjustments. Considerations of when to

perform a running average, however, were beyond the scope of the current study.

For correlation purposes, the time associated with each 500-ms sample of time-integrated squared sound pressures was assumed to be the midpoint of the 500-ms period. The relative data-processing start time at 0.0 sec was assumed to be at the beginning of the first 500-ms sample.

With regard to the second major correction factor (namely, background noise contamination), it is a requirement of §A36.5(d)(3) of FAR 36 that the 1/3-octave band sound pressure levels of the aircraft noise signal, at each 0.5-s interval over the duration from when the PNLT is first equal to 10-dB less than PNLTM to when it is last equal to 10-dB less than PNLTM (or the duration between the 10-dB-down times), must be at least 5 dB greater than the corresponding equivalent sound pressure levels of the background noise. It also is a requirement of §A36.5(d)(3) that no test-time EPNL may be computed or reported from data from which more than four 1/3-octave-band sound pressure levels have been excluded because of background noise contamination for any spectrum within the 10-dB-down times.

Sound pressure levels that exceed the background noise level by more than 5 dB may have the background noise contribution removed using the rule

$$L_{p,s} = 10 \log \left[10^{0.1\, L_{p,m}} - 10^{0.1\, L_{p,b}}\right] \qquad (47)$$

where $L_{p,s}$ is sound pressure level of the aircraft noise signal, $L_{p,m}$ is the measured level of the combination of the signal and the background noise, and $L_{p,b}$ is the sound pressure level of the background noise. Equation (47) applies with the restriction that $L_{p,m} - L_{p,b} > 5$ dB.

Because the true level of a high-frequency aircraft noise signal can be very low as a result of atmospheric absorption, it is extremely important that an accurate and appropriate background noise spectrum be obtained and that the 5-dB rejection rule be carefully observed. When the propagation path is relatively long, or the atmospheric conditions are quite absorptive, or both then many of the high-frequency, or even low- or mid-frequency, band levels may be rejected because of background noise contamination. Reference 15 describes

background noise considerations in analyses of aircraft noise measurements for certification purposes.

Some aircraft noise analyses have attempted to use an estimate of the spectral shape, or other procedures, to supply estimated values for 1/3-octave-band test-time sound pressure levels that have been excluded by the 5-dB rule. Atmospheric absorption adjustments have been then applied to the estimated band levels in order to determine reference-day sound pressure levels.

As part of an analysis of simultaneous measurements made in the period from January to March 1975 by the NASA Langley Research Center and the Douglas Aircraft Company of the noise produced by a McDonnell Douglas DC-9 powered by a refanned version of the JT8D engine and by a McDonnell Douglas DC-9 powered by JT8D engines with no acoustical treatment, Hosier[16] of NASA-Langley described the use of an arbitrary -2 dB per 1/3-octave-band rolloff for high-frequency sound pressure levels that had been rejected because of contamination by background noise. Because the level of the background noise was quite high and the level of the high-frequency aircraft noise signals was rather low, the arbitrary rolloff was applied by Hosier starting at band center frequencies of 1600 to 2000 Hz. The NASA-Langley data-processing system also used a running (or moving) average procedure to simulate the exponential time weighting of the SLOW response of a sound level meter. Reference-day high-frequency sound pressure levels were calculated by NASA from test-time sound pressure levels determined using the -2 dB per band rule. In analyzing the same noise recordings, Hosier noted that Douglas Aircraft Company used a spectral truncation rule similar to that used for the data analyzed for the present study.

In general, there is no valid basis for determining the true values for sound pressure levels rejected because of background noise contamination. Therefore, in this study, when the measured sound pressure level was not more than 5 dB above the background noise level, the indicated sound pressure level was set equal to the arbitrary value of 0.0 dB. A value of 0.0 dB was chosen since, with the systems that were used for data acquisition, the minimum measurable 1/3-octave-band sound pressure level was between 30 and 35 dB.

No spectrum synthesis, or spectrum estimation, was used in this study to make up a complete 24-band spectrum from available valid sound pressure levels from a spectrum that was missing some one-third-octave-band sound pressure levels because of background noise contamination. If a band sound pressure level of 0.0 dB was included in the spectrum to be adjusted for atmospheric absorption losses, then no adjustment was calculated for that band. If a band sound pressure level was set to 0.0 dB, the perceived noisiness for that band was set to 0.0 noys.

Procedures used during data processing for time averaging and for correcting for background noise contamination have been discussed in some detail here because a variety of procedures are employed in practice.[13,15,16] The discussions above in Sections 2 and 3 pointed out the importance of having valid measurements of the sound pressure levels at the receiver (or microphone) and showed that adjustments for atmospheric absorption losses could lead to spurious estimates of reference-day sound pressure levels if the test-day sound pressure levels were not valid. Time-averaging and background-noise-correction procedures can have a significant effect on the validity of the test-day sound pressure level data.

Basic Assumptions Related to Atmospheric Absorption Adjustments

Four basic assumptions were made in applying the analytical methods to determine atmospheric-absorption adjustment factors for aircraft flyover noise measurements. Those assumptions are commonly used in analyses of data for an aircraft-noise-certification compliance demonstration.

(1) For each frequency band of interest, the effective source of the sound produced by the aircraft at any point on the flight path is at the location of an aircraft reference point. The aircraft reference point is that which is used when tracking the aircraft during the flyover noise recording. This assumption is tantamount to an assumption that the aircraft-to-microphone distance is always large enough that the microphone is in the acoustic and geometric far field and that the aircraft's noise sources can be considered to radiate from an equivalent acoustic point source.

(2) Sound from the equivalent point source of aircraft noise propagates outward without distortion of the wavefronts as a result of refraction by temperature gradients or scattering by atmospheric turbulence

caused by inhomogeneities in air temperature or wind velocity. Sound is, therefore, assumed to travel along straight ray paths from the source to the microphone.

(3) Nonlinear propagation effects on the waveform, and hence spectrum, of high-amplitude sound pressure signals can be neglected. (This assumption, while it has almost universally been applied in previous analyses, may need closer scrutiny for future studies. Webster and Blackstock, Ref. 17 conducted a study which indicated that the high-frequency spectrum in the far field of a high-amplitude sound source could be significantly affected by nonlinear propagation effects.)

The assumptions, that the airplane noise sources could be represented by an equivalent acoustic point source and that the sound propagation paths were straight lines from the location of the source on the flight path to the microphone, were used (in conjunction with time synchronization of the systems for recording acoustical, aircraft, and tracking data and with the identification of each 0.5-s sample of noise data at the midpoint of the 500-ms averaging period) to define the geometrical relationships between the noise source and the receiver.

(4) The fourth basic assumption was that the spectrum of the sound at the microphone contained no discrete-frequency components. The spectrum was assumed to be broadband with a relatively smooth distribution of acoustic energy over the 10 to 20,000-Hz frequency range of interest. [The frequency range of interest contains frequencies that are below and above the usual frequency range (45 to 11,200 Hz) to account for energy transmitted through the lower and upper stopbands of the 1/3-octave-band filters.]

For the aircraft types and engine power settings for which data were available, the assumption that no discrete-frequency components were present in the spectra was reasonable, especially for the high frequencies where atmospheric-absorption effects are most noticeable. Atmospheric absorption adjustments for discrete-frequency components within a 1/3-octave-band spectrum should, theoretically, be treated separately especially if their frequency is near the bandedge of a filter. Changes in the apparent frequency of sound as the airplane approaches and recedes from the microphone (i.e., Doppler frequency shifts caused by changes in the magnitude of the relative speed of the source and the receiver) should also be considered in calculating atmospheric-absorption losses for discrete-frequency and broadband aircraft sounds.

Assumptions Regarding Calculation of Tone-Correction Factors

Determination of effective perceived noise level requires calculation of a tone-correction penalty which is to be added to the perceived noise level to form the tone-corrected perceived noise level. Section B36.5 of Appendix B provides details of the procedure to be used to calculate tone-correction factors.

However, straightforward application of the procedures of §B36.5 would have produced spurious and inconsistent results because (1) some of the 24 band levels in many of the 0.5-s data samples were expected to be missing since they had been rejected because of contamination by high background noise, and (2) all spectral data samples were known to contain spectral irregularities caused by cancellation and reinforcement effects resulting from interference between the sound that directly impinged on the microphone and sound that was reflected from the ground to the microphone and arrived out of phase. Ground reflection effects were contained in the spectral data because the microphone was placed, as required by FAR 36, at a height of 1.2 m above the ground surface. The requirements of Appendix B of FAR 36 were interpreted, as allowed, to avoid calculating tone-correction penalties for spectra with missing band levels or spectral irregularities from ground reflections. The intent of Appendix B is to calculate a penalty for an aircraft noise spectrum having pronounced irregularities caused by discrete-frequency aircraft noise sources, not spectral irregularities caused by background-noise contamination or ground-reflection effects. The wording of §B36.5(f) reflects this intent.

Another specific interpretation that had to be made was to ignore the requirement of §A36.5(d)(3) that no EPNL be calculated or reported if more than four band levels are missing from any spectrum within the range of the 10-dB-down times. That requirement, which may be reasonable for data-acquisition systems in use after 1978, could not be retroactively applied to the older systems used to acquire the data available for the study. To have incorporated the requirement of §A36.5(d)(3) in the analyses would have eliminated most, if not all, the data that were available.

Section B36.5(m), in the 3 April 78 version of FAR 36, Appendix B, permits the exclusion of tone-correction penalties resulting from pseudotones caused by ground-reflection effects in the 1/3-octave bands with center frequencies of 800 Hz and lower (i.e., band numbers 29 and lower). Spectral irregularities

produced by ground-reflection effects are most pronounced at low frequencies (usually in the 50 to 400-Hz bands) and are generally negligible above 1000 Hz. In Ref. 18, Rackl discusses problems caused by pseudotones in calculations of tone-correction factors and recommends changing the microphone height from 1.2 m to 10 m for future aircraft-noise-certification tests.

Because there was no convenient way to eliminate the spectral irregularities caused by ground-reflection effects in the measured sound pressure levels, subroutine P36TC in the computer program incorporated the option of §B36.5(m) and calculates tone corrections only over the range of band center frequencies from 1000 Hz (band 30) to 10,000 Hz (band 40), see Volume II.

Tone corrections were, however, calculated for band sound pressure level differences (F values) down to 0.0 dB according to Table B2 of §B36.5.

To avoid the calculation of a tone correction for a spectrum with band levels missing in the 1000 to 10,000 Hz range, a procedure was adopted which was derived from a flyover-noise-analysis computer program called OMEGA 5.5. That program was prepared for the Biodynamics and Bioengineering Branch of the USAF Aerospace Medical Research Laboratory at Wright-Patterson Air Force Base. A description of the USAF computer program is given in Ref. 19.

The procedure for avoiding tone corrections caused by missing band levels was to limit the spectral search to those bands around the band containing the maximum sound pressure level (in the 1000 to 10,000-Hz range) which had sound pressure levels > 20.0 dB. A minimum sound pressure level of 20.0 dB was chosen because the level in a band contaminated by background noise was set equal to 0.0 dB. Therefore, if the indicated sound pressure level was $\geq$ 20.0 dB, that level had to be valid.

The eleven bands from 1000 to 10,000 Hz (i.e., band 30 to band 40) are first searched to locate the maximum 1/3-octave-band sound pressure level and its band number. The spectrum is then searched from the maximum sound pressure level toward band 24 to find the band number where the level is first less than 20.0 dB. The search is then repeated from the band having the maximum band level toward band 14 to find the first band number where the level is again less than 20.0 dB. Tone corrections are then calculated over the range of consecutive sound pressure levels that are all $\geq$ 20.0 dB. A rule is used that there

have to be at least six consecutive bands of valid data (out of eleven) for the tone-correction computation to proceed. If there are fewer than six consecutive bands where the sound pressure levels are $\geq$ 20.0 dB, the tone correction factor is set equal to 0.0 dB and a flag is set as a warning that there were insufficient valid data in that particular data sample.

The rationale for limiting the tone-correction search to sound pressure levels $\geq$ 20.0 dB was derived from §B36.5(c) of Part 36 which permits the use of a frequency analyzer with a bandwidth less than 1/3-octave band if it is suspected that a calculated tone-correction penalty results from other than a discrete-frequency aircraft noise source.

Two other problems addressed in development of the subroutine to calculate tone-correction factors were band sharing and the identification of "tones" resulting from sharp spectral changes caused by atmospheric absorption. For many aircraft noise measurements, both of these problems are often present in the 11-band frequency range from 1000 to 10,000 Hz.

Band sharing means that the sound pressure level in some band is affected by the presence of a high-amplitude discrete-frequency component in an adjacent band. Band sharing is often encountered when a discrete-frequency component has a frequency near the edge of a band. The problem of band sharing is caused by the non-ideal response characteristics of practical filters. The influence of the sharing of energy between adjacent bands will vary with time during a measurement of aircraft flyover noise. Furthermore, because of band sharing, two adjacent 1/3-octave-band sound pressure levels can be "encircled" in the tone-correction calculation process prescribed in Appendix B of FAR 36.

If two adjacent bands are encircled [meaning identified as possibly containing discrete-frequency components], the rules of Appendix B in the April 1978 version of FAR 36 do not provide a means to distinguish which band actually does contain the discrete-frequency component and to assign the tone-correction penalty to that band and not to the adjacent band which could be in a frequency range where larger F factors were calculated and which could thereby yield an inappropriate value for the maximum tone-correction factor. Even though the aircraft signals available to this study did contain discrete-frequency components

from fan noise which could have caused a band-sharing problem such as described above, it was not within the scope of the study to attempt to develop a special rule for computing tone corrections when two adjacent bands were encircled. The rules of §B36.5 were simply applied in a straightforward manner to all valid sound pressure levels between 1000 and 10,000 Hz and the largest tone-correction penalty so calculated was identified as the tone-correction factor for the spectrum.

The other aspect of band sharing whereby the frequency of some particular discrete-frequency component (e.g., the fundamental of the fan-blade-passing frequency) shifts from one band to another because of Doppler effects as the airplane passes overhead was also specifically not included in the program for analyzing the flyover noise data. For this problem, paragraph B36.5(n) of Part 36 requires that the average of the five tone-correction factors around the time of occurrence of the maximum tone-corrected perceived noise level (two before and two after) be computed and compared with the tone-correction factor calculated for the maximum test-time tone-corrected perceived noise level. The average tone-correction factor is to be substituted for the tone-correction factor that had been calculated for the spectrum at the time of PNLTM, if it is larger, and thus increase the previously determined value of PNLTM but not change its time of occurrence.

Incorporating the requirement to compute an average tone-correction factor into the computer program might have increased the value of the test-time PNLTM. The test-time duration-correction factor would either decrease or remain the same. Adjustment factors from test-time to reference-day conditions would be the same for the 1/3-octave-band sound pressure levels whether or not an average tone-correction factor was calculated. However, changes in PNL, PNLT, and EPNL would have been distorted because the sound pressure level adjustment factors are calculated only for one 0.5-s data sample and hence there would be no way to determine the change in the average tone-correction factor for reference-day conditions. Calculation of reference-day adjustment factors at every 0.5-s interval might be one way to eliminate the potential distortion that arises when the tone-correction factor for the test-time PNLTM is increased because of band sharing.

With regard to the problem of tone-correction penalties being identified for sharp spectral changes caused by atmospheric absorption, consider a broad-band source of sound such as jet noise. If the signal from such a source propagates a long distance under moderate to highly-absorptive atmospheric conditions, the high-frequency portion of the spectrum will decrease rapidly with increasing frequency. The tone-correction calculation procedure in Appendix B of Part 36 will treat any sudden change in spectral slope as a spectral irregularity and compute a corresponding tone-correction penalty. Since the source of sound does not contain any actual discrete-frequency components, the tone-correction penalty associated with the effect of atmospheric absorption could be the largest of the tone-correction penalties for that spectrum. The resulting tone-corrected perceived noise level could turn out to be the PNLTM for that recording of flyover noise.

Although assignment of a tone-correction penalty for a spectral irregularity caused by atmospheric absorption was considered to be as inappropriate as tone-correction penalties for irregularities caused by ground-reflection effects, there was no obvious way to modify the tone-correction procedures to eliminate the problem. Thus, again because of the limited scope of the study, the procedure from the April 1978 version of Appendix B was used without modification and the probable occurrence of tone-correction penalties for atmospheric-absorption effects was anticipated. Note that tone-correction penalties for spectral irregularities caused by atmospheric absorption are similar to those caused by spectra from which band levels were missing because of contamination by high-level background noise. However, there was no easy way to eliminate the spurious penalty as there was for the missing-band-level problem or for the ground-reflection problem.

Before it was used for analyzing flyover noise data, the computer subroutine P36TC for calculating tone-correction factors was modified to cover a complete 24-band spectrum and checked against the example in Table B3 of §B36.5 of FAR 36. The check also included the calculation of perceived noise level. All entries in Table B3 of Appendix B were replicated by the subroutines given in Volume II.

Calculation of perceived noise level by the computer program uses a mathematical formulation that can reproduce the perceived noisiness values in Table B1

of Appendix B. Table B1 was extended, in the 3 April 78 version of Appendix B, to a perceived noisiness of 0.1 noy from the minimum value of 1.0 noy in an earlier version. The mathematical formulation given in §B36.13 of FAR 36 (3 April 78) is consistent with a previous version of Table B1 and is not applicable for perceived noisiness values less than 1.0 noy. Additional slope factors and breakpoints had to be developed and included in the computer program in order to be able to compute PNL according to §B36.3 and Table B1. The mathematical formulation that was used for perceived noise level calculations is given in subroutine CPNL in Volume II.

Assumptions Regarding Calculation of Duration-Correction Factors

The duration-correction factor, DCF, for the test-time effective perceived noise level was found from

$$DCF = EPNL - PNLTM \tag{48}$$

while the duration, DSEL, of the test-time sound exposure level, SEL, was determined from

$$DSEL = SEL - ALM \tag{49}$$

where ALM is the maximum value of the time series of A-weighted sound levels, AL(i).

Effective perceived noise level was calculated from

$$EPNL = 10 \log \left[\sum_{i=t_1}^{t_2} 10^{0.1\ PNLT(i)} \right] + 10 \log (\Delta t / t_E) \tag{50}$$

where Δt is the sample length of 0.5 s, t_E is the effective-perceived-noise-level reference time of 10 s, and t_1 and t_2 are times corresponding to the values of test-day PNLT which are closest to (PNLTM - 10.0) decibels, i.e., the times for the 10-dB-down points.

Sound exposure level was calculated by a similar expression, namely

$$SEL = 10 \log \left[\sum_{i=t_1}^{t_2} 10^{0.1\ AL(i)} \right] + 10 \log\ (\Delta t/t_0) \qquad (51)$$

where Δt is also equal to 0.5 s, but the SEL reference time, t_0, is equal to 1.0 s instead of 10.0 s. The summation interval in Eq. (51) is for a duration $(t_2 - t_1)$ corresponding to test-time AL values closest to (ALM - 10.0) decibels. No tone corrections are applied to the AL values in the calculation of SEL.

The only interpretation of the requirements in §B36.9 of FAR 36 that was made in preparing computer-program subroutine INTEG to perform the summations in Eqs. (50) and (51) was in the definition of the initial and final times t_1 and t_2.

By the requirement of §B36.9(b), the summation interval is supposed to be determined to the nearest 1.0 second. To comply with this requirement means using some form of a round-off rule such as to always round up if the duration $(t_2 - t_1)$ has a non-integral value from the series of 0.5-s data samples. The rounding up could be done by either reducing t_1 or increasing t_2 . An alternative rule would be to round up if the number to the left of the decimal point was odd and round down if the number was even, again by changing either t_1 or t_2.

Since by the rules of FAR 36, the duration correction factor is assumed to be the same for test-time conditions as for acoustical reference conditions, any consistent definition for t_1 and t_2 would have been suitable for a study of atmospheric absorption adjustments. Therefore, the rule that was chosen was based on §B36.9(c) wherein the applicable limits are specified to be those times when PNLT(i) is closest to PNLTM - 10.0 and also chosen to yield the largest possible value for the duration time from the 0.5-s data samples.

If there are several PNLT values which are equal or close to PNLTM - 10.0, then the starting time t_1 is at the midpoint of that 0.5-s interval when PNLT is for the first time equal, or closest, to PNLTM - 10.0. Similarly, t_2 is at the midpoint of the very last 0.5-s interval when PNLT is equal, or closest, to PNLTM - 10.0. No attempt is made to round the duration $(t_2 - t_1)$ up or down to the nearest 1.0 second. The determination of t_1 starts with the first data sample

at a relative test time of 0.0 seconds at the beginning of the sample and proceeds toward the relative time of the last data sample. Determination of t_2 starts at the relative time of the last data sample and proceeds backwards toward the first sample.

Description of Test Cases

Nine samples of flyover noise data were used to study the application of the various adjustment methods. The nine samples included five different aircraft: two commercial jet transports, a business/executive jet, a turboprop-powered commercial airliner, and a propeller-powered general-aviation airplane. Table 1 lists the model numbers of the five aircraft and gives some general information about their propulsion systems.

For the DC-9-14, there were five test data samples. For each of the other four aircraft, there was only one test data sample.

The data for the 727, Learjet, HS-748, and Beech Debonair were obtained from Bolt Beranek and Newman, Inc. (BBN). The particular samples of 1/3-octave band sound pressure levels for these four aircraft were from the same test runs that provided the narrow-band sound pressure levels that were to have been used (as described in Section 2) for validating the atmospheric-absorption calculation method. The 727, Learjet, HS-748, and Beech Debonair airplanes were selected to provide data having different spectral characteristics and acquired under different weather conditions than the DC-9 data.

The five samples of DC-9 data were chosen from recordings made during a series of tests conducted under the joint sponsorship of the FAA and NASA in October 1974 at Fresno Air Terminal. The main purpose of those tests was to study the effects of different atmospheric conditions on the sound measured at ground level. The test airplane was flown along a level flight path at various heights over microphones mounted on or above a taxiway.

During the 1974 test program, recordings were made of approximately 270 test flights. In 1977, DyTec Engineering, under NASA contract, conducted a study[20] of ground-reflection effects present in the measured data. A con-

Table 1.-Description of aircraft used for test cases.

Type	Aircraft	Propulsion
Commercial jet transport	McDonnell Douglas DC-9-14	two P&WA JT8D-1 turbofan engines
Commercial jet transport	Boeing 727-100	three P&WA JT8D-7 turbofan engines
Business/executive jet	Raisbeck-modified Learjet	two GE CJ610 6 turbojet engines
Turboprop-powered commercial airliner	Hawker Siddeley HS-748 Series 2A	two Rolls Royce Dart RDa.7 Mk 532-2L turboprop engines developing 2290 eshp and driving Dowty Rotol 4-blade, constant-speed fully feathering, 144-inch-diameter propellers
Propeller-powered general aviation airplane	Beech Debonair (Beechcraft model F33) (straight-tail Bonanza)	single Continental IO-470-K six-cylinder piston engine developing 225 hp at sea level at 2650 rpm and driving a McCauley 2-blade, constant-speed, 84-inch-diameter propeller

sistent set of data was obtained by re-processing [illegible]n of the recordings to yield 37 sets of 1/3-octave-band sound pressure levels at 0.5-s intervals throughout the duration of each flyover. Each of the 37 sets of data contained sound pressure levels recorded at six microphone locations.

The 37 runs represented data acquired under a variety of atmospheric conditions with the DC-9 test airplane flown at various heights above ground level (i.e., various sound propagation pathlengths at equal sound emission angles). The 222 individual data samples (6 microphones times 37 runs) were examined to select the five samples analyzed for this study. Most of the available DC-9 data had the same problem noted in Section 2 in the description of the attempt to obtain narrow-band flyover noise levels, namely high-level background noise which contaminated the high-frequency portion of the spectrum at most (or often all) of the 0.5-s data times.

High-frequency contamination of the flyover noise levels was of little concern to the ground-reflection study because the spectral irregularities caused by ground reflections are primarily low-frequency phenomena. However, since atmospheric absorption is primarily a high-frequency problem, the loss of most of the high-frequency data was a significant limitation on the usefulness of the available data for the present study.

The 37 available runs included data at three nominal heights (152, 335, and 610 m) and three nominal thrust settings. The seven runs at the nominal 610-m height were eliminated because none had any spectral samples with sound pressure levels in the 8 and 10-kHz bands and only a few had data for the 5 and 6.3-kHz bands. The five runs at the highest engine power setting (at nominal heights of 152 and 335 m) also had no data samples with valid sound pressure levels to the 10-kHz band. Of the remaining 25 runs, 22 were for one nominal thrust setting and 3 were for the lowest thrust setting. The 25 runs were examined to select data sets having at least several 0.5-s intervals with valid sound pressure levels to the 10-kHz band.

Table 2 lists some of the relevant parameters for the nine runs that were examined. The five DC-9 runs include four at the nominal 152-m height and one (run 374) at the nominal 335-m (actual 341-m) height. Except for run 322, the

Table 2.-Test and airplane parameters

run no.	test date	airplane	test location	time of day# hours, minutes seconds	height∠ overhead, m	climb angle, deg	airspeed, m/s	flight Mach number
272	21 Oct 74	DC-9-14	Fresno Air Terminal	09 11 57.3	157*	0.0	71.7	0.213
322	24 Oct 74	"	" " "	11 22 07.9	155*	0.0	78.3	0.229
358	25 Oct 74	"	" " "	07 27 38.5	154*	0.0	74.4	0.219
374	25 Oct 74	"	" " "	11 51 20.7	341*	0.0	73.5	0.215
378	25 Oct 74	"	" " "	12 16 39.7	158*	0.0	72.6	0.212
25	29 Jan 76	727-100	LAX	19 00 05.6	336+	+10.0	79.2	0.233
12	28 Aug 75	Learjet	Fresno Air Terminal	11 55 01.0	1359+	0.0	77.7	0.229
7	24 May 71	HS-748	Fresno Air Terminal	10 40 20.4	659+	+ 7.6	59.7	0.175
119	20 Jan 75	Debonair	Ventura County Airport	10 50 08.8	298+	0.0	84.5	0.245

\# at overhead

∠ height of airplane above ground plane

* microphone 1.2 m over concrete surface

\+ microphone 1.2 m over asphalt surface

DC-9 runs were all at the moderate thrust of 26.7 kN per engine. For run 322, the airplane was flown at the low thrust setting of 13.3 kN per engine. Data for the lower power setting were included in order to study the effect of the different spectral shape associated with the lower thrust setting. Data for the 341-m height of run 374 were included to study the effect of adjusting data measured over longer pathlengths even though there were no 10-kHz data available. Run 374, however, was about the best of the 17 runs available at the nominal 335-m height in terms of having several valid samples of data in the 8, 6.3, and 5-kHz bands.

The four sets of data obtained from BBN were for a variety of conditions. The Learjet and the Debonair data were obtained for level-flight conditions as were the DC-9 data. The 727 and HS-748 data were obtained for climbing flight paths; the 727 data were recorded below an actual takeoff flight path from Los Angeles International Airport.

For all nine data sets shown in Table 2, the data were measured by a microphone located 1.2 m above a concrete or asphalt ground surface. The 1.2-m height is specified in FAR 36 and was used for all data here even though some of the DC-9 data were measured with a microphone flush in a plywood sheet. The flush microphone data were not used because the spectra would not have been compatible with the spectra from the 1.2-m-high microphones used for the BBN data and because there was no significant difference in the number of high-frequency bands contaminated by high background noise levels for the flush and 1.2-m data.

As a final remark about the data runs in Table 2, note that the heights of the 727 and Debonair tests were comparable to the heights for the DC-9 tests. The HS-748 height, however, was two to four times greater than the height for the DC-9/727 tests; the Learjet height was four to nine times greater than the height for the DC-9/727 tests. The turbojet engines on the Learjet were capable of providing a high signal-to-noise ratio over a wide range of frequencies even over such a long propagation path.

Test-Time Meteorological Data

The nine test cases of Table 2 were chosen to provide a variety of temperature and humidity conditions and vertical profiles as well as propagation pathlengths and sound-source spectral shapes.

The most-complete meteorological data were measured during the FAA/NASA tests. For those tests, an instrumented meteorological test airplane was used to sample the atmospheric conditions. Vertical profiles of temperature and humidity were measured several times on each noise-measurement test day. For each set of meteorological measurements, data were provided at 30 heights ranging from 30.5 to 915 m at intervals of 30.5 m. A set of data at a height of 1.2 m was also provided.

For each height, a linear interpolation method was used to obtain meteorological data that would be applicable to the time (at overhead) of the flyover noise recording. A short computer program was written to read all the measured temperature and relative humidity data, to calculate corresponding values at the times of the 37 flyover noise recordings, and to list the interpolated data onto a computer file. Data corresponding to a height of 10 m (for the so-called surface conditions according to FAR 36) were interpolated between data for heights of 1.2 and 30.5 m.

In contrast to the detailed meteorological data available from the FAA/NASA DC-9 tests, the four sets of data from BBN only had surface meterological data for two runs. For the other two runs, meteorological data were available to a limited number of heights. For the Beech Debonair, meteorological data were measured at the surface and at the airplane height. For the Learjet, meteorological data were measured at several heights.

Table 3 summarizes the meteorological conditions for the nine test cases. Air temperatures and relative humidities are listed for the 10-m height and for the height of the airplane when it was over the microphone. Note that the temperature ranged from cool to rather warm with lapse rates ranging from negative, to isothermal, to positive (temperature inversion).

To help visualize the vertical variation of temperature and relative humidity, Fig. 24 shows the vertical profiles for the six runs where data were measured at several heights, i.e., the five DC-9 runs and the Learjet run. For each test run in Fig. 24, the data were plotted at the height of the midpoint of the horizontal layer of the atmosphere defined by the heights where the meteorological data were measured. The DC-9 data were plotted to

Table 3.-Meteorological conditions for test cases

run no.	height overhead, m	surface (10-m) met. conditions		met. conditions at airplane	
		air temp., °C	rel. hum., %	air temp., °C	rel. hum., %
272	157	11.4	54.3	10.2	56.0
322	155	17.4	57.7	16.4	59.7
358	154	9.6	87.6	13.5	70.0
374	341	19.4	50.9	17.5	51.0
378	158	20.5	47.8	19.0	51.5
25	336	14.4	74.0	14.4*	74.0*
12	1359	21.6	40.1	13.5	34.5
7	659	19.4	76.0	19.4*	76.0*
119	298	23.9	47.0	23.3	45.0

*only surface conditions were measured, conditions aloft were assumed equal to those at the surface

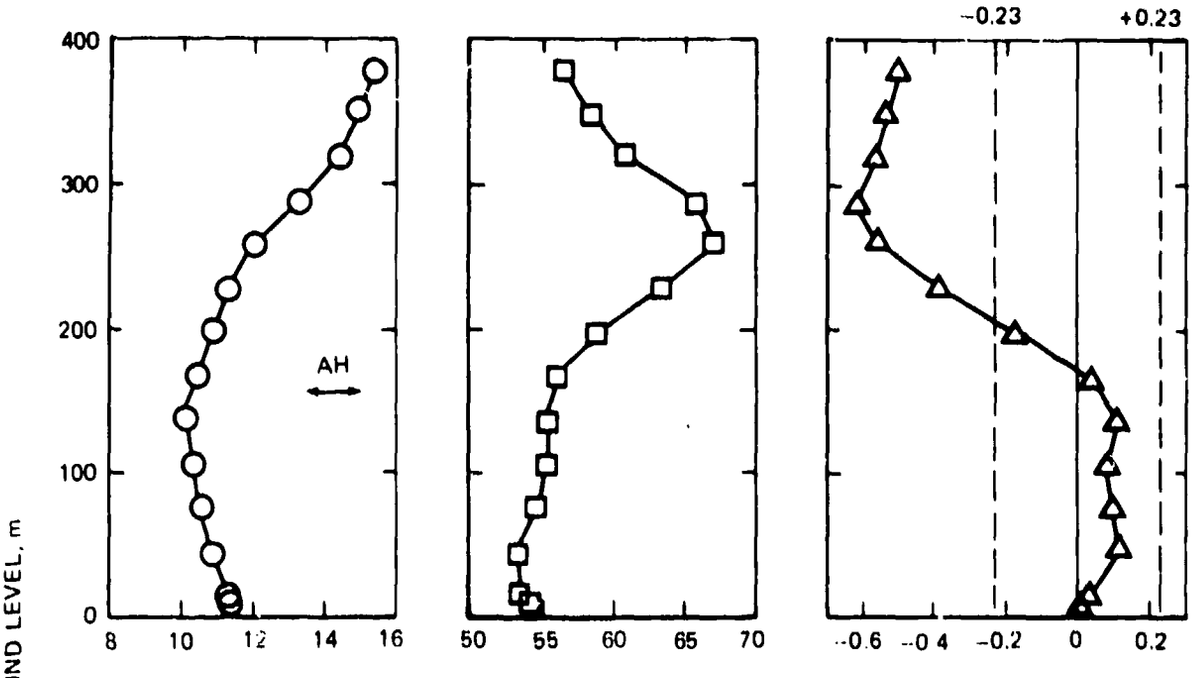

(a) DC-9-14; RUN 272; AIRPLANE HEIGHT, AH, 157 m.

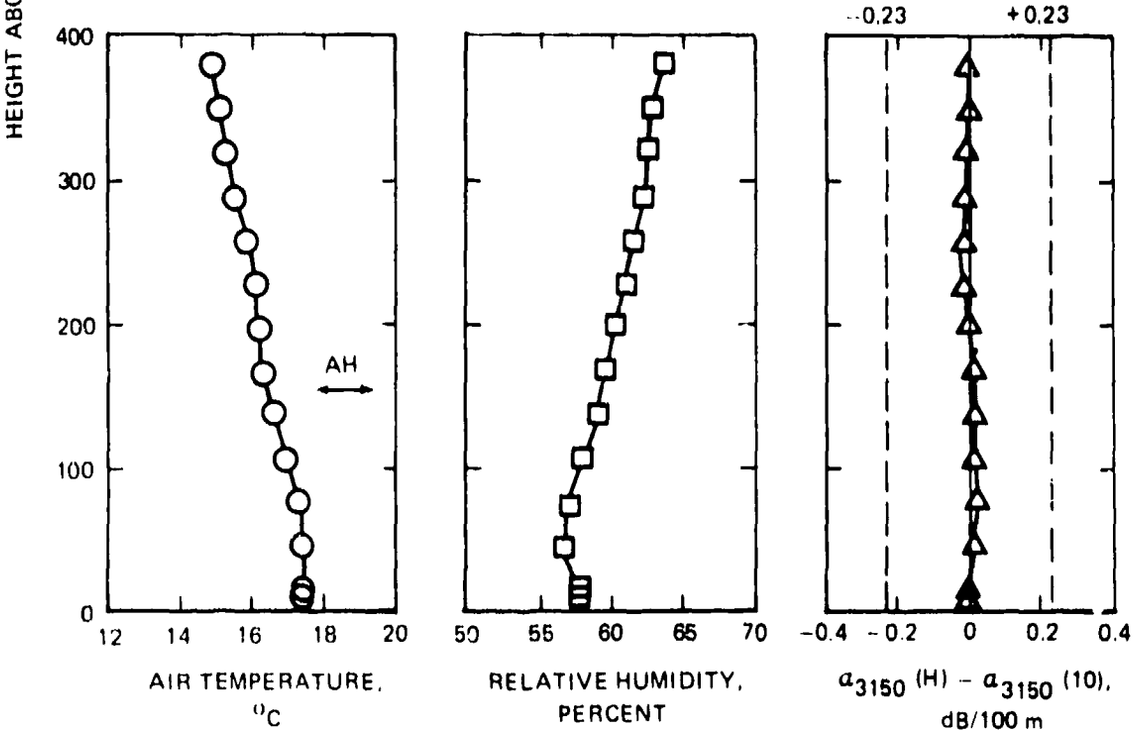

(b) DC-9-14; RUN 322; AIRPLANE HEIGHT, AH, 155 m.

Figure 24.-Measured vertical profiles of air temperature and relative humidity for test cases; also profiles of difference between atmospheric absorption coefficient by SAE ARP866A at 3150 Hz at height and at 10 m height.

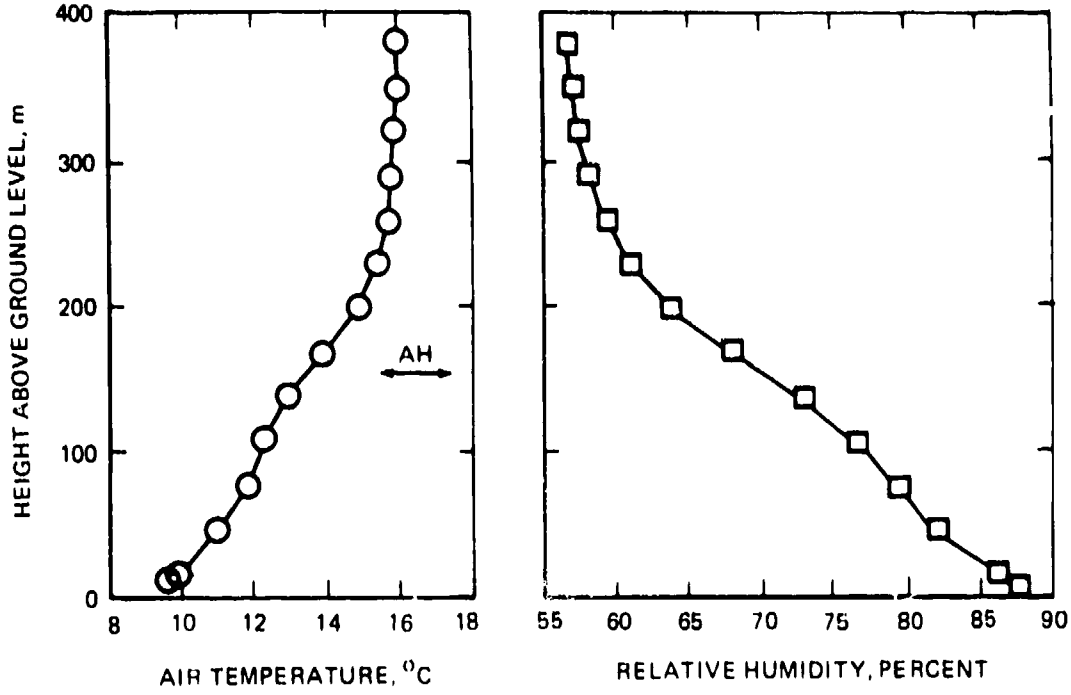

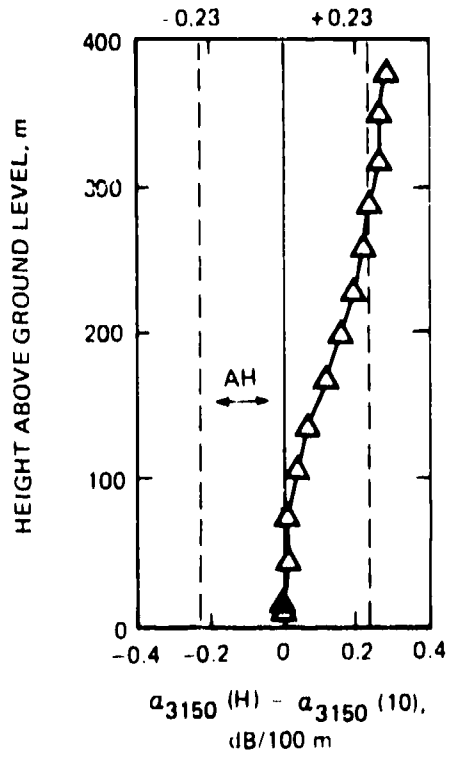

(c) DC-9-14; RUN 358; AIRPLANE HEIGHT, AH, 154 m.

Figure 24.-Continued.

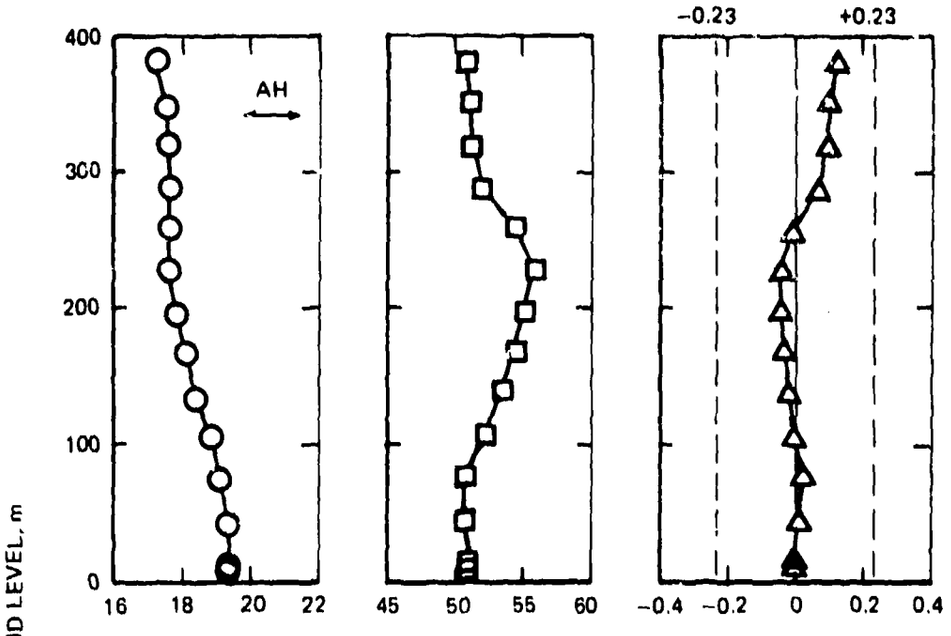

(d) DC-9-14; RUN 374; AIRPLANE HEIGHT, AH, 341 m.

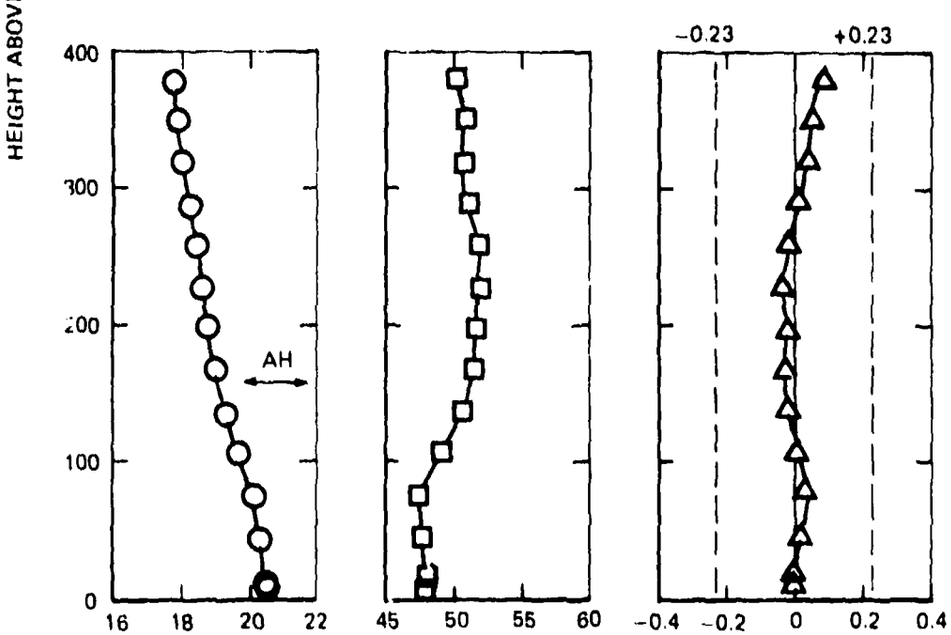

(e) DC-9-14; RUN 378; AIRPLANE HEIGHT, AH, 158 m.

Figure 24.-Continued.

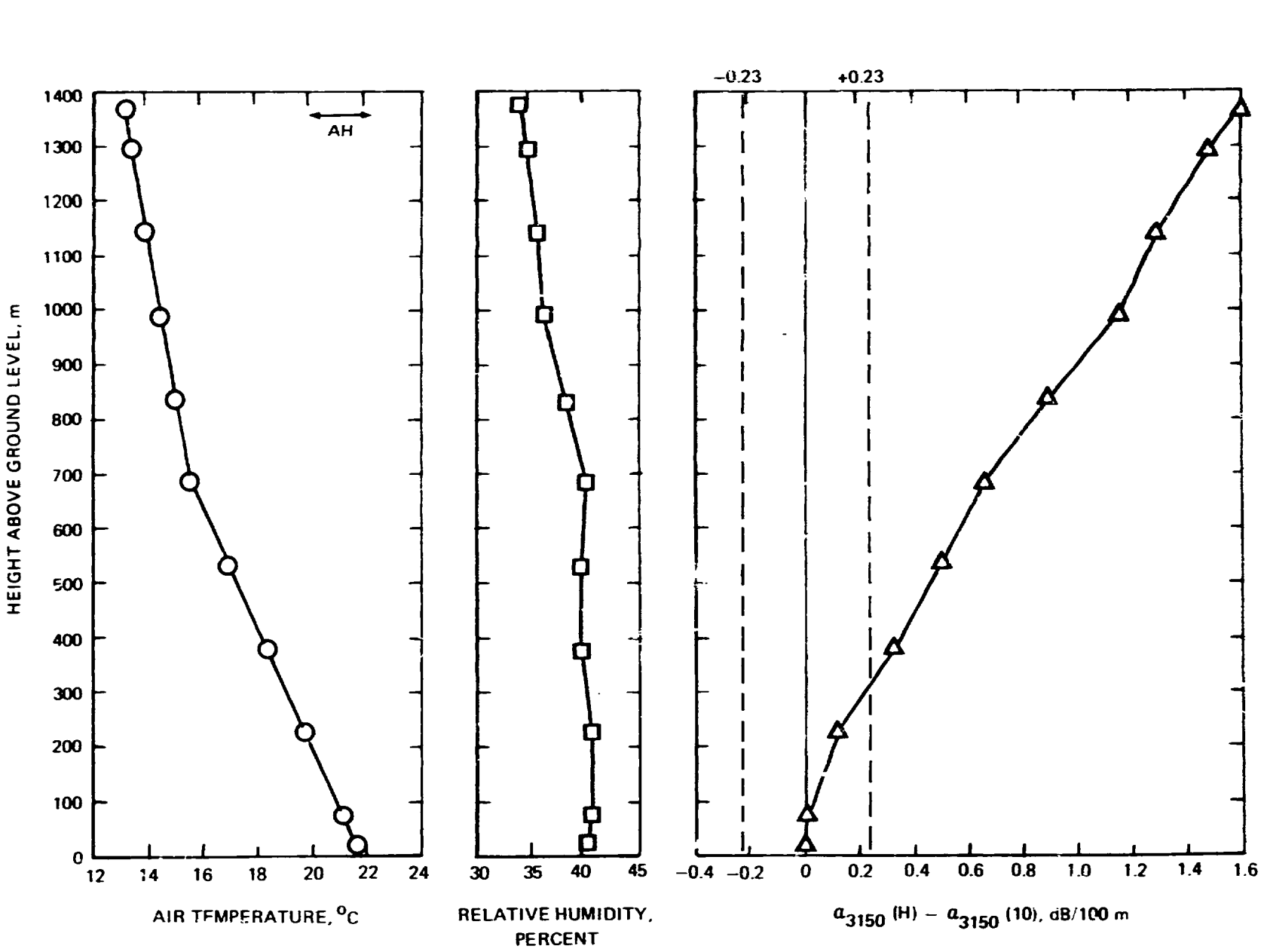

(f) RAISBECK-LEARJET; RUN 12; AIRPLANE HEIGHT, AH, 1359 m.

Figure 24.-Concluded.

a midpoint height of about 380 m to illustrate the trends and to extend the profile above the 341-m airplane height of run 374 in Fig. 24(d). In all cases, the height of the airplane is shown by the double-headed horizontal arrow in the temperature profile with the label AH for airplane height.

As explained in an earlier part of this Section, the FAR 36 criterion for applying a layered atmosphere analysis in calculating adjustments from test to reference conditions depends on the difference between the atmospheric absorption coefficient (as calculated by SAE ARP866A), at a frequency of 3150 Hz, at any height up to the height of the airplane at the time of sound emission and the atmospheric absorption coefficient at 3150 Hz at the surface (i.e., at the 10-m height). If this difference exceeds +0.23 dB/100 m, then a layered atmosphere analysis has to be performed.

The difference in atmospheric absorption coefficients, $\alpha_{3150}(H) - \alpha_{3150}(10)$, is also plotted for each test run in Fig. 24. It is interesting to note that none of the five DC-9 runs that were selected would have required a layered-atmosphere analysis, even for run 358 in Fig. 24(c) where there was a relatively strong temperature inversion in conjunction with a rapid reduction of relative humidity with increasing height. For run 272 in Fig. 24(a), the atmospheric conditions above a height of 200 m were quite absorptive and data (if there had been any) from tests at such heights would have required a layered-atmosphere analysis.

For the Learjet run in Fig. 24(f), the relative humidity was low and did not decrease by much while the temperature decreased rapidly from the surface to the height of the aircraft at 1359 m. As a result, the absorption along the sound propagation path was quite a bit greater than at the surface and the +0.23 dB/100 m criterion was exceeded at a height of about 300 m. A layered-atmosphere analysis would have been required for the Learjet data.

A basic quantity affecting the absorption of acoustic energy by the atmosphere is the amount of water vapor present. In the current model of atmospheric absorption[7], the molar concentration of water vapor is used as the measure of humidity. Molar concentrations were calculated at each height where meteorological data were available. For each test case, the air pressure

at any height was assumed to have the value measured at the 10-m height. Subroutine MOLAR in Volume II was used to perform the calculations.

The resulting vertical profiles of the molar concentration of water vapor are shown in Fig. 25. Four of the five DC-9 runs [Fig. 25(b)] had similar profiles with molar concentrations ranging from 1.0 to 1.15 percent over the range of heights to 380 m. Run 272 [Fig. 25(a)] was different in that the atmosphere was quite dry (a molar concentration between 0.69 and 0.73 percent) to a height of about 170 m. Above that height, the humidity increased rapidly to a value of about 1.0 percent. The more-humid layer aloft accounts for the fact that the absorption coefficient was lower than at the surface at heights above 170 m in Fig. 24(a).

The humidity profile for the Learjet, Fig. 25(c), was significantly different than those for the DC-9 tests. The humidity at all heights up to 1370 m was less than at the surface. The drier conditions at altitude account for the absorption coefficient being greater aloft than at the surface and for the positive values of the profile of differences in absorption coefficients in Fig. 24(f).

The molar concentrations in Fig. 24 ranged from 0.5 to 1.15 percent with the driest conditions being associated with the August test of the Learjet at Fresno Air Terminal. The October tests of the DC-9 (all at Fresno also) were generally somewhat more humid. All measured humidity values in Fig. 25 were significantly lower than the humidity associated with the FAR 36 conditions for an acoustical reference day. At 25° C, 70-percent relative humidity, and one standard atmosphere of air pressure, the molar concentration is 2.18774 percent or two to four times that existing at the time of the flyover noise measurements. Thus, in general, it was expected that the adjustment factors from test to reference conditions would be positive, i.e., that the sound pressure levels would be greater under reference conditions than under test conditions, especially at high frequencies.

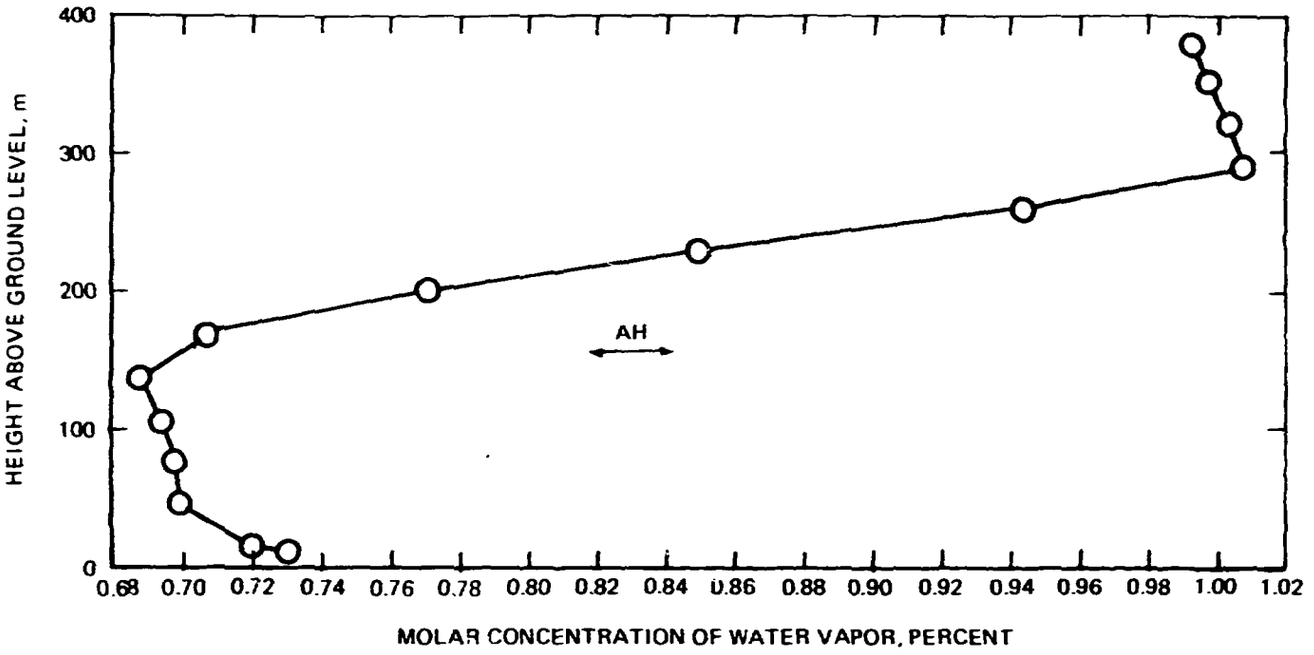

(a) DC-9-14; RUN 272; AIRPLANE HEIGHT, AH, 157 m.

Figure 25.-Measured vertical profiles of molar concentration of water vapor for test cases; reference molar concentration of water vapor at 25°C, 70 percent relative humidity, and one standard atmosphere of air pressure is 2.18774 percent.

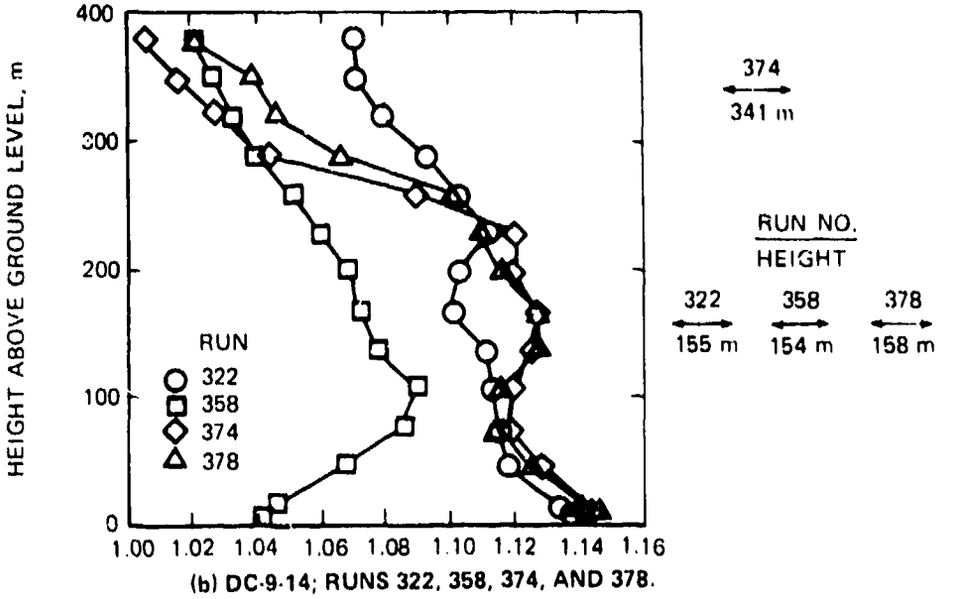

(b) DC-9-14; RUNS 322, 358, 374, AND 378.

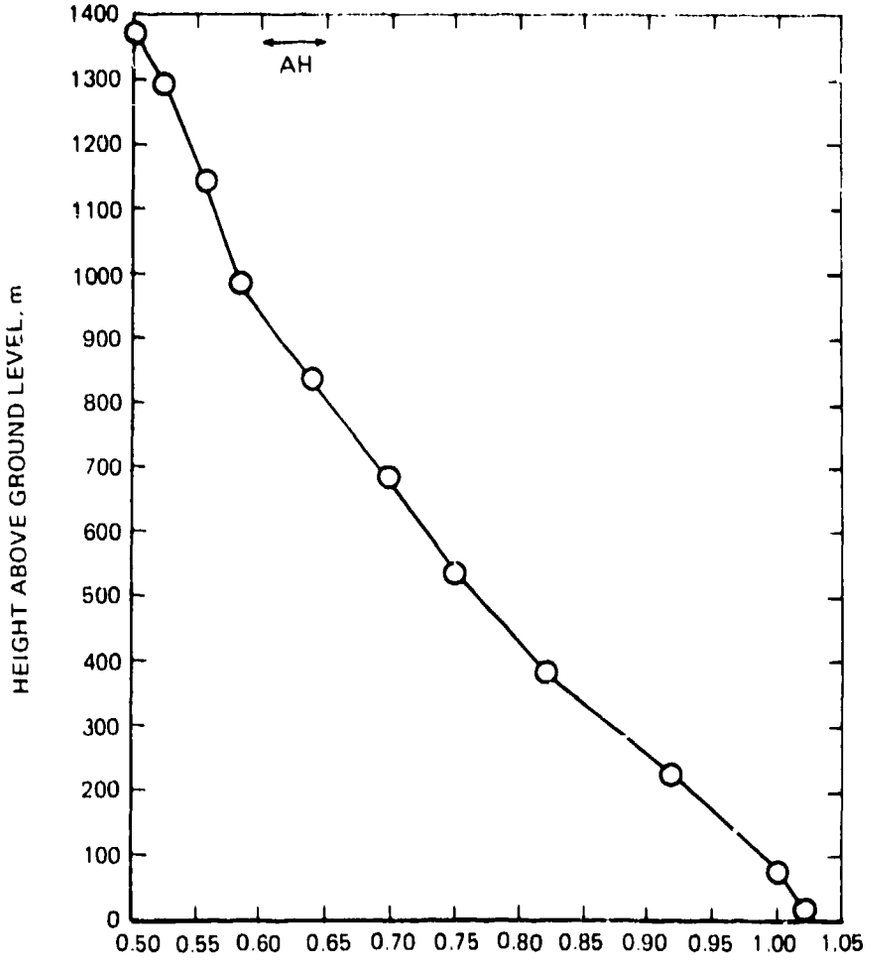

(c) RAISBECK-LEARJET; RUN 12; AIRPLANE HEIGHT, AH, 1359 m.

Figure 25.-Concluded.

Sound Propagation Paths

In order to calculate the attenuation of sound during propagation through the atmosphere it is necessary to determine the length of the sound propagation path. If the meteorological conditions are not constant over the path, then the path must be segmented according to intervals of height over which average meteorological conditions are known (i.e., by strata or horizontal layers of the atmosphere).

A description is presented here of the procedure that was developed to calculate the incremental distances along a sound propagation path. The procedure is specifically applicable to the geometry of the test cases; it could, however, be readily adapted to other noise-measurement situations. The symbols and terminology used here are consistent with the corresponding usage for the computer program in Volume II.

We begin by enumerating certain assumptions relevant to the test cases.

(1) The airplane flies at constant speed, V_a, and Mach number, M_a, along the flight path for the duration of the recording of the noise.

(2) The airplane is always at a large enough distance that the noise that it produces can be considered to be emitted from a single equivalent acoustic source located at the airplane reference point, i.e., the point used for determining the location of the airplane on the flight path.

(3) The flight path is straight for the duration of the noise recording and inclined at an angle, γ, to the horizontal where γ is positive for climbing flight and negative for descending flight.

(4) The sound from the aircraft source propagates at constant speed, c, along a straight line to the microphone, i.e., variations in propagation direction (refraction) caused by temperature variations (hence sound speed variations) can be neglected.

(5) The airplane's flight path is directly over the microphone.

(6) The height of the airplane, AH, is measured when the airplane is overhead (i.e., when the airplane reference point is over the microphone).

(7) The microphone is mounted on a stand at a height ZM above the flat ground plane.

(8) A timing mark is recorded when the overhead position of the airplane is measured, i.e., at time TOH. The timing mark and the measurements of height, airspeed, and flight-path angle are the only information available for tracking the airplane's position as a function of time along the flight path.

(9) Noise data samples are averaged over 0.5-s periods and are available at 0.5-s intervals throughout the duration of the noise recording.

(10) The position of the equivalent airplane noise source along the flight path is correlated with the time at the midpoint of a corresponding 0.5-s sample of noise data.

It was convenient to analyze the general situation according to a relative test-data-sample time, TR, defined as time relative to the time at the overhead position.

Time at overhead, TOH, was provided as part of the input data in seconds on a 24-hr (86,400 s) basis. The time, TS, at the beginning of the first 0.5-s sample of noise data was also provided in seconds on a 24-hr basis. Thus (TOH - TS) represents the time at overhead, in seconds, relative to the time at the start of the first data sample.

The stream of 0.5-s noise data samples was designated as TT(1) = 0.0, TT(2) = 0.5, TT(3) = 1.0, TT(4) = 1.5, and so on, where TT represents test time and TT(1) is identified with 0.0 seconds at the beginning of the first data sample. For the i-th data sample, the test time at the midpoint of the sample is thus [TT(I) + 0.25] in seconds relative to the beginning of the first data sample.

Time, in seconds, for the midpoint of any data sample relative to time at overhead is thus

$$TR(I) = [TT(I) + 0.25] - [TOH - TS]. \qquad (52)$$

For any particular sample of data (e.g., the set of 1/3-octave-band sound pressure levels associated with the maximum value of the tone-corrected perceived noise level), the determination of the corresponding sound propagation path depended on whether the value of TR was less than, equal to, or greater than zero, that is, on whether the airplane was prior to, at, or past the overhead point.

Figure 26 shows the relevant geometrical relationships for the three possibilities and defines the important angles ϕ and ψ and the auxiliary angle η.

The airplane flies at constant speed V_a, and Mach number M_a, along the flight path inclined at angle γ. The microphone is at the receiver position R near the ground plane.

At point E on the flight path the airplane emits a noise signal which propagates at speed c toward the microphone at sound-emission angle ψ relative to the flight path and the direction of flight. In the time, Δt, that it takes for the noise signal to propagate the distance $c(\Delta t)$ from E to R, the airplane moves along the flight path a distance $V_a(\Delta t)$ to point P. The airplane position at point P is at angle ϕ relative to the flight path and the microphone.

The auxiliary angle η can be readily found from the law of sines for plane triangles as

$$[c(\Delta t)]/\sin(\pi - \phi) = [V_a(\Delta t)]/\sin \eta \qquad (53)$$

from which we obtain

$$\eta = \arcsin(M_a \sin \phi) \qquad (54)$$

where $M_a = V_a/c$.

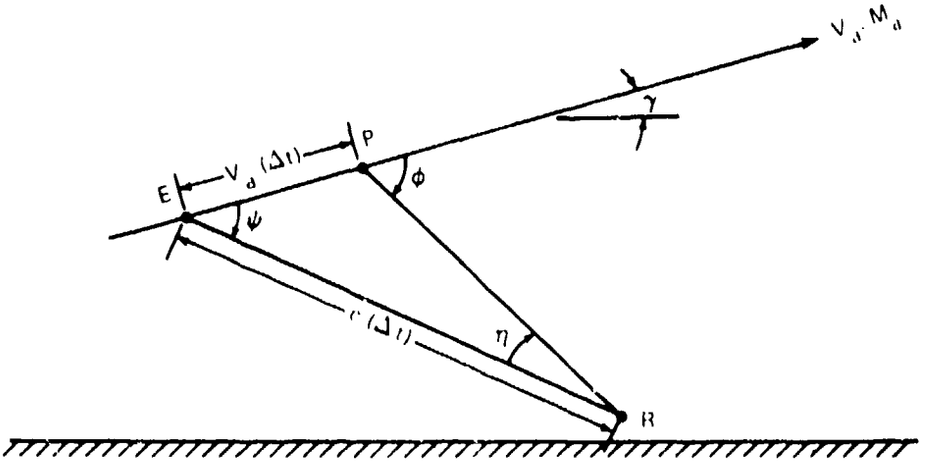

(a) BEFORE AIRPLANE IS OVERHEAD, TR < 0.

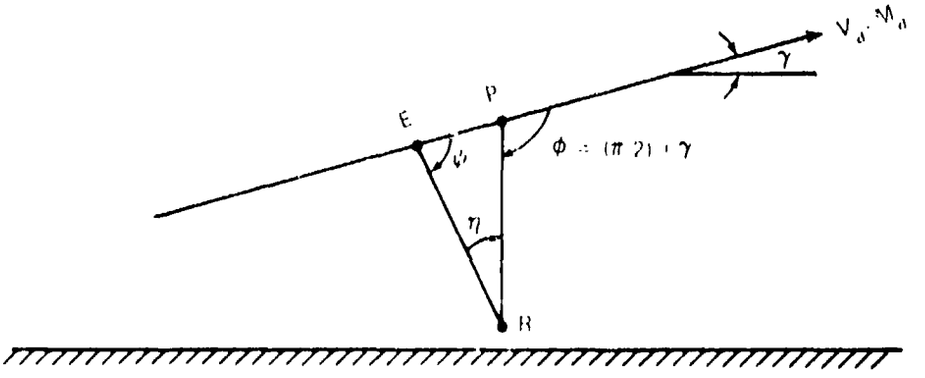

(b) AIRPLANE OVERHEAD, TR = 0.

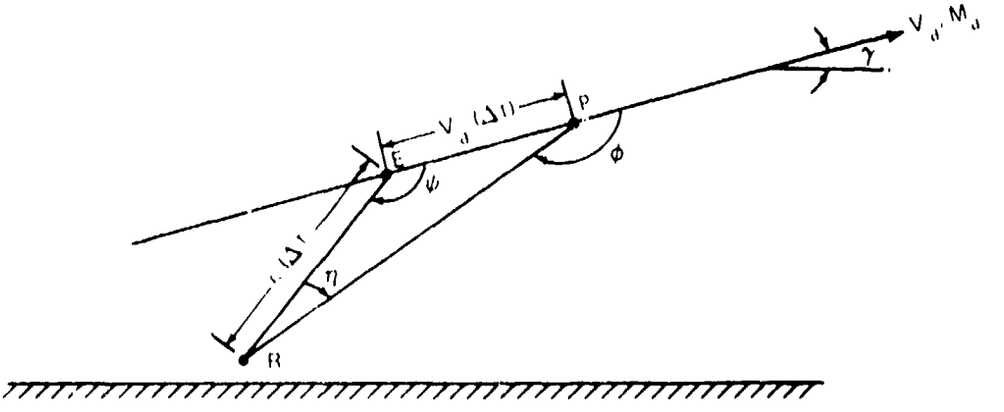

(c) AFTER AIRPLANE IS OVERHEAD, TR > 0.

Figure 26.-Geometrical relationships between aircraft and microphone at different relative times during a flyover.

The sound-emission angle, ψ, which needs to be determined, can be related to ϕ and η using the trigonmetric relation

$$\phi = \psi + \eta$$

from which

$$\psi = \phi - \eta \tag{55}$$

Therefore, if angle ϕ can be found, then angle ψ can be determined using Eqs. (55) and (54) for a specified aircraft Mach number.

In the special case at overhead when TR = 0, Fig. 29(b), angle $\phi = (\pi/2) + \gamma$. Note that for level-flight flyovers with $\gamma = 0$, the sound-emission angle becomes $\psi = (\pi/2) - \arcsin(M_a) = \arccos(M_a)$ when the airplane is over the microphone.

To determine the values of ϕ and ψ at times other than overhead requires the use of some geometrical relationships derived from the available information. Figure 27 illustrates the definition of quantities used to determine angle ϕ on the assumption that angle γ, aircraft Mach number M_a, and distance from the microphone to the flight path at the instant when the aircraft is overhead are all known.

The calculation process proceeds as follows:

(1) Determine the distance AMH from the airplane to the microphone at the time of overhead, i.e., AMH = AH - ZM.

(2) From AMH and flight path angle γ, find the minimum distance DM to the flight path from the microphone at point R (DM = AMH cos γ) and the distance DB back along the flight path from the overhead point to the point of the closest approach (DB = AMH sin γ). [Distance DB is positive for climbing flight paths when γ is positive and negative for descending flight paths when γ is negative.]

(3) The point P on the flight path is where the airplane is when the sound emitted at point E reaches the microphone at point R at some specific relative time TR. The distance DO along the flight path from the overhead point to point P is given by DO = $(V_a)(TR)$. Distance DO is negative when TR is negative, Fig. 27(a), and positive when TR is positive, Fig. 27(b).

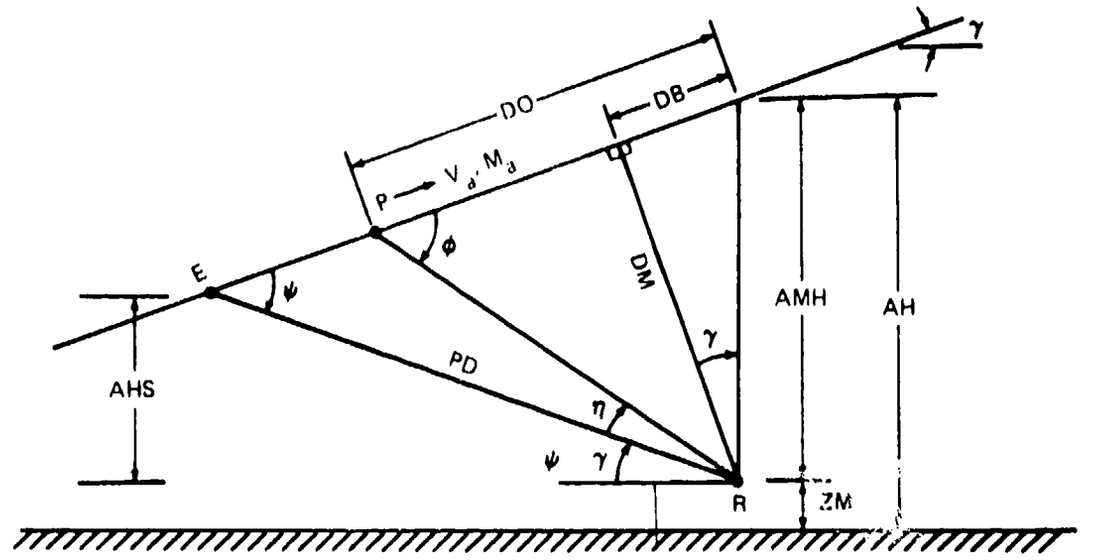

(a) BEFORE AIRPLANE IS OVERHEAD, TR < 0.

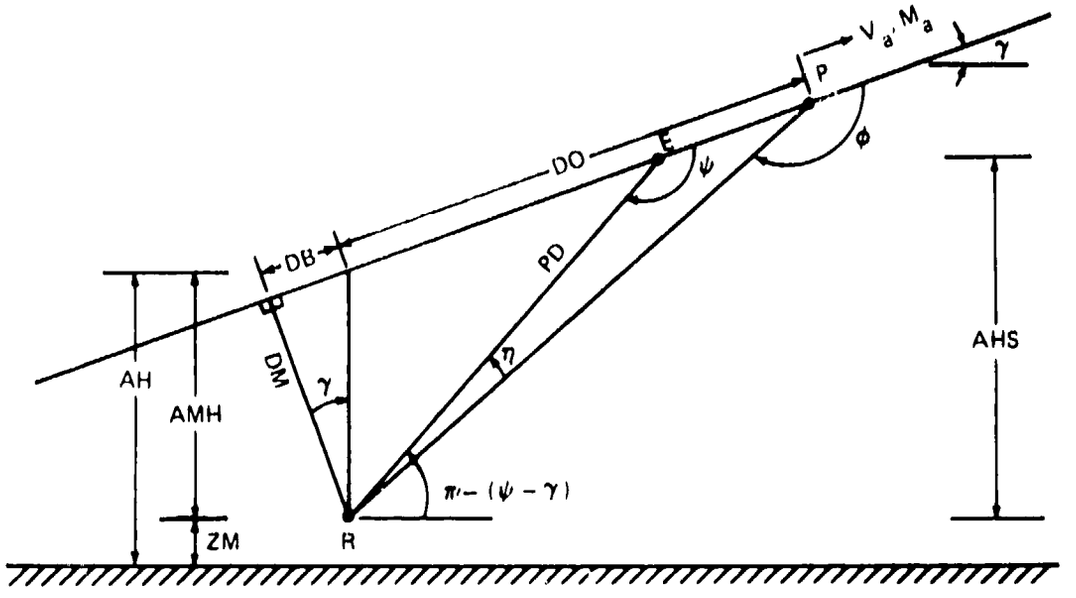

(b) AFTER AIRPLANE IS OVERHEAD, TR > 0.

Figure 27.-Definition of quantities used in calculating angles ϕ, η, and ψ; sound propagation distance PD; and aircraft height above the microphone height at the time of sound emission AHS.

(4) Calculate angle ϕ, in radians, from

$$\phi = \arctan[-DM/(DB + DO)] \tag{56}$$

when DB + DO < 0, and from

$$\phi = \pi - \arctan[DM/(DB + DO)] \tag{57}$$

when DB + DO > 0. When distance (DB + DO) = 0, then point P is at the minimum distance point and $\phi = \pi/2$. (The minus sign before DM in the numerator of the argument of the arctangent in Eq. (56) was included to eliminate negative values for angle ϕ when DB + DO is negative.)

(5) Calculate auxiliary angle η, in radians, by using Eq. (54) knowing M_a and ϕ.

(6) Find angle ψ, in radians, by applying Eq. (55) using the calculated values of ϕ and η.

(7) Determine the total sound propagation pathlength or distance, PD, from

$$PD = DM/\sin \psi \tag{58}$$

for any relative time.

(8) Finally, determine the difference between the height, ZM, of the microphone and the height of the airplane noise source at point E when it emitted the sound that reached the microphone at the specified relative time. The height difference, AHS, is found from

$$AHS = PD \sin(\psi - \gamma) \tag{59}$$

for any relative time.

The incremental distances, D(K), along a sound propagation path can now be determined given angles ψ and γ and the height difference AHS. Figure 28 illustrates the general scheme for calculating the lengths of the segments of

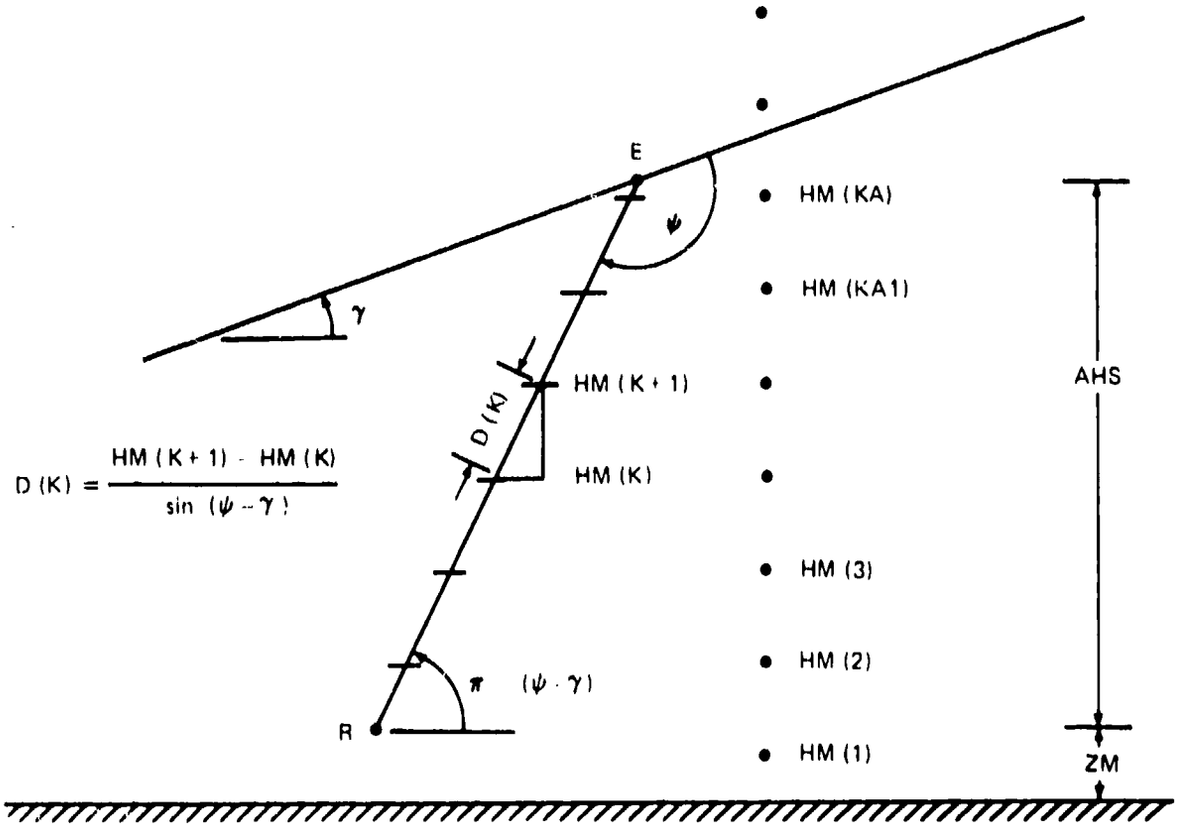

Figure 28. -Illustration of procedure for calculating incremental distances, along sound propagation path of length PD from R to E, which correspond to heights HM (K) where meteorological data were measured.

the propagation path according the the heights, HM(K), where meteorological data were measured. The index, K, for the array of heights and pathlength segments starts at 1 for the height or segment nearest to the ground.

Except for the first and last pathlength segments, the general expression for calculating the length of a pathlength segment is

$$D(K) = [HM(K+1) - HM(K)]/\sin(\psi - \gamma) \tag{60}$$

for any relative time.

For the first pathlength segment, the array of heights is searched to identify the first height which is greater than the microphone height ZM. For example, in Fig. 28 that first height is HM(2). The index of the first meteorological data height which is greater than the height ZM is designated in the computer program by index KK and the first pathlength distance is found from

$$D(1) = [HM(KK) - ZM]/\sin(\psi - \gamma). \tag{61}$$

The distance along the last segment of the propagation path (or really the first segment for propagation proceeding from the location of the equivalent source of noise toward the microphone) requires special consideration because the height of the airplane at point E will not, in general, coincide with the height of a meteorological data measurement. The array of meteorological data heights is again searched during a calculation to identify those heights (or indexes) which are one and two less than the height of the airplane at point E (indexes KA and KA1 in Fig. 28).

Index KA1 is used to terminate the calculations of D(K) using the standard formula in Eq. (60), that is, distance interval D(KA1) is the next to last interval between the microphone and the source.

The length of the last pathlength segment is found from

$$D(KA) = [AHS - |HM(KA) - ZM|]/\sin(\psi - \gamma). \tag{62}$$

Equations (60), (61), and (62) are applied sequentially to generate the array of pathlength segment distances over the total propagation distance for some specified relative test time.

Data Analysis and Adjustment Procedures

The previous parts of this Section have attempted to establish an understanding about the general requirements of FAR 36 relative (a) to measurement of aircraft noise levels during a noise certification demonstration test and (b) to adjustment of the measured test-time EPNL to an equivalent EPNL under reference meteorological conditions.

We have also described the characteristics of the flyover noise data that were available for analysis. These characteristics included: (1) the 500-ms averaging time for each set of 1/3-octave band sound pressure levels, (2) the system used for synchronizing in time the recorded aircraft noise signal and the position (at overhead) of the aircraft on its flight path, (3) the procedure used to account for contamination of the signal by high-level background noise, (4) the geometrical relations available for use in establishing (a) the angle of sound emission between the flight path and the ray to the microphone and (b) lengths along the sound propagation path corresponding to the heights where meteorological data were measured, and (c), for the nine selected test cases, the nature of the flight paths that were flown and the accompanying meteorological conditions aloft.

The computer program that was developed to analyze the flyover noise data from the nine test cases and to calculate atmospheric absorption adjustment factors was given the name TESTREF for the study of test-to-reference adjustment procedures. Volume II contains all the statements for the program.

For each test case, the measured 1/3-octave-band sound pressure levels (corrected for background noise) and the associated test-time meteorological data, time-synchronization data, flight path data, and identification data were all stored in an input data file.

An analysis begins by reading from the input data file. After reading identification and flight-path data, the program reads sound pressure level

data denoted by the array SPL(I,J). The index, or subscript, I indicates the time variable (at 0.5-s intervals) and the index J indicates the frequency-band-number variable. The J index ranges from 1 to 24 for center frequencies from 50 to 10,000 Hz.

For each 0.5-s set of 1/3-octave-band levels, the program calculates the corresponding perceived noise level, PNL(I), using subroutine CPNL, tone-corrected perceived noise level, PNLT(I), using subroutine P36TC, and A-frequency-weighted sound level, AL(I), using frequency weighting factors for 1/3-octave bands from American National Standard S1.4-1971 for Precision Sound Level Meters.

The sets of PNL(I), PNLT(I), and AL(I) data are then searched to find the maximum value in each set [i.e., PNLM, PNLTM, and ALM, respectively] and the relative time of its occurrence. The sets of 1/3-octave-band sound pressure levels that are associated with the times of PNLTM and ALM are identified. The sound pressure levels are identified by codes for the two particular times as SPL(IPTM, J) and SPL(IAM, J) and, for convenience, are given the special names SPLPTM(J) and SPLAM(J) for the sets of band levels at the relative test-time indexes IPTM and IAM.

Adjustment factors for atmospheric absorption losses are calculated for the sound emission angles and propagation pathlengths applicable to the relative test-time indexes IPTM and IAM. The adjustment factors are applied to the test-time measured sound pressure levels SPLPTM(J) and SPLAM(J) to yield corresponding values for reference-day band levels. The program also reads the input file to obtain the measured values of air temperature and relative humidity at each height and the air pressure at the 10-m height.

The next step is to calculate the effective perceived noise level and the sound exposure level for the PNLT(I) and AL(I) data, respectively, using Eqs. (50) and (51). Program subroutine INTEG is used to integrate the data given the 10-dB-down values, in decibels, of PNLTM - 10.0 and ALM - 10.0. The duration factors, DCF and DSEL, for the test-time values of EPNL and SEL are found by application of Eqs. (48) and (49).

Reference meteorological conditions are defined for air temperature, relative humidity, and air pressure.

If test-time meteorological data were not measured at a height of 10 m, then data at 10 m are estimated by interpolating between data measured at heights which are less than and greater than 10 m. The second height is assumed to be always greater than 10 m. The first height where data were measured is assumed to be $\leq$ 10 m.

The average temperature and average relative humidity over each layer of the atmosphere are then calculated from the measured data interpolated to the time of the test and read from the input data file. The air pressure measured at the height of 10 m is assumed to apply to all heights up to the height of the airplane.

The final step before calculating the atmospheric-absorption adjustment factors is to determine, at the relative times corresponding to PNLTM and ALM, the total length of the sound propagation path and the lengths of the segments corresponding to the heights where the meteorological data were measured. The relative test times at time indexes IPTM and IAM are found using Eq. (52). Given the flight path angle, the airplane height at overhead, the airspeed, the airplane Mach number, and the microphone height from the input data file, the program determines the propagation path distances using Eqs. (58), (60), (61), and (62). Airplane height at the time of sound emission is found using Eq. (59).

Four alternative procedures for calculating 1/3-octave-band atmospheric-absorption adjustment factors were included in the study. They were

(1) absorption coefficients and band attenuation by SAE ARP866A and meteorological data measured only at 10 m;

(2) Absorption coefficients and band attenuation by SAE ARP866A and a layered-atmosphere analysis using meteorological data measured at various heights;

(3) absorption coefficients by ANSI S1.26-1978, a band-integration method to calculate attenuation, and a layered-atmosphere analysis using meteorological data aloft; and

(4) absorption coefficients by ANSI S1.26-1978, attenuation calculated at the band center frequencies only, and a layered-atmosphere analysis using meterological data aloft.

For each procedure, the set of calculated reference-day band levels is used to determine values for PNL'_{ref}, $PNLT'_{ref}$, and AL'_{ref}. The reference-day effective perceived noise level and sound exposure level are then found by applying Eq. (46), namely from

$$EPNL_{ref} = PNLT'_{ref} + DCF_{test} \tag{63}$$

and

$$SEL_{ref} = AL'_{ref} + DSEL_{test} \tag{64}$$

using the previously calculated values for DCF_{test} and $DSEL_{test}$.

Procedures (1) and (2) are the 10-m and layered-atmosphere procedures of FAR 36. Procedure (4) is similar to procedure (2) except that absorption is calculated by the method of ANSI S1.26.-1978 instead of SAE ARP866A and center frequencies are used for all frequency bands instead of just to 4000 Hz with lower bandedge frequencies for the 5000 to 10,000-Hz bands. Procedure (3) uses the method of ANSI S1.26-1978 to calculate absorption but evaluates the adjustment factor by integrating over the bandwidth of a filter.

The methods used for procedures (1), (2), and (4) are relatively straightforward. The method used for procedure (3) is more complex because of the requirement to evaluate an integral.

For procedure (1), the reference-day band level for any band is found from

$$SPL_{ref,(1)} = SPL_{test} + (\alpha_{test,\ 10m} - \alpha_{ref})(PD) \tag{65}$$

using the calculated value of total propagation distance PD in meters for absorption coefficients α in decibels/meter.

The absorption coefficients $\alpha_{test,\ 10m}$ and α_{ref} are determined using a computer-program subroutine called ARP866A. To find $\alpha_{test,\ 10m}$, the subroutine is supplied with the air temperature and relative humidity at the 10-m height for test-time conditions. The 25° C and 70-percent relative humidity conditions are supplied to calculate α_{ref}.

For procedure (2), the reference-day band levels are found using

$$SPL_{ref,(2)} = SPL_{test} + (\bar{\alpha}_{test} - \alpha_{ref})(PD) \tag{66}$$

where $\bar{\alpha}_{test}$ is the average absorption coefficient under test-time conditions over the sound propagation path.

The average absorption coefficient is determined from

$$\bar{\alpha}_{test} = atten/PD \tag{67}$$

where atten is the total attenuation in decibels over the path. The total attenuation is found from

$$atten = \sum_{K=1}^{KL} [\alpha_{test}(K)][D(K)] \tag{68}$$

where $\alpha_{test}(K)$ represents the average atmospheric absorption coefficient by SAE ARP866A for the K-th segment of the sound propagation path. The index KL represents the last segment of the path from the microphone to the airplane. For each of the K-th segments, the average temperature and relative humidity for the layer is used with subroutine ARP866A to determine the value of $\alpha_{test}(K)$.

The structure of Eq. (66) was chosen to be parallel to the wording of FAR 36. Equations (66), (67), and (68) could have been combined as

$$SPL_{ref,(2)} = SPL_{test} + \sum_{K=1}^{KL} [\alpha_{test}(K) - \alpha_{ref}][D(K)] \tag{69}$$

since α_{ref} is a constant and $\sum D(K) = PD$. The method implied by Eq. (69) is superior to that of Eqs. (66), (67), and (68) from a computational point of view because the adjustment terms in the summation are all relatively small numbers and hence the overall accuracy should be better.

For procedure (4), the formalism of Eq. (69) is used to calculate the reference-day band levels, namely

$$SPL_{ref,(4)} = SPL_{test} + \sum_{K=1}^{KL} [a_{test}(K) - a_{ref}][D(K)] \tag{70}$$

where now the atmospheric absorption coefficients are determined by program subroutine ANSAB for American National Standard ABsorption for the test and reference meteorological conditions.

The band-integration method for procedure (3) is described in the next Section.

Description of Band-Integration Procedure

For procedure (3), the expression for calculating the reference-day sound pressure levels is given by

$$SPL_{ref,(3)} = SPL_{test} + BA_{(3)} \tag{71}$$

where the band-adjustment factor, $BA_{(3)}$, in decibels, is determined by a computer-program subroutine called NUMINT for NUMerical INTegration.

The basis for the method of calculating the band-adjustment factor was derived using an analysis similar to that in Section 2. The 1/3-octave-band filters were assumed to have ideal filter-transmission-response characteristics because indicated or measured band levels that were not the same as those which would be indicated by filters having ideal response characteristics were considered to have, effectively, a measurement system error. The "correct" band levels were considered to be those which would have been indicated by filters having ideal response characteristics.

In making the assumption about ideal filters, it was recognized, as a result of the analysis presented in Section 3, that some of the measured flyover noise data may have contained high-frequency band levels which were influenced by energy transmitted through the filter's lower stopband. Nevertheless, because there was no way to confirm the suspicion of real-filter effects for the data that were available and because development of a procedure to use the response characteristics of real filters with actual aircraft noise spectra was not within the scope of the present program, the band-integration method of procedure (3) was based on the assumption of ideal filter-response characteristics.

The assumption of ideal characteristics for the 1/3-octave-band filters was considered to have negligible effect on the validity of the relative evaluation of the four alternative atmospheric-absorption adjustment procedures, especially for evaluations in terms of time-integrated measures such as EPNL or SEL. Evaluation in terms of relative differences in band sound pressure levels, especially the high-frequency bands, was considered likely to be influenced more than evaluations in terms of time-integrated measures by the assumption of ideal filter transmission response. However, for the data available to the study, the number of 1/3-octave-band sound pressure level evaluations that could be made was limited because of contamination by high-level background noise in the high-frequency bands.

The band-adjustment factor for procedure (3) was derived as follows using

notation introduced in Sections 2 and 3.

The sound pressure level in any band that would have been measured at the receiver location under reference meteorological conditions (i.e., the band level LR_{ref}) can be obtained from the level measured at the receiver location under the actual, or test, meteorological conditions, LR_{test}, by applying an adjustment factor as

$$LR_{ref} = LR_{test} + (LR_{ref} - LR_{test}) \tag{72}$$

where the band-level difference $(LR_{ref} - LR_{test})$ is the adjustment factor $BA_{(3)}$ in Eq. (71).

The band-adjustment factor in Eq. (72) can be written in terms of the ratio of the mean squared sound pressures as

$$(LR_{ref} - LR_{test}) = 10 \log \left[p^2_{R,ref} \Big/ p^2_{R,test} \right] \tag{73}$$

which can also be expressed in terms of the ratio of the Fourier transforms of the power spectrum, G_R, of the sound pressure at the receiver location as

$$(LR_{ref} - LR_{test}) = 10 \log \left\{ \left[\int_{f_L}^{f_U} G_{R,ref} \, df \right] \Big/ \left[\int_{f_L}^{f_U} G_{R,test} \, df \right] \right\} \tag{74}$$

if the filters have ideal response characteristics so that the range of integration only needs to cover the filter's passband.

To evaluate the integrals in Eq. (74) requires an expression for $G_{R,ref}$ in terms of measured or known quantities. By analogy to the development of Eqs. (17) and (26), the required expression is obtained by writing the spectrum at the receiver in terms of the spectrum at the source and an atmospheric-absorption function.

Thus, symbolically, the sound pressure spectrum at the receiver under the two meteorological conditions can be written as

$$G_{R,test} = (G_S)(AF^-_{test}) \tag{75}$$

and

$$G_{R,ref} = (G_S)(AF^-_{ref}) \tag{76}$$

where AF^- is the absorption function over the sound propagation path from the source to the receiver under the noted atmospheric conditions.

If the sound emission angle is constant, then the source pressure spectrum, G_S, in Eq. (75) is equal to the source pressure spectrum in Eq. (76). (The sound propagation pathlengths and the source strengths are assumed to be identical under the two meteorological conditions.)

From Eq. (75), the source pressure spectrum is

$$\begin{aligned} G_S &= G_{R,test}/AF^-_{test} \\ &= (G_{R,test})(AF^+_{test}) \end{aligned} \tag{77}$$

where the notation AF^+ indicates the absorption factor along the path from the receiver to the source, see Eq. (26).

With Eq. (77), the sound pressure spectrum, $G_{R,ref}$, in Eq. (76) can be written as

$$G_{R,ref} = (G_{R,test})(AF^+_{test})(AF^-_{ref}). \tag{78}$$

Substitution of Eq. (78) into Eq. (74) yields

$$(LR_{ref} - LR_{test}) = BA_{(3)} =$$

$$10 \log \left\{ \left[\int_{f_L}^{f_U} (G_{R,test})(AF^+_{test})(AF^-_{ref})\, df \right] \Big/ \left[\int_{f_L}^{f_U} G_{R,test}\, df \right] \right\} \tag{79}$$

Referring back to Section 2, the form of Eq. (79) is seen to be similar to that of Eq. (28) with the inclusion of the AF^- term as a factor in the integral in the numerator.

Because the sound path is to be divided into segments according to the layers of the atmosphere, the absorption function at any frequency has the form of Eq. (20) namely

$$AF^+_{test} = 10^{\sum_k a_{k,test}\, \xi_{k,test}/10} \tag{80}$$

and

$$AF^-_{ref} = 10^{\sum_k a_{k,ref}\, \xi_{k,ref}/10} \tag{81}$$

where a_k is the atmospheric sound absorption coefficient applicable to the k-th segment of the propagation path under test or reference meteorological conditions and ξ_k is the length of the k-th segment. Meteorological parameters applicable to a path segment are assumed to be the average temperature, humidity, and pressure at the middle of each layer of the atmosphere.

If the sound path is divided into the same segments under the two atmospheric conditions (as it usually would be), then $\xi_{k,test} = \xi_{k,ref} = \xi_k$ and the product of the absorption functions in Eqs. (80) and (81) can be written as

$$(AF^+_{test})(AF^-_{ref}) = 10^{\sum_k (a_{k,test} - a_{k,ref})\, \xi_k/10} \tag{82}$$

and Eq. (79) for the band-adjustment factor becomes

$$BA_{(3)} = 10 \log \left\{ \left[\int_{f_L}^{f_U} (G_{R,test}) \left(10^{\sum_k (a_{k,test} - a_{k,ref})\, \xi_k/10} \right) df \right] \Big/ \left[\int_{f_L}^{f_U} G_{R,test}\, df \right] \right\} \tag{83}$$

Equation (83) defines the band-integration method carried out by subroutine NUMINT for calculation of adjustment factors by procedure (3). Evaluation of the integrals is relatively straightforward if an expression can be supplied for the power spectrum of the sound pressure at the microphone, $G_{R,test}$, given the measured 1/3-octave-band sound pressure levels. Subroutine ANSAB is used to calculate the values of $a_{k,test}$ and $a_{k,ref}$ by the method of ANSI S1.26-1978.

The technique selected to approximate the power spectrum of the sound pressure was the same two-straight-line or two-slope technique used to evaluate the integrals in Eq. (28), see Figs. 8 and 9. Any method of approximating the actual shape of the power spectrum of the sound pressure at the microphone, $G_{R,test}(f)$, over the frequency range of the passband of a filter that was more sophisticated than the two-straight-line or two-slope method was not felt to be appropriate. (Sutherland and Bass[7] discuss the use of a spline function as a general interpolation method between two band-level data points but recommend a log-linear equation to interpolate a spectral shape based on band levels for the bands below, at, and above the band of interest.) The two-straight-line method was considered to be the best choice because the data were available only in 1/3-octave-wide frequency bands, because the possible contribution of energy transmitted through the lower or upper stopbands was neglected as a result of making the assumption that the filters had ideal response characteristics, and because of the necessity to work with practical spectra from which band levels were missing because of background noise contamination.

Montegani[21] has developed an alternative method for numerically evaluating the integrals [such as those in Eq. (83)] which express atmospheric absorption loss over the frequency range of an ideal bandpass filter. As for the present analysis, Montegani uses band-level differences, or a two-slope technique, to approximate the power spectrum of the sound pressure at the receiver, G_R, but he defines frequency steps across the range of integration on a logarithmic rather than a linear scale as done here for use with the numerical integration routine available in subroutine QSF. For the i-th frequency band, Montegani recommends dividing the interval from f_L to f_U into j steps according to

$$(f_j/f_c)_i = 10^{(3/10b)[j/(2m+1)]} \tag{84}$$

where b denotes the type of fractional-octave-band filter (b = 3 for 1/3-octave band filters) and m is an integer whose value is specified by the user. For all bands, Montegani recommends m = 3, to give seven frequencies equally spaced [from j = -m to j = m] between f_L and f_U on a logarithmic scale.

For long-distance measurements of sound, the high-frequency portion of the spectrum can decrease very rapidly with frequency, e.g., see Fig. 4. Determination of atmospheric absorption losses for such cases may require calculation at more than three frequencies in each half of a frequency band to maintain accuracy. However, for those cases, the indicated band sound pressure level is most likely to be contaminated by energy transmitted through the lower stopband and the approximation of the power spectrum by the two-slope method will also be less accurate. Montegani's computer program in Ref. 21 could be modified to use m = 3 for some range of low- and mid-frequency bands and increasingly larger m values for the higher-frequency bands. A more-fundamental need, however, is for a method which, in a computationally efficient manner, is able to estimate the contribution to the indicated band sound pressure level caused by real-filter effects and then to calculate the atmospheric absorption loss over the frequency range of significant response for practical fractional-octave-band filters.

Sutherland, in Ref. 22, has refined the iteration method described in Ref. 7 and has proposed an analytical procedure to estimate what the band sound pressure levels would have been if the filters had ideal rather than practical transmission-response characteristics.

The method used here for calculating band absorption loss made use of the same approach as that used to derive Eq. (29). The frequency range over the passband of a filter was split into two parts from f_L to the band center frequency, f_c, and from f_c to f_U. The two terms in the numerator of Eq. (83) [which are identical to those in Eq. (29) except that they include the absorption function as shown in Eq. (83) instead of just ΔF^+ as in Eq. (29)] are evaluated numerically using band-level differences (or slopes) defined by Eqs. (30) and (31). The two denominator terms are evaluated using Eqs. (32) or (33) as appropriate for the value of the slope of the applicable straight-line approximation to $G_{R,test}$.

Subroutine NUMINT carries out the calculation of the adjustment factor according to the above-described process for evaluating the integrals in Eq. (83). The subroutine requires specification of (1) the test-time sound pressure

levels that are to be adjusted to reference conditions, (2) the reference air temperature, (3) the reference relative humidity, (4) the reference air pressure, (5) the array of average test-time air temperatures over each layer of the atmosphere starting at the height of the microphone, (6) the corresponding array of average test-time relative humidities over each atmospheric layer, (7) the test-time air pressure, (8) the array of pathlength segments between the microphone and the aircraft at the time associated with the sound pressure levels, and (9) the value of the final index along the path from the microphone to the aircraft for the arrays of air temperature, relative humidity, and pathlength segments.

The total number of frequency intervals (or number of frequency steps) over the passband of a filter that were used to evaluate the numerator terms for Eq. (83) were the same as used with subroutine QSF in Section 2 for the eleven bands with center frequencies from 1000 to 10,000 Hz. Thus, for example the band at 10,000 Hz was divided into 30 equally-spaced steps, 15 from f_L to f_c and 15 from f_c to f_U. The 13 bands from 50 to 800 Hz were each divided into 8 steps, 4 from f_L to f_c and 4 from f_c to f_U. Four steps is the minimum number recommended for use with the QSF integration routine.

Given the test-time sound pressure levels, meteorological and pathlength data, and the number of frequency intervals to use for the numerical integrations, the process of calculating the band-adjustment factor is straightforward with one exception. The exception is the calculation of the slopes of the straight-line approximations to $G_{R,test}$ over the frequency range of each filter.

Calculation of band-level differences or slopes was not as straightforward as in Section 2 because of the need to be able to handle spectra from which band levels were missing because of background noise contamination. The various possibilities for spectra having missing band levels are shown in Fig. 29. Subroutine DIFFS, which is called by subroutine NUMINT, was prepared to handle all the possibilities and to calculate appropriate band slopes for any test-time spectrum.

Figure 29(a) illustrates the case when a complete spectrum with no missing band levels is available. Slopes (or band-level differences) are computed for

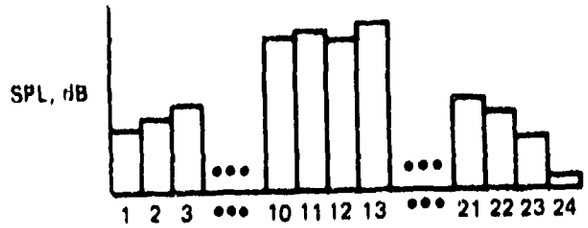

SLOPE (1,2) $L_2 - L_1$
SLOPE (1,1) SLOPE (1,2)
•••
SLOPE (J,1) = SLOPE (J,2)
SLOPE (J,2) = $L_{J+1} - L_J$
•••
SLOPE (23,2) = $L_{24} - L_{23}$
SLOPE (24,1) = SLOPE (23,2)
SLOPE (24,2) = SLOPE (24,1)

(a) CASE 1: DATA AVAILABLE FOR ALL BANDS.

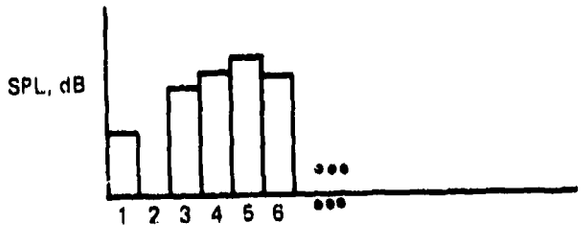

SLOPE (1,1) = SLOPE (1,2) = SS (1)
SLOPE (2,1) = SLOPE (2,2) = 1.0
SLOPE (3,2) = $L_4 - L_3$
SLOPE (3,1) = SLOPE (3,2)
AND SO ON TO BAND 24

(b) CASE 2: NO DATA FOR BAND NUMBER 2; ISOLATED BAND AT BAND NUMBER 1.

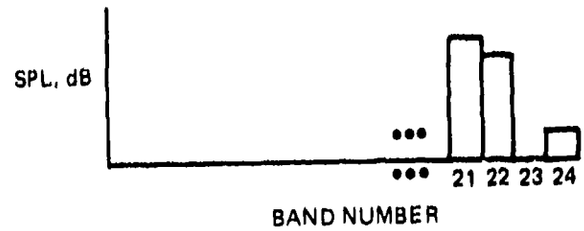

••• FROM BAND 1
SLOPE (21,2) = $L_{22} - L_{21}$
SLOPE (22,1) = SLOPE (21,2)
SLOPE (22,2) = SLOPE (22,1)
SLOPE (23,1) = SLOPE (23,2) = 1.0
SLOPE (24,1) = SLOPE (24,2) = SS (24)

(c) CASE 3: NO DATA FOR BAND NUMBER 23; ISOLATED BAND AT BAND NUMBER 24.

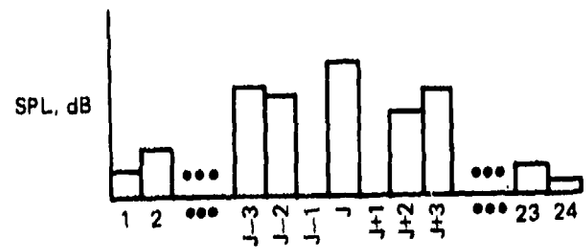

••• FROM BAND 1
SLOPE (J-2,1) = SLOPE (J-3,2)
SLOPE (J-2,2) = SLOPE (J-2,1)
SLOPE (J-1,2) = SLOPE (J-1,2) = 1.0
SLOPE (J,1) = SLOPE (J,2) = SS (J)
SLOPE (J+1,1) = SLOPE (J+1,2) = 1.0
SLOPE (J+2,2) = $L_{J+3} - L_{J+2}$
SLOPE (J+2,1) = SLOPE (J+2,2)
AND SO ON TO BAND 24

(d) CASE 4: DATA FOR BAND AT J, BUT NO DATA FOR BANDS AT J-1 OR J+1; ISOLATED BAND AT BAND NUMBER J.

Figure 29.-Illustration of rules for calculating band-level differences.

the lower half and the upper half of each band, see Fig. 9. For a band at frequency-index J, the slopes over the lower and upper halves of the passband are denoted by the two-dimensional arrays SLOPE(J,1) and SLOPE(J,2), respectively.

Figure 29(a) also indicates the rules used for computing the slopes for any of the 24 bands. Note that a special rule was required for the lower half of band 1 and the upper half of band 24. The slope over the lower half of band 1 [SLOPE(1,1)] was assumed to equal that over the upper half of band 1 [i.e., SLOPE(1,1) = SLOPE(1,2) = $L_2 - L_1$]. The slope over the upper half of band 24 was assumed to equal the slope over the lower half of band 24, i.e., SLOPE(24,2) = SLOPE(24,1) = $L_{24} - L_{23}$. Montegani[21] made the same assumptions for his computer program.

Figures 29(b) to 29(d) illustrate the three special cases that needed to be considered as a result of band levels missing from a spectrum because of background noise contamination. The three special cases involve the question of how to specify a set of slopes for a band that is isolated in the sense of not having valid sound pressure levels in the bands above and below. The three cases also involve the question of what to specify for slopes for the band for which the sound pressure level is missing because of contamination.

The general rules adopted for the isolated-band and missing-band problems were (1) that the slopes to use for isolated bands were the substitute slopes shown in Fig. 30, and (2) that a slope of +1.0 dB/band should be used for bands having no valid sound pressure levels.

The band-level slope of +1.0 dB/band was chosen as a convenient, though arbitrary, value to use with the numerical integrations performed by subroutine NUMINT. A slope of +1.0 dB/band represents a white-noise spectrum with equal energy per unit frequency. By Eq. (30), the power spectrum of a white-noise signal is a constant (i.e., $\ell^L = \ell^U = 0$).

When the band-level slopes are +1.0 dB/band, the band-adjustment factor from Eq. (83) represents the difference in the average attenuation resulting from atmospheric absorption over the frequency range of the passband of the

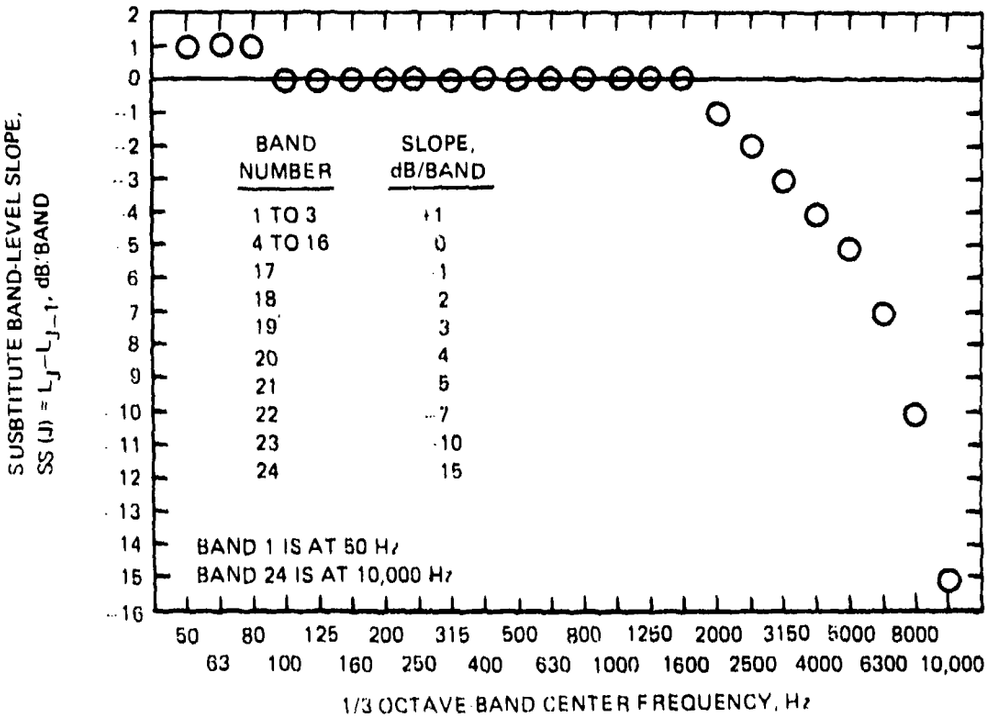

Figure 30.-Substitute slopes for 1/3-octave-band levels of broadband aircraft noise in the free field. (Substitute slope for band 1 estimated from slope derived for band 2.)

ideal filter and over the length of the sound propagation path. For a white-noise spectrum, Eq. (83) reduces to

$$BA_{(3)} = 10 \log \left\{ \left[\int_{f_L}^{f_U} \left(10^{\sum_k (a_{k,test} - a_{k,ref}) \xi_k / 10} \right) df \right] \Big/ (f_U - f_L) \right\} \quad (85)$$

where the denominator $(f_U - f_L)$ represents the bandwidth of the ideal filter.

Although subroutine DIFFS does supply subroutine NUMINT with slope values for the lower and upper halves of all 24 bands including those bands that have no valid data because of background noise contamination and although subroutine NUMINT does calculate a band-adjustment factor for every band from band 1 to band 24 regardless of the value of the test-time sound pressure level, the main computer program is instructed to set the reference-day band sound pressure level to 0.0 dB if the test-time band sound pressure level was not valid. That is

$$SPL_{ref}(J) = 0.0, \text{ if } SPL_{test}(J) = 0.0 \quad (86)$$

for any band and for any band-adjustment method.

The rule expressed by Eq. (86) was adopted to avoid creating values for reference-day band sound pressure levels when the test-time sound pressure level was missing. Because of Eq. (86), any convenient slope could have been selected to use for SLOPE(J,1) and SLOPE(J,2) when the band sound pressure level was missing. The value of +1.0 dB/band was selected because it yields a measure of the average adjustment factor. The average adjustment factor was considered to have intrinsic interest. All adjustment factors are available internally within the program and could be listed in the output, if desired, with minor changes to the program statements.

The problem of specifying reasonable values to use for band-level slopes in the case of an isolated band sound pressure level [cases 2, 3, and 4 in Figs. 29(b) to 29(d)] was resolved by developing the set of so-called substitute slopes shown in Fig. 30.

The slopes in Fig. 30 represent average values obtained from examination of band-level slopes from 1/3-octave-band spectra at various times during the recordings of DC-9 flyover noise levels from the five samples of test data. In the low-frequency bands (center frequencies from 63 to 630 Hz), large variations in slope (±8 to ±10 dB/band) were observed. The large variations were attributed to ground-reflection effects in the measured spectra. An average slope of zero dB/band was estimated to be appropriate for the broadband component of the spectrum in an acoustic free field. For the high-frequency bands (1250 to 5000 Hz), variations in observed slope values were somewhat smaller than those observed for the low-frequency bands and were attributed to discrete-frequency components in the JT8D engine noise signal.

The high-frequency rolloff of the spectrum implied by the increasingly negative slopes for the bands above 1600 Hz in Fig. 30 was regarded as being representative of the broadband component of the jet-noise spectrum for the moderately absorptive atmospheric conditions and moderate pathlengths applicable to the available aircraft noise data.

Alternatives to the use of the substitute slopes in Fig. 30 for specifying band-level slopes to use with subroutine NUMINT to calculate an absorption adjustment factor for an "isolated" band were also considered. The alternatives were either to specify some arbitrary slope that was the same for all bands that might have isolated values of sound pressure level or to calculate a slope based on the nearest valid sound pressure levels in bands above and below the band containing the "isolated" band sound pressure level. Specification of an arbitrary slope (such as +1.0 dB/band) would have been somewhat easier to incorporate in the computer program than the use of substitute slopes; the substitute slopes, however, were regarded as being more realistic in the high-frequency bands. Calculations of slopes by extrapolating over one, two, or more bands having missing sound pressure levels would have been more complicated and would not have been any more accurate or appropriate than the technique of using a set of substitute slopes.

The slope over the upper half of the band prior to a band where the data were missing [e.g., the band at J-2 in Fig. 29(d)] was calculated as though

the band was the last in a complete spectrum [i.e., band 24 in Fig. 29(a)]. Similarly, the slope over the lower half of the band above a band where the data were missing [e.g., the band at J+2 in Fig. 29(d)] was calculated as though the band was the first one in a complete spectrum [i.e., band 1 in Fig. 29(a)].

As a final observation on the band-integration procedure for determining the attenuation caused by atmospheric absorption, it is important to note that the power spectrum of the sound pressure at the microphone (i.e., $G_{R,test}$) has always implicitly been assumed to be a relatively smooth and continuous function of frequency. This assumption was the basic justification for the reasonableness of approximating $G_{R,test}$ in Eq. (83) by line segments over the lower and upper halves of the theoretical passband of the 1/3-octave-band filters. If the spectrum of the sound contains discrete-frequency components such that the sound pressure level in a band is controlled by the level of one, or a few, spectral components within the passband of the filter, then the two-slope or band-level-difference method for approximating $G_{R,test}$ as a function of frequency will not provide a reasonable estimate of the actual variation of $G_{R,test}$ with frequency.

If discrete-frequency components are present in the passband of a filter and if a procedure were available to determine their level and frequency, then the integration of Eq. (83), or the summation carried out by the numerical integration procedure in subroutine NUMINT, would only need to include the discrete-frequency components. If there is only one discrete-frequency component within the passband and its level determines the indicated band level, then the integration would include only one spectral component and, for that band, the calculation of the adjustment factor would be reduced to the form of Eq. (70) for procedure (4) but evaluated at the frequency of the component instead of the band center frequency.

In order to be able to apply the integration method of Eq. (83) separately to the broadband, continuous component of a spectrum and to the discrete-frequency components, some procedure must be available to provide an estimate of the level and frequency distribution of the components. The procedure should have an analytical base so that it can be described mathematically and incor-

porated into routine data processing by a digital computer. The procedure should be capable of accounting for band-sharing effects caused by strong discrete-frequency components or by moderate-amplitude components whose frequency is near the edge of the passband of a filter. The procedure should also be able to account for the apparent change in frequency due to Doppler effects as the magnitude and sign of the component of the speed of the sound sources on the aircraft in the direction of the sound ray propagating toward the microphone (and consequently the apparent wavelength and hence frequency) change with time during a flyover.

A procedure to determine the separate components of a complex time-varying sound such as aircraft noise does not exist. The nearest approximation to such a procedure is the tone-identification routine in Appendix B of Part 36 but that method only provides a crude estimate of the broadband, continuous component and no information on the true frequency and level of the discrete-frequency components. No analytical procedure is available to account for band-sharing or Doppler-frequency-shift effects. Thus, either because information is not available or cannot be provided in a practical manner, application of the band-integration method of Eq. (83) will usually be accomplished in a straightforward manner by ignoring any suspected or actual discrete-frequency components and simply estimating the pressure spectrum function $G_{R,test}$ by the band-level difference method across the passband of every filter.

The straightforward approach was adopted for this study when using the band-integration method of procedure (3). The band-level adjustment factor determined by such an approach will be incorrect although the error, as Montegani[71] has pointed out, will potentially be no larger than using the band-center-frequency method of procedure (4) and ignoring the integral approach.

Results of Comparative Evaluations of Alternative Atmospheric-Absorption Adjustment Procedures

Previous parts of this Section have described the nine cases of flyover noise data that were available for analysis. The description included consideration of the procedures used for acquisition and processing of the flyover noise data as well as consideration of the available test-time meteorological data. The method of calculating the lengths of the sound propagation paths

and the angles of sound emission at times during a flyover was shown for the geometry of the test cases. Also described was the computer program, TESTREF, that was prepared to analyze flyover-noise test data and to determine the sound pressure levels that would have been measured under specified reference-day meteorological conditions instead of the actual test-time meteorological conditions. Four alternative procedures were considered for calculating the band-level adjustment factors for differences in atmospheric absorption under test and reference conditions. Evaluation of those four procedures is presented in this part.

Evaluation of the atmospheric-absorption adjustment procedures is given here primarily in terms of the effect on the 1/3-octave-band sound-pressure-level spectra. Evaluation also includes a discussion of the effect of using the various procedures on the following noise descriptors: PNLM, PNLTM, EPNL, ALM, and SEL

Measured Perceived Noise Levels and A-Weighted Sound Levels.- We begin by considering the variation of PNLT and AL with time during a typical flyover noise measurement. Figure 31 presents the results at 0.5-s time intervals relative to the time when the airplane was over the microphone, i.e., time TR(I) by Eq. (52). The PNLT and AL values were normalized by their respective maximum levels, PNLTM and ALM. The data are from run 272 of the set of DC-9-14 tests, see Table 2. The subcaptions for the two sets of data in Fig. 31 list the values of the maximum quantities (PNLM, PNLTM, and ALM) as well as the time-integrated quantities (EPNL and SEL).

The plots in Fig. 31 illustrate some features that are significant to a study of atmospheric-absorption adjustments. The primary scale for the abscissa is the linear scale for the time TR(I) at the midpoint of a data sample relative to the time at overhead. A secondary abscissa scale is shown below the time scale for the sound emission angle ψ. Note the rapid variation in the value of ψ around the overhead position. In the two-second interval from TR= -1 s to TR = +1s, ψ varied from 53.2° to 102.3° or about 25° per second. The rapid variation in angle emphasizes the need for having a high-quality airplane-tracking system during a test and for having accurate synchronization in time between the airplane tracking system and the noise recordings.

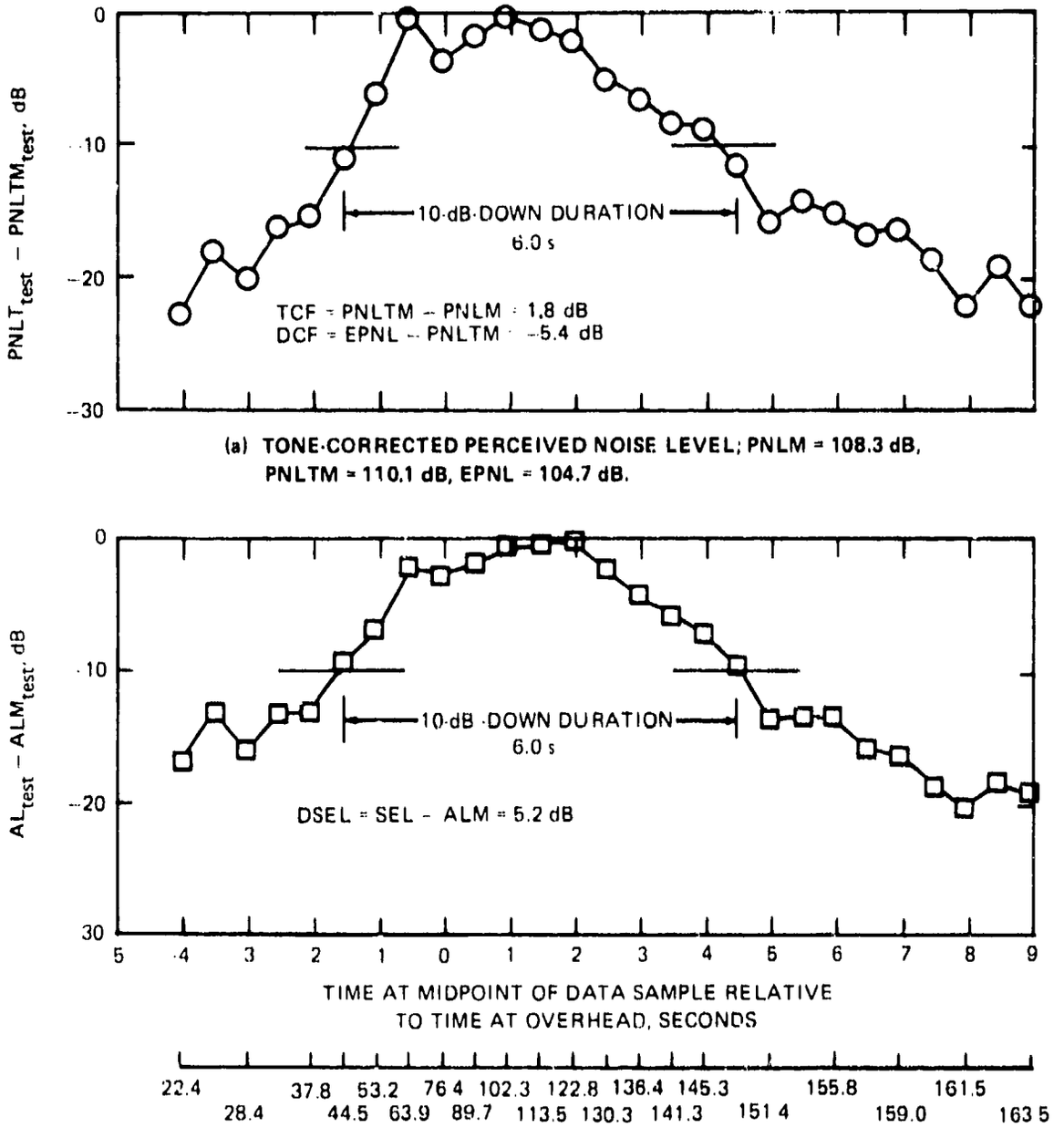

(a) TONE-CORRECTED PERCEIVED NOISE LEVEL; PNLM = 108.3 dB, PNLTM = 110.1 dB, EPNL = 104.7 dB.

(b) A-WEIGHTED SOUND LEVEL; ALM = 93.7 dB, SEL = 98.9 dB.

Figure 31.-Variation of normalized PNLT and AL with time during a DC-9-14 flyover, from run 272.

Another point is that, although the time variation of PNLT and AL in Fig. 31 is relatively smooth, the time pattern can contain several short-duration peaks. Indeed, for the PNLT data in Fig. 31(a), the peak at the relative time of -0.55 s has a value which is only 0.1 dB below the maximum at +0.95 s. If the peak at -0.55 s had been 0.1 dB higher and the peak at 0.95 s had been 0.1 dB lower, then the sound emission angle associated with PNLTM would have shifted from 102.3° to 63.9° with a correspondingly large change in the length of the sound propagation path and the magnitude of the calculated band-level attenuation due to atmospheric absorption.

Note also that if there had been two or more peaks having the same maximum values, the one chosen to be designated as PNLTM (and its corresponding time or emission angle) is always the last one in a search from the first to the last data sample. The choice of which maximum to designate as PNLTM or ALM does not affect the determination of the 10-dB-down integration times or the value of the integrated measures EPNL or SEL. The choice of the time of occurrence of PNLTM or ALM does, however, affect the length of the sound propagation path and the calculation of the band-level adjustment factors from test to reference meteorological conditions.

In five out of the nine test cases, the time of occurrence of PNLTM was the same as the time of occurrence of ALM. Figure 31, however, shows one of the cases where the relative times were not the same. The maximum sound level occurred at +1.95 s at an angle of 122.8° or one second later than PNLTM at an angle of 102.3°. Depending on the spectrum of the sound signal, the time of ALM could precede or follow the time of PNLTM, although in three of the four cases where the times were not equal, the time of ALM occurred after the time of PNLTM by 0.5 to 1.0 seconds.

The tone-correction factor (TCF) of 1.8 dB shown in Fig. 31(a) was the largest value obtained for the nine test cases although a value of 1.8 dB was also obtained for run 358 as indicated below.

Run		TCF = PNLTM-PNLM, dB	Center frequency of band with largest tone-correction factor, Hz
DC-9-14:	272	1.8	3150
	322	0.6	3150
	358	1.8	3150
	374	1.3	3150
	378	1.5	3150
727-100:	25	0.4	2500
Learjet:	12	0.4	2500
HS-748:	7	0.5	1600
Beech:	119	0.3	1250

The smaller tone-correction factor for run 322 is understandable because, as shown in Table 4, run 322 was flown at a significantly lower engine power setting than the other four DC-9 runs and the tone should have had a lower frequency by the ratio of shaft speeds (by the ratio 61/75 = 0.8) and hence might have shifted to the next lower band at 2500 Hz or perhaps have shared some energy between the 2500 and the 3150-Hz bands. The slightly smaller tone-correction factor for run 374, compared with that for the other runs at the same power setting, is attributed to the fact that run 374 was flown at almost twice the height of runs 272, 358, and 378, see Table 4(b). The small variation of TCF from 1.5 to 1.8 dB for runs 272, 358, and 378 is an indication of the good repeatability of the data from that test series.

The small TCF values for the 727 and the Learjet runs are attributed to the fact that the sound signal from those two airplanes is dominated by broadband jet noise at the takeoff power setting. The tone-correction algorithm in program TESTREF, as explained previously, does not compute tone corrections for ground-reflection effects in the frequency range below a band center frequency of 1000 Hz.

The fact that the band producing the largest tone-correction factor was the 2500-Hz band for the 727 and the Learjet is the result of the rapid spectral rolloff caused by atmospheric absorption at high frequencies. A large change in band-level slope in the test-time sound pressure level spectrum is regarded as a spectral irregularity for which a tone-correction penalty is calculated

Table 4.-Engine/airplane parameters for DC-9 runs

(a) engine parameters

run no.	nominal thrust per engine, kN	engine pressure ratio		engine exhaust gas temperature, °C		engine LP shaft speed, pct	
		left	right	left	right	left	right
272	26.7	1.44	1.44	370	375	75.1	75.0
322	13.3	1.205	1.205	322	321	61.2	60.9
358	26.7	1.44	1.44	380	380	75.9	75.2
374	26.7	1.44	1.44	390	380	76.0	75.5
378	26.7	1.44	1.44	390	385	76.1	75.8

(b) airplane parameters

run no.	airplane gross weight at overhead, kN	airplane height over mic, m	flap deflect, deg	nominal airspeed, m/s	nominal flight Mach no.
272	344.9	155.8	33	71.7	0.213
322	312.2	153.8	0	78.3	0.229
358	334.3	152.8	38	74.4	0.219
374	315.8	339.8	38	73.5	0.215
378	302.1	156.8	36	72.6	0.212

even though no discrete-frequency is present.

For the two propeller-powered airplanes, the spectral irregularities related to the fundamental and harmonics of the blade-passing frequency in the bands at 100, 200, and 400 Hz were ignored in calculating tone corrections. Spectral irregularities for center frequencies above 1000 Hz were caused by atmospheric absorption and yielded the 0.5 and 0.3-dB tone-correction factors shown in the table on page 144.

To complete the discussion of the results in Fig. 31, consider the duration factors DCF for EPNL and DSEL for SEL. It is interesting to note that DSEL can be closely approximated by the quantity (DCF + 10). To see why this should be, and to derive a useful relation, we re-write Eqs. (50) and (51) by introducing

the maximum values PNLTM and ALM. The working definitions for EPNL and SEL can then be re-cast into the format of Eqs. (48) and (49) where the duration factors are given by

$$DCF = 10 \log \left\{ \sum_{i=t_1}^{t_2} 10^{0.1(PNLT(i) - PNLTM)} \right\} + 10 \log (\Delta t/t_E) \qquad (87)$$

and

$$DSEL = 10 \log \left\{ \sum_{i=t_1}^{t_2} 10^{0.1[AL(i) - ALM]} \right\} + 10 \log (\Delta t/t_0). \qquad (88)$$

If, as suggested by the two plots in Figs. 31(a) and 31(b), the time variation of the normalized quantities [PNLT(i) - PNLTM] and [AL(i) - ALM] is approximately the same over the period of time between the 10-dB-down times t_1 and t_2, then the two duration correction factors should only differ by 10 times the logarithm of the ratio of the reference times t_E/t_0.

Thus, the following approximation should hold:

$$DSEL = DCF + 10 \log (t_E/t_0) \qquad (89)$$

or

$$DSEL = DCF + 10. \qquad (90)$$

The reference times of $t_E = 10.0$ s and $t_0 = 1.0$ s were used to obtain Eq. (90).

Equation (90) could be useful in a situation where the EPNL and the duration factor DCF were known and ALM was also known and it was desired to obtain an estimate of SEL for the same recording of flyover noise.

Another useful relation between the duration factors can be obtained by approximately the shape of the time variation of PNLT or AL between the 10-dB-down times by a triangle with a base equal to the 10-dB-down duration time

($t_{D,E}$ or $t_{D,A}$ or simply t_D). The vertex of the triangle is at 0.0 dB for the normalized quantities at the time of PNLTM or ALM.

The height of the triangle is given by the difference between the power ratios at 0.0 dB and at 10.0 dB, i.e., by the difference between 1.0 and 0.1 or a height of 0.9 in terms of power ratios for the normalized ordinate scale.

The area of the triangle approximates the area under the plot of [PNLT(i) - PNLTM] or of [AL(i) - ALM] in Figs. 31(a) and 31(b) and, effectively, provides an alternative way of evaluating Eqs. (87) and (88).

Thus, for the normalized PNLT plot we obtain

$$\begin{aligned} DCF &\approx 10 \log \{[(1/2)(t_{D,E})(0.9)]/t_E\} \\ &\approx 10 \log t_{D,E} + 10 \log (0.9/2t_E) \\ &\approx 10 \log t_{D,E} - 13.5 \end{aligned} \tag{91}$$

and for the normalized AL plot we obtain

$$\begin{aligned} DSEL &\approx 10 \log \{[(1/2)(t_{D,A})(0.9)]/t_0\} \\ &\approx 10 \log t_{D,A} - 3.5. \end{aligned} \tag{92}$$

We can use the value of 6.0 seconds shown in Figs. 31(a) and 31(b) for $t_{D,E}$ and $t_{D,A}$ to test the validity of the approximations in Eqs. (91) and (92) Thus, for run 272, Eq. (91) gives -5.7 dB against the calculated value of -5.4 dB, while Eq. (92) gives +4.3 dB against the calculated value of +5.2 dB. Additional comparisons are given in Table 5 for the approximations given by Eqs. (90), (91), and (92) with duration-factor values calculated from Eqs. (50) and (51) using computer-program subroutine INTEG. The approximate duration correction factors are within one decibel of the values obtained from the measured data.

The data shown in Fig. 31 were typical of the time variation of airplane noise level in the sense of being representative of the shape and the 10-dB-down duration time that would be measured during an Appendix C aircraft-noise-

Table 5.-Measured and approximate duration factors for EPNL and SEL

(a) Duration factors for EPNL

Run no.	Prop.[a] dist., m	Angle[a] ψ, deg	Airspeed, m/s	DCF= EPNL-PNLTM, dB	Eq.(90) DCF≈ DSEL -10.0, dB	$t_{D,E'}$ s	Eq. (91) DCF≈ 10 log $t_{D,E}$ -13.5, dB
272	159.5	102.3	71.7	-5.4	-4.8	6.0	-5.7
322	156.8	101.3	78.3	-6.9	-7.2	5.0	-6.5
358	154.4	98.2	74.4	-6.0	-5.3	5.0	-6.5
378	162.3	105.0	72.6	-5.5	-5.4	5.0	-6.5
374	369.4	113.1	73.5	-3.9	-4.6	9.5	-3.7
25	507.2	139.5	79.2	-2.0	-1.4	13.0	-2.4
12	1925.7	135.2	77.7	-0.8	+0.2	29.5	+1.2
7	652.5	92.1	59.7	-3.5	-3.4	10.5	-3.3
119	298.9	83.2	84.5	-4.4	-5.4	7.0	-5.0

(b) Duration factors for SEL

Run no.	Prop.[b] dist., m	Angle[b] ψ, deg	Airspeed, m/s	DSEL= SEL-ALM, dB	Eq.(90) DSEL≈ DCF +10.0, dB	$t_{D,A'}$ s	Eq. (92) DSEL ≈ 10 log $t_{D,A}$ -3.5, dB
272	185.3	122.8	71.7	5.2	4.6	6.0	4.3
322	156.8	101.3	78.3	2.8	3.1	5.0	3.5
358	163.2	110.5	74.4	4.7	4.0	5.5	3.9
378	174.1	115.8	72.6	4.6	4.5	6.0	4.3
374	369.4	113.1	73.5	6.4	6.1	10.5	6.7
25	507.2	139.5	79.2	8.6	8.0	13.5	7.8
12	1925.7	135.2	77.7	10.2	9.2	32.5	11.6
7	652.5	92.1	59.7	6.6	6.5	11.0	6.9
119	298.9	83.2	84.5	4.6	5.6	6.5	4.6

[a]At the time of PNLTM

[b]At the time of ALM

certification exercise for many large jet-powered airplanes. The results in Fig. 31 are also representative of most of the data available to this study. However, for high-performance airplanes (e.g., most business-executive jets) and for relatively quiet aircraft (e.g., airplanes powered by modern high-bypass-ratio engines including new or re-engined business-executive jets), the time variation shown in Fig. 31 is not too representative, especially for noise measurements at the FAR 36 takeoff or sideline points.

Airplanes that have a high thrust-to-weight ratio and consequently attain a great height by the time they reach the 6500-m takeoff-noise-measuring point, as well as airplanes that are relatively quiet, may both generate noise levels which, at most, are only a few decibels above the background noise, especially under highly absorptive atmospheric conditions. In such cases, determination of the 10-dB-down integration times t_1 and t_2 can be difficult. Noise levels measured during the Ralsbeck-Learjet test, run 12, are representative of such data with the results shown in Fig. 32. Note that the increments along the time scale on the abscissa in Fig. 32 differ from those in Fig. 31 by a factor of two. The range of sound emission angles covered by the data in Fig. 32 is smaller than in Fig. 31 because the maximum values occurred well after the overhead point at an angle of approximately 135° and because the rate of change of emission angle with time is slow when the height of the flight path above ground level is as great as it was for the Learjet test (i.e., 1357.8 m).

When the propagation distance is long, the noise level is often observed to fluctuate by several decibels over relatively short periods of time. The fluctuations may be caused by atmospheric turbulence or by refraction effects resulting from variations in the wind or air temperature along the sound propagation paths. For the data in Fig. 32, the 10-dB-down duration times, determined in accordance with the rules described earlier, were approximately 30 seconds. Noise levels between relative times of 10.75 and 13.25 seconds are not shown in Fig. 32 because for those test times there were so few measured band sound pressure levels which exceeded the background sound pressure levels that the calculated perceived noise levels and A-weighted sound levels for those times were not reliable.

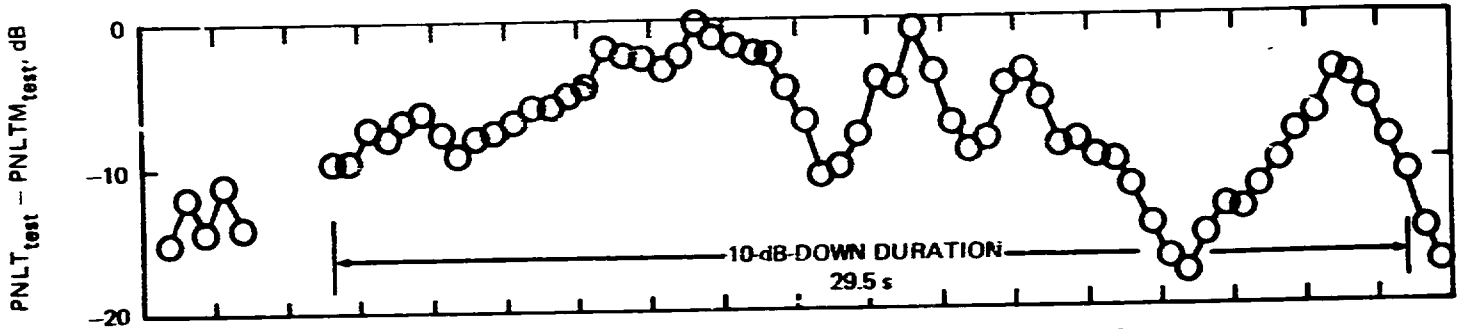

(a) TONE-CORRECTED PERCEIVED NOISE LEVEL; PNLM = 89.8 dB, PNLTM = 90.2 dB, EPNL = 89.4 dB.

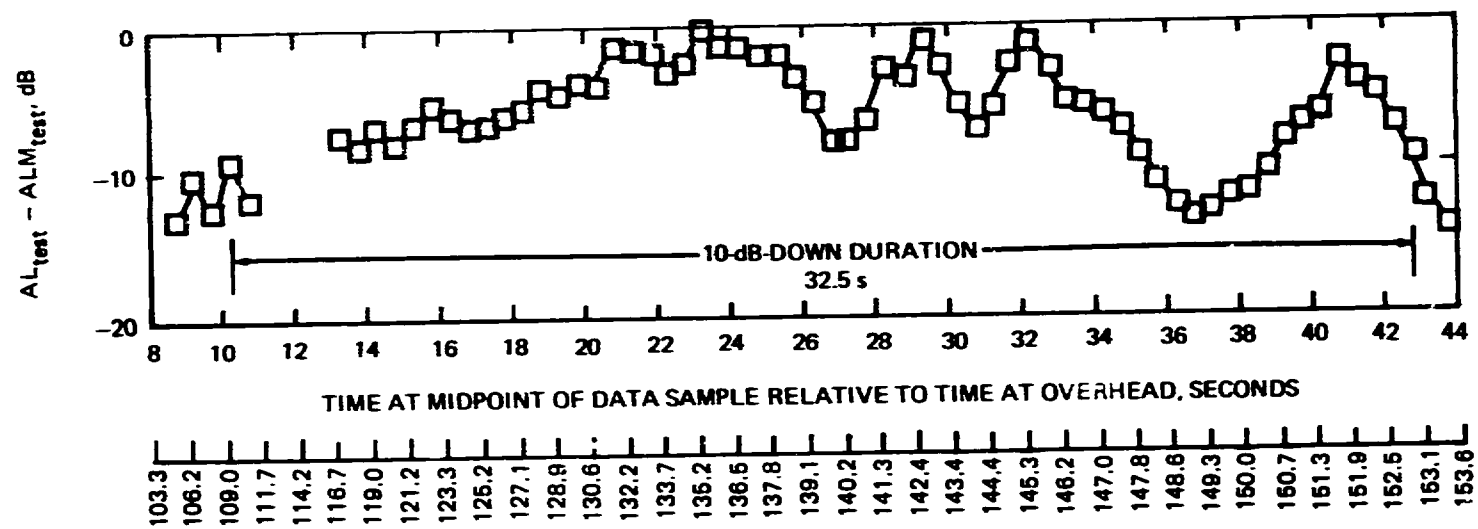

(b) A-WEIGHTED SOUND LEVEL; ALM = 80.4 dB, SEL = 90.6 dB.

Figure 32.-Variation of normalized PNLT and AL with time for the Raisbeck-Learjet, run 12.

1/3-Octave-Band Sound Pressure Levels at the Time of PNLTM.-Thus far we have discussed the time variation of perceived noise level and A-weighted sound level. We have also discussed tone-correction factors for perceived noise level and the duration factors in the calculation of effective perceived noise level and sound exposure level. We now turn to the 1/3-octave-band sound pressure level spectra.

The sound pressure levels at the time of occurrence of PNLTM are shown in Fig. 33 for all nine test cases.

The spectra for the four DC-9 runs that were at the same nominal height over the microphone (at the distance designated AMH in the legends for the figures) are shown in Fig. 33(a). The propagation distances, PD, and sound emission angles, ψ, are tabulated in the legend. Note that the low-frequency component of the spectrum is significantly lower for run 322 than for the other three runs because run 322 was flown at a lower power setting (see Table 4). All runs had a spectral peak in the band at 3150 Hz.

Note also that the high-frequency sound pressure levels in the 4000 to 10,000-Hz bands were significantly lower for run 272 than for the other three runs. The lower levels are probably the result of more-absorptive conditions along the sound path at the time of run 272 because, as shown in Figs. 25(a) and 25(b), the atmosphere was considerably drier during run 272 than during the other runs. The adjustment factors from test-to-reference conditions should therefore be greater for run 272 than for the other runs in Fig. 33(a).

Figure 33(b) shows the spectra for DC-9 run 374 and for the 727. Those two runs were flown at about the same height overhead, but the propagation distances and sound emission angles were different because the 727 was climbing while the DC-9 was flown in a level flight path. The emission angles also differ because the 727 was at takeoff power instead of the reduced power setting used for the DC-9 runs. Note the much higher level of low-frequency jet noise for the 727 even though the propagation distance was 507 m compared with 369 m for the DC-9. The 727 and the DC-9 are both powered by JT8D turbofan engines.

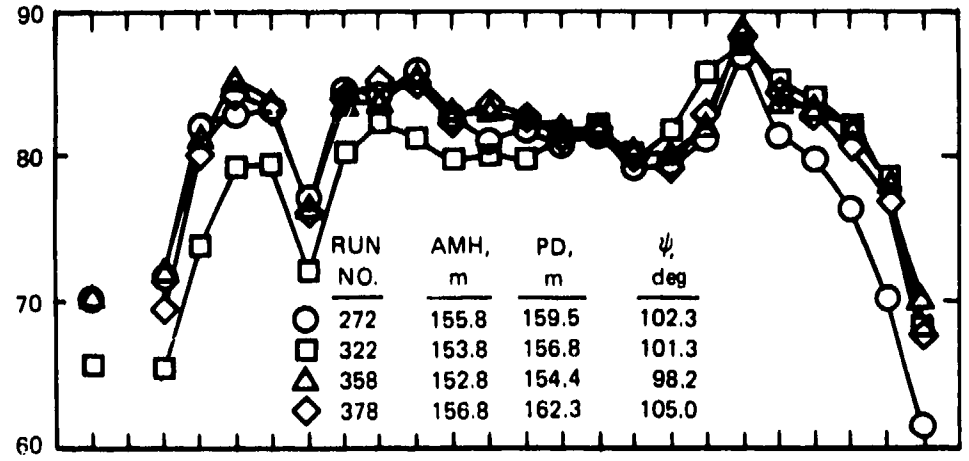

(a) DC-9-14 AT OVERHEAD HEIGHTS FROM 152.8 m TO 156.8 m.

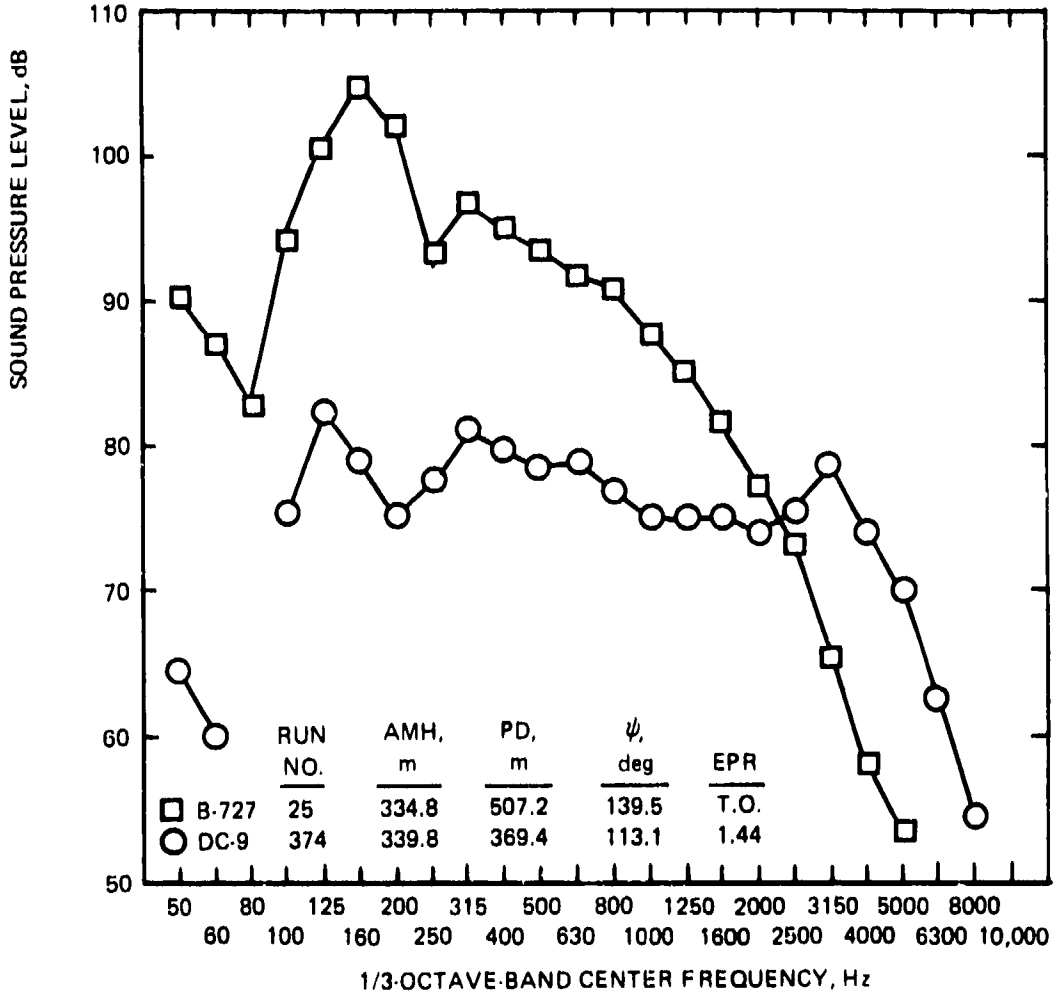

(b) 727-100 AND DC-9-14 AT OVERHEAD HEIGHTS OF 334.8 m AND 339.8 m; NOTE DIFFERENT POWER SETTINGS.

Figure 33.-Aircraft sound pressure level spectra at the time of occurrence of the maximum test-time tone-corrected perceived noise level, $PNLTM_{test}$.

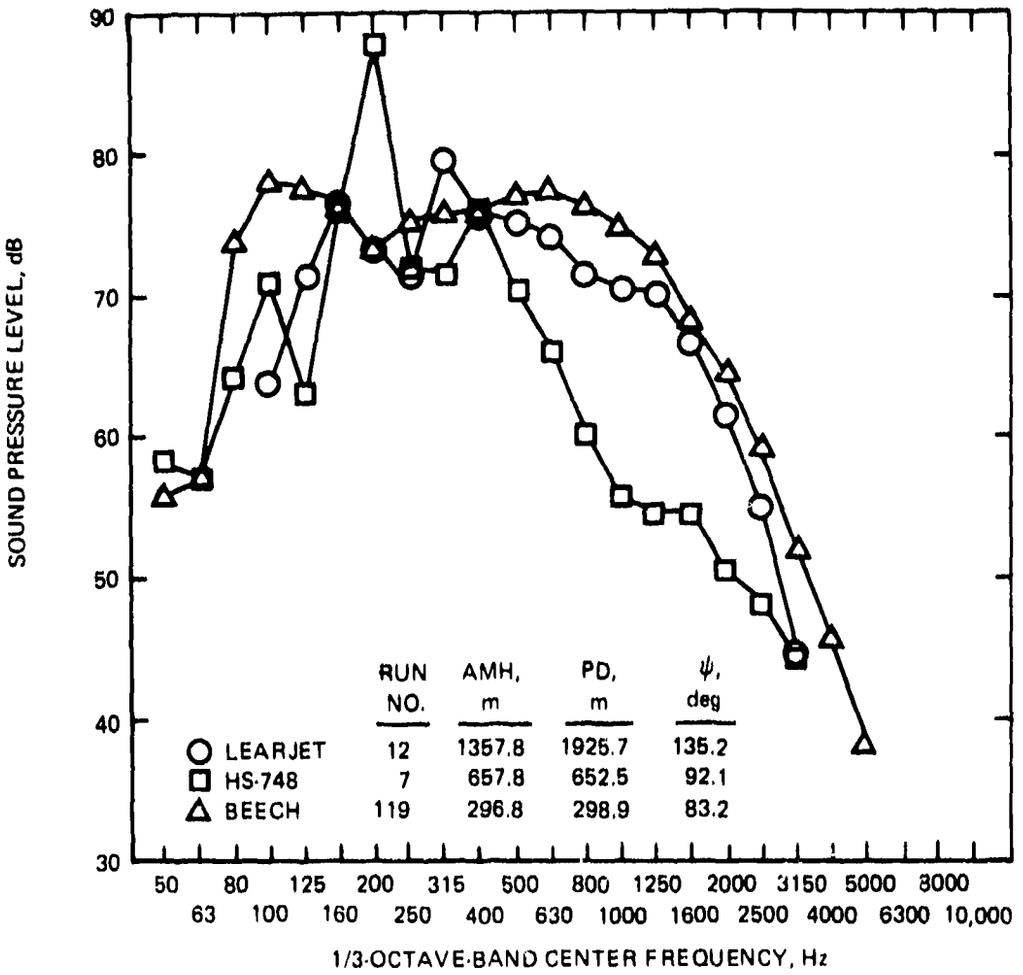

(c) LEARJET, HS-748, AND BEECH DEBONAIR.

Figure 33.-Concluded.

Figure 33(c) presents the spectra for the Raisbeck-Learjet (the run with the longest propagation distance at 1925.7 m) and the two propeller-powered airplanes — the Hawker Siddeley HS-748 and the Beech Debonair. The strong spectral peaks in the HS-748 spectra in the 100, 200, and 400-Hz bands are related to the fundamental and harmonics of propeller blade-passing frequency. The spectrum from the Beech Debonair did not contain the sharp spectral peaks that the HS-748 spectra contained.

The spectra in Fig. 33 illustrate some of the missing-band problems discussed in an earlier part of this Section. Data for the 63-Hz band are missing from the DC-9 data in Fig. 33(a) leaving an isolated sound pressure level in the first band at 50 Hz. Data for the 80-Hz band is missing from the DC-9 spectra for run 374 in Fig. 33(b). Data from the runs with long propagation distances have several band levels missing because of background noise contamination, especially in the high frequencies where the effect of atmospheric absorption has reduced the signal to a very low level. The Learjet run is also missing low-frequency data in the 50, 63, and 80-Hz bands.

The spectrum for the 727 for the bands at 4000 and 5000 Hz also seems to indicate the problem of inadequate rejection in the filter stopbands that was discussed in the previous Section. On the basis of the 507-m pathlength and the relatively absorptive conditions at the surface, the spectral slope should have continued to decrease from the 3150-Hz to the 4000-Hz to the 5000-Hz bands. The increase rather than decrease in slope is similar to the filter effect shown, for example, in Figs. 19 and 22.

The ensuing discussion of atmospheric-absorption effects will concentrate on the four DC-9 runs at the same nominal power setting (omitting run 322) and the Learjet, run 12. The adjustments for the 727 and the HS-748 are not too interesting because only surface meteorological data were measured. The adjustments for the Beech Debonair are also not very interesting because meteorological data were measured only at the surface and at the airplane and, as shown in Table 3, there was not much difference in temperature or humidity between the two heights. Also, for the Beech data, because the temperature was only 1° to 2° C less than the reference temperature of 25° C, though the rela-

tive humidity was less than 70 percent, the magnitude of the spectral adjustments would probably be relatively small. Therefore, because conditions along the sound propagation paths were not measured during the Beech Debonair tests, discussion of the effects of the alternative adjustment procedures on the 1/3-octave-band sound pressure levels is omitted for the Beech Debonair data as well as the 727 and HS-748 data.

Atmospheric Sound Absorption Coefficients.-One of the objectives of this study was an evaluation of the differences in calculated band-level adjustment factors caused by differences in computing atmospheric absorption by the method in SAE ARP866A and that in ANSI S1.26-1978. To anticipate the magnitude and sign of the differences, Fig. 34 shows how the atmospheric sound absorption coefficients from the two methods vary with the frequency of a sound wave and the relative humidity and temperature of the air.

The absorption coefficients for the ANSI S1.26-1978 method are presented as a smooth continuous function of frequency in accordance with the method in the Standard. However, the coefficients for the method of SAE ARP866A have a discontinuity at 5000 Hz [see, in particular, Fig. 34(b)]. The discontinuity, while it could have been eliminated by just using the equations for the method and simply varying the frequency in regular steps, was included in Fig. 34 because the discontinuity is a central part of the method of SAE ARP866A when dealing with 1/3-octave band data. Thus, the absorption coefficient by SAE ARP866A that is plotted at 5000 Hz was actually calculated for a frequency of 4500 Hz; at 6300 Hz it was calculated for 5600 Hz; at 8000 Hz it was calculated for 7100 Hz; and at 10,000 Hz it was calculated for 9000 Hz. The result is a displacement to the right of the high-frequency end of the absorption-coefficient curve.

It is interesting to observe that a displacement to the left of the high frequency portion of the SAE ARP866A curves would make them almost coincide with the high-frequency curves calculated by the ANSI S1.26-1978 method.

Neglecting the built-in differences between the two methods at high frequencies, the main differences is in the absorption coefficients at low

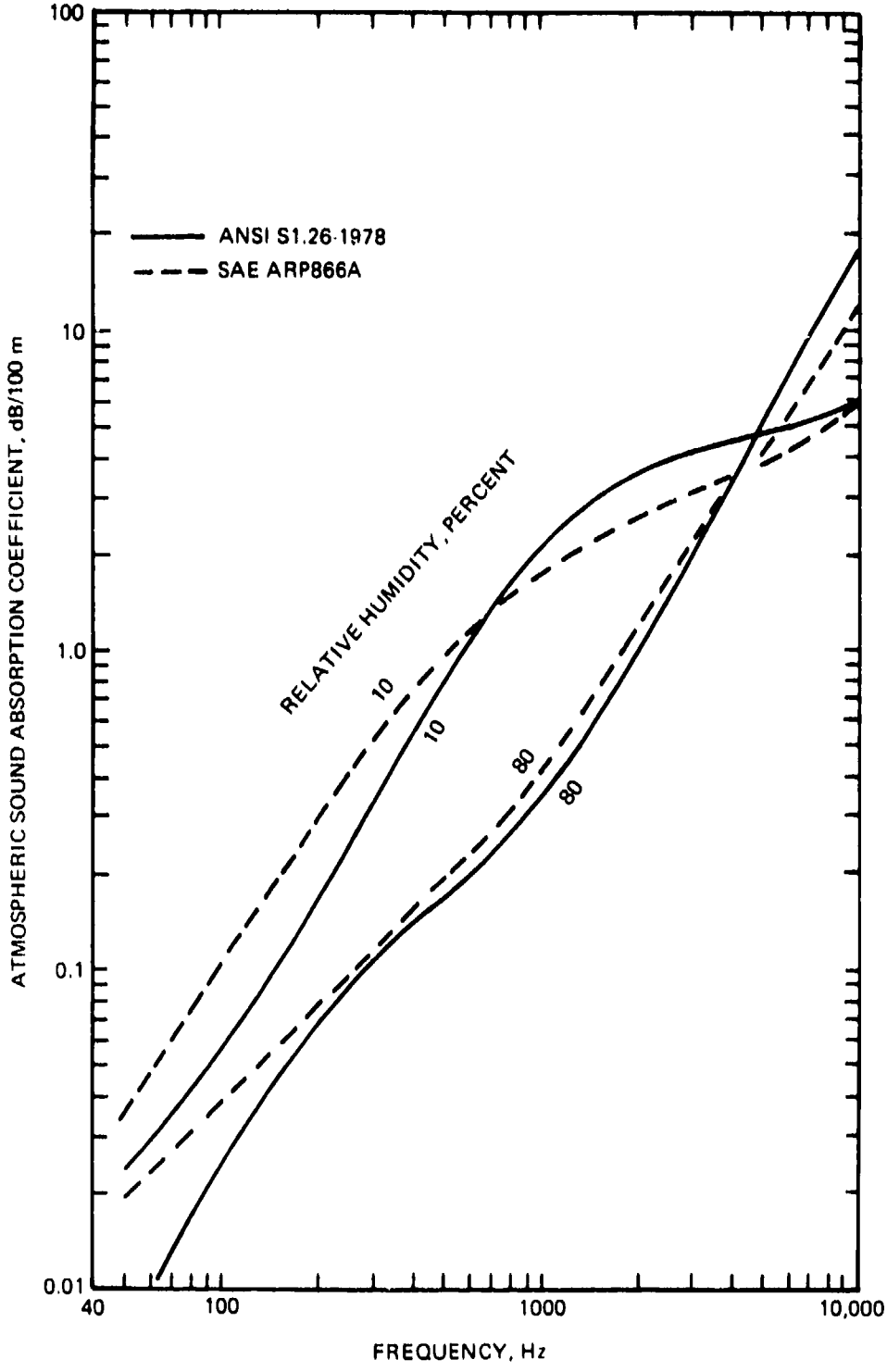

(a) AIR TEMPERATURE: 5° C.

Figure 34.-Pure-tone atmospheric sound absorption coefficients by ANSI S1.26-1978 and SAE ARP866A.

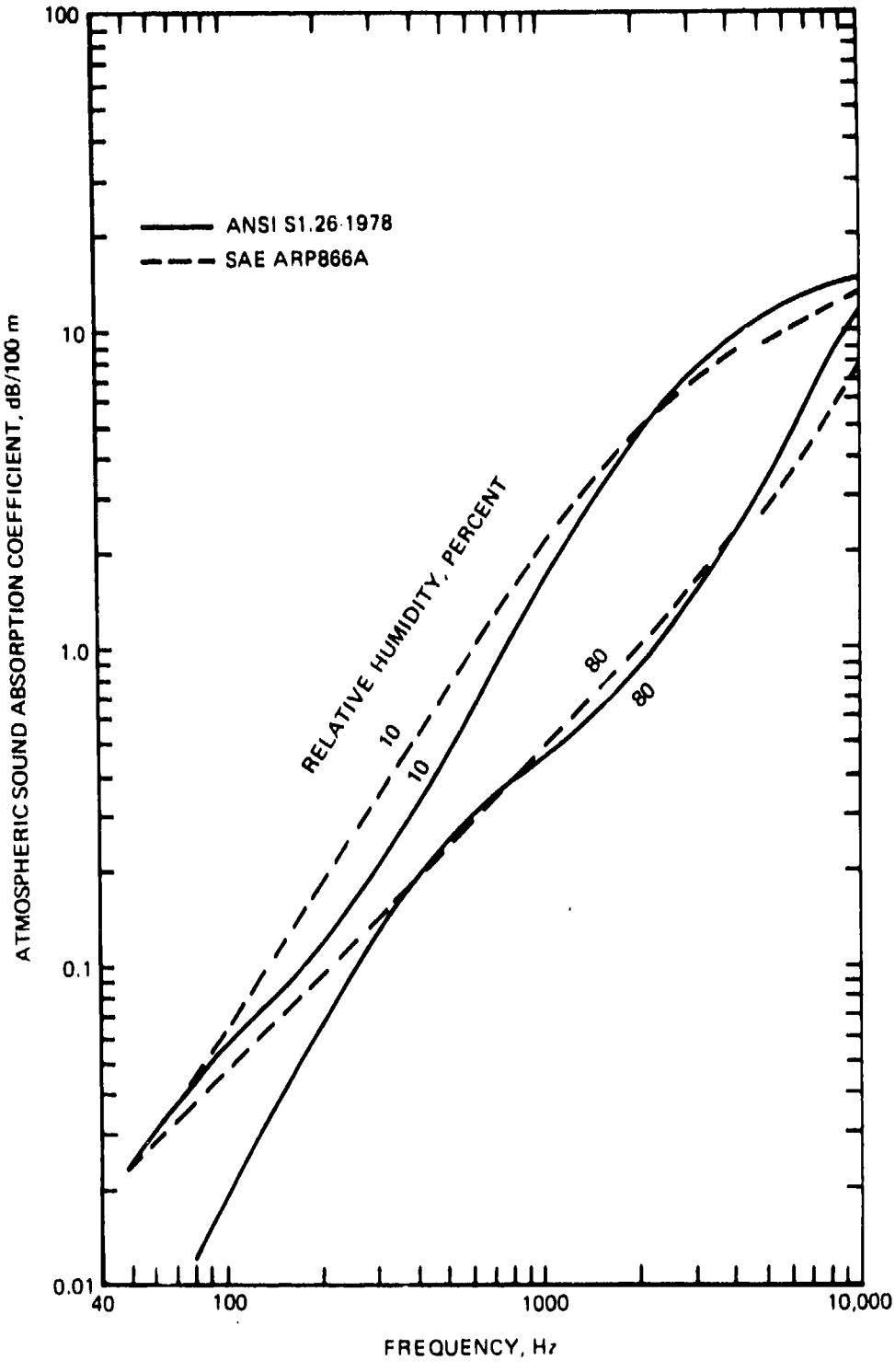

(b) AIR TEMPERATURE: 15° C.

Figure 34.-Continued.

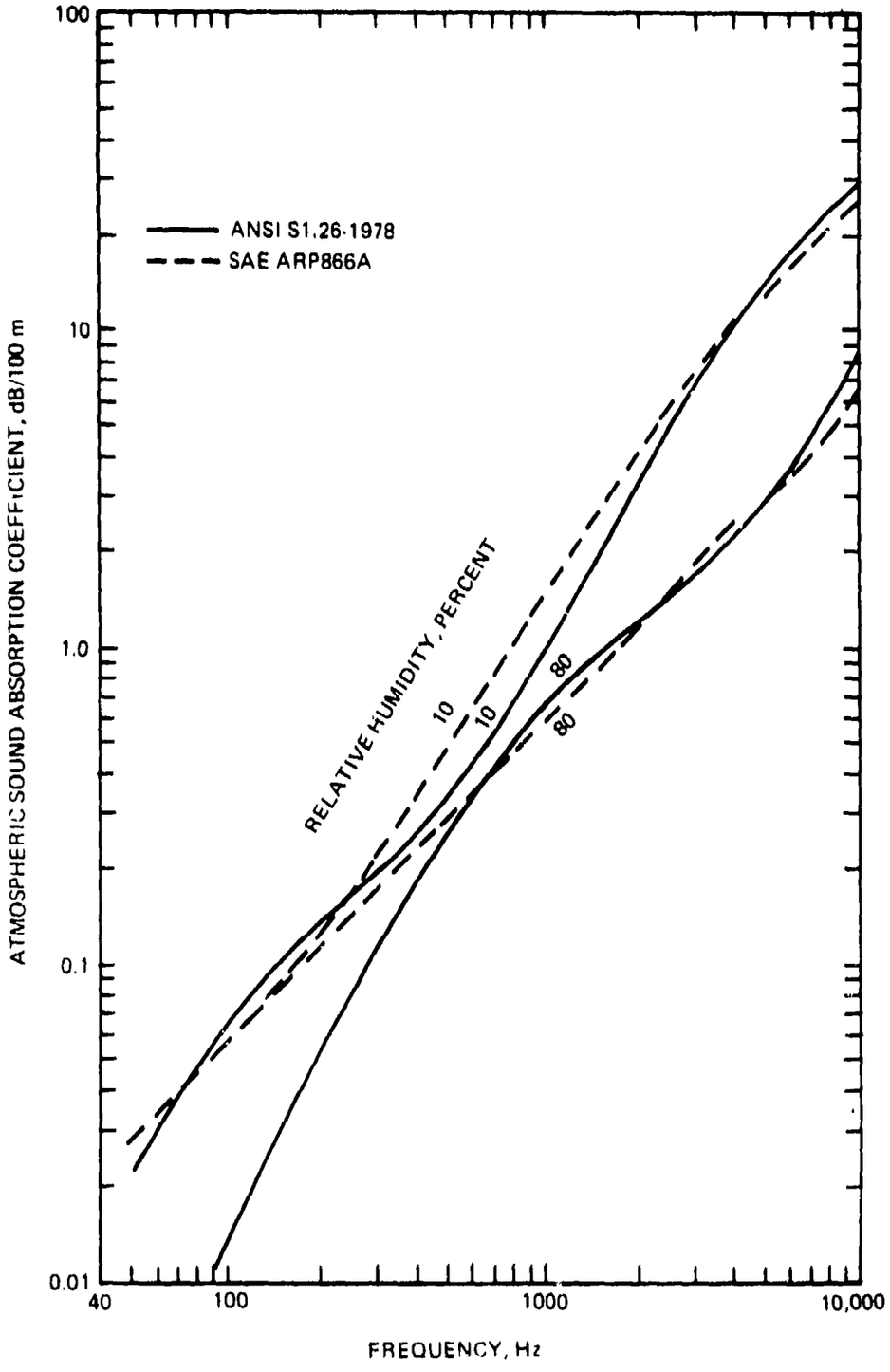

(c) AIR TEMPERATURE: 25° C.

Figure 34.-Concluded.

frequencies when the humidity is moderate to relatively high, see Figs. 34(b) and 34(c). The difference at these frequencies would be most significant for long propagation paths. In the frequency range from about 500 to about 2000 Hz, the method of ANSI S1.26-1978 generally indicates a smaller absorption coefficient than the method of SAE ARP866A. Thus, for data in that range of frequencies, the band-level adjustment factors to reference conditions should be somewhat smaller, for most test conditions, for the method of the ANSI Standard than for the method of SAE ARP866A.

Band-Level Test-to-Reference-Day Adjustment Factors.-The first set of 1/3-octave-band sound-pressure-level adjustment factors are shown in Fig. 38 for DC-9 runs 358, 378, and 272. Those three runs had approximately equal propagation distances and sound emission angles at the time of PNLTM. Also, they all were flown at nearly equal engine power settings, see Table 4.

The sound pressure level adjustment factors for the three runs in Fig. 35 are arranged in order ranging from run 358 which had the smallest values for the test-to-reference-day adjustment factors to run 272 which had the largest adjustments of the three runs. The fact that the adjustments were largest for run 272 was expected because the test-time high-frequency sound pressure levels for that run were significantly lower, as shown in Fig. 33(a), for that run than for runs 358 or 378. Also, on the basis of the low temperature and low humidity during run 272 [see Figs. 24(a) and 25(a)], it was expected that the adjustments to 25° C and 70 percent relative humidity should have been relatively large for the data from run 272.

The fact that the adjustments were somewhat larger for run 378 than for run 358 was expected because, again as shown in Fig. 33(a), the test-time high-frequency sound pressure levels were lower for run 378 than for run 358. For the same propagation distance, emission angle, and engine power setting, the lower values of sound pressure level should have been associated with a larger amount of atmospheric absorption along the sound path. Thus, the lower values of sound pressure level should have the larger adjustments to reference meteorological conditions.

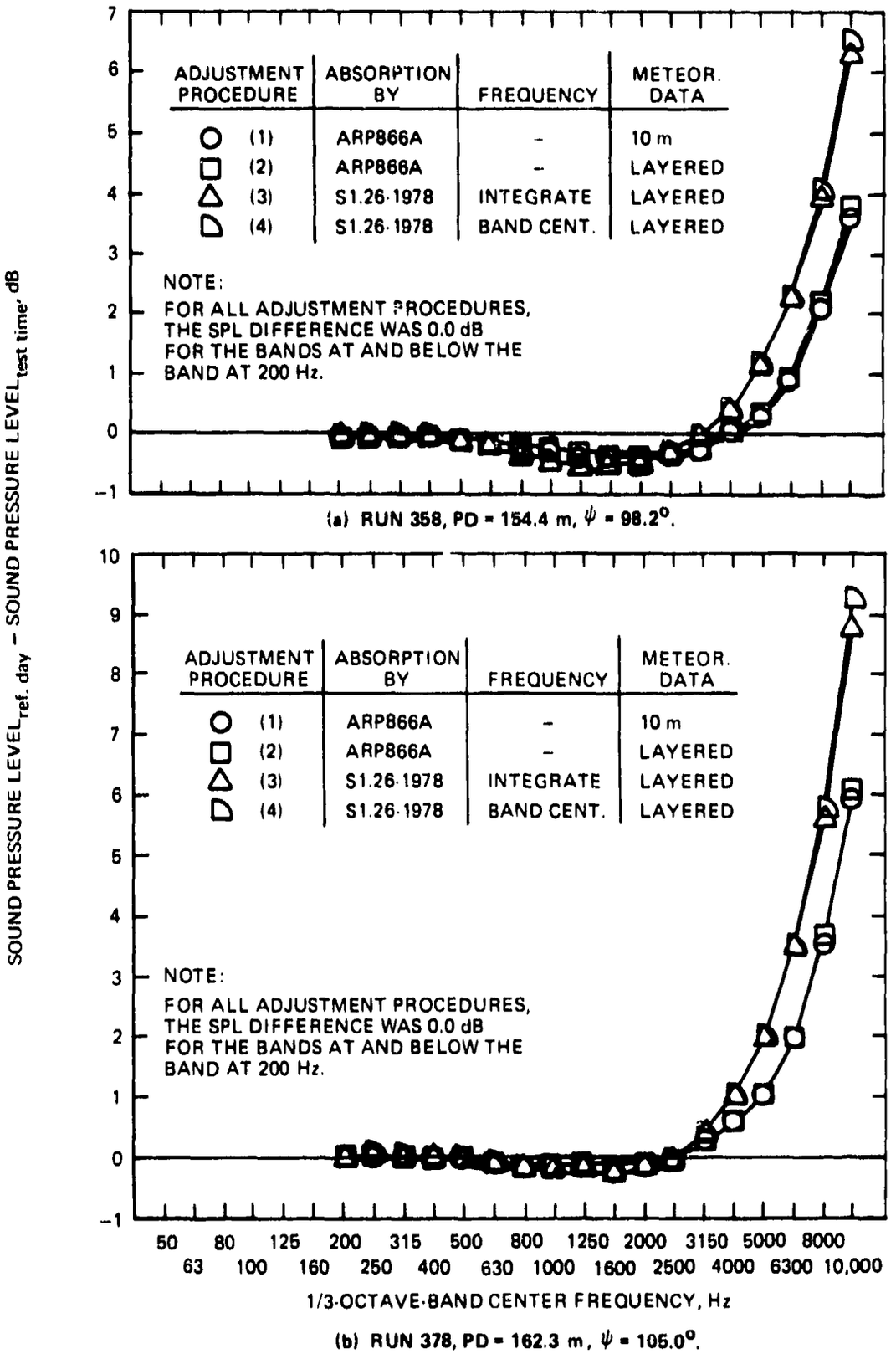

Figure 35.-Band sound-pressure-level adjustment factors at the time of $PNLTM_{test}$ for DC-9-14 runs at nearly-equal sound propagation distances, PD, and emission angles, ψ, but different meteorological conditions along the sound path.

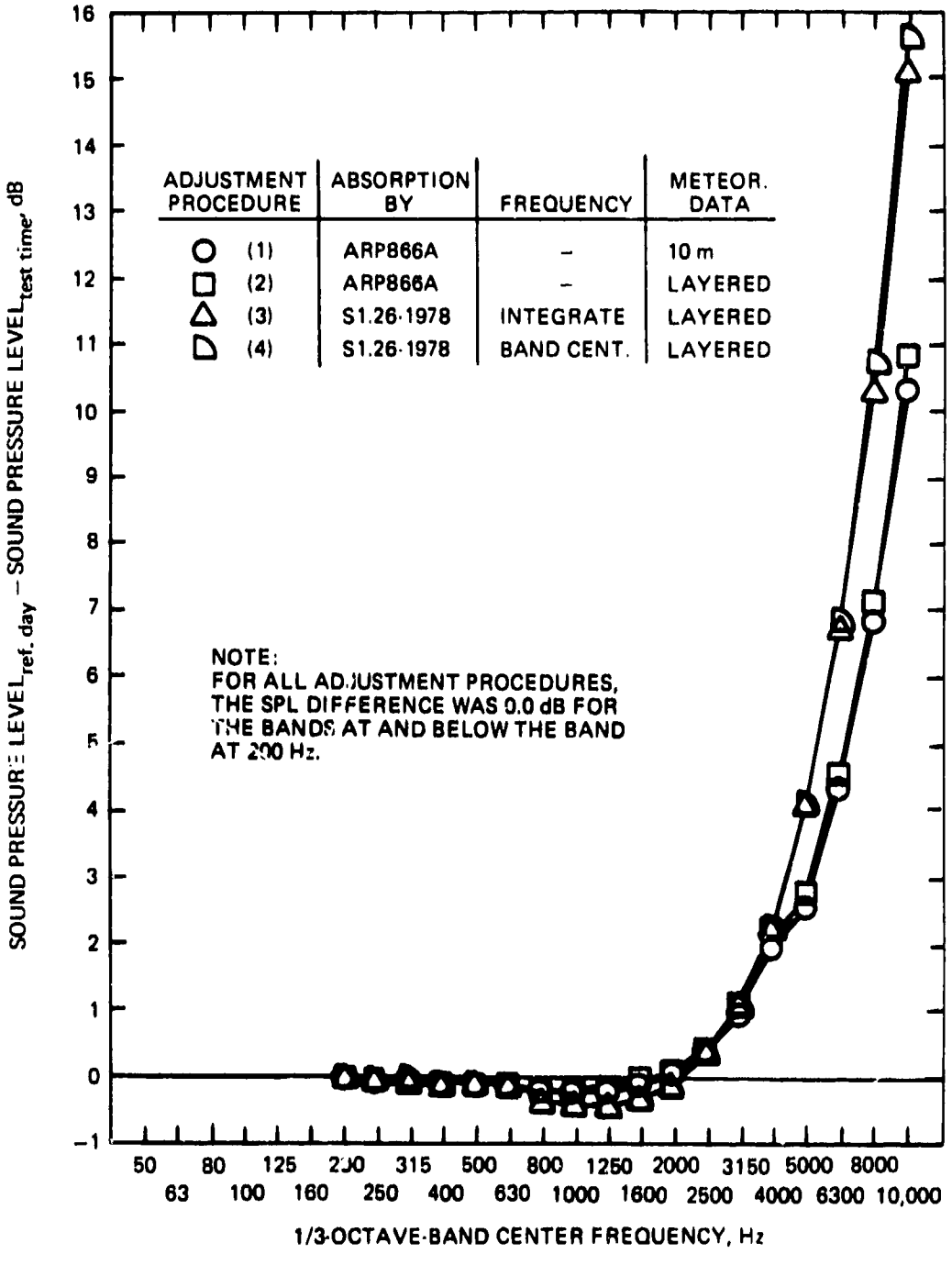

(c) RUN 272, PD = 159.5 m, ψ = 102.3°.

Figure 35.-Concluded.

The reason the test-time atmospheric conditions should have been more absorptive for run 378 than for run 358 is not obvious from inspection of the meteorological data in Figs. 24 and 25. It is noted, however, that the profiles of the molar concentration of humidity in Fig. 25 had a *negative* lapse rate for all runs [including the Learjet run in Fig. 25(c)] except run 358 for the range of heights between the surface and the height of the airplane. For run 358, the lapse rate of humidity was *positive*, as was the temperature lapse rate shown in Fig. 24(c). Apparently, the meteorological conditions along the path kept changing in such a way that the test-time absorption loss was closer to the absorption loss under reference conditions for run 358 than for run 378.

The data shown in Fig. 35 illustrate some general trends observed for the six of the nine test cases where meteorological data were measured along the sound propagation path. First, there was some frequency below which the test-to-reference adjustment factors equalled zero decibels (actually less than ±0.05 dB because of rounding to the tenth of a decibel in the calculations). The frequency below which the adjustment factor was always zero decibels was a function of (1) which model was used to calculate atmospheric absorption losses, (2) the meteorological conditions at the time of the test, and (3) the length of the propagation path. In general, the frequency above which the adjustment factors were always nonzero was higher using the ANSI S1.26-1978 method than the method of SAE ARP866A, i.e., by adjustment procedures (3) or (4) than by procedures (1) or (2).

This result is consistent with the differences in the low-frequency absorption coefficients in Fig. 34. Compare, for example, the curves in Fig. 34(c) for the reference temperature of 25° C, at frequencies below 500 Hz, with those for colder temperatures in Figs. 34(a) or 34(b). The differences arise because the model in SAE ARP866A is independent of humidity at low frequencies for warm temperatures [25° C], while the model in ANSI S1.26-1978, which is based on an improved understanding of absorption mechanisms at low frequencies, indicates a strong dependence on humidity at all temperatures. The consequence of the differences in the low-frequency absorption losses calculated by the two models is not large in an absolute sense unless the propagation path is of the order of thousands rather than hundreds of meters.

The second interesting feature of the band-level adjustment factors in Fig. 35 is that over a relatively large frequency range (generally from 250 to 2000 Hz in Fig. 35) the adjustment factors are negative rather than positive. A negative factor indicates that the sound pressure level under reference conditions is lower than under the test-time conditions, i.e., that the test-time meteorological conditions are less absorptive than the reference conditions. Although, as can be seen from the data in Fig. 34 or by examination of the tabulated values of absorption coefficients in Volume III of this report, the absorption coefficients for the warm and humid conditions at 25° C and 70-percent relative humidity are usually smaller than for other temperatures or humidities, they can be greater at some frequencies. At high frequencies, the reference-day absorption coefficients are almost always smaller than those under practical test-time conditions with the result that the adjustment factors are generally positive at high frequencies and the sound pressure levels are greater for reference than for test-time conditions.

The magnitude of the negative adjustment factors was always less than one decibel for the pathlengths corresponding to the data in Fig. 35. Longer pathlengths would be expected to result in calculation of factors that are more negative than those for the pathlengths of Fig. 35. The importance of negative adjustment factors is that they tend to offset, to a degree, the influence of positive adjustment factors at high frequencies. For a particular aircraft, the net effect on perceived noise level or A-weighted sound level depends on the shape of the spectrum of the sound signal at the microphone. For aircraft that produce a spectrum having a large amount of low-frequency energy, for example the Learjet at takeoff power as in Fig. 33(c), the offsetting effect of the negative adjustment factors could yield a lower, rather than a higher, reference-day EPNL and SEL compared with the test-time values.

For most aircraft noise-certification tests, the relatively small, negative adjustment factors will not be large enough to offset the larger, positive, high-frequency adjustment factors. Hence, reference-day EPNLs will usually tend to be greater than test-time EPNLs. It may be significant, however, to note from Fig. 35 that the method of ANSI S1.26-1978 [procedures (3) and (4)] produced mid-frequency adjustment factors that were consistently more negative than those calculated using the method of SAE ARP866A [procedures (1) and (2)].

The most-significant feature of the data in Fig. 35 is the large and positive values of the adjustment factors in the higher-frequency bands starting, approximately, in the 2000-Hz band for the pathlengths of Fig. 35. The magnitude of the adjustment factor, in a particular high-frequency band, increased as the test-time meteorological conditions became increasingly more absorptive, i.e., from run 358, to 378, to 272. The frequency where the adjustment factor changed from negative to positive decreased as the test-time conditions became more absorptive.

Of greater interest, however, are the differences between the sole use of meteorological conditions at the 10-m height, procedure (1), and the use of conditions along the path in a layered-atmosphere analysis, procedure (2). On the basis of the differences shown in Fig. 24 in test-time absorption coefficient at 3150 Hz over the height range, it was not expected that there would be large differences for the DC-9 runs between using 10-m and sound-path meteorological conditions. That expectation was confirmed by the results in Fig. 35 where the difference in band-level adjustment factor between the methods of procedures (1) and (2) was no more than 0.5 dB at 10,000 Hz for the more-absorptive conditions of run 272, Fig. 35(c). The longer-pathlength and very-absorptive conditions for the Learjet test, see Fig. 24(f), should show more influence of the effect of the choice of test-time meteorological conditions than any of the DC-9 runs.

For data in Fig. 35, however, high-frequency band-level adjustment factors calculated using only 10-m meteorological conditions were always smaller than those calculated using the sound-path conditions for the layered-atmosphere analysis of procedure (2). This result is expected to be applicable to most aircraft noise test conditions likely to be encountered in practice because meteorological conditions aloft are generally associated with larger test-time sound absorption coefficients than test-time conditions at 10 meters above the ground surface.

Another feature of the results in Fig. 35 is that, as expected, the adjustment factors for the high-frequency bands are larger when calculated using the atmospheric-absorption model of ANSI S1.26-1978 than using the model of SAE ARP866A. For center frequencies between 4000 and 10,000 Hz, the difference

ranged from less than 0.5 dB to as much as 5 dB at 10,000 Hz for the absorptive test-time conditions of run 272.

Most of the difference between the results obtained using the two models can be attributed to the use of the lower bandedge frequency in the SAE ARP866A procedure to represent the loss over the four 1/3-octave-bands from 5000 to 10,000 Hz. In fact, if the dashed lines in Fig. 34 representing the SAE ARP866A model were to be shifted to the left by an amount representing the ratio of the center frequency to the lower bandedge frequency, the resulting band-adjustment factors would be in closer agreement than they are in Fig. 35.

The change from using the band center frequency to using the band lower cutoff frequency introduces a kink or discontinuity in the adjustments calculated using the SAE ARP866A model in procedures (1) and (2). The discontinuity occurs between the bands at 4000 and 5000 Hz and is most easily seen for the results in Fig. 35(c).

One final remark from the results in Fig. 35 is that the band-center-frequency method of procedure (4) always produced a somewhat larger adjustment factor for the high-frequency bands than did the band-integration method of procedure (3). The difference increased as the slope of the high-frequency portion of the test-time spectrum became steeper with increasingly more-absorptive test-time conditions. For the data in Fig. 35, there was no difference in adjustment factors by procedures (3) and (4) for band center frequencies up to 5000 Hz. The larger factors calculated by the band-center-frequency method for spectra with steep high-frequency slopes and the agreement at low frequencies are both consistent with the results obtained by Montegani[21] and with the results of the analytical study in Section 2, see Fig. 14.

For spectra containing steep negative slopes in the high-frequency bands, the adjustment calculated by the band-integration method is intrinsically more correct than the adjustment calculated by the band-center-frequency method.

Unless one has available aircraft noise data measured at different distances under reference meteorological conditions and under a variety of test-time conditions and were able to compare the ability of the various procedures

to adjust the measured non-reference-condition data to the measured reference-condition data, there does not seem to be any analytical technique to use aircraft noise measurements for determining the absolute accuracy of any particular adjustment method. Indeed, aircraft noise data may well be the poorest choice for trying to make such a judgment because of the difficulty of trying to assure repeatability for those physical parameters which can be controlled as well as repeatability of the atmospheric parameters which can be measured, not controlled. Pernet[14], in a review of aircraft noise propagation literature for the National Physical Laboratory, has described measuring techniques which should be improved in order to make better use of aircraft noise measurements for understanding aircraft noise propagation phenomena.

Mueller and Hilton[23] conducted an analysis similar to that described above using data extracted from the same series of DC-9 tests in 1974 at Fresno Air Terminal and at Yuma International Airport. They considered adjustments to sound pressure levels obtained during tests under three different test conditions at Fresno [none of which was among those analyzed here] and to sound pressure levels obtained at Yuma under nearly constant temperature and humidity conditions. The Yuma tests were considered to represent reference data. Because of background noise, they had no data in the bands from 5000 to 10,000 Hz.

They used absorption-loss models of SAE ARP866A and ANSI S1.26-1978. An undefined "bandwidth correction procedure" was developed and used with the model of ANSI S1.26-1978 to give a quasi band-integration procedure for calculating an adjustment factor from test-to-reference conditions.

Mueller and Hilton concluded that the method based on ANSI S1.26-1978 gave results closer to the measured reference data than did the method based on SAE ARP866A. They also concluded that an adjustment method using a layered-atmosphere analysis gave results closer to the measured reference data than the method based on using only meteorological data measured at a height of 10 meters.

The study reported here does not provide any fundamental data for assessing the validity of the atmospheric-absorption model of ANSI S1.26-1978 over that in SAE ARP866A. The study does provide data that can be used to evaluate the

magnitude of the differences in test-to-reference-day band-level adjustment factors and the resulting changes in PNL, PNLT, EPNL, AL, and SEL.

Figure 36 presents a comparison of the sound pressure levels calculated for the 25° C, 70-percent-relative-humidity acoustical reference day according to procedures (2) and (3) for runs 358 and 272. Procedures (2) and (3) both used sound-path weather. Procedure (2) used SAE ARP866A. Procedure (3) used ANSI S1.26-1978.

For the relatively short propagation distances at the time of PNLTM for these runs, the differences between the spectra for the two runs in Fig. 36 are not considered significant for band center frequencies at and below 3150 Hz. Differences between the spectra in the four bands from 5000 to 10,000 Hz are considered to be significant in that they illustrate the influence of the two atmospheric-absorption models.

If all other factors involved in a measurement of aircraft noise (engine power setting, airspeed, propagation distance, sound emission angle, wind, atmospheric turbulence, and so forth) are equal, then a *reference-day* spectrum calculated from one set of test-time data should be the same as another *reference-day* spectrum calculated from another set of test-time data. This rationale was the basis for comparing the reference-day spectra from runs 358 and 272 in Fig. 36. The other factors were as close as the available data permitted.

Therefore, on that basis, the atmospheric-absorption adjustment procedure that yielded the smallest set of differences between the two reference-day spectra could be considered superior to other adjustment procedures. For the four bands from 5 to 10 kHz, inspection of the data plotted Fig. 36 shows a closer grouping of the reference-day band levels by procedure (3) [Fig. 36(b)] than by procedure (2) [Fig. 36(a)]. The evidence indicates a preference for the atmospheric absorption model of ANSI S1.26-1978 over that in SAE ARP866A. Because of the relatively short propagation distances, the differences shown in Fig. 36. between the two procedures were not large although they appear to be consistent. The trends agree with those observed by Mueller and Hilton[23].

The reference-day sound pressure levels in the 5 to 10-kHz bands by pro-

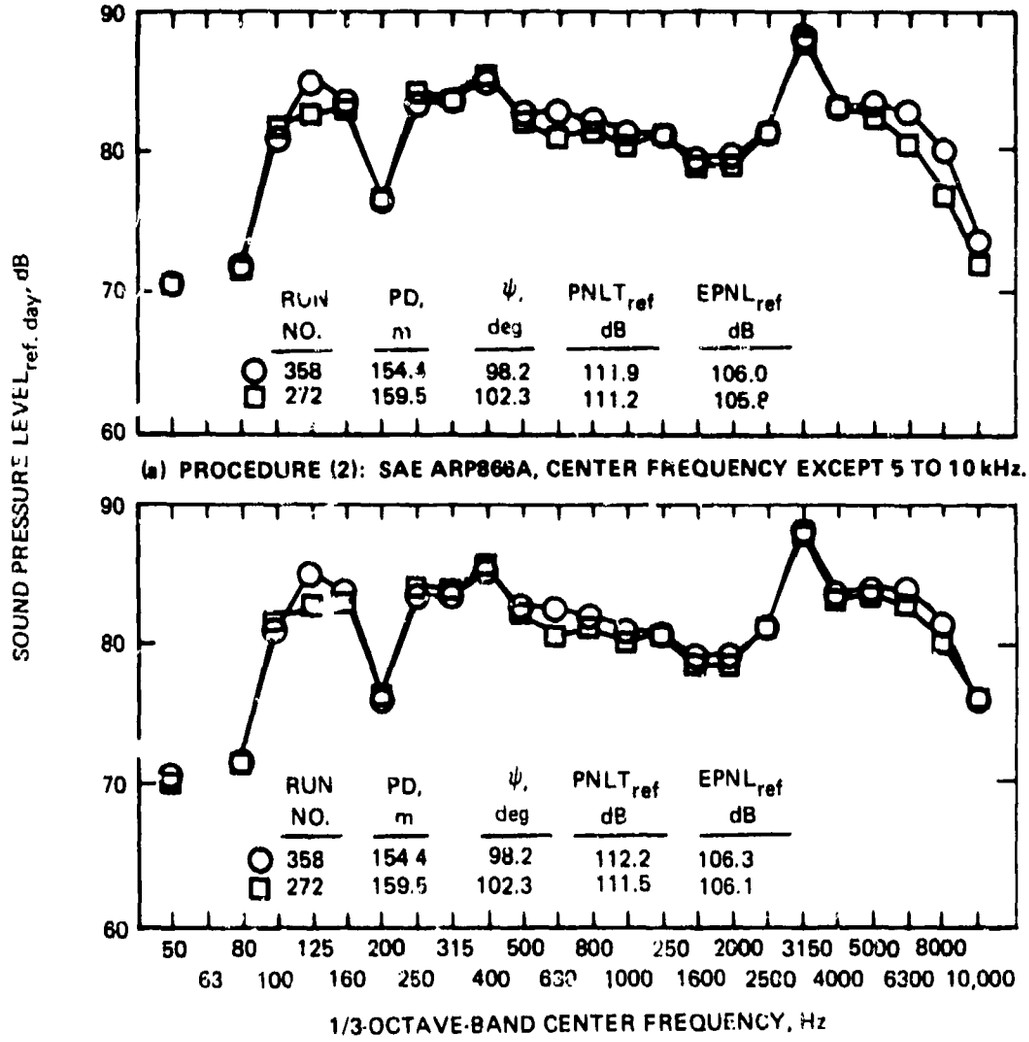

Figure 36. Illustration, for DC-9-14 runs 272 and 358, of difference between reference-day sound pressure levels calculated by adjustment procedures (2) and (3). Propagation distances and sound emission angles are for the time of PNLTM$_{test}$.

cedure (2) are, of course, lower than those by procedure (3) because of the use of the lower bandedge frequency to represent the absorption over the band. The higher levels in the 5 to 10-kHz bands did not alter the value of the tone-correction factor calculated for the various spectra in Fig. 36. A 1.8-dB tone-correction factor was calculated for the reference-day spectra as it was for the corresponding test-time spectra, see Fig. 31. The band producing the maximum tone-correction factor was always the band at 3150 Hz. The tone-corrected perceived noise levels and the effective perceived noise levels for the reference-day spectra were 0.3 dB greater according to procedure (3) than procedure (2), primarily because of the higher sound pressure levels in the 5 to 10-kHz bands by procedure (3).

As the pathlength increases, the magnitude of the adjustment factors would generally be expected to increase. The data analyzed above had a pathlength of about 160 m. Figure 37 shows the band-level adjustment factors from run 374 for a pathlength of about 369 m. The results are similar to those shown in Fig. 35 except that (1) the first low-frequency band with nonzero adjustments is now the 125-Hz band instead of the 250-Hz band, (2) the adjustments in the mid-frequency range have values which are more negative than any of the corresponding values in Fig. 35, and (3) the high-frequency adjustments are larger (more positive). There are no data for the band at 10,000 Hz because the test-time sound pressure levels in that band were missing and hence no reference-day sound pressure levels were calculated.

For the high-frequency bands, the methods of procedures (1) and (2) again showed that the use of meteorological data at a height of 10 m consistently produced smaller adjustments than the use of meteorological data along the sound path. The kink that was observed for the results in Fig. 35 in the slope of the adjustment factors between the bands at 4000 and 5000 Hz for procedures (1) and (2) using the model of SAE ARP866A is also evident in Fig. 37.

In Fig. 35, there was no difference between adjustment factors calculated by the band-integration method of procedure (3) and the band-center frequency method of procedure (4) except for the very high-frequency bands where the spectral slope was quite steep. For runs 358 and 374, the smaller adjustments

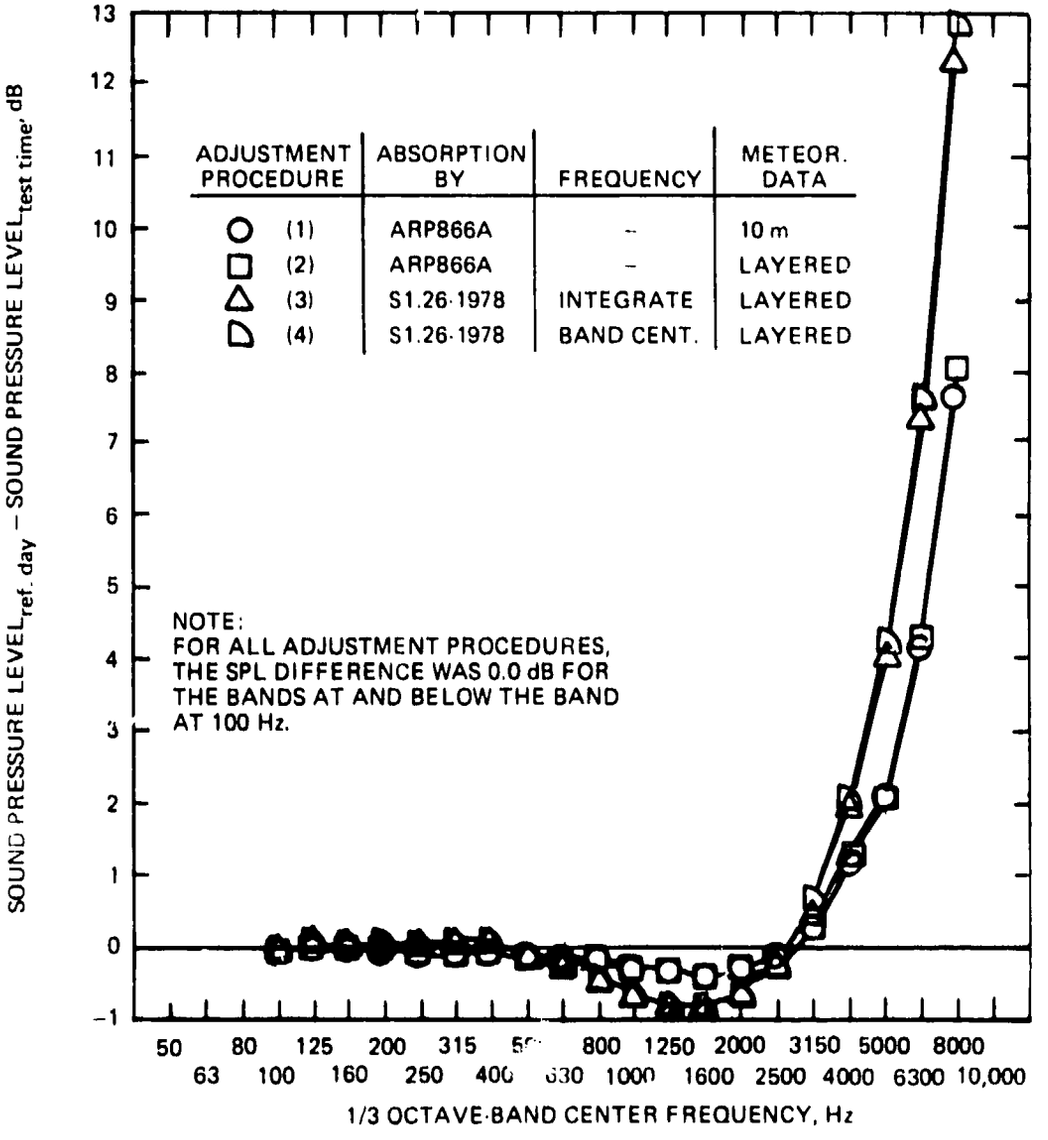

Figure 37.-Band sound-pressure-level adjustment factors at the time of $PNLTM_{test}$ and of ALM_{test} for DC-9-14 run 374, PD = 369.4 m, $\psi = 113.1^{o}$.

by the band-integration method were first noted in the 8000-Hz band. For run 272 in Fig. 35(c), the smaller adjustments by the band-integration method were first noted in the 6300-Hz band. For run 374 in Fig. 37, the even-more-steeply-sloped high-frequency spectrum of the noise signal after propagation over the longer pathlength caused the center-frequency method to produce larger adjustments than the band-integration method starting in the 4000-Hz band. The largest difference, however, was about 0.5 dB in the 8000-Hz band where the slope of the test-time spectrum was -8 dB/band.

The reference-day sound pressure levels calculated for run 374 can be used to obtain additional insight into the relative differences between the atmospheric absorption models of SAE ARP866A and ANSI S1.26-1978. During the analysis of data acquired from a noise-certification test program, it is often required that the reference-day results be further adjusted for propagation-pathlength differences that stem from the actual airplane flight path not being equal to the flight path calculated for the airplane under the specified reference conditions. Thus, it is often necessary to include an additional adjustment factor for propagation over shorter or longer pathlengths. Adjustment of a sound pressure level spectrum to a longer, or shorter, propagation distance is also required when generating predictions of aircraft noise levels at large distances, as, for example, in determination of the data base for calculations of the locations of contours of aircraft noise exposure around airports.

Comparisons of aircraft noise spectra at different distances should be made at the same sound directivity angle because the spectrum can change relatively rapidly with angle. For the data available for analysis, reference-day spectra were only produced for two sound emission angles (i.e., for two times). The angles were those associated with the time of occurrence of $PNLTM_{test}$ and ALM_{test}. For run 374, the two maximum values both occurred at an angle of 113.1°. For the three runs at the shorter distance and at the power setting used for run 374 (namely, runs 358, 378, and 272), the angle at the time of $PNLTM_{test}$ was less than the angle at the time of ALM_{test}. From Table 5(b), we see that runs 358 or 378 could be used to provide data at an angle close to the 113.1° angle of run 374. For run 358, the emission angle at ALM_{test}

was 110.5°, for run 378 it was 115.8°. We chose run 358 to provide a spectrum to compare with run 374 because, as shown in Fig. 35, the test-time meteorological conditions were closer to those for an acoustical reference day than were those for run 378.

Figure 38 shows the measured test-time and the calculated reference-day spectra for runs 358 and 374. The results obtained using the model of SAE ARP866A are presented in Fig. 38(a); those obtained using ANSI S1.26-1978 are shown in Fig. 38(b). The generally similar appearance of the spectra from the two runs is another indication of the good reproducibility of the data from these 1974 FAA/NASA flyover noise tests.

For constant directivity angle, the process of extrapolating a sound pressure level, in some band of frequencies, from distance s_1 from the source to a larger distance s_2 can be represented analytically by

$$L_2 = L_1 - 20 \log (s_2/s_1) - A_a \tag{93}$$

where the $-20 \log (s_2/s_1)$ term accounts for inverse-square divergence loss under the assumption that sound waves spread spherically outward from an effective acoustic source and the A_a term accounts for losses resulting from atmospheric absorption.

For propagation outward from a source, the atmospheric-absorption-loss term for sound analyzed by ideal filters can be represented by the following general expression*

$$A_a = -10 \log \left\{ \left[\int_{f_L}^{f_U} [G_{R1}][\exp(-\int_{s_1}^{s_2} 2\alpha \, ds)] \, df \right] \Big/ \left[\int_{f_L}^{f_U} G_{R1} \, df \right] \right\} \tag{94}$$

where, as before, G_{R1} represents the pressure spectral density of the sound as a function of frequency at a receiver location at distance s_1 and α is the atmospheric absorption coefficient as a function of frequency. The coefficient α in Eq. (94) has units of nepers/meter for distances in meters.

*See Eq. (A2) of Ref. 2.

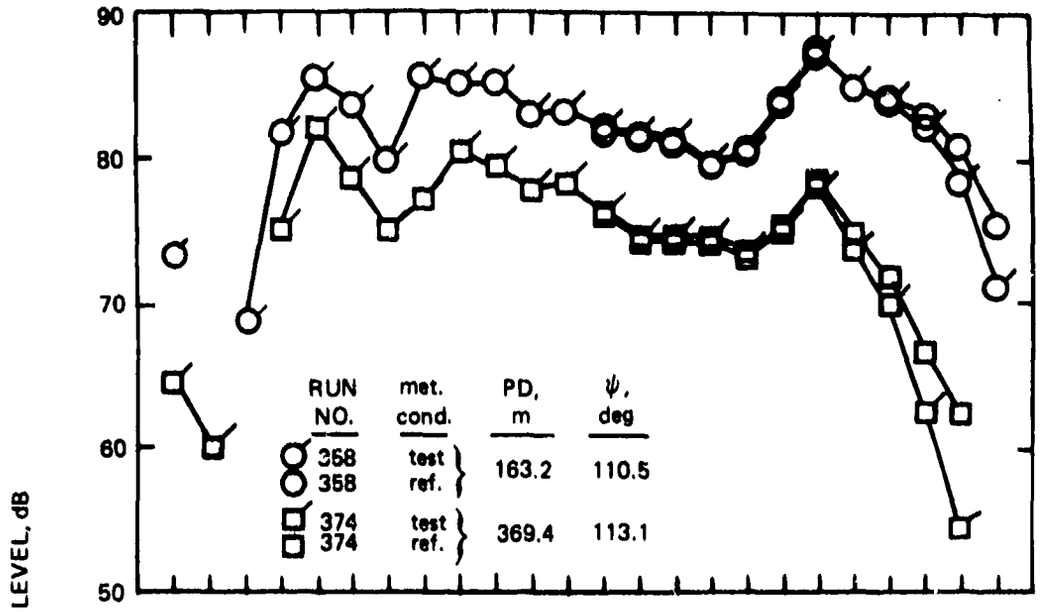

(a) BAND-LEVEL ADJUSTMENT FACTORS BY PROCEDURE (2), SAE ARP866A, CENTER FREQUENCY EXCEPT 5 TO 10 kHz.

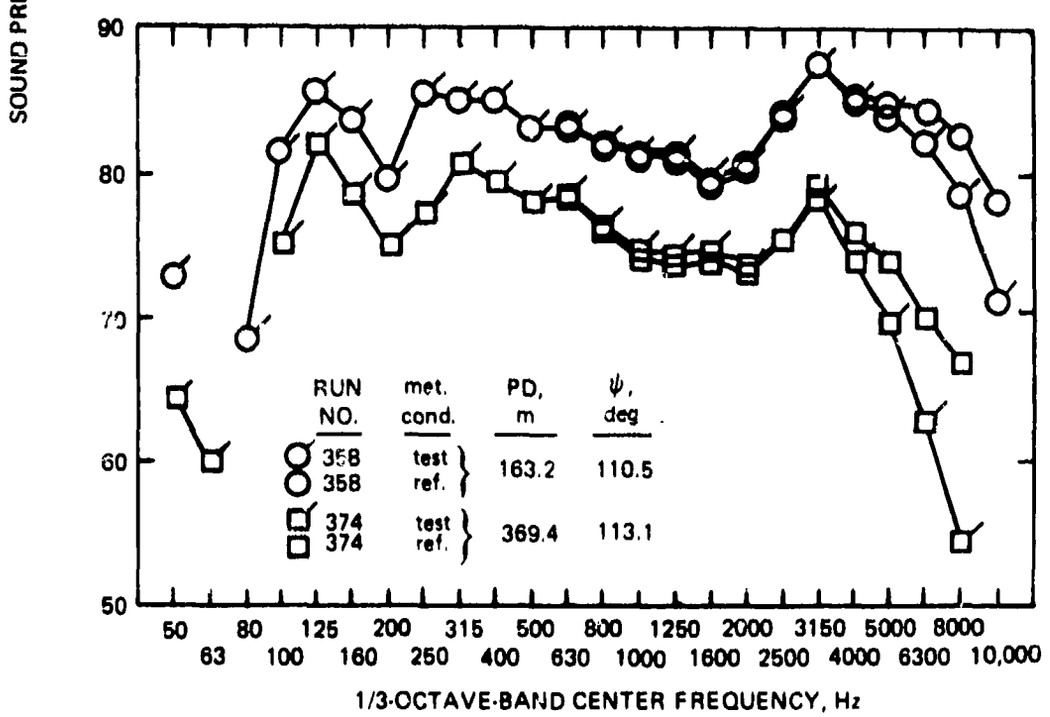

(b) BAND-LEVEL ADJUSTMENT FACTORS BY PROCEDURE (3), ANSI S1.26–1978, BAND INTEGRATION.

Figure 38.-Sound-pressure-level spectra for test and reference meteorological conditions from DC-9-14 runs 358 and 374 at nearly-equal sound-emission angles but different propagation distances.

Over the frequency range of the filter from f_L to f_U, evaluation of the integral in the numerator of Eq. (94) requires a separate evaluation at each frequency of the integral in the exponent of the exponential term because the absorption coefficient α is also a function of temperature, pressure, and humidity and those meteorological parameters may not be constant along the path from distance s_1 to distance s_2. Evaluation of the integral over the path from s_1 to s_2 for the exponential term requires knowledge of the variation of temperature, pressure, and humidity as a function of distance along the path. In practice, the path would be divided into segments over which average conditions were known and the integral would be replaced by a summation as done for Eqs. (80) and (81).

If the meteorological conditions were constant over the path (as they are for the acoustical reference-day conditions in the current version of FAR 36) then, as for Eq. (21), the absorption-loss expression of Eq. (94), for constant reference conditions, becomes

$$A_{a,ref} = -10 \log \left\{ \left[\int_{f_L}^{f_U} \left[G_{R1} \right] \left[10^{-(a_{ref})[(s_2 - s_1)/10]} \right] df \right] \Big/ \left[\int_{f_L}^{f_U} G_{R1} \, df \right] \right\} \tag{95}$$

where $(s_2 - s_1)$ is the pathlength and a_{ref} is the absorption coefficient for constant reference meteorological conditions in units of decibels/meter as a function, now, only of frequency.

As a further simplification, if the sound is a pure tone at some frequency between f_L and f_U or if the absorption loss is being calculated by treating the pressure spectral density of a broadband sound analyzed by a bandpass filter as though it were a pure tone sound, then Eq. (95) reduces to

$$A_{a,ref} = (a_{ref})(s_2 - s_1) \tag{96}$$

where a_{ref} is at some frequency within the frequency band associated with $A_{a,ref}$.

Because the method of SAE ARP866A uses a single frequency to approximate the absorption loss over a frequency band, Eq. (96) was used to approximate the absorption-loss term in Eq. (93). For constant reference conditions along the sound path, the general expression in Eq. (93) thus becomes

$$L_{2,ref} = L_{1,ref} - 20 \log (s_2/s_1) - (a_{ref})[s_2 - s_1)/100] \qquad (97)$$

where a factor of 100 has been introduced in the absorption-loss term because a_{ref} now has the more-convenient units of dB/(100 m) instead of dB/m.

The use of the format of Eq. (97) to project a spectrum from one distance to a larger distance permitted a direct comparison of the two atmospheric absorption models as well as the different methods [as used in procedures (2) and (4)] of approximating the absorption losses for the 1/3-octave bands with center frequencies from 5000 to 10,000 Hz.

For the sound pressure levels $L_{1,ref}$ in Eq. (97), we take the spectra shown in Fig. 38 for run 358 as calculated for reference conditions. Equation (97) was used to project the reference-day sound pressure levels of run 358 to the 369.4-m distance of run 374. The difference between the sound pressure levels projected using run 358 data and the data calculated for run 374 is then a measure of validity of the extrapolation procedure. If there is no difference between the levels projected from run 358 and those calculated for run 374, then the extrapolation method is capable of duplicating the data at the larger distance. Negative values for the difference mean that the extrapolation from run 358 underpredicted the levels from run 374, and *vice versa*.

The differences between the band levels projected from run 358 and those from run 374 are shown in Fig. 39 as a function of band center frequency. The inverse-square divergence-loss term was a constant 7.1 dB from 161.2 to 369.4 meters.

The results in Fig. 39 are shown only for band center frequencies from 800 to 8000 Hz. No data were available for run 374 at 10,000 Hz. There was no difference between the two adjustment procedures for frequencies at and below 800 Hz.

The general trend shown by the results in Fig. 39 is for the band levels projected from the 163.2-m distance of run 358 to the 369.4-m distance of run 374 to be about 2 dB lower than those of run 374. The differences in the lower-frequency bands from 100 to 630 Hz agreed with this trend but ranged from +1.0 to -3.8 dB. The larger scatter in those bands was attributed to differences caused by variations in the interference effects resulting from ground reflections in the measured test-time spectra for the two runs.

The reasons the levels projected from the 169.2-m distance for run 358 were approximately 2 dB lower than those of run 374 over the spectrum from the 100 to the 6300-Hz bands are not known. On the basis of the engine and airplane data listed in Table 4, the strength of the noise at the source should have been nearly the same for the two runs. The accuracy of the photographic technique for determining height overhead, however, is about ±5 to ±10 percent. The accuracy of the time synchronization between the taking of the photograph and the recording of the noise signal could also account for some of the 2-dB difference. If the height at overhead for run 374 was too large by 10 percent while that for run 358 was too short by 5 percent, then the inverse-square-loss term would have been approximately 1.3 dB smaller and the across-the-spectrum difference would have been reduced to about 0.7 dB. The small difference in sound emission angle might be able to account for another 0.2 dB of the difference because of the difference in the directivity of the noise at the source.

The most-striking and principal feature of the results in Fig. 39 is the gross difference in the trends shown for the 5000, 6300, and 8000-Hz bands. The method of procedure (4) based on the model of ANSI S1.26-1978 produced band-level differences for those bands which were consistent with the trends observed at lower frequencies.

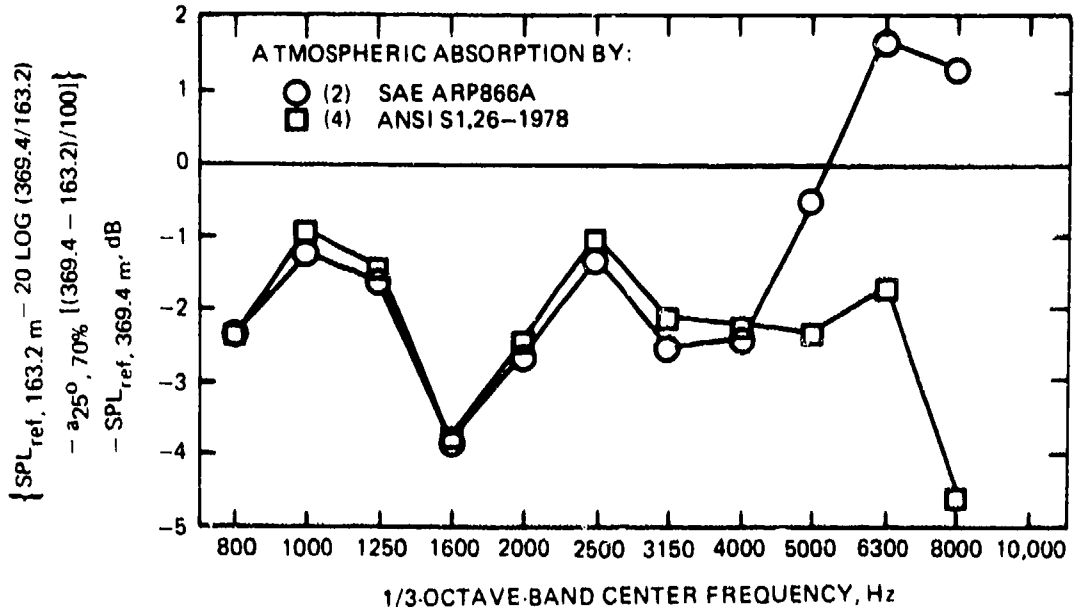

Figure 39.-For nominally equal sound-emission angles (110.5° and 113.1°), illustration of effect of choice of atmospheric-absorption model on ability to extrapolate reference-day SPLs. Comparision of differences between reference-day SPLs from run 358 at 163.2 m extrapolated to 369.4 m and reference-day SPLs at 369.4 m from run 374.

The larger negative value for the 8000-Hz band for procedure (4) is attributed partly to the use of the band center frequency instead of the band-integration method and partly (probably mostly) to the suspicion that the test-time sound pressure level for the 8000-Hz band for run 374 was contaminated by power transmitted through the lower stopband. That suspicion is based on the shape of the high-frequency part of the test-time spectrum shown in Fig. 38 for run 374. Judging from the absorptivity of the test-time meteorological conditions for runs 374 and 358 and from the roll-off rates for the shorter-distance data of run 358, the test-time level indicated for the 8000-Hz band of run 374 appears to be higher than would have been expected.

If the test-time level in the 8000-Hz band for run 374 had been lower, then the reference-day level would also have been lower and the difference between the level projected from run 358 and that of run 374 would have been less negative (more positive). A change of 2 dB in the 8000-Hz band level for run 374 would have made the difference at 8000 Hz consistent with the differences in the lower frequencies for procedure (4).

The differences in the 5000, 6300, and 8000-Hz bands using the SAE ARP866A model in procedure (2) showed an unusual trend in that the data projected from run 358 were *greater* than the reference-day data from run 374 in these bands. The levels in all three of these bands would be larger than those of run 374 if a reason could be justified for making a 1.5-dB to 2.0-dB net positive adjustment to all differences in Fig. 39. The fact that the projected data overpredict the reference-day levels of run 374 is considered to be the consequence of using the lower bandedge frequency in SAE ARP866A to represent absorption loss over a band of frequency.

Note that the downward trend from the 6300 to the 8000-Hz bands in Fig. 39 for procedure (2) would have been continued as the steady upward trend from the 4000 to the 6300-Hz bands if the 2-dB reduction in the 8000-Hz reference-day band level for run 374 was proper as postulated above in the explanation of the more-negative difference in the 8000-Hz band for procedure (4).

Overprediction of high-frequency band levels when using the method of SAE ARP866A to extrapolate to larger distances is regarded as a significant shortcoming of the method. If the process had been reversed and the data of run 374 had been used to estimate the band levels of run 358, the results would have been reversed and the method of procedure (2) would have underpredicted the levels of run 358. Errors arising from the use of a single frequency to calculate atmospheric absorption loss over a frequency band were also pointed out by Montegani in Ref. 21.

The conclusion here is that a band-center-frequency or band-integration method appears to be better able to reproduce high-frequency data measured at a longer or shorter distance than does the lower-bandedge-frequency method of SAE ARP866A. Moreover, for all bands between 1000 and 4000 Hz, the method of procedure (4) with ANSI S1.26-1978 was consistently better (i.e., produced band-level differences in Fig. 39 that were closer to zero) than the method of procedure (2) with SAE ARP866A, though only by 0.2 to 0.4 dB. The consistency of the trend and the fact that it was observed in each of the seven bands between 1000 and 4000 Hz are, however, considered to be significant factors in favor of the use of the ANSI S1.26-1978 model instead of the SAE ARP866A model for atmospheric absorption when adjusting measured test-time sound pressure levels to acoustical-reference-day conditions. Furthermore, smaller differences (i.e., improved correlation) would be expected for the high-frequency bands, where atmospheric absorption effects are most noticeable and the spectral slopes can be very steep, if the atmospheric-absorption loss were computed by integrating over the response of a filter and if a procedure were used to remove real-filter effects (i.e., effects caused by non-ideal filter-transmission characteristics) from the measured test-time sound pressure levels *before* adjusting the data to acoustical-reference-data conditions.

The procedure for removing real-filter effects must, however, be an approximate one because there is no exact analytical method to determine ideal-filter band levels from real-filter band levels and the frequency response characteristics of the filter.

The analysis of the data from the DC-9 flyover noise tests at Fresno for propagation pathlengths of about 160 and 370 m has yielded certain conclusions

relative to calculation of adjustment factors from test-to-reference meteorological conditions. The conclusions were concerned with (1) the use of meteorological data at the 10-m height *versus* meteorological data along the sound path, (2) the use of the atmospheric-absorption model of SAE ARP866A *versus* that of ANSI S1.26-1978, (3) the use of the band center frequency to calculate atmospheric-absorption loss *versus* a method of integrating over the response of a filter band, and (4) the need to account for real-filter response effects in the measured test-time 1/3-octave-band sound pressure levels.

The spectral effects on which the conclusions were based depended on the length of the sound propagation path and the absorptive character of the atmosphere. For the DC-9 runs, the absorptive quality of the atmosphere was not greatly different from run to run and the pathlengths were relatively short. For the one remaining set of flyover noise data with meteorological data available along the sound path (i.e., that from the test of the Raisbeck-modified Gates Learjet in run 12), the atmosphere was much more absorptive and the 1926-m pathlength was much longer. Differences between the four adjustment procedures were expected to be larger for the Learjet data than for the DC-9 data.

Figure 40 shows the band-level adjustment factors calculated for the data from the Raisbeck-Learjet test by the four alternative procedures. The results in Fig. 40 apply to adjustment of the test-time spectrum associated with both $PNLTM_{test}$ and ALM_{test} since the maximum values of both quantities occurred at the same relative time (i.e., the same sound emission angle). The results in Fig. 40 are limited to band center frequencies from 100 to 3150 Hz because of background noise contamination of the test-time sound pressure levels in the low- and high-frequency bands.

Differences among the four alternative adjustment procedures that were seen in the results from run 374 in Fig. 37, in comparison with the results for the other DC-9 runs in Fig. 35, are much more evident for the results in Fig. 40. The low-frequency band where the adjustment was zero for all procedures was not determined because it was at a frequency below the limit of the data at 100 Hz.

Differences between the methods based on SAE ARP866A [procedures (1) and (2)] and the methods based on ANSI S1.26-1978 [procedures (3) and (4)] were

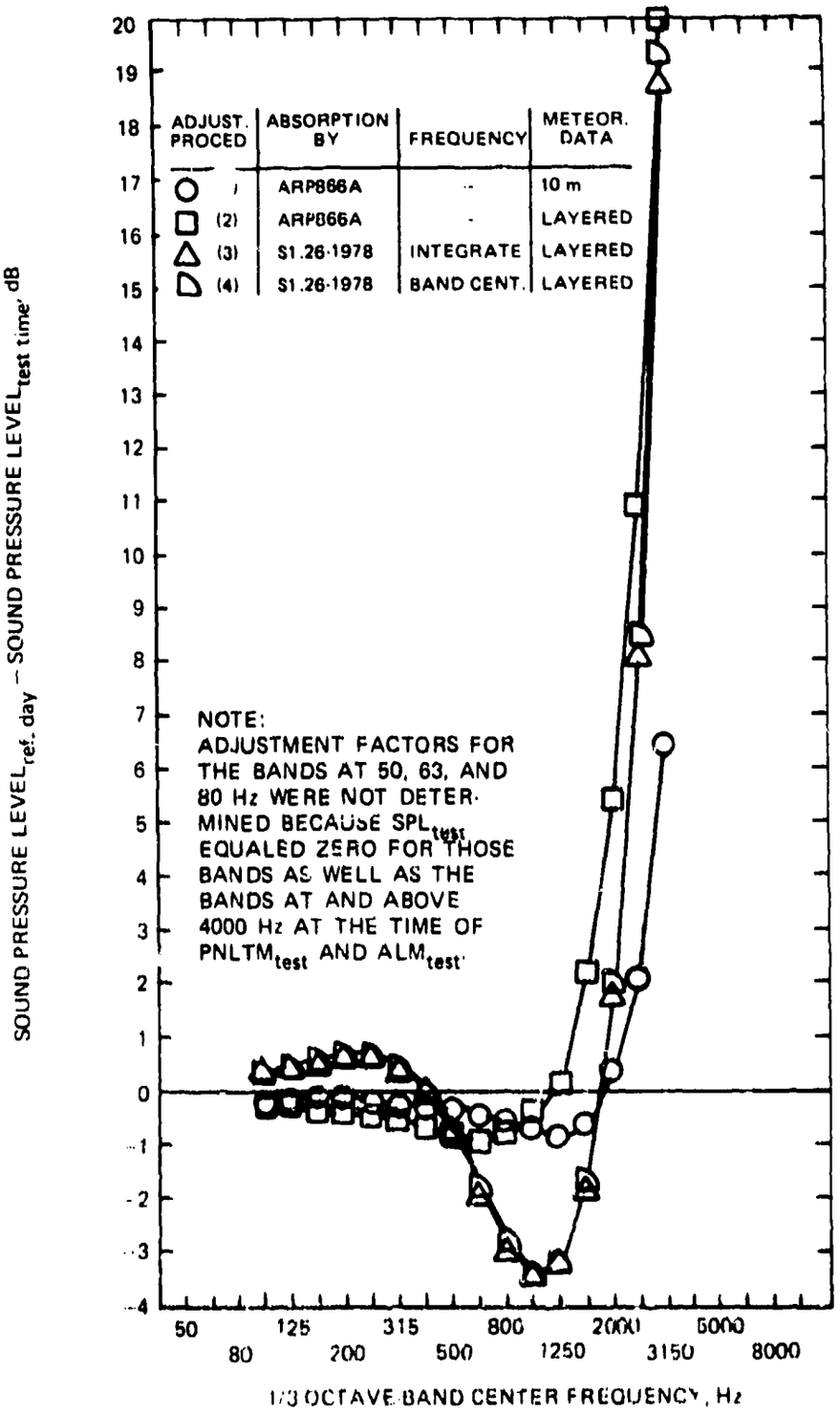

Figure 40.-Band sound-pressure-level adjustment factors at the time of PNLTM$_{test}$ and of ALM$_{test}$ for Raisbeck - Learjet, run 12, PD = 1925.7 m, ψ = 135.2°.

particularly evident for band center frequencies from 100 to 1600 Hz. From 100 to 400 Hz, procedures (3) or (4) showed positive adjustment factors; between 500 and 1600 Hz, the adjustments decreased to relatively large negative values. The adjustments by procedures (1) and (2) were always negative over this frequency range, but not as negative as those calculated by procedures (3) and (4). The same trends for the differences between the two absorption models were also in the results from run 374 in Fig. 37, though not as prominent as in Fig. 40. The differences in adjustment factors are the result of differences between the two models for atmospheric absorption as shown by the curves in Fig. 34.

Comparing the results using procedures (1) and (2), Fig. 40 shows that, as expected, sole use of meteorological data measured at the 10-m height results in significantly smaller adjustments than use of meteorological data measured along the sound path. The meteorological conditions aloft [see Figs. 24(f) and 25(c)] were quite different, and more absorptive, than the conditions at the 10-m height. Since FAR 36 requires measurements, at various times throughout each test day, of the meteorological conditions of the atmosphere at various heights above ground level, it would appear to be logical, and for no significant increase in test cost, to always use the meteorological conditions along the sound path when computing adjustment factors for differences in atmospheric absorption under test and reference conditions.

Referring again to Fig. 40, the frequency where the higher-frequency adjustment factors changed from negative to positive was significantly lower than for the shorter-pathlength adjustment factors shown in Figs. 35 and 37. For procedure (2) using SAE ARP866A, the crossover frequency was between the 1000- and 1250-Hz bands. For procedures (3) and (4) using ANSI S1.26-1978, the crossover frequency was between the 1600- and 2000-Hz bands.

If we consider just the methods that use the meteorological conditions aloft [procedures (2), (3), and (4)], it is interesting to note that the adjustments calculated using the procedure of SAE ARP866A were greater (i.e., more positive) than those calculated using the procedure of ANSI S1.26-1978 for every band center frequency from 630 to the upper limit of the data at 3150 Hz. The effect of the offset or kink in the procedure of SAE ARP866A

between the 4000 and 5000-Hz bands is not evident in Fig. 40 because the data terminate at the 3150-Hz band. The adjustments calculated by making use of the SAE ARP866A method (i.e., the greater absorption losses) were larger than those calculated using the method of ANSI S1.26-1978 because the absorption coefficients in ARP866A are larger at those frequencies than the absorption coefficients from ANSI S1.26-1978 for the cold and dry conditions prevailing at the time of the test.

As a final observation about the results in Fig. 40, we note that the difference between the adjustment factors calculated by the band-integration method of procedure (3) and the band-center-frequency method of procedure (4) was small-to-negligible for all frequency bands covered by the available data. The largest difference was 0.5 dB in the highest-frequency band at 3150 Hz where the test-time spectral slope was also steepest and the band-center-frequency method probably overestimated the actual absorption loss.

Effect of Different Adjustment Procedures on Reference-Day Sound Pressure Levels.-The discussion of the effect on the 1/3-octave band sound pressure levels of using different procedures to calculate adjustment factors for atmospheric absorption losses concludes with examination of the test-time and reference-day sound pressure levels in Fig. 41 at the time of PNL(M)$_{tes}$ and A$_{tes}$ for the Raisbeck-Learjet data. Only reference-day levels by procedures (1), (2), and (3) are shown because the levels by procedure (4) were almost identical to those by procedure (3).

At low frequencies (i.e., the 100 to 400-Hz bands), the differences between the calculated reference-day sound pressure levels are noticeable, but not too important. The differences among the higher-frequency sound pressure levels (i.e., the 500 to 3150-Hz bands) are significant.

The relatively small adjustments calculated using the 10-m meteorological data and procedure (1) make the high-frequency reference-day spectrum by that procedure have an entirely different shape than the spectrum determined using procedures (2) and (3). The method of procedure (1) essentially preserves the rapid high-frequency rolloff of the test-time spectrum. The absorption-loss adjustment factors determined by procedure (1) are not considered to be a reasonable representation of the actual losses over the 1926-m pathlength for the meteorological conditions as they existed at the time of the test.

The reference-day sound pressure levels calculated using procedures (2) and (3) both have a more-gradual high-frequency rolloff than the levels calculated using procedure (1). The levels determined using ARP866A are higher than those determined using ANSI S1.26-1978 because the adjustment factors were greater as indicated in Fig. 40.

The most-interesting aspect of the results shown in Fig. 41 is the high-frequency "turning up" of the reference-day spectra determined by procedures (2) and (3). The "turning up" of the spectra at high frequencies is considered to likely be an incorrect result because the Learjet was operated at a high power setting and the spectrum measured in the far field at an emission angle of

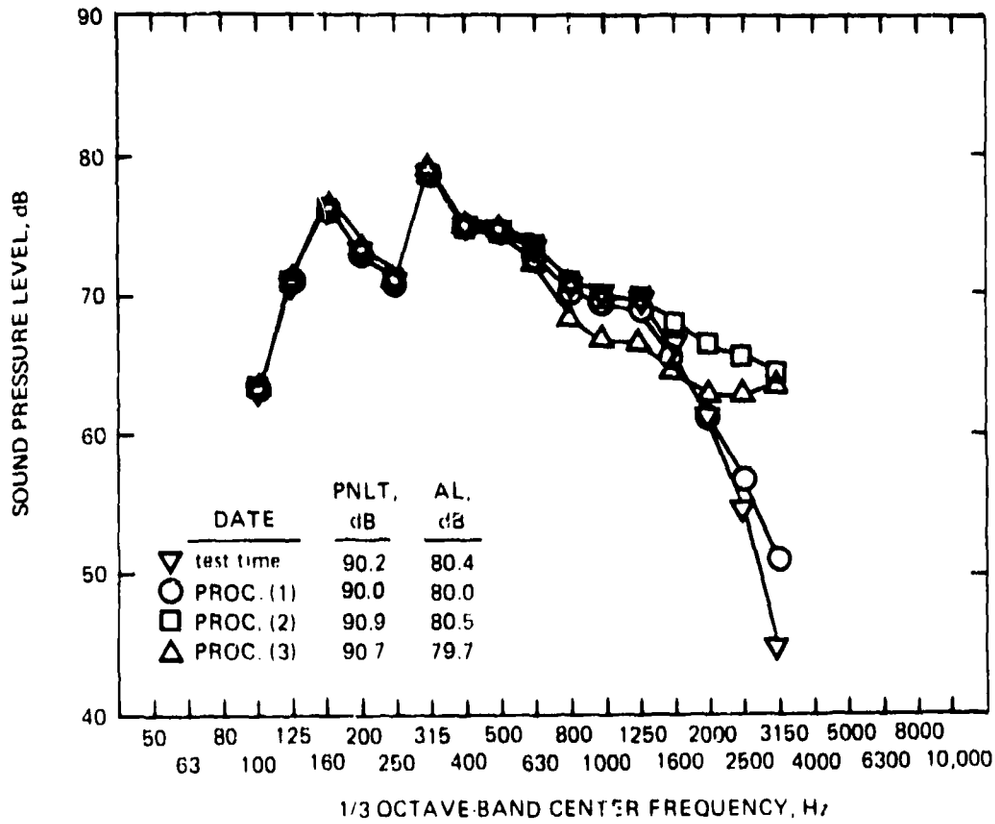

Figure 41.-Sound-pressure-level spectra for test and reference meteorological conditions for Raisbeck-Learjet at time of $PNLTM_{test}$ or ALM_{test}, run 12, PD = 1925.7 m, $\psi = 135.2^{o}$.

135° should have been that produced by broadband jet-noise sources in the exhaust streams from the two turbojet engines. A jet-noise spectrum, with a maximum occurring between the 200 and 315-Hz bands, would be expected to decrease, not increase, at high frequencies under any meteorological conditions, especially for a propagation distance of 1926 meters.

The high-frequency "turning up" of the reference-day sound pressure levels is more noticeable for the levels determined using procedure (3) than using procedure (2). For procedure (2), the sound pressure levels in the 2500- and 3150-Hz bands are the only levels that appear to be affected by the "turning-up" phenomenon in that the band-level slopes over those bands did not decrease with increasing frequency as would be expected for a spectrum produced by a jet-noise source. In other words, the level change from the 1600-Hz band to the 2000-Hz band was -1.9 dB; then from the 2000 to the 2500-Hz band the level change decreased to only -2.0 dB; from the 2500 to the 3500-Hz band the level change increased to -0.9 dB instead of decreasing. Even for the minimal absorption conditions associated with 25° C and 70-percent relative humidity, the band-level slope should continually decrease with increasing frequency for a pathlength as long as 1926 meters.

For procedure (3), the sound pressure levels in the three bands at 2000, 2500, and 3150 Hz seem to be influenced because the slope of -2.0 dB from the 1250 to the 1600-Hz band increases to -1.6 dB from 1600 to 2000 Hz, increases again to -0.2 dB from 2000 to 2500 Hz, and increases again to +0.8 dB from 2500 to 3150 Hz. The "turning up" is more noticeable for the procedure (3) results because the band-level slope actually becomes positive from the 2500 to the 3150-Hz bands. The trend indicated by the positive slope is that the level in the 4000-Hz band (had there been any test-time data at 4000 Hz) would have been quite a bit higher than the level in the 3150 Hz band, and so on. Such a result would be considered to be ludicrous for a jet-noise source. Such trends are similar to those obtained for the hypothetical spectrum considered in Section 3 for filters having non-ideal response characteristics with the results as shown in Fig. 22.

"Turning up" of reference-day high-frequency sound pressure levels calculated by adjusting measured test-time sound pressure levels for differences in atmospheric absorption losses has been observed by others, e.g., see Refs. 24 to 28. The reasons put forward to explain the "turning up" of the reference-day sound pressure levels

have included speculations that atmospheric absorption losses were not properly modeled, that meteorological conditions along the sound propagation path were not measured properly or with adequate resolution and hence that the adjustments from test-to-reference conditions could not be expected to apply to the measured test-time sound pressure levels;[29] or that the calculated high-frequency adjustment factors were too large because they were calculated at a single frequency that was too high to be representative of the loss over the width of the higher-frequency bands. The latter concern is the reason the nominal lower bandedge frequency is used in SAE ARP866A for the four bands from 5000 to 10,000 Hz.

Analysis of DC-9 flyover noise data from the 1974 tests at Fresno and Yuma that was performed by McCollough and True[25] resolved the problem of a high-frequency turning up of the reference-day spectrum by arbitrarily rolling off the adjusted spectrum starting in the 4000 or 5000-Hz bands. The rolloff was applied after visual inspection of the adjusted sound pressure levels. The rolloff rate appears to have been -6 dB/band for the 1/3-octave-band data. The difference in reference-day EPNL between using and not-using the arbitrary rolloff of high-frequency data was said to be less than 0.5 dB for the path-length distances that were examined.

Calculated values for the high-frequency sound pressure levels reported here have not included any arbitrary rolloff. Any single rolloff rate was not likely to be applicable to all engine power settings and measurement distances. Nor would a single rolloff rate apply to all sources of aircraft noise. The requirement to inspect each spectrum to determine the frequency at which to start applying the rolloff was considered neither desirable nor compatible with automated processing of aircraft flyover noise data by a digital computer.

It was considered that the cause of the high-frequency turning up of reference-day spectra should be determined and a solution developed which could be used by a digital computer when analyzing any set of aircraft noise data. If as suspected, the fundamental problem was incorrect test-time band levels because of contamination from power transmitted through the lower stopbands of the filters, than a method should be developed to estimate what the band levels would have been if the filters had ideal transmission response charac-

teristics. Development of an appropriate method to accomplish that task was not within the scope of the effort reported here.

Effect of Different Adjustment Procedures on Reference-Day EPNL and SEL.- Thus far we have discussed the effect of alternative atmospheric-absorption adjustment procedures on 1/3-octave-band sound pressure levels and the maximum values of the frequency-weighted quantities PNL, PNLT, and AL. We now turn to an examination of the effect of the alternative adjustment procedures on the time-integrated measured EPNL and SEL.

Since the aircraft noise data used for the analyses reported here had been previously acquired and analyzed by the FAA and NASA or by BBN for other purposes, it was felt that it would be instructive to compare certain results obtained from the present analyses with those obtained by the FAA and BBN. Table 6 presents a compilation of a number of comparisions between the values of various quantities determined from the present study (abbreviated as P.S.) with those reported by McCollough and True in Ref. 25. Comparisons are shown for each of the five DC-9 runs from the Fresno tests. Except for the last two entries, the comparisons in Table 6 are all for test-time meteorological conditions.

With the exception of a few anomalies, the comparisons in Table 6 indicate good agreement between the results from the present study and the previous results in Ref. 25. The differences, in general, are consistent and explainable.

The maximum A-weighted sound levels, ALM, determined in the present study are all higher than those from Ref. 25. The differences range from 0.1 dB to 1.8 dB [for run 322] with an average difference of 0.7 dB for all five runs, or 0.4 dB if the 1.8 dB difference for run 322 is excluded.

The reason for the differences may be related to differing practices used during processing of the data - by the Department of Transportation's Transportation Systems Center for the data reported by the FAA in Ref. 25 and by DyTec and The Boeing Company for the data[20] used for the present study.

Table 6.-Comparison of results from present study with those from Ref. 25 for five DC-9 runs.

Quantity to be compared	Data from present study (P.S.) or Ref. 25									
	272		322		358		374		378	
	P.S.	25	P.S.	25	P.S.	25	P.S.	25	P.S.	25
ALM, dB	93.7	93.6	94.9	93.1	95.4	95.2	87.2	86.5	95.1	94.6
PNLTM, dB	110.1	109.2	109.8	108.0	112.0	111.3	102.5	101.7	111.1	110.9
tone-correction factor, dB	1.8	1.1	0.6	0.8	1.8	1.5	1.3	1.3	1.5	1.4
center freq. of band producing TCF, Hz	3150	3150	3150	6300	3150	3150	3150	3150	3150	3150
EPNL duration-correction factor, dB	-5.4	-4.5	-6.9	-5.3	-6.0	-5.4	-3.9	-2.6	-5.5	-5.1
EPNL, dB	104.7	104.7	102.9	102.6	106.0	105.9	98.6	99.2	105.6	105.8
time of PNLTM - time at overhead, sec	0.95	2.0	0.85	2.0	0.75	2.0	3.05	4.0	1.05	2.5
sound emission angle at PNLTM, deg	102.3	129	101.3	129	98.2	126	113.1	125	105.0	135
propagation pathlength at PNLTM, m	159.5	200.3	156.8	194.8	154.4	200.3	369.4	379.8	162.3	210.3
PNLTM adjustment factor using SAE ARP866A and 10-m met. data, dB	1.0	1.2	0.1	0.2	-0.1	-0.3	0.2	0.1	0.4	0.4
PNLTM adjustment factor using SAE ARP866A and layered - atmosphere analysis, dB	1.1	1.4	0.2	0.2	-0.1	-0.2	0.2	0.2	0.4	0.0

The effective perceived noise levels in the sixth row in Table 6 reflect the differences in PNLTM and duration-correction factor. The differences in EPNL tend to be less than the differences in the preceding quantities because the more-negative duration-correction factors calculated for the present study tend to offset the higher PNLTM values. There is no consistent trend to the differences in EPNL because of variations in the combinations of the differences in PNLTM and duration-correction factor.

The three quantities following the effective perceived noise level in the sixth row of Table 6 are related to the time synchronization of the recorded noise signal and the position of the airplane on the flight path. For each quantity [(1) the difference between the time of occurrence of PNLTM and the time at overhead, (2) the sound emission angle at the time of occurrence of PNLTM, and (3) the length of the sound propagation path at the time of occurrence of PNLTM] there are significant and consistent differences. In each case, the FAA data from Ref. 25 show later times, larger angles, and longer pathlengths.

For the data that were used for the present study, timing data were initially reviewed and checked with NASA personnel. During data processing, the timing data were re-read and checked by the Boeing personnel who transcribed the time-code recordings from the original data tapes. Time code on the magnetic tape recordings of the aircraft noise signals was read for each of the two sets of microphones for each of the 37 aircraft noise recordings that were analyzed[20]. For each test, the original photographs of the test airplane were re-examined to determine the height at overhead. Several errors in previous height calculations were found and corrected. Aircraft speed during the flyovers was determined for each test from the distance between the timing cameras and the time interval. The airplane speed from those calculations was checked against the airspeed noted on the cockpit log for each test. Thus, the timing, airspeed, and height data used for the present study from the DC-9 tests are as accurate as the data-acquisition system permitted.

With regard to the reported timing and angle/pathlength data, Ref. 25 states that the data which were listed are average values for a number of nominally identical test runs. There could be ±0.5-s variations in the calculation of the average time for a set of test runs. Reference 25 also does not specify

the convention that was used to specify a reference time within the 500-ms span of a sample of data. The mid-point of the data span was used for the present study.

Because of the sensitivity of sound-emission angle and propagation distance to changes in timing data for these flyovers at heights between 150 to 160 m, the relatively small timing differences caused relatively large shifts in the calculated value of the sound emission angle and propagation pathlength. The layered-atmosphere method of calculating an atmospheric-absorption adjustment factor should thus have yielded larger factors for the longer pathlengths of the data reported in Ref. 25.

Test-to-reference-day adjustment factors, using SAE ARP866A and meteorological data at the surface or aloft [i.e., procedures (1) and (2) in the notation of the present study], are shown in the final two rows of Table 6. There was no consistent trend for the differences between the values obtained from the present study and from Ref. 25. Adjustment factors from the present study were sometimes larger, sometimes equal to, and sometimes smaller than those from Ref. 25.

There should have been no difference in calculation of atmospheric absorption since both sets of calculations used the same method. There might have been minor differences in the determination of test-time meteorological conditions. Reference 25 showed plots of vertical profiles of temperature and relative humidity for two of the five runs analyzed for the present study. The data in those plots showed good agreement with the corresponding data in Fig. 24. The meteorological data used for the present study were obtained from and reviewed with NASA personnel to verify and eliminate certain anomalies. For each aircraft height, interpolations to derive meteorological parameters applicable to the test times were carried out for each of the 37 test runs.

Therefore, like the timing and height data, the meteorological data for the present study should have been as accurate as the measuring system permitted and should have been close to the data used in Ref. 25. Indeed, the differences, in general, were small and did not exceed ±0.2 dB.

Data for the remaining four of the nine test cases were obtained from BBN. Table 7 compares the values of ALM, PNLM, PNLTM, and EPNL calculated by BBN and the present study for those four test cases. There are only negligible differences in the ALM data as there should have been since the 1/3-octave-band sound pressure levels were not re-processed for the BBN data as they were for the DC-9 runs discussed above for the comparisons in Table 6.

Table 7.-Comparison of test-time quantities calculated by BBN and by present study (P.S.) for data obtained from BBN.

Quantity	Source	727	Learjet	HS-748	Beech
ALM, dB	BBN	100.2	80.5	78.9	82.7
	P.S.	100.1	80.4	78.9	82.7
PNLM, dB	BBN	112.1	90.5	91.8	92.1
	P.S.	111.9	89.8	91.2	91.9
PNLTM, dB	BBN	112.7	91.5	95.0	93.7
	P.S.	112.3	90.2	91.7	92.2
EPNL, dB	BBN	110.0	91.1	91.0	89.1
	P.S.	110.3	89.4	88.2	87.8

The BBN data, as supplied to us, were not processed to remove background noise contamination. For our analysis of the four sets of data from BBN, we identifed an appropriate set of 1/3-octave-band sound pressure levels to represent background noise levels for each run. Data representing aircraft noise signals were then obtained by making use of Eq. (47) to remove the contaminating effects of background noise.

Differences in the sound pressure levels caused by removal of background noise contamination are considered to be the reason for the 0.2 to 0.7-dB lower PNLM values shown in Table 7 for the present study.

Differences in the values of PNLTM in Table 7 are attributed partly to the lower values of sound pressure level (and hence perceived noise level) and partly to the fact that the calculations of tone corrections for the present study started in the 800-Hz band while those calculated by BBN appear to have started in the 80-Hz band and thus included ground-reflection effects as well as spectral peaks at the funda-

mental and harmonics of the propeller blade-passing frequency for the HS-748 and Beech Debonair data.

Differences in EPNL in Table 7 reflect differences in sound pressure levels, perceived noise levels, tone-correction factors, and duration-correction factors. The differences are considered to be consistent with the above explanations for the differences in perceived noise levels and tone-correction factors.

The various comparisons in Tables 6 and 7 have established the credibility of the results of the present study and of the basic methods used to analyze the aircraft flyover noise data. For the nine test cases that were studied, Tables 8 and 9 list the test-time and reference-day values for the various frequency-weighted and time-integrated quantities of interest. Results are listed for each of the four atmospheric-absorption adjustment procedures.

The data in Table 8 are for the six runs for which vertical profiles of meteorological parameters aloft were measured, i.e., the five DC-9 runs and the Learjet run. The data in Table 9 are for the three runs (727, HS-748, and Beech Debonair) for which vertical profiles of the meteorological parameters were not measured and only surface data were available. The data in Table 9 are shown here for the record; the reference-day data in Table 9 are essentially the same for all adjustment methods because the meteorological parameters measured near the ground had to be assumed to apply all along the sound path. The results in Table 9 will not be discussed further.

The data in Table 8 corroborate the trends illustrated by the previous discussion of the effects of the different adjustment procedures on the 1/3-octave-band sound pressure levels. The changes in EPNL should be the same as the changes in PNLT since the duration-correction factor was assumed to be the same under reference-day conditions as it was under test-time conditions. Similarly, the changes in SEL should be the same as the changes in AL.

For the shorter sound-propagation pathlengths, the tone-correction factors were approximately the same under reference-day conditions as they were under test-time conditions. For the two runs with moderate and long pathlengths (DC-9 run 374 and Learjet run 12), the tone-correction factor under reference-

Table 8.-Summary of frequency-weighted and time-integrated noise levels for DC-9 and Learjet test cases where meteorological data aloft were measured.

Test-time or ref.-day levels for indicated run number	PNL, dB	PNLT, dB	TCF, dB	EPNL, dB	AL, dB	SEL, dB
DC-9, run 272, test time	108.3	110.1	1.8	104.7	93.7	98.9
adj. proc. 1	109.3	111.1	1.8	105.7	94.4	99.6
adj. proc. 2	109.4	111.2	1.8	105.8	94.5	99.7
adj. proc. 3	109.7	111.5	1.8	106.1	94.8	100.0
adj. proc. 4	109.7	111.5	1.8	106.1	94.8	100.0
DC-9, run 322, test time	109.2	109.8	0.6	102.9	94.9	97.7
adj. proc. 1	109.4	109.9	0.5	103.1	95.1	97.9
adj. proc. 2	109.4	110.0	0.6	103.1	95.1	97.9
adj. proc. 3	109.8	110.3	0.5	103.4	95.5	98.3
adj. proc. 4	109.8	110.3	0.5	103.4	95.5	98.3
DC-9, run 358, test time	110.2	112.0	1.8	106.0	95.4	100.1
adj. proc. 1	109.9	111.9	2.0	105.9	95.3	100.0
adj. proc. 2	110.0	111.9	1.9	106.0	95.4	100.1
adj. proc. 3	110.3	112.2	1.9	106.3	95.7	100.4
adj. proc. 4	110.3	112.2	1.9	106.3	95.7	100.4
DC-9, run 374, test time	101.2	102.5	1.3	98.6	87.2	93.6
adj. proc. 1	101.6	102.7	1.1	98.8	87.3	93.7
adj. proc. 2	101.6	102.7	1.1	98.9	87.3	93.7
adj. proc. 3	102.0	103.2	1.2	99.3	87.5	93.9
adj. proc. 4	102.1	103.2	1.1	99.3	87.6	93.9
DC-9, run 378, test time	109.6	111.1	1.5	105.6	95.1	99.7
adj. proc. 1	110.0	111.5	1.5	105.9	95.5	100.0
adj. proc. 2	110.0	111.5	1.5	105.9	95.5	100.1
adj. proc. 3	110.3	111.8	1.5	106.2	95.9	100.4
adj. proc. 4	110.3	111.8	1.5	106.2	95.9	100.4
Learjet, run 12, test time	89.8	90.2	0.4	89.4	80.4	90.6
adj. proc. 1	89.7	90.0	0.3	89.2	80.0	90.2
adj. proc. 2	90.7	90.9	0.2	90.1	80.5	90.7
adj. proc. 3	90.5	90.7	0.2	89.9	79.7	89.8
adj. proc. 4	90.5	90.7	0.2	89.9	79.7	89.9

*Reference-day duration factors for EPNL and SEL are not tabulated here because they are, by definition, the same as the test-time duration factors (at least to ± 0.1 dB from rounding).

day conditions was always 0.1 to 0.2 dB smaller than [illegible] under test-time meteorological conditions. In determining the effective perceived noise level, the smaller tone-correction factors for those larger pathlengths tended to offset the larger perceived noise levels associated with the adjusted reference-day 1/3-octave-band sound pressure levels.

Table 9.-Summary of frequency-weighted and time-integrated noise levels for 727, HS-748, and Beech Debonair test cases where only surface meteorological data were measured.

Test-time or ref.-day levels for indicated run number	PNL, dB	PNLT, dB	TCF, dB	EPNL, dB	AL, dB	SEL, dB
727, run 25, test time	111.9	112.3	0.4	110.3	100.1	108.7
adj. proc. 1	111.7	112.1	0.4	110.1	99.9	108.5
adj. proc. 2	111.7	112.1	0.4	110.1	99.9	108.5
adj. proc. 3	111.7	112.1	0.4	110.1	99.8	108.4
adj. proc. 4	111.7	112.1	0.4	110.1	99.8	108.4
HS-748, run 7, test time	91.2	91.7	0.5	88.2	78.9	85.5
adj. proc. 1	91.1	91.5	0.4	88.1	78.8	85.4
adj. proc. 2	91.1	91.5	0.4	88.1	78.8	85.4
adj. proc. 3	91.1	91.6	0.5	88.2	78.9	85.5
adj. proc. 4	91.1	91.6	0.5	88.1	78.9	85.5
Beech, run 119, test time	91.9	92.2	0.3	87.8	82.7	87.3
adj. proc. 1	91.9	92.2	0.3	87.8	82.7	87.3
adj. proc. 2	91.9	92.2	0.3	87.8	82.7	87.3
adj. proc. 3	91.9	92.2	0.3	87.8	82.6	87.2
adj. proc. 4	91.9	92.2	0.3	87.8	82.6	87.2

Figure 42 was prepared to help visualize the trends resulting from the use of the four adjustment procedures. Figure 42(a) shows trends for the changes in effective perceived noise level by plotting the change in tone-corrected perceived noise level, i.e., from Eq. (46) using

$$EPNL_{ref} - EPNL_{test} = PNLT'_{ref} - PNLTM_{test}. \tag{98}$$

Figure 42(b) shows the trends for changes in sound exposure level by plotting the change in A-weighted sound level, i.e., from

$$SEL_{ref} - SEL_{test} = AL'_{ref} - ALM_{test}. \tag{99}$$

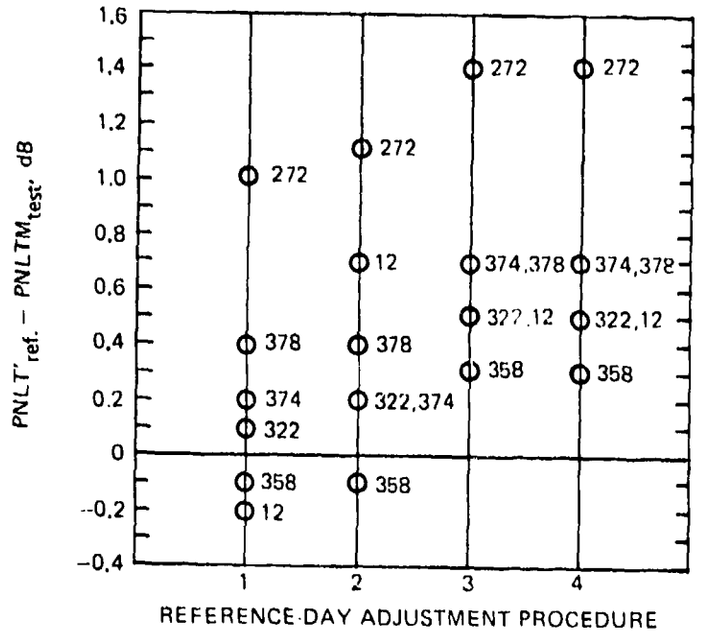

(a) FOR TONE-CORRECTED PERCEIVED NOISE LEVEL.

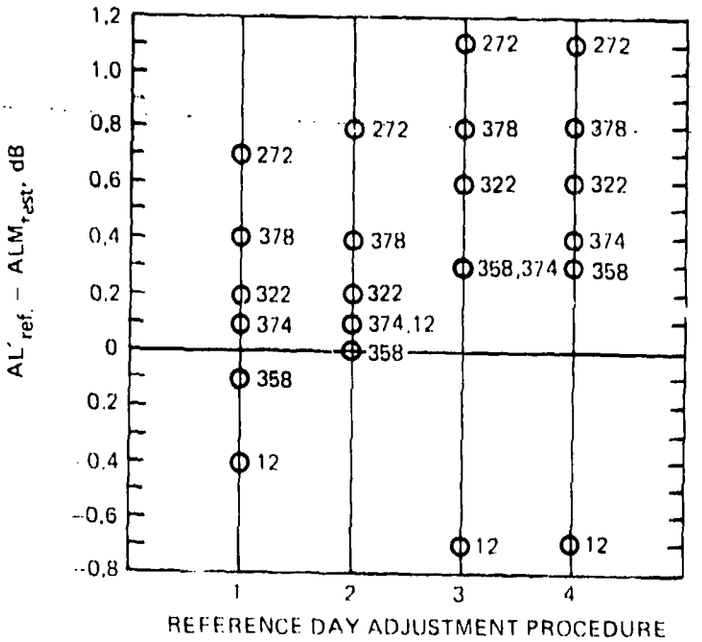

(b) FOR A-WEIGHTED SOUND LEVEL.

Figure 42.-Test-to-reference-day adjustment factors by the four adjustment procedures for PNLT and AL for DC-9 test cases (runs 272 to 378) and Learjet (run 12).

The primed quantities in Eqs. (98) and (99) represent the tone-corrected perceived noise levels and A-weighted sound levels calculated for reference-day meteorological conditions from the spectra corresponding to $PNLTM_{test}$ and ALM_{test}, respectively.

Examination of the data in Fig. 42 provided the following observations:

(1) The largest positive adjustment factors were those for DC-9 run 272 which had a pathlength of about 160 meters and which was flown under cold and dry meteorological conditions.

(2) Negative adjustment factors were generally noted for the Learjet run 12 which had a pathlength of about 1926 meters and which was flown under meteorological conditions along the sound path that were drier than those of DC-9 run 272 but not quite as cold.

(3) Except for the Learjet run 12, the trends for, and the magnitude of, the changes in PNLT were very nearly identical to those for AL. The adjustment factors for the Learjet data were strongly affected by the length of the path, the test-time meteorological conditions, the shape of the measured spectrum of the sound signal, the apparent contamination of the measured 1/3-octave-band levels by power transmission through the stopbands of the real filters, and on whether it is the change in PNLT or AL that was being considered.

(4) For each run, procedure (1), which used only the meteorological data at the 10-m height, always yielded the smallest adjustment factors.

(5) Except for the Learjet run 12, the use of atmospheric layering by procedure (2) produced adjustment factors which were equal to, or at most 0.1 decibel larger than, those calculated using the surface conditions of procedure (1). For the Learjet, the adjustment factor by procedure (2) was 0.9 decibels greater than by procedure (1) for PNLT and 0.5 decibels greater for AL.

(6) With the exception again of the data from the Learjet test, the use of the method of ANSI S1.26-1978 to calculate atmospheric absorption instead of the method of SAE ARP866A yielded adjustment factors that were larger by

0.3 to 0.4 decibels. For the Learjet data, the adjustment factor by procedure (3) was smaller than by procedure (2) by 0.2 decibels for PNLT and by 0.8 decibels for AL; the difference of 0.6 dB was the result of differences in the calculated reference-day spectra as shown in Fig. 41.

(7) Adjustment factors calculated by the band-center-frequency method of procedure (4) were identical to those calculated by the band-integration method of procedure (3) with one exception. That exception was DC-9 run 374 where the factor by procedure (4) was 0.1 dB greater for PNLT than by procedure (3). That single difference is not significant because of the rounding performed by the computer.

5. CONCLUSIONS

1. The magnitude of the measured, test-time 1/3-octave-band sound pressure levels depends on (a) the spectrum of the sound at the source, (b) the length of the sound propagation path, (c) the meteorological conditions along the path, and (d) the response characteristics of the bandpass filters used to produce the measured 1/3-octave-band sound pressure levels. For measurements made during an aircraft noise-certification test, decisions made by a particular organization regarding data acquisition and data processing, within the various options available under FAR Part 36, also affect the measured 1/3-octave-band sound pressure levels.

2. The magnitude and sign of the adjustments to the measured, test-time 1/3-octave-band sound pressure levels to determine equivalent band levels for reference meteorological conditions along the propagation path depend on the choice of analytical model for the atmospheric absorption of sound and on whether the test-time atmospheric conditions are represented by meteorological data measured at the surface or aloft.

3. The study reported here does not provide any fundamental data to assess the validity of the atmospheric-absorption models given in American National Standard ANSI S1.26-1978 and in SAE Aerospace Recommended Practice ARP866A-1975. However, the study does provide data that can be used to evaluate the magnitude of the differences in test-to-reference-day band-level adjustment factors and the resulting changes in PNL, PNLT, EPNL, AL, and SEL.

4. For most cases, use of ANSI S1.26-1978 instead of SAE ARP866A-1975 to calculate atmospheric-absorption losses along the sound propagation path will probably yield higher reference-day levels by an amount ranging from zero to 0.5 decibels. The maximum increase will probably not exceed one decibel for frequency-weighted or time-integrated quantities associated with the sound spectra and meteorological conditions of practical interest for aircraft noise certification.

5. However, in some cases, use of ANSI S1.26-1978 may result in certification noise levels which are lower than those calculated using SAE ARP866A-1975.

Examples of cases where that result may occur include aircraft that generate sound dominated by low- and mid-frequency acoustic energy. Smaller test-to-reference-day adjustment factors from use of ANSI S1.26-1978 will be noted when the noise from such a source is measured under highly absorptive test-time atmospheric conditions after propagation over a relatively long path such as the paths occurring at the takeoff and sideline noise-certification measuring points. Again, the differences in certification noise levels that may result from use of the different atmospheric-absorption models will probably not be more than one decibel.

6. Using meteorological data measured aloft at closely spaced height intervals produces better estimates of atmospheric-absorption losses under actual test conditions than does the assumption that the meteorological conditions measured near the surface adequately represent conditions all along the length of the propagation path.

7. With meteorological data measured at various heights above ground level and an atmospheric layering procedure, the calculated atmospheric-absorption losses over the sound propagation path will produce test-to-reference-day adjustment factors that are, in general, greater than those calculated using only the meteorological conditions measured near the surface (e.g., at a height of 10 meters). Generally, the difference in adjustment factors for frequency-weighted or time-integrated quantities should be between zero and 0.5 decibels for most cases. The maximum difference is expected to be approximately one decibel. For five of the six test cases examined here, the atmospheric-absorption adjustment factors calculated using the atmospheric-layering method ranged from zero to 0.1 dB greater than those calculated using only the surface meteorological conditions. For the sixth case with the data from the Learjet test, the difference was 0.9 dB for PNLT (or EPNL) and 0.5 dB for AL (or SEL).

8. For the four 1/3-octave bands with nominal band-center frequencies ranging from 5000 to 10,000 Hz, calculation of atmospheric-absorption losses by substituting the nominal lower bandedge cutoff frequency for the band-center frequency did not provide as good an estimate of the actual atmospheric-absorption losses as did the use of the band-center frequency for moderately absorptive conditions and moderate pathlengths.

9. Except for measured sound spectra having very rapid high-frequency rolloff rates (resulting, for example, from an aircraft that generates relatively little high-frequency sound, or from measurements made under very absorptive conditions or at long distances, or a combination of those factors), a band-center-frequency method provides as accurate an estimate of atmospheric-absorption losses as does a band-integration method for 1/3-octave-band sound pressure levels with center frequencies to 10,000 Hz.

10. For measured sound spectra with rapid high-frequency rolloff rates, a band-integration method provides a more-accurate estimate of the high-frequency atmospheric-absorption loss over the length of the propagation path than does the band-center-frequency method.

11. Test-to-reference-day adjustment factors for high-frequency sound pressure levels are generally larger when using the band-center-frequency method than the band-integration method. The magnitude of the difference depends on frequency, pathlength, and meteorological conditions. Typical maximum differences (at the highest band center frequency for which data were available) were of the order of 0.5 decibel for the test cases examined for this study.

12. For band-center frequencies from 500 to 2000 Hz, the test-to-reference-day adjustment factors for the 1/3-octave-band sound pressure levels are smaller (i.e., more negative) when determined using the method of ANSI S1.26-1978 to calculate absorption losses than using the method of SAE ARP866A-1975.

13. For band-center frequencies greater than 2000 Hz, test-to-reference-day adjustment factors calculated using the method of ANSI S1.26-1978 are generally larger (i.e., more positive) than those calculated using the method of SAE ARP866A-1975, though comparisons here are complicated by the use of the nominal lower bandedge frequency to calculate the absorption loss over a band in the SAE ARP866A method for the 5000 to 10,000 Hz bands.

14. Because of finite electrical rejection capability in the stopbands, currently available 1/3-octave-band filters (analog or digital) can indicate higher sound pressure levels than equivalent ideal filters because of energy

transmitted through the stopbands, particularly the lower stopbands for high-frequency sound pressure levels. Real-filter effects are encountered most often when attempting to measure sound pressure signals that have propagated over a long propagation path through a relatively absorptive atmosphere such that the high-frequency portion of the sound pressure spectrum decreases rapidly with frequency. If the influence of real-filter effects is not recognized and removed before attempting to adjust the measured high-frequency sound pressure levels from test-time to reference-day conditions, then the adjusted reference-day sound pressure levels will be incorrect. The magnitude of the error can be many decibels.

6. REFERENCES

1. SAE Committee A-21, "Standard Values of Atmospheric Absorption as a Function of Temperature and Humidity," Aerospace Recommended Practice ARP866A, Society of Automotive Engineers, Warrendale, PA 15096 (issued 31 August 1964, revised and re-issued 15 March 1975).

2. Anon., "American National Standard Method for the Calculation of the Absorption of Sound by the Atmosphere," American National Standards Institute ANSI S1.26-1978, Standards Secretariat, Acoustical Society of America, New York, NY 10017 (issued in 1978).

3. F. Douglas Shields and H. E. Bass, "Atmospheric Absorption of High Frequency Noise and Application to Fractional-Octave Bands," National Aeronautics and Space Administration Contractor Report CR-2760 (June 1977).

4. Alan H. Marsh, "Atmospheric-Absorption Adjustment Procedure for Aircraft Flyover Noise Measurements," Federal Aviation Administration Contractor Report FAA-RD-77-167 (December 1977).

5. Anon., "Noise Standards: Aircraft Type and Airworthiness Certification," Part 36 of the Federal Aviation Regulations (Part 36 was first published 1 December 1969; Part 36 includes Changes 1 to 12 with Change 12 effective 15 January 1979.)

6. Anon., "American National Standard Specification for Octave, Half-Octave, and Third-Octave-Band Filter Sets," American National Standards Institute ANSI S1.11-1966 (R-1971), Standards Secretariat, Acoustical Society of America, New York, NY 10017 (issued in 1966, re-affirmed in 1971).

7. L. C. Sutherland and H. E. Bass, "Influence of Atmospheric Absorption on the Propagation of Bands of Noise," J. Acoust. Soc. Am. 66, No. 3, 885-894 (September 1979).

8. Anon., "Recommendations for Octave, Half-Octave, and Third-Octave-Band Filters Intended for the Analysis of Sounds and Vibrations," IEC Recommendation, Publication 225, International Electrotechnical Commission, Geneva, Switzerland (1966).

9. L. W. Sepmeyer, "Bandwidth Error of Symmetrical Bandpass Filters Used for the Analysis of Noise and Vibration," J. Acoust. Soc. Am. 34, 1653-1657 (1962).

10. L. W. Sepmeyer, "On the Bandwidth Error of Butterworth Bandpass Filters," J. Acoust. Soc. Am. 35, 404-405 (1963).

11. Sound Level Meters. IEC Standard, Publication 651, International Electrotechnical Commission, Geneva, Switzerland (First Edition 1979).

12. D. J. Stouder and J. C. McCann, "Evaluation of Proposed Standards for Aircraft Flyover Noise Analysis Systems," J. Aircraft 14, No. 8, 713-719 (August 1977).

13. D. J. Stouder, "Use of Digital Averaging Techniques for the Analysis of Aircraft Flyover Noise," in *INTERNOISE 74, Proceedings of the International Conference on Noise Control Engineering*, edited by John C. Snowdon (Institute of Noise Control Engineering, Poughkeepsie, NY, 1974), pp. 137-140.

14. D. F. Pernet, "A Review of Aircraft Noise Propagation," National Physical Laboratory Acoustics Report Ac 92, Teddington, Middlesex, England (October 1979).

15. L. C. Sutherland, J. Parkinson, and D. Hoy, "Correction Procedures for Aircraft Noise Data, Volume II: Background Noise Considerations," Federal Aviation Administration Contractor Report FAA-EE-80-1, Vol. II (December 1979).

16. Robert N. Hosier, "A Comparison of Two Independent Measurements and Analyses of Jet Aircraft Flyover Noise," National Aeronautics and Space Administration Technical Note TN D-8379 (June 1977).

17. Don A. Webster and David T. Blackstock, "Experimental Investigation of Outdoor Propagation of Finite-Amplitude Noise," National Aeronautics and Space Administration Contractor Report CR-2992 (August 1978).

18. R. Rackl, "Correction Procedures for Aircraft Noise Data, Volume I: Pseudotones," Fede: Aviation Administration Contractor Report FAA-EE-80-1, Vol. I (December 1979).

19. Henry T. Mohlman and John N. Cole, "Computer Programs (Omega 5, 6, and 8) for Processing Measured Aircraft Flyover/Runup Noise Data for USAF Community Noise Prediction Procedures (NOISEMAP/NOISEFILE)," University of Dayton Research Institute and Aerospace Medical Research Laboratory, Draft AMRL report, unpublished but available from AMRL, Wright-Patterson Air Force Base, OH.

20. Robert L. Chapkis and Alan H. Marsh, "Investigation of Ground Reflection and Impedance from Flyover Noise Measurements," National Aeronautics and Space Administration Contractor Report CR-145302 (February 1978).

21. Francis J. Montegani, "Computation of Atmospheric Attenuation of Sound for Fractional-Octave Bands," National Aeronautics and Space Administration Technical Paper 1412 (February 1979).

22. Louis C. Sutherland, "Correction Procedures for Aircraft Noise Data, Volume III: Filter Effects," Federal Aviation Administration Contractor Report FAA-EE-80-1, Vol. III (December 1979).

23. Arnold W. Mueller and David A. Hilton, "Statistical Comparisons of Aircraft Flyover Noise Adjustment Procedures for Different Weather Conditions," National Aeronautics and Space Administration Technical Paper 1430 (May 1979).

24. Carole S. Tanner, "Experimental Atmospheric Absorption Coefficients," Federal Aviation Administration Contractor Report FAA-RD-71-99 (November 1971).

25. 'JB' McCollough and Harold C. True, "Effect of Temperature and Humidity on Aircraft Noise Propagation," Federal Aviation Administration Report FAA-RD-75-100 (September 1975).

26. Harold C. True, "The Layered Weather Correction for Flyover Noise Testing," Amer. Inst. of Aero. and Astro. Paper No. 76-895 (28 September 1976).

27. G. J. Cooper, "Atmospheric Layering," British Aerospace Acoustic Report 559, British Aerospace, Weybridge, Surrey, England (21 June 1978).

28. D. G. Crighton, "Nonlinear Propagation Effects in Aircraft Noise," J. Acoust. Soc. Am. Suppl. 1, 65, S95, Paper KK7 (Spring 1979).

29. R. C. Payne and D. F. Pernet, "The Effects of Temperature and Relative Humidity Gradients on Sound Attenuation in Air-to-Ground Propagation," National Physical Laboratory Acoustics Report Ac 86, Teddington, Middlesex, England (June 1978).